



Provided by the author(s) and University of Galway in accordance with publisher policies. Please cite the published version when available.

Title	In-situ Formed Bioactive Stem Cell Hydrogel Dressings from PEG-based Multifunctional Copolymers for Wound Healing
Author(s)	Dong, Yixiao
Publication Date	2013-07-23
Item record	http://hdl.handle.net/10379/3762

Downloaded 2024-04-25T15:57:22Z

Some rights reserved. For more information, please see the item record link above.





***In-situ* Formed Bioactive Stem Cell Hydrogel Dressings from
PEG-based Multifunctional Copolymers for Wound Healing**

A thesis submitted to the National University of Ireland for the
degree of Doctor of Philosophy

By

Yixiao Dong (M.Sc.)

July 2013

Network of Excellence for Functional Biomaterials

National University of Ireland, Galway

Research Supervisor: Dr. Wenxin Wang

Table of Contents

Table of Contents.....	i
List of Appendices.....	vii
List of Figures.....	viii
List of Tables.....	xviii
List of Abbreviations.....	xix
Acknowledgements.....	xxi
Abstract.....	xxiii
1. Chapter One: Introduction.....	1
1.1 Wound Healing.....	2
1.1.1 Acute Wound Healing.....	2
1.1.2 Chronic Wound Healing.....	10
1.2 Common Wound Dressings.....	13
1.3 Allo- and Autologous Skin Graft.....	20
1.3.1 Autologous Skin Graft.....	20
1.3.2 Allogeneic Skin Graft.....	21
1.4 Tissue Engineering Skin Substitutes.....	24
1.4.1 Acellular Skin Substitutes.....	24
1.4.2 Cellular Skin Substitutes.....	29
1.4.3 Limitations of Current Skin Substitutes.....	33
1.5 Drug & Growth Factors Delivery.....	33
1.6 Stem Cell Therapy for Wound Healing.....	39
1.6.1 Bone Marrow Stem Cells.....	39
1.6.2 Adipose-Derived Stem Cells.....	40
1.7 Injectable Hydrogels for Tissue Engineering.....	45
1.7.1 Physical Cross-linking Hydrogels.....	45
1.7.2 Chemical Cross-linking Hydrogels.....	49

1.8	Hypotheses and Objectives.....	50
1.8.1	Phase I.....	50
1.8.2	Phase II.....	51
1.8.3	Phase III.....	52
1.9	References.....	56
2.	Chapter Two: Synthesis of Thermoresponsive and Photo-crosslinkable Hyperbranched Copolymer via <i>In-situ</i> Deactivation Enhanced Atom Transfer Radical Polymerization (DE-ATRP).....	91
2.1	Introduction.....	92
2.2	Materials and Methods.....	95
2.2.1	Materials.....	95
2.2.2	Synthesis and Purification of PEGMEMA-MEO ₂ MA-EGDMA Copolymers.....	95
2.2.3	Characterizations of PEGMEMA-MEO ₂ MA-EGDMA Copolymers.....	95
2.2.4	Thermoresponsive Behavior of PEGMEMA-MEO ₂ MA-EGDMA Copolymers.....	96
2.2.5	Preparation of Photo-crosslinked Gels and SEM Imaging.....	96
2.2.6	Cytotoxicity Assessment.....	97
2.2.7	Statistical Analysis.....	97
2.3	Results and Discussion.....	99
2.3.1	Synthesis of PEGMEMA-MEO ₂ MA-EGDMA Copolymers via <i>In-situ</i> DE-ATRP Approach.....	99
2.3.2	Characterization of Hyperbranched PEGMEMA-MEO ₂ MA-EGDMA Copolymers with Vinyl Functional Groups.....	100
2.3.3	Thermoresponsive Behavior of PEGMEMA-MEO ₂ MA-EGDMA Copolymers.....	106
2.3.4	Photo-crosslinked Hydrogels and SEM Analysis.....	111
2.3.5	Cytotoxicity Assessment.....	111

2.4	Conclusion.....	114
2.5	References.....	115
3.	Chapter Three: <i>In-Situ</i> Cross-linked Semi-IPN Hydrogel Prepared from Thermoresponsive Hyperbranched Copolymer with Multi-acrylate Functionality and Hyaluronic Acid.....	119
3.1	Introduction.....	120
3.2	Materials and Methods.....	124
3.2.1	Materials.....	124
3.2.2	Synthesis of PEGMEMA-MEO ₂ MA-PEGDA Copolymers via <i>In-Situ</i> DE-ATRP.....	124
3.2.3	Characterizations of PEGMEMA-MEO ₂ MA-PEGDA Copolymers.....	125
3.2.4	Preparation of Non-IPN and Semi-IPN Gels.....	125
3.2.5	Determination of HA Retention in Semi-IPN Hydrogels.....	126
3.2.6	Swelling Studies.....	126
3.2.7	Cytotoxicity Assessment.....	127
3.2.8	Cellular Viability Assessments, 2D-Cell Seeding and 3D-Cell Encapsulation Experiments.....	127
3.3	Results and Discussion.....	128
3.3.1	Synthesis of PEGMEMA-MEO ₂ MA-PEGDA Copolymers via <i>In-Situ</i> DE-ATRP.....	128
3.3.2	Thermoresponsive Behavior of Copolymers.....	135
3.3.3	<i>In-Situ</i> Semi-IPN Gelation and HA Retention Assay.....	135
3.3.4	Swelling Characteristics of Non-IPN and Semi-IPN Hydrogels.....	136
3.3.5	Cytotoxicity of the Copolymer and 2D/3D Cell Culture on Non-IPN and Semi-IPN Hydrogels.....	141
3.4	Conclusion.....	147
3.5	References.....	148

4.	Chapter Four: <i>In-Situ</i> Cross-linked Hybrid Hydrogel for ADSCs Encapsulation Prepared from Thermoresponsive Hyperbranched Copolymer and Thiolated Hyaluronic Acid.....	153
4.1	Introduction.....	154
4.2	Materials and Methods.....	157
4.2.1	Materials.....	157
4.2.2	Synthesis of Hyperbranched PEGMEMA-MEO ₂ MA-PEGDA Copolymer.....	157
4.2.3	Thermoresponsive Behavior of Copolymers.....	158
4.2.4	Synthesis of Thiol Derivatized Hyaluronic Acid (HA-SH).....	158
4.2.5	Preparation of P-SH-HA Hybrid Hydrogel via Michael-type Addition Reaction.....	159
4.2.6	Morphological Characterization.....	159
4.2.7	Swelling Behavior.....	160
4.2.8	Cell Viability, Proliferation and Metabolic Activity Analysis of ADSCs-embedded Hydrogel from PEGMEMA-MEO ₂ MA-PEGDA Copolymer and Commercially Available HA-SH.....	160
4.2.9	Determination of Growth Factor Secretion.....	162
4.2.10	Statistical Analysis.....	163
4.3	Results and Discussion.....	163
4.3.1	Polymer Synthesis.....	163
4.3.2	Synthesis of Thiol Derivatized Hyaluronan (HA-SH).....	164
4.3.3	Fabrication of Hybrid Hydrogels	165
4.3.4	Morphological Characterisation and Swelling Behaviour of the Hydrogels	167
4.3.5	Cell Metabolic Activity, Viability and Proliferation in 3D Culture..	175
4.3.6	Determination of Growth Factor Secretion.....	180
4.4	Conclusion.....	183
4.5	References.....	184

5.	Chapter Five: Assessment of Material Responce and Theraputic Performance of <i>In-situ</i> Formed Bioactive Stem Cell Hydrogel Dressing in Rat Dorsal Excisional Wound Model.....	187
5.1	Introduction.....	188
5.2	Materials and Methods.....	190
5.2.1	Materials and Reagents.....	190
5.2.2	Polymer Synthesis and Hydrogel Fabrication.....	190
5.2.3	<i>In Vivo</i> Model.....	191
5.2.4	Harvesting and Processing of Tissue.....	192
5.2.5	Analysis for <i>In Vivo</i> Study.....	192
5.3	Results.....	199
5.3.1	Wound Closure.....	199
5.3.2	Wound Contraction and Epithelialization.....	199
5.3.3	Cell Retention.....	199
5.3.4	Inflammatory.....	200
5.3.5	Angiogenesis.....	210
5.4	Discussion.....	216
5.5	Conclusion.....	218
5.6	References.....	219
6.	Chapter Six: Summary and Future Direction.....	223
6.1	Introduction.....	224
6.2	Summary.....	226
6.2.1	Phase I: Multifunctional Polymer Synthesis.....	226
6.2.2	Phase II: <i>In-situ</i> Chemical Cross-linked Hydrogel Fabrication.....	227
6.2.3	Phase III: <i>In vivo</i> Assessments.....	229
6.3	Limitations.....	231
6.4	Conclusions.....	232

6.4.1	Phase I.....	232
6.4.2	Phase II.....	233
6.4.3	Phase III.....	234
6.5	Future Directions.....	234
6.5.1	Bioactive Modification of PEG-based Hydrogels.....	234
6.5.2	Semi-degradable <i>In-situ</i> Formed Hydrogel Dressing with ADSCs.....	238
6.5.3	Degradable <i>In-situ</i> Formed Hydrogel Skin Substitutes with ADSCs.....	238
6.5.4	Degradable Injectable Hydrogel for Growth Factor Delivery for Wound Healing	239
6.6	References.....	241

List of Appendices

A.	Materials and Reagents.....	250
B.	Polymer Synthesis and Purification.....	253
C.	Swelling Assessment for Non-IPN & Semi-IPN Hydrogels.....	256
D.	HA Release Assessment from Semi-IPN Hydrogel.....	257
E.	Thiolated HA Preparation.....	258
F.	Ellman’s Test.....	259
G.	P-SH-HA Hydrogel Fabrication and Swelling Assessment.....	260
H.	Rat ADSCs Cell Extraction.....	261
I.	Differentiation Test for rADSCs.....	263
J.	Cell Culture.....	269
K.	Cell Metabolic Assessment (alamarBlue [®] Assay).....	274
L.	Cell Proliferation Assessment (Picogreen [®] Assay).....	275
M.	Procedures for Animal Studies.....	277
N.	Tissue Harvest and Slides Preparation.....	283
O.	Hematoxylin and Eosin (H&E) Staining.....	285
P.	Immunohistochemistry.....	286
Q.	Hoechst Stain (for Cell Retention Analysis).....	289
R.	Stereology.....	289
S.	Publications.....	293

List of Figures

Chapter 1

- Figure 1.1: An overview of the stages of the normal wound healing process describing major biological processes, characteristic cell types and molecules as well as the main growth factors and cytokines involved in their regulation.....9
- Figure 1.2: Schematic of *in-situ* cross-linked hydrogel cell delivery system for wound healing: the hybrid polymer mixture is a solution at room temperature but form physical gels once applied onto the skin to cover and seal wound sites at body temperature. Furthermore, chemical cross-linking with ECM biopolymers occurs in minutes to achieve a stable hydrogel with enhanced mechanical properties. Thus the implanted ADSCs can survive, proliferate in the hydrogel, and secrete growth factors and cytokines which would affect the wound healing process.....54
- Figure 1.3: Project overview.....55

Chapter 2

- Scheme 2.1: Synthesis of hyperbranched polymers via an *in-situ* DE-ATRP copolymerization of poly(ethylene glycol) methyl ether methacrylate (PEGMEMA), 2-(2-methoxyethoxy) ethyl methacrylate (MEO₂MA) and ethylene glycol dimethacrylate (EGDMA). Ethyl 2-bromoisobutyrate and N,N,N',N'',N''-Pentamethyldiethylenetriamine (PMDTA) was used as the initiator and ligand. The dimethacrylate monomer of EGDMA provided the copolymer hyperbranched structure and the vinyl functionality.....94
- Scheme 2.2: Mechanism of *in-situ* deactivation enhanced atom transfer radical polymerization (DE-ATRP). (a) *In-situ* producing Cu^I species from Cu^{II} species by reducing agent L-ascorbic acid (AA); (b) A small amount of AA addition ensures the excessive Cu^{II} species in the reaction system which leads to enhanced deactivation reaction, suppression of the growth rate and delayed gelation.....98
- Figure 2.1: GPC traces from RI detector for the samples of entry 2 in Table 2.1. Note: the peak became broader and moving forward indicated that the

increased molecular weights and polydispersities with monomer conversion were observed.....	102
Figure 2.2: Kinetic plots of the <i>in-situ</i> DE-ATRP polymerization of PEGMEMA-MEO ₂ MA-EGDMA copolymers by using 15 mol %, 30 mol % and 50 mol % of reducing agent of L-ascorbic acid (AA).) Increase of the monomer conversion along with the reaction progress. Note: the polymerization speed can be sensitively affected by varying the amount of the reducing agent AA. For example, the same level of monomer conversion (i.e. 45 %) needed 9 h of reaction time by using 15 mol % AA, 6 h with 30 mol % AA and only 1 h with 50 mol %.....	103
Figure 2.3: Kinetic plots of the <i>in-situ</i> DE-ATRP polymerization of PEGMEMA-MEO ₂ MA-EGDMA copolymers by using 15 mol %, 30 mol % and 50 mol % of reducing agent L-ascorbic acid (AA). Increase of the polydispersity Index (PDI, Mw/Mn) along with the monomer conversion.	104
Figure 2.4: ¹ H NMR for the PEGMEMA-MEO ₂ MA-EGDMA copolymer (entry 1 in Table 2.1) in CDCl ₃ . Note: the spectrum shows the double bonds within the structure at the chemical shifts of 6.1 and 5.6 ppm (Insert).....	105
Figure 2.5: FTIR analysis of freeze-dried polymer of PEGMEMA-MEO ₂ MA-EGDMA (entry 1 in Table 2.1). The main chemical groups were characterized by a standard and labeled. Note: the spectrum shows the double bond within the polymer structure at the wavenumber around 1650 cm ⁻¹	108
Figure 2.6: Thermoresponsive properties of PEGMEMA-MEO ₂ MA-EGDMA copolymers (S4, S5 and S6 in Table 2.2). LCST behavior of the copolymer in 0.03 % w/v deionized water determined by UV-vis spectrophotometer. Insert: copolymer solution (S5 in Table 2.2, 40 % w/v) became physical cross-linked gel when the temperature was raised above its LCST from 20 °C to 37 °C.....	109
Figure 2.7: Size distribution measured by dynamic light scattering. Polymer solutions (S5 in Table 2.2, 0.01% w/v) were prepared in deionized water and filtered prior to measurements using a 0.45 μm disposable	

filter. Light incident angle was 90°. Note: at 37 °C, polymer particles aggregated together to form the microgel structure.....	110
Figure 2.8: SEM images of freeze-dried photo-crosslinked gels prepared from 20 % (a) and 40 % (b) (w/v) PEGMEMA-MEO ₂ MA-EGDMA copolymer (S5 in Table 2.2) solution. Note: the photo-crosslinked gel formed using a low polymer concentration sample demonstrated more porous and looser structure (a) than the gel formed using a high polymer concentration (b).....	112
Figure 2.9: Cellular metabolism viability assessment of 3T3 cells after one and four days treatment with PEGMEMA-MEO ₂ MA-EGDMA polymer (S5 in Table 2.2) using alamarBlue [®] assay. Cells alone as the control; the polymer concentrations were at 0.5 and 1 mg/ml. Note: there is no significant difference of cells viability between the control (cells alone) and polymer samples after four days (mean ± SD, n = 3, p < 0.005).....	113

Chapter 3

Scheme 3.1: Synthesis of thermoresponsive hyperbranched PEGMEMA-MEO ₂ MA-PEGDA copolymer via an <i>in-situ</i> DE-ATRP approach. The copolymer can physically cross-link at body temperature and can be cross-linked with thiol cross-linker of pentaerythritol tetrakis (3-mercaptopropionate (QT) via thiol-ene Michael-type addition. Meanwhile, by mixing with hyaluronic acid (HA) macromolecule, a semi-IPN hydrogel system was formed.....	123
Figure 3.1: GPC traces from RI detector for the samples of entry 1-5 in Table 3.1. Note: the peak became broader and moving forward indicated that the increased molecular weights and polydispersities with monomer conversion were observed.....	131
Figure 3.2: ¹ H NMR for the PEGMEMA-MEO ₂ MA-PEGDA copolymer (entry 6 in Table 3.1) in CDCl ₃ . Note: the spectrum shows clearly the double bonds within the structure at the chemical shifts between 6.4 and 5.8 ppm (Insert).....	132
Figure 3.3: Physical and chemical cross-linking properties of PEGMEMA-MEO ₂ MA-PEGDA copolymer (entry 6 in Table 3.1). (a) Chemical	

gelation of copolymer (10 wt %) with QT (equal molar ratio of thiol and vinyl group). (b) LCST behaviour of the copolymer which was dissolved in deionized water at the concentration of 0.03 % (w/v), determined by UV-vis spectrophotometer. Insert: Polymer solution (30 wt %) became physical cross-linked gel when the temperature was raised above its LCST from 20 °C to 37 °C.....137

Figure 3.4: SEM images for the freeze-dried gels samples prepared from PEGMEMA-MEO₂MA-PEGDA copolymers (20 wt %) cross-linked with QT with different concentrations of HA from 0 mg/ml (non-IPN gel) to 20 mg/ml. Note: the higher HA concentration leads to looser hydrogel microenvironment with more space and porous structure138

Figure 3.5: HA release study. Cumulative release of HA from semi-IPN hydrogels at 37 °C determined by carbazole assay. The absorbance of the samples at 550 nm was determined by a Varioskan Flash Reader. (Mean ± SD, n = 3). Note: after 12 h the HA release had leveled off indicating most of HA molecules (70 - 80 %) were kept in the hydrogels after gelation to form a semi-IPN structure.....139

Figure 3.6: Swelling of chemically cross-linked (P) and IPN (P/HA) gels in PBS (1 M, pH 7.4) at 20 °C and 37 °C within first 24 h (a) and total 19 days (b) (Mean ± SD, n = 3). Note: the lower cross-linking density (10 wt %) or at lower temperature (20 °C) demonstrated a higher swelling ratio than the higher cross-linking density (20 wt %) or at 37 °C. The IPN structure significantly enhanced the swelling capability of the gels.....140

Figure 3.7: Cellular metabolism viability assessment of 3T3 cells after 48 h treatment with PEGMEMA-MEO₂MA-PEGDA (entry 6 in Table 3.1) and Pentaerythritol tetrakis (3-mercaptopropionate) (QT) using alamarBlue[®] assay. Note: there was no significant difference between copolymer and QT treatment with control of cell alone (n = 3, *p* < 0.05).....143

Figure 3.8: LIVE/DEAD[®] viability assay for 2D and 3D cell culture. The hydrogels were formed from 10 % w/v polymer solution in PBS and the QT was added with equal molar ratio of thiol and vinyl group. (a and b) ADSCs seeded on the surface of gels. (c and d) Cells were

encapsulated into gelling system. (a and c) Non-IPN gels without HA. (b and d) Semi-IPN gels with HA (16 mg/ml). The hydrogels fluorescently labeled with a dye that green fluoresces upon the presence of intracellular esterase activity in living cells (calcein-AM) and a dye that red fluoresces (ethidium homodimer-1) when bound to the DNA of dead cells with compromised membranes. The samples were directly visualized on an Olympus 1X81 inverted microscope. Note: cell adhesion and cell viability were significantly improved in semi-IPN hydrogels both in 2D and 3D models.....144

Figure 3.9: LIVE/DEAD[®] viability assay for 3D culture of ADSCs with different gelling condition after 3 and 6 days. Green fluoresces (calcein-AM) labeled living cells and red fluoresces (ethidium homodimer-1) labeled dead cells. The samples were directly visualized on an Olympus 1X81 inverted microscope. Scale bars in all cases represent 100 μm . Note: it seemed that the ratio of 10 % polymer with 1 % HA showed higher cell survival ratio after 6 days, which is confirmed by quantified analysis as shown.....145

Figure 3.10: Quantification analysis of LIVE/DEAD[®] viability assay for 3D culture with different gelling condition after 3 and 6 days. Percentage of live cells to total cell number calculated from LIVE/DEAD[®] staining micrographs (Mean \pm SD, n = 3). Note: a significant drop on percentage cell viability was found in “10 % P - 2 % HA” group after 6 days (n = 3, $p < 0.05$).....146

Chapter 4

Scheme 4.1: Synthetic route and chemical structures of PEGMEMA-MEO₂MA-PEGDA and HA-SH hydrogel. (i) modification of HA with cysteamine (EDAC-NHS) carbodiimide coupling; (ii) ‘One-pot and One-step’ *in-situ* DE-ATRP in butanone at 50 °C; (iii) hydrogel from *in-situ* cross-linking of components via thiol-ene Michael-type addition reaction at pH 7.4.....156

Figure 4.1: (a) LCST of the PEGMEMA-MEO₂MA-PEGDA copolymer determined by UV-vis spectrophotometer. (b) A temperature ramp rheological measurement for the copolymer (30 wt%). Note: the LCST of the copolymer was around 27 °C; and the rheological

modulus were dramatic increased due to the aggregation of polymer particles above LCST.....	168
Figure 4.2: ¹ H NMR (300Hz) spectrum of HA and thiolated HA (HA-SH) in DO ₂ . Note: the protons from 2.6 (1) to 2.4 (2) ppm confirm the conjugation of thiol groups.....	169
Figure 4.3: Content of free thiol groups on HA and thiolated HA (HA-SH), determined by Ellman's assay. Note: the content of free thiol group on the modified HA showed significant higher than control group of normal HA.....	170
Figure 4.4: Chemical gelation via Michael-type addition between PEGMEMA-MEO ₂ MA-PEGDA copolymer and thiolated HA (HA-SH) at room temperature. The molar ratio between thiol groups on the HA-SH and the vinyl groups on the copolymer were (a) 1:0 (without polymer), (b) 1:1, and (c) 1:2, which were calculated based on ¹ H NMR and Ellman's analysis. Note: HA-SH solution without polymer stay as liquide form, while in the other two groups, stable hydrogels were formed.....	171
Figure 4.5: Compression tests on chemical cross-linked hydrogels fabricated from PEGMEMA-MEO ₂ MA-PEGDA with thiolated HA. (a) Storage Modulus of hydrogels prepared at different polymer concentration (n = 3, Mean ± SD). (b) A hydrogel sample (diameter 12.5 mm, thickness 2.5 mm) was under a compression test using DMA. Note: the hydrogel prepared from higher polymer concentration exhibited the strengthened mechanical properties.....	172
Figure 4.6: SEM images of the cross-linked hydrogel using (a) 10 wt% and (b) 15 wt% PEGMEMA-MEO ₂ MA-PEGDA polymer and fixed concentration of HA-SH. Note: slight larger pore formed with lower polymer concentration.....	173
Figure 4.7: Swelling ratio of hydrogel with 10 wt% and 15 wt% PEGMEMA-MEO ₂ MA-PEGDA copolymer and HA-SH at 37 °C.....	174
Figure 4.8: Cell viability of ADSCs encapsulated in P-SH-HA hydrogels at 3, 7, 14 and 21 days. (a) Representative fluorescent images of encapsulated ADSCs stained with calcein AM (green) for live cells and ethidium homodimer-1 (red) for dead cells by LIVE/DEAD®	

stain kit. (b) Hydrogel prepared on Teflon tape (molar ratio of thiol:vinyl as 1:1).....	176
Figure 4.9: Cell viability of ADSCs encapsulated in P-SH-HA hydrogels at 3, 7, 14 and 21 days. Percentage of live cells to total cell number calculated from LIVE/DEAD® staining micrographs (Mean ± SD, n = 3). Note: there is no significant difference of cell viability from every time point ($p < 0.05$).....	177
Figure 4.10: Cellular proliferation assessment by PicoGreen® assay. Note: total DNA content in the hydrogel is significant increased from 7 days (n = 3, $p < 0.05$) and maintain at the same level after that, which means the proliferation of the cells were restricted after 7 days.....	178
Figure 4.11: Cell metabolic activity assessment by alamarBlue® assay. Percentage of deduced alamarBlue® was calculated by the absorbance at 550 and 595 nm. Note: total cellular metabolic activity were significantly reduced after 14 days (n = 3, $p < 0.05$).....	179
Figure 4.12: Secretion profile of cytokines of hADSCs in both P-SH-HA hydrogel (3D) and tissue culture plastic (2D) over 7 days. Cells were seeded at 0.5×10^6 cells/ml in both 3D and 2D culture conditions in 48-well plates. Supernatant from both conditions was analysed using multiplex ELISA kit for IL-2, IL-10 and INF- γ . (n = 3, $p < 0.05$). Note: inflammatory cytokines of IL-2 and INF- γ reduced after 7 days in 3D hydrogel microenvironment, while remained at the same level for 2D seeded cells (a-b); anti-inflammatory cytokine of IL-10 in hydrogel seemed higher level than 2D control (c).....	181
Figure 4.13: Secretion profile of growth factors of hADSCs in both P-SH-HA hydrogel (3D) and tissue culture plastic (2D) over 7 days. Cells were seeded at 0.5×10^6 cells/ml in both 3D and 2D culture conditions in 48-well plates. Supernatant from both conditions was analysed using multi-plex ELISA kit for PlGF, VEGF and TGF- β . (n = 3, $p < 0.05$). Note: the angiogenic growth factors of PlGF, VEGF significantly increased in hydrogel system over time (a-b); TGF- β was also showed increased production over time in both 2D and 3D conditions, but there was no significant difference in concentration levels at any time for 3D culture (c).....	182

Chapter 5

- Figure 5.1: The identified parameters for measurement of wound contraction and epithelialization on H&E staining slides. E: epidermal; D: dermal; E1/E2: regenerated epidermal; G: granulation tissue. Note: wounds are contracted along with healing process.....195
- Figure 5.2: Representative photographs of wounds at 3, 7 and 14 days. NA: no treatment group; C: ADSCs cell alone group; H: hydrogel alone group; H+C: hydrogel + ADSCs group. Note: obvious wound contraction occurred in no treatment and cell alone control groups at 7 and 14 days.....197
- Figure 5.3: Percentage of wound area at 3, 7 and 14 days comparing to original wound area measured by ImagePro® Plus, (Media Cybernetics, USA). (*) labels the significant differences between each time point and groups (Two way ANOVA with Tukey's post analysis method, Mean \pm SD, n = 7, $p < 0.05$). Note: wound areas of hydrogel treatment groups (with or without cells) were significantly larger than no treatment and cell alone control groups at 14 days due to the skin contraction.....198
- Figure 5.4: Percentage of wound contraction. Note: no significant difference between each treatment group at each time point (Two way ANOVA with Tukey's post analysis method, Mean \pm SD, n = 7, $p < 0.05$), but a trend can be found that hydrogel treatment groups (with or without rADSCs) contracted less than other groups at 7 and 14 days.....201
- Figure 5.5: *In vitro* 2D cell attachment assessment. Fibroblast (3T3), normal human keratinocytes (NHK) and ADSCs were seeded on the cell culture plate (Cont.) and on the surface of the P-SH-HA hydrogels (Gel) and detected by LIVE/DEAD® stain after 48 h. Scale bars in all cases represent 100 μ m. Note: neither of these cells can attach on the hydrogel surface compared with the cells seeded on tissue culture plates.....202
- Figure 5.6: Percentage of wound epithelialization. Note: no significant difference between each treatment group at each time point (Two way ANOVA with Tukey's post analysis method, Mean \pm SD, n = 7, $p < 0.05$).....203

Figure 5.7: Representative fluorescent images of rADSCs embedded hydrogels at 3, 7 and 14 days. Implanted cells were marked with CellTracker™ CM-Dil (red) counterstained with Hoechst 33258 (blue). The yellow dotted line labeled the hydrogel area above wound bed.....204

Figure 5.8: The stereological quantification of the volume fraction of implanted rADSCs based on the fluorescent images labelled by CellTracker™ CM-Dil/Hoechst 33258. Note: no significant difference between each time point (Student's t-test, Mean ±SD, n = 7, $p < 0.05$).....205

Figure 5.9: Representative fluorescent images of CD68⁺ immunohistochemistry stained macrophages (green) counterstained with Hoechst 33258 (blue) for different treatment groups at 3, 7 and 14 days. Scale bars in all cases represent 50 μm.....206

Figure 5.10: Quantification of volume fraction of macrophages at 3, 7 and 14 days based on the immunohistochemistry images (CD68⁺/Hoechst 33258). Note: no significant difference between each treatment group at each time point (Two way ANOVA with Tukey's post analysis method, Mean ±SD, n = 7, $p < 0.05$).207

Figure 5.11: Representative images (x 600 magnification) of H&E stained tissue slides at 3, 7 and 14 days. W: skin tissue at wound area; H: hydrogel. The arrows highlight the neutrophils cells. Scale bars in all cases represent 10 μm. Note: the neutrophils surrounding the hydrogels was obviously more than control groups at day 3, but clearly decreased at day 7, which indicated that the hydrogel triggered higher acute inflammatory response than control groups at the early stage of wound healing.....208

Figure 5.12: Volume fraction of total inflammatory cells at days 3, 7 and 14. Counted inflammatory cells included neutrophils, eosinophils, lymphocytes and macrophages. Note: because of the increased neutrophils, total inflammatory cells in Hydrogel with/without cells groups are significantly higher than control groups at day 3 and day 7 (Two way ANOVA with Tukey's post analysis method, Mean ±SD, n = 7, $p < 0.05$).....209

Figure 5.13: Representative fluorescent images of Collagen type IV immunohistochemical staining (green) counterstained with Hoechst 33258 (blue) for different treatment groups at each time point. Note:

the angiogenesis with hydrogel treatment groups (with or without cells) were obvious increased at 14 days compared with control groups.....211

Figure 5.14: Vascular surface density at 3, 7 and 14 days. Note: Hydrogel + rADSCs group shows significant higher than control groups (One way ANOVA with Tukey’s post analysis method, Mean \pm SD, n = 7, $p < 0.05$).212

Figure 5.15: Vascular length density at 3, 7 and 14 days. Note: Hydrogel + rADSCs group shows significant higher than control groups (One way ANOVA with Tukey’s post analysis method, Mean \pm SD, n = 7, $p < 0.05$).213

Figure 5.16: Total vascular surface area at 3, 7 and 14 days. Note: no significant difference between each treatment group at each time point (One way ANOVA with Tukey’s post analysis method, Mean \pm SD, n = 7, $p < 0.05$).214

Figure 5.17: Total vascular length at at 3, 7 and 14 days. Note: no significant difference between each treatment group at each time point (One way ANOVA with Tukey’s post analysis method, Mean \pm SD, n = 7, $p < 0.05$).215

Chapter 6

Figure 6.1: Summary of the main outcomes from each phase of this thesis.....225

Figure 6.2: Future direction of bioactive modifications on the PEG-based hyperbranched multifunctional polymer which can be performed for specific wound healing applications.....237

List of Tables

Chapter 1

Table 1.1: Summary of basic wound dressings.....	18
Table 1.2: Commercially available autologous skin grafts for clinical use.....	22
Table 1.3: Commercially available allogeneic skin grafts for clinical use.....	23
Table 1.4: Commercially available acellular skin substitutes for clinical use	26
Table 1.5: Commercially available cellular skin substitutes for clinical use.....	31
Table 1.6: Main growth factors and cytokines in wound healing.....	35
Table 1.7: Injectable hydrogels for tissue engineering.....	43

Chapter 2

Table 2.1: Copolymerization of poly(ethylene glycol) methyl ether methacrylate (PEGMEMA, $M_n = 475$), 2-(2-methoxyethoxy) ethyl methacrylate (MEO ₂ MA) and ethylene glycol dimethacrylate (EGDMA) via <i>in-situ</i> DE-ATRP.....	101
Table 2.2: Properties of PEGMEMA-MEO ₂ MA-EGDMA copolymers.....	107

Chapter 3

Table 3.1: Copolymerizations of PEGMEMA-MEO ₂ MA-PEGDA via <i>in-situ</i> DE-ATRP.....	133
Table 3.2: Properties of PEGMEMA- MEO ₂ MA-PEGDA copolymers.....	134

Chapter 4

Table 4.1: Copolymerization of PEGMEMA-MEO ₂ MA-PEGDA via <i>in-situ</i> DE-ATRP.....	166
--	-----

Chapter 5

Table 5.1: Treatment groups design for <i>in vivo</i> study.....	194
--	-----

List of Abbreviations

¹ H NMR	Proton Nuclear Magnetic Resonance
2D	Two-Dimensional
3D	Three-Dimensional
AA	L-ascorbic Acid
ADSCs	Adipose-Derived Stem Cells
ADSC-CM	Adipose-Derived Stem Cell Conditioned Medium
AGET-ATRP	Activator Generated by Electron Transfer ATRP
ATRP	Atom Transfer Radical Polymerization
BMSCs	Bone Marrow Derived Stem Cells
CCL-2	Chemokine Ligand-2
CSF-1	Colony-Stimulating Factor 1
Cx43	Connexin 43
CXCL-x	Cysteine-X Amino Acid-Cysteine Ligand-x
CXCR	Cysteine-X Amino Acid-Cysteine Ligand Receptor
Cyr61	Cysteine-Rich Angiogenic Inducer-61
DE-ATRP	Deactivation Enhanced ATRP
DLS	Dynamic Light Scattering
DMAEMA	2-(dimethylamino)ethyl Methacrylate
DMEM	Dulbecco's Modified Eagle's Medium
DMF	Dimethylformamide
DVB	Divinyl Benzene
ECM	Extracellular Matrix
EDAC	N-(3-Dimethylaminopropyl)-N'-Ethylcarbodiimide
EGDMA	Ethylene Glycol Dimethacrylate
EGF	Epidermal Growth Factor
FGF	Fibroblast Growth Factor
FTIR	Fourier Transform Infrared Spectroscopy
GP	Glycerophosphate
GPC	Gel Permeation Chromatography
HA	Hyaluronic Acid
HA-SH	Thiolated HA
HB-EGF	Heparin Binding EGF
HDF	Human Dermal Fibroblasts
HGF	Hepatocyte Growth Factor
HSCs	Hematopoietic Stem Cells
ICAM-1	Intercellular Adhesion Molecule-1
IGF-I	Insulin-like Growth Factor I
IL-x	Interleukin-x
INF- γ	Interferon- γ
IPN	Interpenetrated Polymer Network
iPS	Induced Pluripotent Stem cells
ISCT	International Society for Cellular Therapy

KGF	Keratinocyte Growth Factor
LCST	Lower Critical Solution Temperature
MCP-1	Monocyte Chemoattractant Protein 1
MEO ₂ MA	2-(2-methoxyethoxy) ethyl methacrylate
MMPs	Matrix Metalloproteinases
MSCs	Mesenchymal Stem Cells
M _n	Number Average Molecular Weight
M _w	Weight Average Molecular Weight
NETs	Neutrophil Extracellular Traps
NHS	National Health Service (Chapter 1) N-Hydroxysuccinimide (Chapter 4)
NIPAAm	N-isopropylacrylamide
Nrf2	NF-E2-Related Factor 2
OEGMA	Oligo(ethylene glycol) Methacrylate
OPF	Oligo(poly(ethylene glycol) fumarate)
PBS	Phosphate Buffered Saline
PCL	Poly(caprolactone)
PDGF	Platelet-Derived Growth Factors
PDI	Polydispersity Index
PEG	Poly(ethylene glycol)
PEGDA	Poly(ethylene glycol) Diacrylate
PEGMEMA	Poly(ethylene glycol) Methyl Ether Methacrylate
PEO	Poly(ethylene oxide)
PLA	Poly(L-lactic acid)
PLGA	Poly(DL-lactic-co-glycolic acid)
PIGF	Placental Growth Factor
PMDTA	N,N,N',N'',N'''-pentamethyldiethylenetriamine
PMMA	Poly(methyl methacrylate)
PNIPAAm	Poly(N-isopropylacrylamide)
PPF	Poly(propylene fumarate)
PPO	Poly(propylene oxide)
PVA	Poly(vinyl alcohol)
QT	Pentaerythritol Tetrakis (3-mercaptopropionate)
ROS	Reactive Oxygen Species
SEM	Scanning Electron Microscopy
Shh	Sonic Hedgehog Protein
SSGs	Split Skin Grafts
SVF	Stromal Vascular Fraction
TIMPs	Tissue Inhibitor of Matrix Metalloproteinases
TGF- α/β	Transforming Growth Factor α/β
TNF- α	Tumor Necrosis Factor α
UCST	Upper Critical Solution Temperature
UV	Ultraviolet
VCAM-1	Vascular Cell Adhesion Molecule-1
VEGF	Vascular Endothelial Growth Factor

Acknowledgements

I would like to sincerely thank Dr. Wenxin Wang for his valuable guidance and immense support throughout this project. Not only has he helped me to develop my research skills, but also encouraged my growth and independence as a scientist. I would like to thank Prof. Abhay Pandit and Dr. Yolanda Garcia for their support and supervision throughout the project. My gratitude is also extended to Dr. Hongyun Tai in Bangor University, UK for her exceptional help, support and encouragement over these four years. I would also like to thank National University of Ireland, Galway, Science Foundation Ireland, DEBRA Ireland and DEBRA Austria for providing the funds for this project.

I would like to thank both former and current members of the Network of Excellence for Functional Biomaterials. Special thanks are due to Dr. Hongliang Cao and Mr. Waqar UI Hassan who worked closely with me, not only as colleagues but also as friends. I would also like to specifically thank Prof. Xuejun Hu and Dr. Estelle Collin for helping me to develop my research skills in many areas; Dr. Udo Greiser for lots of helping on my thesis and manuscripts preparations; Dr. Oliver Carroll for his assistance in laboratory managements; Mr. Anthony Sloan for his language editing; Mrs. Tara Cosgrave and Mr. Vidoja Kovacevic for their assistance in administrations. My gratitude is also extended to Dr. Micheal Monaghan, Dr. Benjamin Newland, Dr. Carolyn Holladay, Mr. Mohammad Abu-Rub, Mrs. Asha Mathew, Dr. Aram O. Saeed, Mrs. Ciarstan McArdle, Mr. Tianyu Zhao, Mrs. Hong Zhang, Mr. Ahmed Aied, Mr. Bill Daly, Mr. Biraja Dash and Mr. Robert Kennedy for their helping and collaboration in the development of the project.

I deeply appreciate the wonderful support and assistance from the excellent researchers and technical staff in the National Centre for Biomedical Engineering Science and Regenerative Medicine Institute, and Anatomy laboratory. My special thanks to Mr. Charles McHale, Mr. Gerry Mchale, Dr. Cathal O'Flatharta and Dr. Xizhe Chen for their help in animal facility; Prof. Sanbing Shen, Dr. Siobhán Gaughan and Miss Min Liu for assistance with tissue processing; Mr. Mark Canney and Dr. Kerry Thompson for

assistance with staining and imaging analysis; Mrs Eadaoin Timmins for assistance with FTIR, SEM and TEM.

My final acknowledgements are to my parents and my family in China. Without their sacrifices, support and encouragement all the time, I would never go this far in my educational career to pursue my dream. Thank you so much!

Thank the time of the past four years for making me learn and grow up.

Abstract

Wound healing, especially chronic wound healing, has become a major clinical problem all over the world. Among all the treatments for wound healing, wound dressings are the main management approaches for both acute and chronic wounds. However, although significant progress has been made in the development of modern wound dressings over the past few years, there are still restrictions to stimulating the healing process. As an alternative to existing approaches, tissue engineering approaches with stem cell therapy have been widely studied for wound healing applications and showed promising therapeutic effects. Ideally, the next step is to develop a wound dressing with specific therapeutic functions such as delivering therapeutic agents (e.g. growth factors and/or stem cells) to promote the healing process. The overall goal of this doctoral project was to develop an injectable hydrogel cell delivery system which could easily encapsulate and support adipose-derived stem cells' (ADSCs) growth, proliferation and secretion, with the potential use as a temporary bioactive hydrogel dressing for wound healing applications. To this end, the multifunctional PEG-based hyperbranched copolymers with thermoresponsive behavior and *in-situ* photo-/chemical cross-linkable properties have been developed via an advanced one-step *in-situ* deactivation enhanced atom transfer radical polymerization (DE-ATRP) method. At room temperature, this copolymer was water-soluble while forming a gel rapidly at body temperature, so that the cells can be easily encapsulated and applied to any wound size, shape or cavity, which is less invasive than other approaches and minimizes patients' discomfort. In addition, a photo-/chemical gelation occurs within a short time to achieve a stable hydrogel with enhanced mechanical properties, supporting cell growth, proliferation and secretion. Furthermore, in combination with extracellular matrix (ECM) biopolymer of hyaluronic acid (HA), the microenvironment of the hydrogel system has been optimized during the project, so that the encapsulated ADSCs can maintain their viability and secretion level *in vitro*. Finally, the *in vivo* cell survival, material inflammatory response, and the wound healing effect of the optimized hydrogel system with rat ADSCs were evaluated using a rat

dorsal excisional wound model. It was found that this system prevented the wound contraction and significantly enhanced angiogenesis. This is the first study to describe an injectable stem cell bioactive hydrogel dressing for wound healing purpose; and with the advanced multifunctional polymer and injectable hydrogel template developed in this project, there is significant potential for further development of this technique to the next step towards the realization of clinical wound healing applications ultimately.

Chapter One

Introduction

1.1 Wound Healing

The skin is one of the most important protective barriers of the body against the environment and its functional disruption or injury may result in major disability or even death. According to the definition from the Wound Healing Society, wound healing is a “complex dynamic process” involving various mediators, different blood and parenchymal cells, and extracellular matrix (ECM) ¹. Based on the nature of the healing process, wounds can be classified into two categories as *acute wounds* and *chronic wounds* ². Acute wounds, which are usually caused by mechanical injuries and thermal or chemical burns, can generally completely heal with minimal scarring within days to 12 weeks ^{2,3}. In contrast, chronic wounds fail to heal over months, even years, due to repeated tissue insults or specific physiological conditions such as diabetes, obstinate infections and poor management of the wounds ^{4,5}.

1.1.1 Acute Wound Healing

Depending on the biologic and physiologic mechanisms, the acute (normal) wound healing process can be divided into three overlapping phases (**Figure 1.1**): (i) hemostasis and inflammation; (ii) proliferation and repair (neoangiogenesis, proliferation and re-epithelialization); and (iii) tissue remodeling ^{6, 7}. More importantly, these overlapping steps are precisely regulated by local and system mediators such as cytokines, chemokines and growth factors ⁸⁻¹⁰.

1.1.1.1 Hemostasis and Inflammation

Bleeding usually occurs immediately after skin injury, which does not only serve to flush out the bacteria and foreign antigens but also to activate hemostasis. After injury, platelet aggregation initiates the clotting cascade forming a fibrin clot and triggers platelet-mediated vasoconstriction ¹¹. The clot serves as a temporary shield protecting the uncovered wound tissue and the vasoconstriction can prevent further blood loss. In addition, the fibronectin and fibrin composition in the clot supports and guides the fibroblast and keratinocytes as a provisional matrix or scaffold. The platelet activation also results in the release of mediators such as platelet-derived

Introduction

growth factors (PDGF), which induces a series of immune defenses and tissue repair process including the migration of fibroblasts and keratinocytes, the recruitment of inflammatory cells, the production of collagen, glycosaminoglycan or other ECM proteins, and the synthesis of collagenases which are response to reshape the regenerated tissue^{12,13}.

The damage of blood vessels and vasoconstriction also result in a hypoxic microenvironment, which induces the release of anti-microbial substances such as reactive oxygen species (ROS)¹⁴⁻¹⁶, oxidants, cationic peptides, proteases¹⁷ and stimulate the formation of neutrophil extracellular traps (NETs) which can degrade virulence factors and bacteria¹⁸. These anti-microbial substances can kill the microorganisms in the early wound stage, while too many of them may cause further tissue damage and delayed healing process. Moreover, the imbalance of oxidants and antioxidants may cause the prolonged inflammatory phase in chronic wounds^{16,19}. Therefore the balance of ROS production and detoxification by ROS-detoxifying enzymes, antioxidants and hemeoxygenases plays a crucial role in wound healing process¹⁹. A number of studies have aimed at identifying some potential clinical targets based on this mechanism. For example, the intracellular enzyme peroxiredoxin-6 that is expressed in epithelial cells was found to protect cells from the ROS-induced damage^{20,21}. The gene transcription approaches for encoding growth factors, cytokines and chemokines have also been used to control the oxidative stress. A good example for such targets is the transcription factor NF-E2-related factor 2 (Nrf2) which regulates the production of antioxidant molecules in keratinocytes²². Keratinocyte growth factor (KGF) or so called fibroblast growth factor-7 (FGF-7) can increase the expression of Nrf2 and peroxiredoxin-6, therefore indirectly protecting keratinocytes from ROS-induced damage^{23,24}.

The inflammation begins nearly simultaneous with hemostasis and is usually complete within 24 h to 3 days, while sometimes it may last for one week after injury⁷. Within a few minutes after injury, neutrophils are recruited from the circulating blood around the wound site to clean the rush of contaminating bacteria²⁵. In addition, the pro-inflammatory cytokines

Introduction

produced by neutrophils can activate local fibroblasts and keratinocytes at the early wound stage ²⁶. The infiltration of neutrophils ceases once the infection is controlled (normally after a few days) and then are cleared by macrophages phagocytosis ⁷. Monocytes are also recruited to the wound site at this stage, in response to various mediators such as monocyte chemoattractant protein 1 (MCP-1), transforming growth factor β (TGF- β) and fragments of ECM proteins, and then they differentiate into activated macrophages ¹¹. Adherence to the ECM may induce monocytes and macrophages to express important cytokines for inflammation and tissue repair process such as colony-stimulating factor 1 (CSF-1), tumor necrosis factor α (TNF- α), PDGF, transforming growth factor α (TGF- α), TGF- β , interleukin-1 (IL-1), insulin-like growth factor I (IGF-I) ²⁷⁻²⁹. In addition, macrophages can also synthesize nitric oxide (NO) which has been proved to have an important beneficial role in wound healing ^{30,31}. As a “transition cell” between inflammation and wound repair, macrophages not only phagocytose cell debris and clean the wound site, but also regulate the migration and proliferation of epidermal cells, organization of new tissue connection, and angiogenesis ^{29,32}.

Another important cell type acting at the inflammatory phase is leukocytes, which are induced by endothelial and intercellular adhesion factors. For example, the immunoglobulin superfamily members intercellular adhesion molecule-1 (ICAM-1) and vascular cell adhesion molecule-1 (VCAM-1) which are up-regulated by vascular endothelial growth factor (VEGF) and IL-1, may benefit the recruitment of leukocytes and macrophages during the inflammatory phase ³³⁻³⁶. In addition, the effect of the intercellular communication channels (gap junctions) can also promote or delay the wound repair process. It has shown that down-regulation of connexin 43 (Cx43), one of the important gap junction proteins, reduced the chemokine ligand-2 (CCL-2) and TNF- α level, leading to decreased inflammatory response and improved healing ³⁷. As another potential treatment target, chemokines such as cysteine-X amino acid-cysteine ligand 1 (CXCL1) and its receptor (CXCR1) also regulate the recruitment and infiltration of leukocytes and macrophages ³⁸.

Furthermore, vasoactive substances such as serotonin, prostaglandins, histamine and bradykinin also play significant roles in the inflammatory stage of wound healing process²⁹. These factors increase the permeability of endothelium which leads to enhanced infiltration of immune and repair cells. As a result, the fluid starts to leak and the temperature increases at the wound site, leading to a warm and moist microenvironment for healing process⁷. At the end of the inflammation phase, bleeding is controlled and the wound bed is clean, which is suitable for the next phase of proliferation and repair.

1.1.1.2 Proliferation and Repair

The proliferation and repair - the second phase of the healing process - usually occurs within 1-3 weeks after wound injury and includes three major events: re-epithelialization, neovascularization and granulation⁷. Fibroblast and keratinocytes are the key cell types during this stage.

1.1.1.2.1 Re-epithelialization

Re-epithelialization occurs within hours after injury when the epidermal cells from skin appendages (e.g. hair follicles) clear the damaged stroma and blood clots from the wound site. Meanwhile, keratinocytes undergo marked changes in their phenotype: the retraction and dissolution of the intracellular tonofilaments and desmosomes³⁹; and formation of peripheral cytoplasmic actin filaments to support cell movement⁴⁰. The tight adherence of epidermal and dermal cells is broken via dissolution of hemidesmosomal links between the epidermis and the basement membrane. Consequently, these cells interact with several ECM proteins such as fibronectin, vitronectin, and collagen type I⁴¹, and separate eschar tissue from the wound space.

24-48 h after wound injury, epidermal cells start to proliferate following the active migrating cells from the edge towards the center of the wound. The proliferation and migration of keratinocytes include a series of cell transformation and leapfrogging processes⁴², which are induced and regulated by a number of growth factors and cytokines such as FGF family (e.g. FGF-2/-7/-10)⁴³⁻⁴⁶, epidermal growth factor family (EGF, heparin

binding EGF)^{47, 48}, hepatocyte growth factor (HGF)^{49, 50}, IL-6^{51, 52} and TGF- α ⁵³. Furthermore, the role of TGF- β as an important growth factor functioning throughout the entire healing process has been controversially discussed in literature. On the one hand, it stimulated keratinocyte migration and promoted chronic wound healing⁵⁴. On the other hand, inhibited effect on keratinocyte migration and re-epithelialization has also been found after treatment with TGF- β ^{55, 56}. A recent report demonstrated that the association of TGF- β with integrins and ECM materials plays an essential role in the wound healing process⁵⁷.

In addition, some matrix metalloproteinases (MMPs), a family of zinc dependent endopeptidases which cleave specific ECM and basement member proteins^{58, 59}, also play essential roles to encourage cell proliferation and migration, such as MMP-1 (interstitial collagenase)⁶⁰, MMP-9 (gelatinase B)⁶¹ and MMP-10 (stromelysin-2)⁶². Once the migrating cells from opposing sides make contact with each other, a ceasing process is triggered that is known as the contact inhibition. Then, basement membrane reformed as a zipper-like sequence⁶³ and epidermal cells return to their normal phenotype⁶.

1.1.1.2.2 Angiogenesis

Angiogenesis, sometimes also referred as neovascularization, is a restoring process for the vascular network. It is essential for providing nutrients and oxygen during the healing process⁶⁴. As discussed in the former sections, increased endothelial permeability creates a required nutrient-rich microenvironment for wound repair before the new blood vessel system regenerates. Shortly after the injury, the partial pressure of oxygen at the wound site significantly decreases while the partial pressure of carbon dioxide (CO₂) increases to about 80 mm Hg, and the pH decreases to 6.8, leading to increased level of lactic acid. The lactic acid molecules can regulate the cell metabolism and transcription. For example, an increased lactic acid level promotes collagen production within the wound and enhances angiogenesis⁶⁴.

On the other hand, the hypoxic environment induces macrophages secreting growth factors to stimulate angiogenic factors such as VEGF⁶⁵⁻⁶⁸, TGF- β 1⁶⁹, basic FGF⁷⁰, and indirect angiogenic factors such as cysteine-rich angiogenic inducer-61 (Cyr61)⁷¹ and sonic hedgehog protein (Shh)⁷². In addition to these factors, endothelial receptors, ECM and provisional matrix are also important for angiogenesis, which affect the proliferation and migration of endothelial cells⁷³. At the late stage of the proliferation phase, angiogenesis ceases once the wound space is filled with new granulation tissue, and many of the blood vessels are cleared via apoptotic process⁷⁴.

1.1.1.2.3 Granulation

The last mechanism of the proliferation phase is called granulation and begins about four days after injury⁷. Here, new capillaries occur, macrophages, fibroblasts and blood vessels move into the wound space, leading to a development of new tissue rich in hyaluronic acid, fibronectin, collagen and other ECM materials. In this stage of the wound healing process, fibroblasts are the main contributors to the production of new ECM compounds. For instance, hyaluronic acid increases the tissue hydration; fibronectin promotes the cell adhesion and migration; proteoglycans (e.g. chondroitin sulfate) benefit the regulation of several growth factors and secreted proteins; and glycoproteins (e.g. collagen and elastin) provide the mechanical strength of new tissue matrix⁷. During this process, the proliferation and migration of fibroblasts are stimulated by mediators that include PDGF⁷⁵, TGF- β 1⁷⁶ and FGF⁷⁷. Finally, the provisional matrix is replaced by new extracellular matrix caused by the influx of fibroblasts^{78,79}. Once the collagen-rich ECM has formed, the fibroblasts cease to produce collagen and undergo apoptosis⁸⁰.

Another essential mechanism during the ECM regeneration is wound contraction. Usually during the second week of wound repair process, fibroblasts differentiate into an actin containing phenotype, named as myofibroblasts⁷. Utilizing their contractile properties, myofibroblasts pull wound edges together to result in the wound contraction, which increases the healing process at some level via reducing the wound gap; but too much contraction can cause deforming scars, painful contractures and mobility

dysfunction⁸¹. The modulation factors that are involved in this process include TGF- β 1/- β 2⁸², PDGF⁸³, integrin receptors for cell-ECM attachment⁸⁴ and enzymes for collagen remodeling⁸⁵. Furthermore, during the contraction process, collagen molecules accumulate, are remodeled and cross-link with each other. Approximately at three weeks after injury, the wound can achieve about 20 % of its final strength^{6,7}.

1.1.1.3 Remodeling

The final phase of wound healing in which regenerated granulation tissue reorganize into mature connective tissue, is called remodeling. It starts from about three weeks after injury and continues for months, even years to achieve the restoration of physiologic functions¹¹. As discussed earlier, collagen synthesis starts during the proliferation phase to build the granulation tissue, while at the same time, connective tissue is developed to reshape the collagen and ECM production is driven by macrophages and fibroblasts^{63,78}. Released collagen molecules first form a triple helix protein of procollagen that can form fibers with arranged order, and then cross-link to generate stable and stronger collagen strands⁸⁶. In this process, angiogenesis ceases, cell metabolism in ECM is reduced, hyaluronic acid and fibronectin are replaced by collagen fibers. Then composition of type III collagen decreases from 30 % to 10 %, which results in an increased tensile strength in tissue⁷. Meanwhile, the macrophages, keratinocytes, fibroblasts are removed by apoptosis⁷.

The remodeling process, a balance between the new collagen formation and old tissue degradation, is regulated by ECM-bound growth factors and MMPs⁸⁷. The activity of MMPs and their inhibitors (i.e. tissue inhibitor of matrix metalloproteinases, TIMPs) are stimulated by several cytokines, chemokines and growth factors. For example, TGF- β has been reported to up-regulate MMP-9 and down-regulate MMP-1, which sustains the balance between matrix synthesis and degradation, and promotes the remodeling process⁸⁸⁻⁹¹. Other examples include: IL-22 inducing MMP-3 expression; IL-1 results in MMP-1/-3/-9 and inhibits the TIMP-1^{92,93}. In addition, chemokines such as CXCL10 and CXCL11 have also been proved as essential factors regulating the tissue remodeling and dermal formation^{94,95}.

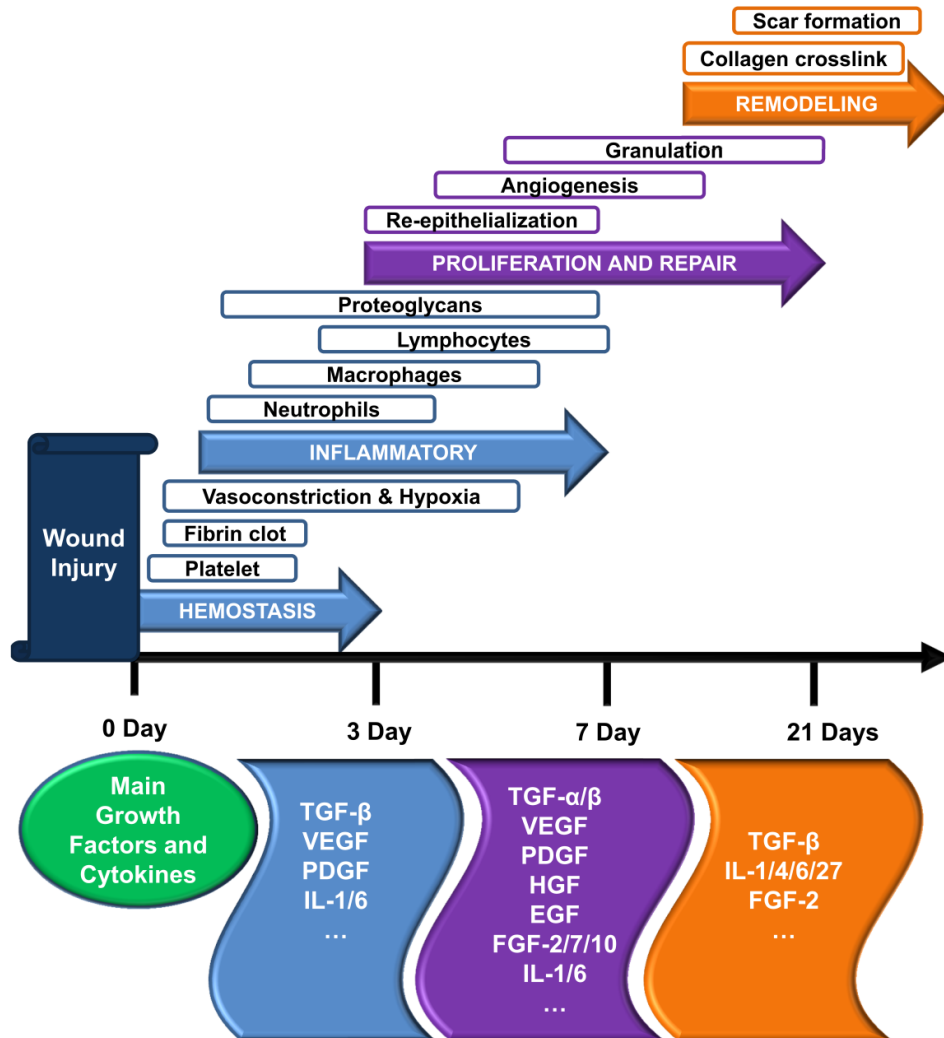


Figure 1.1: An overview of the stages of the normal (acute) wound healing process describing major biological processes, characteristic cell types and molecules as well as the main growth factors and cytokines involved in their regulation.

1.1.2 Chronic Wound Healing

As discussed above, it follows the rapid and acute wound healing process under normal physiologic conditions after injury. However, this process is impeded under certain pathological conditions, leading to a chronic wound with a long duration (over 6 months) or frequent recurrence^{6, 7, 96}. Many factors can impair the normal healing process including local factors (e.g. tissue maceration, infection, ischemia and induced foreign body response) systemic factors (e.g. advanced age, undernourishment and diabetes) and abnormal pathophysiological condition (e.g. genetic mutation in epidermis bullosa⁹⁷ and angiogenesis disorder in keloid scar⁹⁸). In addition, reduction of tissue growth factors⁹⁹, disturbance of proteolytic proteinases⁵⁹ and cell senescence¹⁰⁰⁻¹⁰² are also essential influences in chronic wound.

Chronic wound healing has become a major clinical problem all over the world. Not only the patients suffer from the physical and emotional stress over years or even during their whole lifetime, but also their families and the healthcare system has to bear the enormous financial burden. It is estimated that 1 to 1.5 % of the population in the industrialized countries will suffer from impaired wound healing during their lives¹⁰³. In the UK, there are approximate 200,000 patients with chronic wounds¹⁰⁴. The cost to the UK National Health Service (NHS) for these patients is estimated at £2.3 billion to £3.1 billion every year, which is almost 3 % of the total healthcare expenditure from 2005 to 2006¹⁰⁵.

1.1.2.1 Common Chronic Wounds

Chronic wound healing is a complex pathological phenomenon involving disruption of number of molecular pathways at all phases of the healing process. The most common chronic wounds include venous leg ulcers, pressure ulcers and diabetic foot ulcers^{96, 104, 106}.

1.1.2.1.1 Venous ulcers

Venous ulcers are a major cause of chronic wounds, influencing approximately 1-2 % of the adult population all over the world, and there is a high probability for this type of wound to persist for longer than five years¹⁰⁷⁻¹⁰⁹. In the UK, the annual cost to the NHS for treating and caring the

patients with venous ulcers ranges from £168 million to £198 million ¹⁰⁴. Furthermore the differences of age and gender seem to be related with the incidence of the venous ulcers: female and elder patients are more common than males and younger ¹⁰⁸. Venous ulcers often occur on the leg, caused by long-lasting venous hypertension which results from the venous thrombosis near the malfunctioned valves ^{110, 111}. Persistent venous hypertension will further lead to the swelling that causes the longstanding pain of the patients, and the restricted blood flow that causes the damage to the skin tissues ^{96, 110, 111}.

1.1.2.1.2 Pressure ulcers

Pressure ulcers, or bed sores, are caused by the sustained pressure, friction or shear-force which leads to the reduced blood supply and tissue damage ⁹⁶. The prevalence of the pressure ulcers in the US is around 10-17 % ¹¹² and 18.1 % in Europe ¹¹³. Probably more than 20,000 patients in hospitals have pressure ulcers in the UK at any time and the annual cost to NHS is ranging from £1.8 billion to £2.6 billion ¹⁰⁴. Healthy people normally do not develop the pressure ulcers as our body can prevent the sustain pressure automatically by routine movements. Thus, patients with pressure ulcers usually have other underlying health condition such as restricted mobility, malnutrition, disruption of blood supply (e.g. patients for type-2 diabetes), ageing skin; or extrinsic environmental risks ¹¹⁴. It usually begins with the skin erythema once the excessive pressure is placed on the particular part of the body, and then can develop to full-thickness wound with underlying tissue damage ^{115, 116}.

1.1.2.1.3 Diabetic foot ulcers

Diabetes mellitus is another major incentive for chronic wound, which can cause a poor blood supply and neuropathic disorder. It is estimated that 15% of the patients with diabetes could develop foot ulcers and 70 % of ulcers relapse within five years, ultimately leading to lower limb amputations ^{117, 118}. The prevalence statistics indicate that diabetes has become one of the major burdens for worldwide healthcare systems. In the US, approximate 18.8 million people have been diagnosed with diabetes with a further 7.0

million as yet undiagnosed, and the total of direct and indirect cost for these patients is estimated at \$174 billion in the US per year ¹¹⁹. In the UK, it is estimated there are about 64,000 patients with diabetic foot ulcers at any time and the annual cost to NHS is around £300 million ^{104, 120}. Moreover, it is forecast that the percentage of the patients and the related cost, will significantly increase in the near future mainly due to the aging of the population ^{104, 121}. With this trend, the total number of patients of diabetes was estimated to rise from 171 million in 2000 to 439 million by 2030 ^{122, 123}, and its global health expenditure is expected over \$ 500 billion by 2030 ¹²⁴.

1.1.2.2 Principles of Chronic Wound Care

1.1.2.2.1 Moisture and occlusion

For more than 2,000 years people believed that a dried wound bed is essential for preventing large scale infection and promoting the healing process ¹²⁵. Nowadays the moisture wound bed is widely accepted as the most ideal healing environment. Wound exudate not only supplies the nutrients on the wound bed, but also provides the favorable conditions for certain cell recruitment and migration ^{126, 127}. However, the overhydrated maceration surrounding the wound may impair the healing process by prolonged inflammation, reduced mobility and venous insufficiency ². In addition, the chronic wound fluid obstructs the proliferation and remodeling processes with excessive proteases and growth factors ¹²⁸⁻¹³⁰. Therefore, an ideal wound dressing should maintain the moisture environment while absorbing the extra exudate at the wound bed ².

1.1.2.2.2 Infection

Excessive bacterial accumulation at the wound space may cause the chronic inflammatory and delayed healing ¹³¹. Infected wounds usually present the signs including erythema, edema, exudate, pain or even fever. Some common pathogenic bacteria which can impair wound healing include *Staphylococcus aureus*, *Pseudomonas aeruginosa*, *Streptococcus pyogenes*, *Coliform*, *Clostridium*, *Proteus* and others ¹³²⁻¹³⁴. Antiseptics (e.g. hydrogen peroxide, iodine based preparation and silver releasing devices) and

antibiotics (e.g. mupirocin) are commonly used to reduce the wound infection in modern dressings¹³⁵⁻¹³⁸.

1.1.2.2.3 Debridement

Debridement is the approach to clear eschar, callus and exudate from the wound bed in order to promote healing process^{139, 140}. *Sharp debridement* is the most accurate and fast method to remove the non-healing tissue, so as to convert the chronic wound into an acute wounds. This approach can be used on most of wounds including diabetic ulcers, venous ulcers and pressure ulcers, but not appropriate for arterial ulcers¹⁴¹⁻¹⁴³. *Wet-to-dry debridement* is to leave the saline-moist gauze drying out on the wound bed and then remove the nonviable tissue together with the gauze^{139, 140}. This coarse approach is rarely employed nowadays because it causes a high degree of pain and cannot precisely remove the slough and nonviable tissue. *Autolytic debridement* is a slow approach (it usually takes weeks) using a moisture-donating dressing to rehydrate and separate the dried and nonviable tissue^{139, 140}. *Enzymatic debridement* is another slow approach which uses topical proteases targeting the fibrin and collagen in nonviable tissue^{139, 140, 144}.

1.2 Common Wound Dressings

Wound dressings are the most important therapeutic tools for both acute and chronic wounds. With different type and physiologic conditions of the wounds, specific wound dressings have been developed over the years². In the past, traditional dressings were made from plant fibers, animal fat, honey and latter-day cotton wool, gauzes and lint^{145, 146}. The main functions of these dressings were to absorb the exudates, keep wound bed dry and prevent the bacterial infection. However, as discussed earlier, a warm moist wound environment is essential for healing process, therefore the modern wound dressings focus more on creating an optimal environment for promoting the wound repairing. The most important properties for the modern wound dressings include²:

Introduction

- *Provide debridement action.* Clean the wound space via removing the dead tissue and foreign particles; and indirectly prevent the bacterial infection.
- *Maintain a moist wound environment.* It is essential for preventing cell desiccation and death; and promoting cell migration, re-epithelialization, angiogenesis and ECM remodeling.
- *Absorption.* Excess exudate surrounding the wounds contains undue level of proteases and growth factors, which impair the healing process.
- *Provision of thermal insulation.* Normal body temperature is essential for the angiogenesis and epidermal cell migration.
- *Prevent infection.* Influx of bacteria into the wound space may cause the chronic inflammatory, delayed healing and additional tissue damage.
- *Exchanges of gaseous substances and fluid.* Balance between hypoxia (promoting angiogenesis) and raised oxygen level (inducing re-epithelialization) plays an important role during the healing process. Moreover, permeability to water vapor is significant to manage the wound exudate.
- *Non-adherent.* Ease to remove from wound bed. Prevent extra pain or further trauma.
- *Nontoxic and non-allergic.*
- *Cost effective.*

Based on these aspects, wound dressings can be classified differently. For example, depending on their materials, they can be classified as *passive products* that simply act as a cover (e.g. gauze and tulle); *interactive materials* with decent permeability to vapor and gaseous (e.g. hydrogels and foams); and *bioactive materials* (e.g. hyaluronic acid collagens, chitosan, hydrocolloids and alginates)¹⁴⁷⁻¹⁴⁹. While based on their functions, they can be classified as debridement dressings, antibacterial dressings, occlusive dressing and adherence dressings and so forth¹⁴⁸. Classification criteria can sometimes be helpful for choosing an appropriate dressing, however in most cases one dressing can fit in different categories, which may cause more

confusion for patients. Therefore, in this chapter, the author did not follow any single criteria system, while combining different classifications together depending on their materials and functioning mechanism.

To provide protection from damage by force, bacterial infection, and to keep a moist wound environment, a number of common wound dressings have been developed such as gauzes, films, hydrogels, hydrocolloid, alginates and foams, which is summarized as follows (**Table 1.1**).

Gauze dressings made from cotton, rayon or polyester which are usually used to absorb fluid and exudates on open wounds¹⁵⁰. Dry gauze dressings that promote dehydration of wound bed will disturb healing process as former discussed, and often bind to wounds once it desiccated which cause pain and further trauma at dressing changes¹⁵¹. In addition, when the dressings absorb too much wound exudates and fluid, they become moistened and ease to be infected. Therefore gauzes need to be changed more regularly than other modern dressings (e.g. 1-2 times per day). Although many modern gauze dressings such as petrolatum and sodium chloride impregnated gauze¹⁵² have developed with different adherent and absorbing properties, they are mainly used for cleaning wounds as secondary dressings nowadays¹⁵³.

Films are transparent, semi-permeable and adhesive dressings^{2, 96}. Films have been used for a long time and the original products are made from nylon and polyethylene derivatives¹⁵⁴. These dressings with badly absorb efficiency often caused the bacteria accumulation, skin maceration and infection². Nowadays, advanced film dressings have improved the permeation properties that permit the exchange of oxygen and water vapor between wound and environment, so as to prevent the excess exudates accretion while remain the appropriate moist wound environment. Wounds can be examined through the transparent films without removing the dressings, therefore the frequency of dressing changes can be made as needed; meanwhile most films become non-adherent by moisture surface which minimizes the patient's un-comfort and further trauma at dressing changes¹⁵⁵⁻¹⁵⁷. In addition, the film dressings are elastic and flexible which can be easily applied on knees or elbows areas. Films dressings can be used

as primary dressing or a secondary dressing to seal other non-adhesive dressings, but they are not suitable for the wound with heavy exudate as their limited absorbing property and too thin for the deep cavity wounds¹⁵⁸.

Hydrogel dressings are made from swelling polymeric hydrophilic materials, which can maintain the moist wound environment. Hydrogel dressings contain a large amount of water and can only absorb very limited exudate, which are best suitable for dry wounds or the wounds with light exuding^{156, 157, 159}. Hydrogel dressings can be made as amorphous gel or elastic sheet form. The gel dressings are usually applied together with a secondary dressing (e.g. gauze), while the sheet dressings can be used alone and flexible to cut for specific wound shape². One of the major advantages of hydrogel dressings is non-adherent to wound bed, thus can be easily removed at dressing changes without causing pain and further trauma. In addition, hydrogels cool the wound surface which lead to a pain relief for patients at some level¹⁶⁰⁻¹⁶². Furthermore, hydrogel dressings provide autolytic debridement by rehydrating the necrotic and slough tissue^{159, 163}. The disadvantages of hydrogel dressings include the low mechanical strength and may cause over-moist wound environment^{164, 165}.

Hydrocolloid dressings absorb the wound exudate to form a gel and maintain the moist wound environment¹⁶⁶. Hydrocolloid dressings are one of the most widely used dressings for light and moderately exuding wounds including pressure ulcer, burn and trauma¹⁶⁷. Typical hydrocolloid dressings are made from gelatin, pectin and carboxymethylcellulose^{168, 169}. They may adhere to dry area which resulting a trauma around the wound at dressing changes, therefore barrier and protectant can be used with hydrocolloids together¹⁷⁰. Usually hydrocolloid dressings have a relatively long wear time up to one week, which reduces the cost and inconvenience for patients⁹⁶. Common hydrocolloid dressing products include GranuflexTM, AquacelTM, ComfeelTM, TegaserbTM, DuoDERM[®] CGF[®] and so forth.

Alginates that derived from brown seaweed contain the calcium and sodium salts of mannuronic and guluronic acids¹⁵⁶. These highly absorbent dressings are often used to manage the wounds with heavy level of exudate

^{171, 172}. The ion released from these polysaccharide dressing can reacted with wound fluid cross-linking to form a degradable gel on the wound bed, which maintain the moist environment and protect wound from bacterial contamination ^{173, 174}. The different component of mannuronic and guluronic acids can influence the degradability and swelling property in various alginate dressings ¹⁷¹. In addition, because of the ion exchange reaction in wound space, the unique pharmacological functions of the alginate dressings have been reported such as promoting hemostatic ^{175, 176}, increasing the proliferation of fibroblasts ¹⁷⁷ and activate the secretion of TNF- α from macrophages ¹⁷⁸. The concerns of using alginate dressings include: maceration around wound area ¹⁷⁹ and fibrous debris left in the wound space may cause unexpected immune response ^{180, 181}.

Foam dressings are made from porous polyurethane foam or film ¹⁵³. These dressings can maintain the moist environment, provide thermal insulation, and prevent shear injury ¹⁸². The absorption capacity of foam dressings depends on the pore size, thickness and texture properties. These dressings can be used for light to moderately draining wounds but not suitable for over-dried wound and dry scars ¹⁸³. Examples of the commercial foam dressing products include Allevyn[®], Lyofoam[®], 3M[™] adhesive form and so forth.

Table 1.1: Summary of common wound dressings^{2, 96, 158, 184}.

Classification	Changing Frequency	Advantage	Disadvantage	Applications	Products
Gauzes	12 to 24 h	Inexpensive Accessible	Desiccated wound environment Adherent to wound Poor barrier	Clean and dry wounds Secondary dressing	Curity™ gauze sponge; Vaseline™ gauzes; Xeroform™ gauzes; Mesalt® sodium chloride impregnated gauzes
Films	Up to 1 week (until fluid leaks)	Moisture maintaining Transparent Elastic and flexible Protect from bacterial infection	Non-absorption Skin stripping Only for shallow wounds	Wounds with minimal exudate Secondary dressing	Bioclusive™ film Cutifilm™ plus film Tegaderm™ dressing OpSite™ Flexifix film Blisterfilm™ film
Hydrogels	1 to 3 days	Moisture maintaining Non-traumatic change Pain relief	Non-absorption Low mechanical strength May cause over-moist environment	Dry wounds Wounds with minimal exudate Painful wounds	Nu-gel™ dressing Purilon™ dressing SAF-Gel® dressing Curage™ hydrogel Carrasyn® gel

Table 1.1: Summary of common wound dressings (continued)^{2, 96, 158, 184}.

Classification	Changing Frequency	Advantage	Disadvantage	Applications	Products
Hydrocolloids	Up to 1 week	Absorbent	Low permeation	Wounds with light to moderate exudate	Granuflex™ dressing
		Long wearing time	Fluid trapping		Aquacel™ dressing
		Occlusive	Skin stripping		Comfeel™ dressing
		Protect from bacterial infection	Malodorous discharge		Tegasorb™ dressing DuoDERM® CGF® dressing
Alginates	Keep until soaked with exudate	Highly absorbent	Fibrous debris	Wounds with heavy exudate	Kaltostat™ dressing
		Hemostatic	Lateral wicking		Sorbsan™ dressing
				Mild hemostasis	Tegasorb™ dressing
					AlgiSite-M dressing
Foams	3 days	Absorbent	Malodorous discharge	Wounds with light to moderate exudate	Allevyn® hydrocellular dressing
		Thermal insulation	Opaque		Allevyn® cavity dressing
		Occlusive			Lyof foam® dressing 3M™ adhesive form dressing

1.3 Allo- and Autologous Skin Graft

1.3.1 Autologous Skin Graft

Autologous skin graft, or known as skin transplantation has been used for many years as a gold standard for full-thickness wounds (especially for burn wounds) ^{185, 186}. Autologous split skin grafts (SSGs) are harvested from a patient's body with the whole epidermis and part of dermis tissue. Once SSGs are transplanted on the wound bed, its capillaries will merge with the host capillary network to supply the nutrients for grafts surviving and regeneration of new skin tissue ¹⁸⁶. Over the past few years, and thanks to improved techniques such as early excision, fluid resuscitation and infection control, the mortality of patients with extensive burn injury has significantly decreased ^{187, 188}. However, autologous skin grafts suffer from obvious limitations and drawbacks. First of all, donor grafts are harvested from patients, which results in secondary wounds. Although the split skin donor site usually heals within a week and can be repeatedly harvested up to four times, it will cause scarring at the harvest site, prolongs the hospital stays which leads to an increase in the risks for infection and complication ^{185, 186}. Furthermore, the application of SSGs donor sites is actually limited to extensive injury in which patients have lost most of the skin tissue.

To solve these problems, autologous cultured skin replacements have been developed since the 1970s ¹⁸⁹. By this technique, relatively few autologous epidermal cells are harvested from the patients, cultured *in vitro* to form a skin graft and then transplanted back to patients' wound site. This technique was first clinically applied in 1980 ¹⁹⁰, and since then these cultured autografts have been used to treat various wounds without causing any rejection response and the functional recovery of the wounded skin area showed to be as good as treating by SSGs ¹⁹¹⁻¹⁹³. Several products of cultured autografts are shown in **Table 1.2**. Epicel[®] autograft (Genzyme Biosurgery, Cambridge, MA, USA) was the first commercially available autologous cultured epidermal product that utilized autologous keratinocytes sheet for deep-dermal or full-thickness burns¹⁹⁴. The disadvantages of this product include fragility to sheer force and slow cell expansion (the culturing takes approximately three weeks). Burn wounds have a high risk

to develop hypertrophic scar by delayed healing process, therefore early cell coverage is essential for burn wounds treatment. CellSpray[®] (Avita Medical, Woburn, MA, USA) was designed for such purpose¹⁹⁴. A suspension of keratinocytes can be produced for spraying on to the wound bed with an aerosol device within 5 days after harvesting a small slit-thickness donor biopsy from patients¹⁹⁴. These sprayed cells can grow, proliferate and migrate into an even confluent cell cover over the wounds. The aerosolizing technique is a simple and rapid approach, particularly for the wounds with complex shape for grafting. Moreover, a new technical process called ReCell[®] kit has been developed by the same company, which can prepare the autologous cell suspension within approximately 20-30 min. Another cultured autograft product is EpiDex[®] (Modex Therapeutics, Lausanne, Switzerland), which uses patients' hair as a cell source¹⁹⁴. The outer root sheath stem cell from hair follicle can differentiate into keratinocytes by a co-culturing process within 2 weeks. This process takes a longer time than the former discussed techniques but it does not require any skin biopsy.

1.3.2 Allogeneic Skin Graft

Another option to address the challenges in wound healing are acellular allogeneic skin grafts which are made from cadaveric skin to temporary prevent the contamination and fluid loss¹⁹⁵. For dermal allografts, human cadaveric skin is cryopreserved, lyophilized and glycerolized to remove cellular components and infectious or antigenic donor tissues so as to reduce the rejection risk. After transplantation, host cells and vascular structures fill into the graft and regenerate to form new skin tissue. Disadvantages for these allografts are obvious and include, apart from the ethical issue, the safety risk (transplant rejection), and as a general concern, disease transmission and contamination^{196, 197}. Moreover, as the number of donors is limited and the shelf life of the product is short, allografts from tissue banks cannot fill the clinical demands. Therefore, it is paramount to develop alternative products for allogeneic skin grafts. Some examples of commercially available allogeneic skin grafts are shown in **Table 1.3**.

Table 1.2: Commercially available autologous skin grafts for clinical use ^{194, 198, 199}.

Brand Name	Manufacturer	Cell Source	Cell Type	Lifespan
Epicel [®]	Genzyme Biosurgery, Cambridge, MA, USA	autologous	Keratinocytes	Permanent
CellSpray [®]	Avita Medical, Woburn, MA, USA	autologous	Keratinocytes	Permanent
EpiDex [®]	Modex Therapeutics, Lausanne, Switzerland	autologous	Keratinocytes	Permanent
EPIBASE	Laboratoires Genevrier, Sophia-Autipolis, Nice, France	autologous	Keratinocytes	Permanent

Table 1.3: Commercially available allogeneic skin grafts for clinical use^{194, 198, 199}.

Brand Name	Manufacturer	Cell Source	Scaffold Material	Lifespan
Allograft	Skin bank (Not-for profit)	allogeneic	Acellular native human skin (cadaveric)	Temporary
Karoderm [®]	Karocell Tissue Engineering AB, Karolinska University Hospital, Stockholm, Sweden	allogeneic	Allogeneic human acellular dermis	Permanent
AlloDerm [®]	LifeCell Corporation, Branchburg, NJ, USA	allogeneic	Allogeneic human acellular lyophilized dermis	Permanent
SureDerm [™]	HANS BIOMED Corporation, Seoul, Korea	allogeneic	Allogeneic human acellular lyophilized dermis	Permanent
GraftJacket [®]	Wright Medical Technology, Inc., Arlington, TN, USA	allogeneic	Allogeneic human acellular pre-meshed dermis	Permanent

1.4 Tissue Engineered Skin Substitutes

Although advanced cultured autologous skin graft techniques have reduced the culturing and processing time, protected from the hypertrophic scar formation, and significantly improved the survival ratio for the patients with extensive burns^{198, 199}, other alternative approaches are still demanded for clinical applications. These include tissue engineered skin substitutes which consist of bioactive natural or synthetic materials combined with/without cells, drugs and growth factors to replace the damaged skin tissue and accelerate the healing process^{2, 198, 199}. Tissue engineered skin substitutes have been developed for many years and can be classified as acellular or cellular skin substitutes.

1.4.1 Acellular Skin Substitutes

1.4.1.1 Bioactive material dressings

Some dressings made from natural biomaterials (e.g. collagen, hyaluronic acid, chitosan and elastin) accomplish more than just protecting the wound area and maintaining a moist environment for healing. They also actively adjust the wound environment by regulating proteolytic enzymes (e.g. MMPs), absorbing the metabolic byproducts from cell or microorganism and promoting the dermal regeneration^{2, 194}. These biomaterials have attractive advantages such as biodegradability, biocompatibility and bioactive functionalities. For example, collagen plays essential roles during the healing process including stimulating migration of dermal cells, regulating granulation tissue construction and remodeling, and affecting scar formation. Hyaluronic acid (HA) is a glycosaminoglycan with a highly hydrophilic property and a lack of immunogenicity²⁰⁰ and has been widely used for drug and growth factors delivery^{201, 202}. Chitosan has also been reported to promote wound repair by accelerating the granulation stage in healing process²⁰³.

These bioactive material dressings have two major therapeutic functions. One is regulating the level of proteolytic enzymes in wound environment and protecting growth factors from MMPs degradation²⁰⁴. Examples for such dressings include: Promogran Prisma[®] wound matrix (Systagenix,

Gargrave Centre of Excellence for Wound Healing, North Yorkshire, UK) and Fibracol[®] Plus Collagen dressing (Johnson and Johnson, New Brunswick, NJ, USA). The other function is promoting the regeneration and reconstruction of the dermal tissue²⁰⁵. The examples for products in this category include Medifil[™] II Particles dressing (Human BioSciences, Inc, Gaithersburg, MD, USA), SkinTemp[™] II dressing (Human BioSciences, Inc, Gaithersburg, MD, USA), Healthcare MatriDerm[®] (Ideal Medical Solutions Ltd, Wallington Surrey, UK) and Oasis[®] Wound Matrix (Cook Biotech, Inc. West Lafayette, IN, USA). More detailed information of such bioactive material dressings is summarized in **Table 1.4**.

1.4.1.2 Synthetic bilayer substitutes

Another type of acellular skin substitute, called synthetic bilayer substitutes, combine ECM biomaterials with a thin layer of silicone to maintain the moisture wound environment and protect against bacterial infection¹⁹⁴. Examples of this type of dressings include Biobrane[®] (UDL Laboratories, Inc., Rockford, IL, USA), AWBAT[®] (Aubrey, Inc., Carlsbad, CA, USA), Integra[™] Bilayer Matrix Wound Dressing (Integra Life Science Corporation, Plainsboro, NJ, USA) and Hyalomatrix[®] (Anika Therapeutics, Inc., Bedford, MA, USA). More detailed information of such acellular synthetic bilayer substitutes is summarized in **Table 1.4**.

Table 1.4: Commercially available acellular skin substitutes for clinical use ^{194, 198, 199}.

Brand Name	Manufacturer	Scaffold Source	Scaffold Materials	Lifespan
Promogran Prisma [®] wound matrix	Systagenix, Gargrave Centre of Excellence for Wound Healing, North Yorkshire, UK	xenogeneic/synthetic	Porcine lyophilized collagen/oxidized regenerated cellulose (ORC)/silver	Permanent
Fibracol [®] Plus Collagen dressing	Johnson and Johnson, New Brunswick, NJ, USA	xenogeneic	Lyophilized collagen/alginate	Permanent
Medifil [™] II Particles dressing	Human BioSciences, Inc, Gaithersburg, MD, USA	xenogeneic	Particles made from bovine collagen	Permanent
SkinTemp [™] II dressing	Human BioSciences, Inc, Gaithersburg, MD, USA	xenogeneic	Bovine collagen	Permanent
MatriDerm [®]	Ideal Medical Solutions Ltd, Wallington Surrey, UK	xenogeneic	Three dimensional matrix consisting of bovine collagen with elastin coating	Permanent

Table 1.4: Commercially available acellular skin substitutes for clinical use (continued) ^{194, 198, 199}.

Brand Name	Manufacturer	Scaffold Source	Scaffold Materials	Lifespan
Oasis [®] Wound Matrix	Cook Biotech, Inc. West Lafayette, IN, USA	xenogeneic	Porcine lyophilized small intestine sub-mucosa	Permanent
Permacol [™] Surgical Implant	Tissue Science Laboratories plc, Aldershot, UK	xenogeneic	Porcine acellular dermal collagen implant	Permanent
E-Z Derm [™]	Brennen Medical, Inc., MN, USA	xenogeneic	Porcine aldehyde reconstituted dermal collagen	Temporary
Biobrane [®]	UDL Laboratories, Inc., Rockford, IL, USA	xenogeneic/synthetic	Porcine collagen/nylon mesh/ultrathin silicone film	Temporary
AWBAT [®]	Aubrey, Inc., Carlsbad, CA, USA	xenogeneic/synthetic	Porcine collagen peptides/thin porous silicone membrane with nylon fabric	Temporary

Table 1.4: Commercially available acellular skin substitutes for clinical use (continued)^{194, 198, 199}.

Brand Name	Manufacturer	Scaffold Source	Scaffold Materials	Lifespan
Integra™ Bilayer Matrix Wound Dressing	Integra Life Science Corporation, Plainsboro, NJ, USA	xenogeneic/synthetic	Bovine tendon collagen with glycosaminoglycan and polysiloxane	Semi-permanent
Hyalomatrix®	Anika Therapeutics, Inc., Bedford, MA, USA	xenogeneic/synthetic	A benzyl ester of hyaluronic acid with semi-permeable silicone member	Semi-permanent
Pelnac™	Gunze Ltd, Medical Materials Center, Kyoto, Japan	xenogeneic/synthetic	Porcine atelocollagen with silicone cover-layer	Semi-permanent
Terudermis	Olympus Terumo Biomaterial Corporation, Tokyo, Japan	xenogeneic/synthetic	Bovine lyophilized cross-linked collagen sponge with silicone	Semi-permanent

1.4.2 Cellular Skin Substitutes

Cellular skin substitutes generally seed or encapsulate the living cells (dermal or stem cells) into a biodegradable scaffold. These degradable scaffolds provide ideal mechanical properties and physiologic conditions for cell growth, proliferation as well as secretion of growth factors to stimulate tissue regeneration and wound repair^{2, 206}. During the healing process, the scaffolds degrade progressively and leave behind a regenerated matrix filled with host cells and tissue which is similar to natural skins. Based on the anatomic skin structure, various cell types and substitute devices have been developed for different wound areas, which can be divided as epidermal substitutes, dermal substitutes and composite epidermal/dermal substitutes (**Table 1.5**)^{198, 199}.

1.4.2.1 Epidermal substitutes

Since it became possible to culture human keratinocytes (the main cell type in the epidermis) *in vitro* and to rapidly expand these cell number *ex vivo*¹⁸⁹, autografts have become one of the most important clinical tools for treating epidermal wound damage. These autograft techniques have been significantly improved over the last few decades as discussed above. Advancing technology beyond pure cell sheets, some tissue engineered autografts grow cells on natural or synthetic biomaterials to further reduce the culturing time, are easy to handle and also protect the wound area from moisture loss and bacterial infection. For example, mySkinTM (CellTran Ltd., Sheffield, UK) uses sub-confluent autologous keratinocytes seeded on a silicone substrate layer for treating diabetic foot ulcers, superficial burns and neuropathic pressure^{207, 208}; Laserskin[®] (Fidia Advanced Biopolymers, Padua, Italy) cultures autologous keratinocytes on a hyaluronic acid membrane¹⁸³; and Bioseed-S[®] (BioTissue Technologies GmbH, Freiburg, Germany) resuspended autologous keratinocytes in a fibrin sealant for chronic venous leg ulcers^{209, 210} (**Table 1.5**).

1.4.2.2 Dermal substitutes

In the cases of full-thickness burns, both epidermis and dermis layers are damaged and need to be replaced, thus application of the cultured

keratinocytes graft is not an optimal treatment option for such wounds¹⁹⁹. Currently the most widely used dermal equivalents are allogeneic or xenogeneic acellular skin grafts. Typical cellular tissue engineering dermal substitutes include Dermagraft[®] (Advanced BioHealing, Inc., New York, La Jolla, CA, USA), TransCyte[®] (Advanced BioHealing, Inc., New York, La Jolla, CA, USA) and Hyalograft[®] (Anika Therapeutics, Inc., Bedford, MA, USA). More detailed information of such dermal tissue engineering substitutes is summarized in **Table 1.5**.

1.4.2.3 Dermal/Epidermal substitutes

Dermal/epidermal substitutes are considered more advanced skin equivalents as they mimic the native architecture of both epidermis and dermis¹⁹⁸. Both fibroblasts and keratinocytes are combined into scaffolds which are made from native ECM or synthetic materials¹⁹⁹. The cells contained in these substitutes provide growth factors, cytokines and ECM materials into host tissue, thus stimulate host cells and accelerate the healing process²¹¹. Current commercial available dermal/epidermal substitutes include Apligraf[®] (Organogenesis, Inc., Canton, Massachusetts, CA, USA), OrCel[®] (Ortec International, Inc., New York, NY, USA), PolyActive[®] (HC Implants BV, Leiden, Netherlands) and TissueTech Autograft System[™] (Fidia Advanced Biopolymers, Abano Terme, Italy), which are summarized in **Table 1.5**.

Table 1.5: Commercially available cellular skin substitutes for clinical use ^{2, 198, 199}

Brand Name	Manufacturer	Type	Cell Source	Scaffold Materials	Lifespan
mySkin™	CellTran Ltd., Sheffield, UK	Epidermal substitutes	autologous keratinocytes	Silicone layer with a specially formulated coating	Permanent
Laserskin®	Fidia Advanced Biopolymers, Padua, Italy	Epidermal substitutes	autologous Keratinocytes	Hyaluronic acid membrane	Permanent
Bioseed-S®	BioTissue Technologies GmbH, Freiburg, Germany	Epidermal substitutes	autologous keratinocytes	Fibrin sealant	Permanent
Dermagraft®	Advanced BioHealing, Inc., New York, LaJolla, CA, USA	Dermal substitutes	allogeneic fibroblasts	Polyglycolic acid/polyglactin mesh	Temporary
TransCyte®	Advanced BioHealing, Inc., New York, La Jolla, CA, USA	Dermal substitutes	allogeneic neonatal fibroblasts	Porcine collagen with silicon film and nylon mesh	Temporary

Table 1.5: Commercially available cellular skin substitutes for clinical use (continued)^{2, 198, 199}.

Brand Name	Manufacturer	Type	Cell Source	Scaffold Materials	Lifespan
Hyalograft [®]	Anika Therapeutics, Inc., Bedford, MA, USA	Dermal substitutes	autologous fibroblasts	Hyaluronic acid membrane	Permanent
Apligraf [®]	Organogenesis, Inc., Canton, Massachusetts, CA, USA	Epidermal/Dermal substitutes	allogeneic fibroblasts and keratinocytes	Bovine collagen	Temporary
OrCel [®]	Ortec International, Inc., New York, NY, USA	Epidermal/Dermal substitutes	allogeneic fibroblasts and keratinocytes	Bovine collagen sponge	Temporary
PolyActive [®]	HC Implants BV, Leiden, Netherlands	Epidermal/Dermal substitutes	autologous fibroblasts and keratinocytes	Polyethylene oxide terephthalate and polybutylene terephthalate	Temporary
TissueTech Autograft System [™]	Fidia Advanced Biopolymers, Abano Terme, Italy	Epidermal/Dermal substitutes	autologous fibroblasts and keratinocytes	Hyaluronic acid membrane	Permanent

1.4.3 Limitations of current skin substitutes

As a result of all the efforts over the last few years, a number of advanced tissue engineering substitutes have been developed as discussed earlier, however there is still no single product that can provide all the properties as an “ideal” skin substitute or fully replace the native skin. Some of the major limitations or concerns of the tissue engineering skin substitutes are summarized as follows.

- High cost ^{2, 198, 199}
- Short shelf-time ^{2, 198, 199}
- Long culture time for cellular substitutes ^{2, 198, 199}
- Create second wound (in case of autologous cell sources) ^{185, 186}
- Immunogenic rejection risk for allogeneic/xenogeneic cell or material sources ^{212, 213}
- Disease transmission risk for allogeneic substitutes ^{196, 197}
- Prone to contamination ^{214, 215}
- Low vascularization ratio in scaffold ²¹⁶
- Allergies caused by xenogeneic cell or material sources ²¹⁵
- Mechanical fragility ^{215, 217}

1.5 Drug & Growth Factor Delivery

Some pharmaceutical agents and antimicrobials are usually included in different dressings. For example, thymol and hydrogen peroxide are often used to clean and debride the wound area, and to protect the wound from bacterial infection ². Silver ^{218, 219} and antibiotics ²²⁰⁻²²² such as dialkylcarbamoylchloride, povidone-iodine, gentamycin, ofloxacin and minocycline are also commonly used for incorporation into wound dressings. However, these antibacterial agents can only protect wounds from infections but do not contribute physiological functions during the healing process. Growth factors, on the other hand, play significant roles in the whole healing process as discussed earlier. Because these approaches are not the focus of this dissertation, the author summarized here only some main growth factors involved in the wound healing process as shown in **Table 1.6**.

Introduction

It is obvious that the wound healing process is regulated by a complex molecular signaling network which is very dynamic during different healing stages, therefore, using gene therapy to deliver a single growth factor can hardly modified all the phases of the wound healing process. Thus a number of studies have tried combined different growth factors together to achieve more effective results, such as combination of PDGF with IGF-I²²³, PDGF with FGF-2²²⁴, and KGF with IGF-I²²⁵. Alternatively, advanced controlled delivery systems have been also developed for slow and sequential release of growth factors and relative genes²²⁶.

Table 1.6: Main growth factors and cytokines in wound healing.

(ECM: extracellular matrix; EGF: epidermal growth factor; FGF: fibroblast growth factor; HB-EGF: heparin binding EGF; HGF: hepatocyte growth factor; IL: interleukin; PDGF: platelet-derived growth factor; ROS: reactive oxygen species; TGF: tumor growth factor; VEGF: vascular endothelial growth factor)

Growth Factors	Source	Target	Key Functions	References
VEGF	keratinocytes, fibroblasts, macrophages, endothelial cells	endothelia cells, macrophages, smooth muscle cells, neutrophils	angiogenesis, inflammation, granulation tissue formation	34, 71, 72, 227-230
TGF- β	keratinocytes, fibroblasts, macrophages, platelets	fibroblasts, keratinocytes, macrophages, leukocytes, endothelial cells ECM	angiogenesis, inflammation, granulation tissue formation, collagen synthesis, tissue remodeling, leukocyte chemotactic function	9, 54-57, 88-91, 231-234

Table 1.6: Main growth factors and cytokines in wound healing (continued).

Growth Factors	Source	Target	Key Functions	References
IL-6	fibroblasts, keratinocytes, macrophages, endothelial cells	macrophages, leukocytes, keratinocytes, fibroblasts, endothelial cells neutrophils	inflammation, angiogenesis, re-epithelialization collagen deposition, tissue remodeling	51, 52, 93, 235
IL-1	macrophages, leukocytes, keratinocytes, fibroblasts	endothelial cells, macrophages, keratinocytes, leukocytes, fibroblasts neutrophils	inflammation, angiogenesis, re-epithelialization, tissue remodeling	6, 26, 33, 34, 93, 236, 237
IL-4	leukocytes	macrophages	collagen synthesis	238, 239

Table 1.6: Main growth factors and cytokines in wound healing (continued).

Growth Factors	Source	Target	Key Functions	References
IL-27	macrophages,	macrophages	suppression of inflammation, collagen synthesis	239
PDGF	platelets	macrophages, keratinocytes, fibroblasts, endothelial cells, leukocytes	inflammation, re-epithelialization, collagen deposition, granulation tissue formation tissue remodeling	240-243
HGF	fibroblasts	keratinocytes, endothelial cells	suppression of inflammation, angiogenesis, re-epithelialization granulation tissue formation	34, 49, 50, 244

Table 1.6: Main growth factors and cytokines in wound healing (continued).

Growth Factors	Source	Target	Key Functions	References
FGF-2	keratinocytes, fibroblasts, endothelial cells	keratinocytes, fibroblasts, endothelial cells mast cells smooth muscle cells chondrocytes	angiogenesis, granulation tissue formation re-epithelialization, tissue remodeling	43-46, 245
FGF-7, FGF-10	fibroblasts, keratinocytes	keratinocytes,	re-epithelialization, detoxification of ROS	23, 24
EGF, HB-EGF, TGF- α	keratinocytes, macrophages	keratinocytes, fibroblasts	re-epithelialization	47, 48, 93, 246-249

1.6 Stem Cell Therapy for Wound Healing

As previously discussed, wound healing is a complex biological and physiological process that involves different cell types, molecules and biomaterials²⁵⁰. Creating an ideal skin substitute to completely mimic and replace the native skin has not been successful^{2, 198, 199, 251}. Therefore, stem cells which have the unique capability to differentiate into various cell types and secrete numerous growth factors have attracted more and more attention for last few years²²⁶. Stem cells has been first discovered by Till and McCulloch in 1961²⁵², and more recently they have been found to be present in different tissues such as skin²⁵³, brain²⁵⁴, liver²⁵⁴, pancreas²⁵⁴, skeletal muscle²⁵⁵, testis²⁵⁶ and blood vessels²⁵⁷. Embryonic stem cells raised momentous ethical concerns and controversies by both the public and scientists. As an alternative, a number of other stem cell sources from the adult tissue have been studied for clinical applications such as bone marrow derived stem cells (BMSCs), hematopoietic stem cells (HSCs), umbilical cord derived stem cells, cutaneous stem cells and adipose-derived stem cells (ADSCs). More recently, Induced Pluripotent Stem cells (iPS) produced by genetic reprogramming of somatic cells have been generated, which have the similar differentiation capability as embryonic stem cells and have shown great potential for clinical applications²⁵⁸⁻²⁶⁰. BMSCs and ADSCs, two major types of stem cells for wound healing are discussed in the following sections.

1.6.1 Bone Marrow Stem Cells

BMSCs was first described by Friedenstein and colleagues in 1968²⁶¹, and firstly named as mesenchymal stem cells (MSCs) by Caplan in the early 1990s²⁶². The International Society for Cellular Therapy (ISCT) identified minimal criteria for characterization of MSCs in the 2000s: (i) plastic-adherent at standard culturing condition; (ii) express surface markers including CD105, CD90 and CD73, but lack to express CD 45, CD34, CD14 (or CD11b), CD79a (or CD19) and HLA-DR surface molecules; (iii) capable to differentiate into osteoblasts, adipocytes and chondroblasts *in vitro*^{263, 264}. Besides the osteoblasts, adipocytes and chondroblasts, MSCs can also differentiate into myocytes, tendocytes and ligaments cells²⁶⁵⁻²⁶⁷.

So far, MSCs have been found in different tissues through the body such as bone marrow, blood vessels, fat, skin, muscle, and teeth ²⁶⁵⁻²⁶⁸, and it has been reported that MSCs possess certain level of plasticity, in other words can differentiate across the lineage boundary ²⁶⁹.

BMSCs have been reported to play essential roles in wound healing process by producing various cytokines, however, the mechanism is not fully understood ²⁷⁰⁻²⁷². The BMSCs are precursor cell of fibroblasts ²⁷³, keratinocytes ²⁷⁴ and fibrocytes ²⁷⁵ in the granulation tissue formation process ^{250, 276}. They also regulate the ratio of collagen type I and collagen type III in the remodeling process, which is essential for scar formation ²⁷⁷. BMSCs have been employed to treat acute burn wounds or chronic wounds (e.g. diabetic foot ulcer) either using alone or in combination with gene therapy ²⁷⁸⁻²⁸¹. For example, transfected BMSCs with PDGF and beta-defensin-2 (BD-2) showed increased collagen deposition, granulation tissue formation and reduced bacterial infection ²⁷⁸. BMSCs with angiogenic factors (e.g. VEGF) showed improved neovascularization and accelerated healing ^{279, 282}. Furthermore, MSC-conditioned medium has been reported to promote angiogenesis, epithelialization, and affect recruit or proliferation of macrophages and endothelial progenitor cells during the healing process ^{250, 283}. In summary, BMSCs have been widely used in researching and clinical studies for wound healing; however, several drawbacks of using BMSCs limited their applications such as painful extracting process, low yield and decreasing cell number with age ^{226, 284, 285}.

1.6.2 Adipose-derived Stem Cells

In comparison to BMSCs, the ADSCs yield from adipose tissue is generally 40-fold higher ²⁸⁶, and the cell sources for ADSCs (e.g. liposuction) are much easier to achieve and the surgical approach is considerable painless for patients. In addition, the isolated cells can be cryopreserved for up to 6 months which can be accessible for the further therapeutic uses ²⁸⁷. It has been proved that ADSCs possess the plasticity to differentiate into various cell lineages including adipocytes, osteoblasts, chondrocytes, myocytes, hepatocytes, endothelial, hematopoietic, and neuronal cells ^{242, 288-295}, and the potential to improve the angiogenesis and stabilize vascular formation

²⁹⁶⁻³⁰⁰. In addition, cytokines secreted by ADSCs have been demonstrated to play essential roles in the healing process ^{299, 301-304}. Therefore, ADSCs have shown great potential and could be used to develop an off-the-shelf substitute product.

ADSCs are generally isolated from the so called stromal vascular fraction (SVF) of adipose tissue, which is comprised of adipocytes and a diverse set of other cells including stromal cells, vascular endothelial cells and vascular smooth muscle cells ³⁰⁵⁻³⁰⁷. The adipose tissue is minced into small pieces, and digested by type I collagenase following centrifugation to get SVF fraction. Then, ADSCs are further separated from other lineages' cells based on their ability to adhere on tissue culture plate ^{289, 290, 308}. ADSCs are commonly characterized by immunophenotype and differentiation capability to osteoblasts, adipocytes and chondroblasts. ADSCs present quite similar surface markers as BMSCs with the exceptions of CD49b (expressed on ADSCs) and CD106 (lack expression on ADSCs) ³⁰⁹⁻³¹¹. It needs to be noted that different surface markers, sometimes even conflicting results, have been reported by different groups over years, which might be due to the differences in antibodies sources, detection methods or cell culturing conditions ³⁰⁷.

Although it has not been long since ADSCs were used for wound healing applications, a number of studies have demonstrated that ADSCs promote wound healing via enhancing angiogenesis, differentiating into various cell types, and paracrine secreting effect ^{312, 313}. For example, Trottier and colleagues reported that ADSCs can be used to replace the fibroblasts and combined with keratinocytes to form a epidermal/dermal substitute for promoting healing *in vivo* ³¹⁴. Ebrahimian and colleagues reported that ADSCs accelerated the healing process by differentiating into keratinocytes and increasing the VEGF and KGF level ³¹⁵. Similar results were also reported by Lin and colleagues, who showed that ADSCs cell sheets significantly increased the blood vessel density in a nude mice wound model ³¹⁶. Furthermore, Altman and colleagues used a ADSCs seeded silk fibroin-chitosan scaffold for murine skin injury repair ³¹⁷. They found that angiogenesis and wound closure were promoted, and ADSCs/scaffold

Introduction

transferred as fibrovascular, endothelial and epithelial tissue components. More recently, Hong and colleagues compared the potential of BMSCs and ADSCs to heal wounds in a rabbit ear model ³¹⁸. They found that transplanted ADSCs differentiated into a fibroblast phenotype, enhanced the recruitment of macrophage and endothelia cells, and promoted granulation tissue formation.

Besides the differentiation into other cell phenotypes as mentioned above, paracrine effects of ADSCs in wound healing process have attracted much attention recently. Kim and colleagues found that ADSCs promote the proliferation of human dermal fibroblasts (HDF) not only by cell-cell contact stimulation, but also through a paracrine activation effect ³¹⁹. They found released factors (including PDGF, IGF and KGF) contained in the adipose-derived stem cell conditioned medium (ADSC-CM) can up-regulate the collagen type I, III and fibronectin while down-regulating MMP-1; as a result, the proliferation and migration of HDFs was stimulated, thus accelerated the re-epithelialization and wound closure. A more recent study reported that ADSCs seeded on a silk fibroin-chitosan scaffold promoted angiogenesis and wound healing ³¹⁷. In addition, Amos and colleagues demonstrated that the use of ADSCs could be used for treating diabetic ulcers, and they also indicated that three-dimensional culturing of ADSCs results in the secretion of significantly more extracellular matrix proteins and soluble factors compared to monolayer culture ³²⁰. ADSCs have shown capability to secrete various growth factors including IGF, HGF, TGF- β 1 and VEGF, which all play essential roles in wound healing process ^{301, 321}.

Table 1.7: Injectable hydrogels for tissue engineering.

(PEG: Poly(ethylene glycol); PEO: Poly(ethylene oxide); PNIPAAm: Poly(*N*-isopropylacrylamide); PPF: Poly(propylene fumarate); OPF: Oligo(poly(ethylene glycol) fumarate); PPO: Poly(propylene oxide); PLGA: Poly(*DL*-lactic-*co*-glycolic acid); PLA: Poly(*L*-lactic acid); PVA: Poly(vinyl alcohol))

	Injectable Hydrogels	Gelation Mechanism	References
Natural Polymer	Collagen/Gelatin	Thermal/Chemical cross-linking	322-324
	Chitosan	Thermal/Chemical/Schiff-base reaction/Photo- crosslinking	325-331
	Hyaluronic acid	Thermal/Chemical/Schiff-base reaction/Photo-crosslinking/ Michael-type addition cross-linking	332-338
	Chondroitin Sulfate	Photo-crosslinking	339-341
	Agar/Agarose	Thermal cross-linking	342, 343
	Fibrin	Thermal cross-linking	344, 345
	Alginate	Ionic/Photo-crosslinking	346-348
	Methylcellulose	Thermal cross-linking	349

Table 1.7: Injectable hydrogels for tissue engineering (continued).

	Injectable Hydrogels	Gelation Mechanism	References
Synthetic Polymer	PEG/PEO	Thermal/Chemical/Michael-type Addition/Photo-crosslinking	350-353
	PNIPAAm	Thermal cross-linking	105, 354-357
	PPF/OPF	Thermal cross-linking	358-361
	PEO-PPO-PEO/PLGA-PEG- PLGA/PLA-PEG	Thermal cross-linking	362-365
	PVA/PLA-PVA	Chemical/Photo- crosslinking	362, 366
	Poly (aldehyde guluronate)	Chemical cross-linking	367

1.7 Injectable Hydrogels for Tissue Engineering

Injectable hydrogels have attracted more and more attention in the fields of drug delivery and tissue engineering as they provide a simple delivery procedure, minimize the patients' discomfort and reduce the scar formation as well as the infection risk³⁶⁸. These hydrogels can be injected to any wound size, shape or cavity with minimized invasive surgery, and then *in-situ* form a three-dimensional (3D) water content polymer network via physical or chemical cross-linking, which mimics precisely the mechanical and swelling/shrinking properties of the native tissue³⁶⁹. Physical cross-linking of the injectable hydrogels takes place mainly in response to the environmental stimulus (e.g. temperature, pH, and ionic strength)³⁷⁰; and chemical cross-linking mechanisms include photo-polymerization, Michael-type addition reaction, Schiff-based gelation and enzymatically triggered systems³⁶⁹. In addition, hydrogel components, living cells and growth factors can be co-injected together effortlessly, and after gelation, hydrogels provide a temporary matrix to support cell adhere, growth, and proliferation^{349, 371}. Various natural and synthetic polymers have been developed for injectable hydrogel systems, and **Table 1.7** summarized some of the major types of these materials for tissue engineering applications.

1.7.1 Physical Cross-linking Hydrogels

1.7.1.1 Thermoresponsive cross-linking hydrogels

Thermoresponsive cross-linking hydrogels have been widely studied as the temperature stimuli can be easily applied without requirements of complex equipment or other external stimulus³⁷². Thus, many of the thermoresponsive hydrogels for biomedical and tissue engineering applications are designed by making use of the change between body temperature and environmental temperature. The phase transition with the varying temperature of this type of materials from a solution to a gel can be called sol-gel transition³⁷². Some materials change from solution phase to gelation phase above a certain temperature which is called lower critical solution temperature (LCST); while others form gels below certain temperature which is called upper critical solution temperature (UCST)³⁷⁰.

This sol-gel transition can be explained by Gibbs equation: $\Delta G = \Delta H - T\Delta S$ (G, Gibbs free energy; H, enthalpy; S, entropy). In the case of polymers exhibiting LCST, the increase of the temperature results in the rise of energy and entropy. The water-water reaction, at this time, is more favorable than polymer-water reaction in the system as the higher entropy (i.e. less ordered). As a result, polymers become more hydrophobic and separated from solution driven by a negative free energy. This phenomenon is also called the hydrophobic effect, and the physical cross-linking or gelation is reversible³⁷³.

Many different thermoresponsive hydrogel systems have been developed from natural, synthetic or hybrid materials. In the following section, four major groups of these hydrogels are reviewed briefly: (i) natural polymers and derivatives; (ii) Poly(N-isopropylacrylamide) (PNIPAAm) and derivatives; (iii) block copolymer hydrogels; (iv) PEG based systems.

1.7.1.1.1 Natural polymers and derivatives

A number of natural materials including polysaccharide (e.g. cellulose derivative, chitosan, dextran and xyloglucan) and proteins (e.g. gelatin) have been used for the construction of thermoresponsive hydrogels either being used alone or in combination with other thermoresponsive materials.

Methylcellulose is a cellulose-derivative polysaccharide. The hydrophobic methyl groups provide methylcellulose thermoresponsive cross-linking behavior with the gelling temperature around 60 to 80 °C depending on the molecular weight, substitution degree and the solvents^{374, 375}. It has been reported that the thermoresponsive behavior and mechanical strength of PNIPAAm based hydrogel altered by combining with methylcellulose with different ratio³⁷⁶. Furthermore, a thermoresponsive hydrogel of methylcellulose combining with laminin was used for neural tissue engineering and has been demonstrated to improve the neural stem cell survival and differentiation^{377, 378}. *Chitosan* which is made from the chitin are also used to construct thermoresponsive materials³⁷⁹. For example, PEG-grafted chitosan has been developed as thermoresponsive hydrogel for drug delivery system^{380, 381}. NIPAAm-chitosan hybrid polymer was used to

deliver hMSCs, and the desired chondrogenic differentiation was achieved both *in vitro* and *in vivo* ³⁸². Another type of thermoresponsive derivative is chitosan-glycerophosphate salt (Chitosan-GP), which has been developed for neural tissue engineering ³²⁵. *Xyloglucan* was also reported exhibiting thermoresponsive behaviors by removing 35 % of the galactose residues on it ^{383, 384}. *Gelatin*, a protein derived from collagen is another natural material which exhibits thermoresponsive behavior. Interestingly, the thermoresponsive property of gelatin is opposite to common thermoresponsive polymer: it forms a gel below 25 °C while becomes as liquid above 30 °C, which is due to a conformation transition between triple helices and flexible coil ³⁸⁵. With this special property, gelatin has been combined with other polymers to construct thermoresponsive hydrogels for drug delivery and tissue engineering applications, such as monomethoxy poly(ethylene glycol)-poly(D,L-lactide) (mPEG-DLLA) ³⁸⁶, NIPAAm ³⁸⁷ and silk fibroin ³⁸⁸.

1.7.1.1.2 PNIPAAm and derivatives

PNIPAAm is the most widely studied thermoresponsive polymer which exhibits a sharp sol-gel transition at 32 °C ^{389, 390}. Below the LCST temperature, isopropyl groups on the polymer bind with water molecules via hydrogen bond, while the intra-/inter-molecular hydrophobic interactions between isopropyl groups and releasing of water molecules are induced by rising temperature above the LCST. Numbers of thermoresponsive PNIPAAm based copolymers have been developed for drug delivery ^{389, 391-393}, tissue engineering ³⁹⁴ and surface coating ³⁹⁵. More information about PNIPAAm based thermoresponsive copolymers have been reviewed elsewhere ³⁹⁶. More interestingly, PNIPAAm are not only used to combine with other synthetic polymers, but also with some biomolecules which can improve the biodegradable property and biocompatibility of the hydrogels, such as dextran ³⁹⁷, chitosan ^{356, 357, 382}, gelatin ³⁸⁷ and hyaluronic acid ^{382, 398, 399}. For example, hyaluronic acid can cross-link with carboxyl-terminated PNIPAAm, which have shown the potential for adipose regeneration and soft tissue engineering ^{382, 398, 399}.

1.7.1.1.3 Triblock copolymer hydrogels

Another important group of synthetic thermoresponsive polymers are triblock copolymers including PEO-PPO-PEO (Pluronic[®]), PLGA-PEG-PLGA, PEG-PLLA-PEG, PCLA-PEG-PCLA, PEG-PCL-PEG and so on³⁶³⁻³⁶⁵. These amphiphilic copolymers can self-assemble into micelles at low temperature in aqueous solutions, and aggregate to form a macroscopic gel at high temperature³⁶⁴. The polymer composition, molecular weight and the solution concentration all influence the gelling properties of these types of thermoresponsive polymers. Among all these copolymers, Pluronic[®] are commercially available with a series of compositions, molecular weight and forms, which have been widely studied for drug delivery⁴⁰⁰, tissue adhesion⁴⁰¹ and wound covering⁴⁰². However, the mechanical strength of this type of thermal gels is generally weak and shows limited stability^{403, 404}. Thus a number of approaches have been studied to improve these properties such as adding the covalent binding unit^{403, 404} or functional end groups for further chemical cross-linking⁴⁰⁴⁻⁴⁰⁷.

1.7.1.1.4 PEG based graft copolymer

Poly(ethylene glycol) (PEG) or named as poly(ethylene oxide) (PEO) have been used for constructing thermoresponsive copolymer for many years as its biocompatible and hydrophilic property^{372, 408, 409}. More recently, Lutz and colleagues reported a new type of PEG-based thermoresponsive polymers with “graft” structures⁴¹⁰⁻⁴¹². By adjusting the composition of hydrophilic/hydrophobic PEG-based monomers, and molecular weight, desired LCST of the copolymer can be fine controlled. As the outstanding biocompatibility of PEG-based structure compare to other synthetic polymers, these copolymers have shown great potential for biomedical and tissue engineering applications⁴¹¹.

1.7.1.2 pH-sensitive cross-linking hydrogels

Another group of physical cross-linking hydrogels are made from pH-sensitive polymers. Either pendant acidic or basic functional groups provide these polymers capability to accept or release protons induced by the variation of environmental pH⁴¹³. These polymers with ionizable groups, also known as polyelectrolytes can further form reversible hydrogel

depending on the pH of the system ⁴¹⁴. Examples of the pH-sensitive hydrogels used in drug delivery and tissue engineering include PMA-PEG ⁴¹⁵, NIPPAm-AAc ⁴¹⁶, NIPPAm-DMAEMA (2-(dimethylamino)ethyl methacrylate) ⁴¹⁷, Pluronic[®] F127-DMAEMA ⁴¹⁸ and so forth.

1.7.2 Chemical Cross-linking Hydrogels

1.7.2.1 Photo-crosslinked hydrogels

In contrast to physical cross-linking mechanism chemical cross-linking forms irreversible and more stable hydrogels by covalent bonds. One of the most studied chemical cross-linked hydrogels are triggered by photo-polymerization between vinyl functional groups (i.e. C=C) on the polymers ^{351, 419}. Mediated by suitable photoinitiators (e.g. 2,2-dimethoxy-1-phenylacetophenone), these polymers can cross-link by exposure under visible or ultraviolet (UV) radiation both *in vitro* and *in vivo* ⁴²⁰. Advantages of the photo-crosslinking systems include rapid gelation, well-controlled reaction process, ease of combination with other chemicals or materials without affecting the cross-linking behavior ^{334, 419}. Many studies have been reported using PEG-based monomers to create photo-crosslinked hydrogels for cell delivery and tissue engineering ⁴²¹⁻⁴²³. In addition, hybrid photo-crosslinking hydrogel systems of PEG-based polymer and bioactive materials such as collagen, alginate, hyaluronic acid, alginate and chondroitin sulfate have also been developed ^{421, 422, 424}. However, there are drawbacks of these hydrogels and concerns about their clinical applications, including the cytotoxicity of photoinitiators, safety issue of UV radiation and extract cost for special equipment ⁴²⁵.

1.7.2.2 Michael-type addition reaction hydrogels

Michael-type addition reaction is another approach for *in-situ* chemical cross-linked hydrogels. For example, thiol and vinylsulfone groups on the natural or synthetic polymers can be cross-linked to form hybrid hydrogels for tissue engineering applications ^{334, 426}. Vinylsulfone, however has been demonstrated to be toxic to cells because it reacts with DNA and glutathione ⁴²⁷. Thus, a number of hydrogel systems used bioactive polymers with high molecular weight (e.g. hyaluronic acid) combining with vinylsulfone group

to reduce the toxic effect, which have been applied for both *in vitro* and *in vivo* studies^{352, 427, 428}. In addition, thiolated hyaluronic acid was also used to cross-link with vinyl-functional PEG-based polymers such as poly(ethylene glycol) diacrylate (PEGDA) via Michael-type addition reaction^{352, 428, 429}.

1.7.2.3 Schiff-base cross-linked hydrogels

Schiff-base reaction has been also used to develop *in-situ* cross-linked hydrogel systems for tissue engineering applications⁴³⁰. For example, Marra and colleagues developed water soluble *N*-Succinyl-chitosan cross-linking with oxidized hyaluronic acid for cartilage tissue engineering⁴³⁰. In this system, a rapid gelation time (about one minute) can be achieved by adjusting the ratio between amine group on *N*-Succinyl-chitosan and aldehyde group on oxidized hyaluronic acid. In addition, other type of polysaccharides can be oxidized and utilized for Schiff base-mediated cross-linking, such as dextran⁴³¹, chondroitin⁴³², gum arabic⁴³³, hyaluronic acid^{434, 435} and cellulose⁴³⁶.

1.8 Hypothesis and Objectives

The overall aim of this project was to develop an *in-situ* cross-linkable hydrogel cell delivery system which could easily encapsulate and support adipose-derived stem cells (ADSCs) growth, proliferation and secretion, with the potential use as a bioactive temporary hydrogel dressing for wound healing applications (**Figure 1.2**). The specific objective of *in vitro* studies was to design, fabricate and optimize a thermoresponsive and photo-/chemical cross-linked hydrogel system for cell delivery. The *in vivo* studies aimed to evaluate the material inflammatory response, ADSCs cell retention and therapeutic effects on wound healing (e.g. wound closure, angiogenesis) as a bioactive dressing system. The whole project was divided into three phases with specific objectives and hypotheses.

1.8.1 Phase I (Chapter Two)

Deactivation enhanced atom transfer radical polymerization (DE-ATRP) approach was first reported by Wang *et al.* for homopolymerization of divinyl monomers to achieve the synthesis of dendritic homopolymers with

multiple-vinyl functional groups without gelation⁴³⁷. The overall objective of this phase is to synthesize and optimize a PEG-based hyperbranched copolymer with thermoresponsive and photo-crosslinkable properties via DE-ATRP approach.

Hypotheses:

- PEG-based hyperbranched copolymers with high content of vinyl functional groups can be achieved by introducing the divinyl monomer into polymerization without gelation via DE-ATRP approach.
- The thermoresponsive behavior of the copolymers can be achieved by two PEG-based monomers with different hydrophilic properties. The lower critical solution temperature (LCST) of the copolymer can be adjusted close to body temperature via varying the ratio between these two monomers.
- The high content of vinyl functional groups which lead to photo-crosslinking property can be adjusted by varying the polymer composition.
- PEG-based polymer composition should not result in toxicity to cells.

Specific Objectives:

- To design and synthesize a thermoresponsive and photo-crosslinkable PEG based hyperbranched copolymer via DE-ATRP polymerization of poly(ethylene glycol) methyl ether methacrylate (PEGMEMA), 2-(2-methoxyethoxy) ethyl methacrylate (MEO₂MA) and ethylene glycol dimethacrylate (EGDMA).
- To characterize and optimize the molecular weights, chemical structures, thermoresponsive and gelation behaviors of the copolymer.
- To adjust the LCST of the copolymer close to body temperature by varying the polymer composition.
- To evaluate the cytotoxicity of this copolymer *in vitro*.

1.8.2 Phase II (Chapter Three and Four)

Compared to the photo-crosslinking hydrogel systems, chemical gelation via thiol-ene Michael-type addition reaction exhibits remarkable advantages including the ease to operate, rapid gelation, the absence of chemical initiator, no specific requirement of equipment and simple gelling condition close to physiological circumstance⁴³⁸. The overall objective of this phase is to modify the multifunctional copolymer that developed in the first phase in order to fabricate an *in-situ* physical and chemical cross-linked hydrogel system and optimize this hydrogel microenvironment with extracellular matrix (ECM) materials to support the ADSCs growth, proliferation and secretion.

Hypotheses:

- Replacement of the methacrylate multifunctional vinyl monomer with acrylate monomer can provide the copolymer *in-situ* chemical cross-linking property with thiol functional materials via Michael-type addition reaction.
- Hyaluronic acid as an important component of ECM can improve the microenvironment in the hydrogel for cell growth and improve cell viability.

Specific Objectives:

- To design and synthesize a thermoresponsive and chemical cross-linkable PEG-based hyperbranched copolymer via DE-ATRP polymerization of PEGMEMA, MEO₂MA and poly(ethylene glycol) diacrylate (PEGDA).
- To fabricate a chemical cross-linked hydrogel system for cell delivery.
- To evaluate and optimize the cell viability, morphology, activity, proliferation and secretion in the established hydrogel system.

1.8.3 Phase III (Chapter Five)

Once the optimized hydrogel system for cell delivery is achieved, the overall objective of the last phase is to evaluate the cell retention, material inflammatory response, and the wound healing effect of this *in-situ* cross-linked bioactive hydrogel dressing system *in vivo*.

Hypotheses:

- ADSCs can survive in the *in-situ* formed hydrogel system *in vivo*.
- Angiogenesis can be enhanced by applying the ADSCs encapsulated *in-situ* cross-linked bioactive hydrogel dressing.
- Wound contraction and closure can be improved by this dressing system.

Specific Objectives:

- To evaluate the ADSCs retention in the *in-situ* cross-linked hydrogel system using a rat dorsal full-thickness wound model.
- To evaluate the wound healing effect via using this bioactive hydrogel dressing system, including wound closure, epithelialization and inflammatory response and angiogenesis.

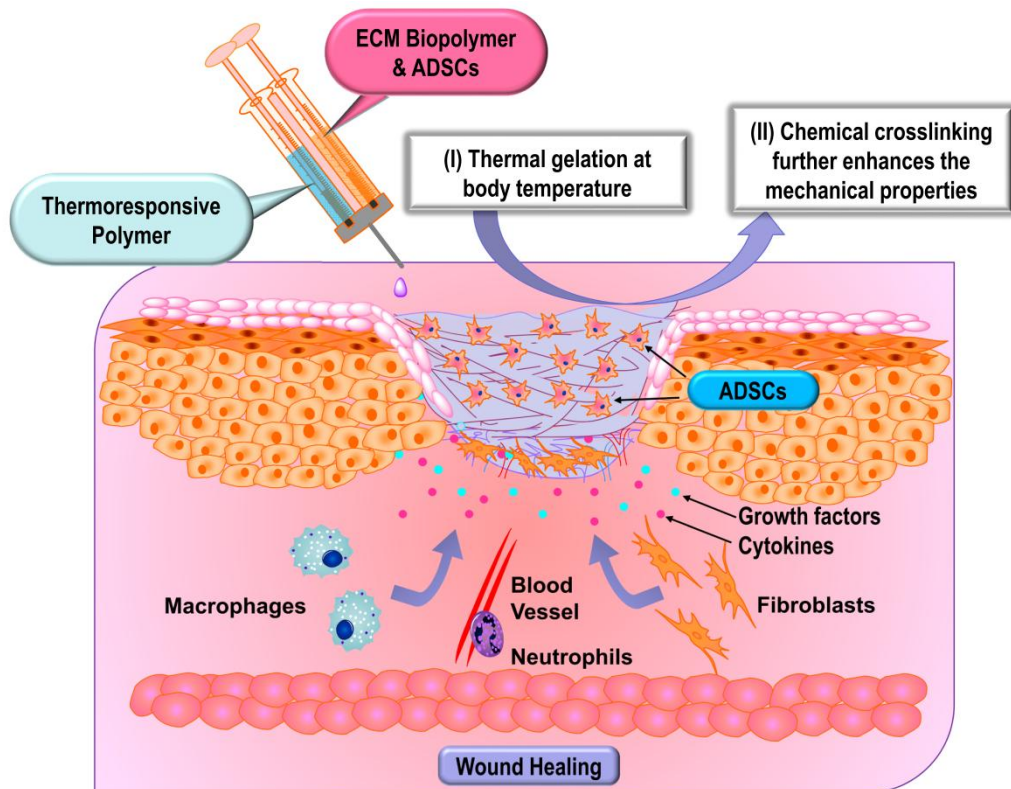


Figure 1.2: Schematic of *in-situ* cross-linked hydrogel cell delivery system for wound healing: the hybrid polymer mixture is a solution at room temperature but form physical gels once applied onto the skin to cover and seal wound sites at body temperature. Furthermore, chemical cross-linking with ECM biopolymers occurs in minutes to achieve a stable hydrogel with enhanced mechanical properties. Thus the implanted ADSCs can survive, proliferate in the hydrogel, and secrete growth factors and cytokines which would affect the wound healing process.

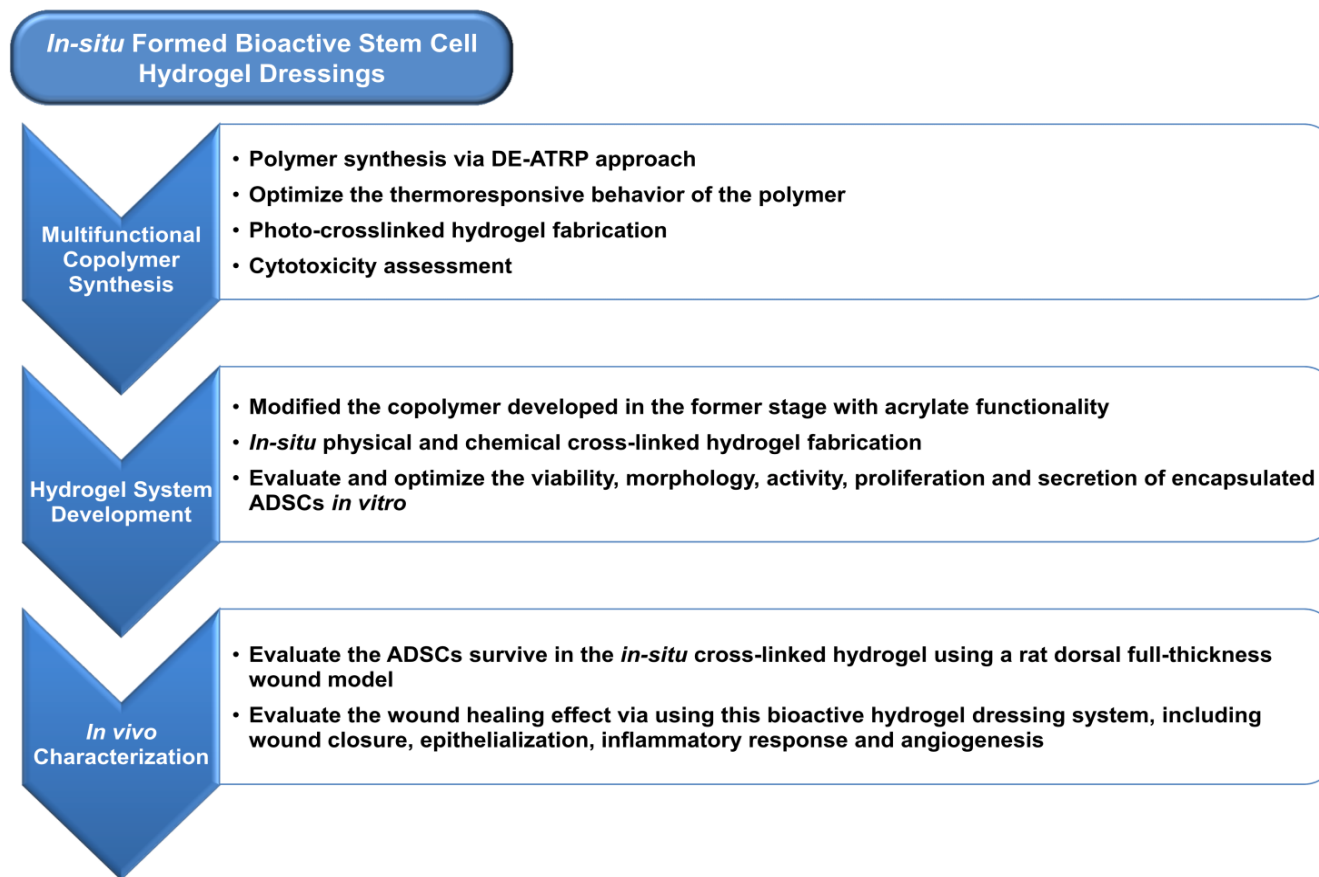


Figure 1.3: Project overview.

1.9 References

1. Lazarus, G. S.; Cooper, D. M.; Knighton, D. R.; Margolis, D. J.; Pecoraro, R. E.; Rodeheaver, G.; Robson, M. C., Definitions and guidelines for assessment of wounds and evaluation of healing. *Archives of Dermatology* 1994, 130, (4), 489-493.
2. Boateng, J. S.; Matthews, K. H.; Stevens, H. N. E.; Eccleston, G. M., Wound healing dressings and drug delivery systems: A review. *Journal of Pharmaceutical Sciences* 2008, 97, (8), 2892-2923.
3. Percival, N. J., Classification of wounds and their management. *Surgery (Oxford)* 2002, 20, (5), 114-117.
4. Harding, K. G.; Morris, H. L.; Patel, G. K., Science, medicine, and the future - Healing chronic wounds. *British Medical Journal* 2002, 324, (7330), 160-163.
5. Moore, K.; McCallion, R.; Searle, R. J.; Stacey, M. C.; Harding, K. G., Prediction and monitoring the therapeutic response of chronic dermal wounds. *International Wound Journal* 2006, 3, (2), 89-96.
6. Singer, A. J.; Clark, R. A. F., Mechanisms of disease - cutaneous wound healing. *New England Journal of Medicine* 1999, 341, (10), 738-746.
7. Strodtbeck, F., Physiology of wound healing. *Newborn and Infant Nursing Reviews* 2001, 1, (1), 43-52.
8. Werner, S.; Grose, R., Regulation of wound healing by growth factors and cytokines. *Physiological Reviews* 2003, 83, (3), 835-870.
9. Barrientos, S.; Stojadinovic, O.; Golinko, M. S.; Brem, H.; Tomic-Canic, M., Growth factors and cytokines in wound healing. *Wound Repair and Regeneration* 2008, 16, (5), 585-601.
10. Behm, B.; Babilas, P.; Landthaler, M.; Schreml, S., Cytokines, chemokines and growth factors in wound healing. *Journal of the European Academy of Dermatology and Venereology* 2012, 26, (7), 812-820.
11. Cooper, D. M., Wound healing: New understandings. *Nurse Practitioner Forum-Current Topics and Communications* 1999, 10, (2), 74-86.
12. Steed, D. L., The role of growth factors in wound healing. *Surgical Clinics of North America* 1997, 77, (3), 575.
13. Garrett, B.; Garrett, S. B., Cellular communication and the action of growth factors during wound healing. *Journal of Wound Care* 1997, 6, (6), 277-80.
14. Gorchach, A.; Brandes, R. P.; Bassus, S.; Kronemann, N.; Kirchmaier, C. M.; Busse, R.; Schini-Kerth, V. B., Oxidative stress and expression of p22phox are involved in the up-regulation of tissue factor in vascular smooth muscle cells in response to activated platelets. *Faseb Journal* 2000, 14, (11), 1518-1528.

15. Schreml, S.; Szeimies, R. M.; Prantl, L.; Karrer, S.; Landthaler, M.; Babilas, P., Oxygen in acute and chronic wound healing. *British Journal of Dermatology* 2010, 163, (2), 257-268.
16. Soneja, A.; Drews, M.; Malinski, T., Role of nitric oxide, nitroxidative and oxidative stress in wound healing. *Pharmacological Reports* 2005, 57, 108-119.
17. Eming, S. A.; Krieg, T.; Davidson, J. M., Inflammation in wound repair: Molecular and cellular mechanisms. *Journal of Investigative Dermatology* 2007, 127, (3), 514-525.
18. Brinkmann, V.; Reichard, U.; Goosmann, C.; Fauler, B.; Uhlemann, Y.; Weiss, D. S.; Weinrauch, Y.; Zychlinsky, A., Neutrophil extracellular traps kill bacteria. *Science* 2004, 303, (5663), 1532-1535.
19. Schaefer, M.; Werner, S., Oxidative stress in normal and impaired wound repair. *Pharmacological Research* 2008, 58, (2), 165-171.
20. Kuemin, A.; Schaefer, M.; Epp, N.; Bugnon, P.; Born-Berclaz, C.; Oxenius, A.; Klippel, A.; Bloch, W.; Werner, S., Peroxiredoxin 6 is required for blood vessel integrity in wounded skin. *Journal of Cell Biology* 2007, 179, (4), 747-760.
21. Wang, X. S.; Phelan, S. A.; Forsman-Semb, K.; Taylor, E. F.; Petros, C.; Brown, A.; Lerner, C. P.; Paigen, B., Mice with targeted mutation of peroxiredoxin 6 develop normally but are susceptible to oxidative stress. *Journal of Biological Chemistry* 2003, 278, (27), 25179-25190.
22. Beyer, T. A.; Keller, U. a. d.; Braun, S.; Schaefer, M.; Werner, S., Roles and mechanisms of action of the Nrf2 transcription factor in skin morphogenesis, wound repair and skin cancer. *Cell Death and Differentiation* 2007, 14, (7), 1250-1254.
23. Davidson, J. M., First-class delivery: Getting growth factors to their destination. *Journal of Investigative Dermatology* 2008, 128, (6), 1360-1362.
24. Braun, S.; Keller, U. A. D.; Steiling, H.; Werner, S., Fibroblast growth factors in epithelial repair and cytoprotection. *Philosophical Transactions of the Royal Society of London Series B-Biological Sciences* 2004, 359, (1445), 753-757.
25. Martin, P., Wound healing - Aiming for perfect skin regeneration. *Science* 1997, 276, (5309), 75-81.
26. Hubner, G.; Brauchle, M.; Smola, H.; Madlener, M.; Fassler, R.; Werner, S., Differential regulation of pro-inflammatory cytokines during wound healing in normal and glucocorticoid-treated mice. *Cytokine* 1996, 8, (7), 548-556.
27. Rappolee, D. A.; Mark, D.; Banda, M. J.; Werb, Z., Wound macrophages express TGF-ALPHA and other growth-factors invivo - Analysis by messenger RNA phenotype. *Science* 1988, 241, (4866), 708-712.

28. Leibovich, S. J.; Ross, R., Role of macrophage in wound repair - Study with hydrocortisone and antimacrophage serum. *American Journal of Pathology* 1975, 78, (1), 71-99.
29. Haas, A., Wound healing. *Dermatology Nursing* 1995, 7, 28-34.
30. Witte, M. B.; Barbul, A., Role of nitric oxide in wound repair. *American Journal of Surgery* 2002, 183, (4), 406-412.
31. Schulz, G.; Stechmiller, J., Wound healing and nitric oxide production: too little or too much may impair healing and cause chronic wounds. *The international journal of lower extremity wounds* 2006, 5, (1), 6-8.
32. Martin, P.; Leibovich, S. J., Inflammatory cells during wound, repair: the good, the bad and the ugly. *Trends in Cell Biology* 2005, 15, (11), 599-607.
33. Kim, I.; Moon, S. O.; Kim, S. H.; Kim, H. J.; Koh, Y. S.; Koh, G. Y., Vascular endothelial growth factor expression of intercellular adhesion molecule 1 (ICAM-1), vascular cell adhesion molecule 1 (VCAM-1), and E-selectin through nuclear factor-kappa B activation in endothelial cells. *Journal of Biological Chemistry* 2001, 276, (10), 7614-7620.
34. Min, J. K.; Lee, Y. M.; Kim, J. H.; Kim, Y. M.; Kim, S. W.; Lee, S. Y.; Gho, Y. S.; Oh, G. T.; Kwon, Y. G., Hepatocyte growth factor suppresses vascular endothelial growth factor-induced expression of endothelial ICAM-1 and VCAM-1 by inhibiting the nuclear factor-kappa B pathway. *Circulation Research* 2005, 96, (3), 300-307.
35. Nagaoka, T.; Kaburagi, Y.; Hamaguchi, Y.; Hasegawa, M.; Takehara, K.; Steeber, D. A.; Tedder, T. F.; Sato, S., Delayed wound healing in the absence of intercellular adhesion molecule-1 or L-selectin expression. *American Journal of Pathology* 2000, 157, (1), 237-247.
36. Yukami, T.; Hasegawa, M.; Matsushita, Y.; Fujita, T.; Matsushita, T.; Horikawa, M.; Komura, K.; Yanaba, K.; Hamaguchi, Y.; Nagaoka, T.; Ogawa, F.; Fujimoto, M.; Steeber, D. A.; Tedder, T. F.; Takehara, K.; Sato, S., Endothelial selectins regulate skin wound healing in cooperation with L-selectin and ICAM-1. *Journal of Leukocyte Biology* 2007, 82, (3), 519-531.
37. Qiu, C.; Coutinho, P.; Frank, S.; Franke, S.; Law, L. Y.; Martin, P.; Green, C. R.; Becker, D. L., Targeting connexin43 expression accelerates the rate of wound repair. *Current Biology* 2003, 13, (19), 1697-1703.
38. Ishida, Y.; Gao, J.-L.; Murphy, P. M., Chemokine receptor CX3CR1 mediates skin wound healing by promoting macrophage and fibroblast accumulation and function. *Journal of Immunology* 2008, 180, (1), 569-579.
39. Paladini, R. D.; Takahashi, K.; Bravo, N. S.; Coulombe, P. A., Onset of re-epithelialization after skin injury correlates with a reorganization of keratin filaments in wound edge keratinocytes: Defining a potential role for keratin 16. *Journal of Cell Biology* 1996, 132, (3), 381-397.
40. Goliger, J. A.; Paul, D. L., Wounding alters epidermal connexin expression and gap junction-mediated intercellular communication. *Molecular Biology of the Cell* 1995, 6, (11), 1491-1501.

41. Clark, R. A. F.; Ashcroft, G. S.; Spencer, M. J.; Larjava, H.; Ferguson, M. W. J., Re-epithelialization of normal human excisional wounds is associated with a switch from alpha v beta 5 to alpha v beta 6 integrins. *British Journal of Dermatology* 1996, 135, (1), 46-51.
42. Garrett, B., Re-epithelialisation. *Journal of Wound Care* 1998, 7, (7), 358-359.
43. Powers, C. J.; McLeskey, S. W.; Wellstein, A., Fibroblast growth factors, their receptors and signaling. *Endocrine-Related Cancer* 2000, 7, (3), 165-197.
44. Bikfalvi, A.; Klein, S.; Pintucci, G.; Rifkin, D. B., Biological roles of fibroblast growth factor-2. *Endocrine Reviews* 1997, 18, (1), 26-45.
45. Robson, M. C.; Hill, D. P.; Smith, P. D.; Wang, X.; Meyer-Siegler, K.; Ko, F.; VandeBerg, J. S.; Payne, W. G.; Ochs, D.; Robson, L. E., Sequential cytokine therapy for pressure ulcers: Clinical and mechanistic response. *Annals of Surgery* 2000, 231, (4), 600-611.
46. Sogabe, Y.; Abe, M.; Yokoyama, Y.; Ishikawa, O., Basic fibroblast growth factor stimulates human keratinocyte motility by Rac activation. *Wound Repair and Regeneration* 2006, 14, (4), 457-462.
47. Shirakata, Y.; Kimura, R.; Nanba, D.; Iwamoto, R.; Tokumaru, S.; Morimoto, C.; Yokota, K.; Nakamura, M.; Sayama, K.; Mekada, E.; Higashiyama, S.; Hashimoto, K., Heparin-binding EGF-like growth factor accelerates keratinocyte migration and skin wound healing. *Journal of Cell Science* 2005, 118, (11), 2363-2370.
48. Oda, K.; Matsuoka, Y.; Funahashi, A.; Kitano, H., A comprehensive pathway map of epidermal growth factor receptor signaling. *Molecular Systems Biology* 2005, 1:2005.0010.
49. Wang, Y.; Weil, B. R.; Herrmann, J. L.; Abarbanell, A. M.; Tan, J.; Markel, T. A.; Kelly, M. L.; Meldrum, D. R., MEK, p38, and PI-3K mediate cross talk between EGFR and TNFR in enhancing hepatocyte growth factor production from human mesenchymal stem cells. *American Journal of Physiology-Cell Physiology* 2009, 297, (5), C1284-C1293.
50. Yoshida, S.; Yamaguchi, Y.; Itami, S.; Yoshikawa, K.; Tabata, Y.; Matsumoto, K.; Nakamura, T., Neutralization of hepatocyte growth factor leads to retarded cutaneous wound healing associated with decreased neovascularization and granulation tissue formation. *Journal of Investigative Dermatology* 2003, 120, (2), 335-343.
51. Lin, Z. Q.; Kondo, T.; Ishida, Y.; Takayasu, T.; Mukaida, N., Essential involvement of IL-6 in the skin wound-healing process as evidenced by delayed wound healing in IL-6-deficient mice. *Journal of Leukocyte Biology* 2003, 73, (6), 713-721.
52. McFarland-Mancini, M. M.; Funk, H. M.; Paluch, A. M.; Zhou, M.; Giridhar, P. V.; Mercer, C. A.; Kozma, S. C.; Drew, A. F., Differences in wound healing in mice with deficiency of IL-6 versus IL-6 receptor. *Journal of Immunology* 2010, 184, (12), 7219-7228.

53. Diegelmann, R. F.; Evans, M. C., Wound healing: An overview of acute, fibrotic and delayed healing. *Frontiers in Bioscience* 2004, 9, 283-289.
54. Gailit, J.; Welch, M. P.; Clark, R. A. F., TGF-BETA-1 stimulates expression of keratinocyte integrins during reepithelialization of cutaneous wounds. *Journal of Investigative Dermatology* 1994, 103, (2), 221-227.
55. Amendt, C.; Mann, A.; Schirmacher, P.; Blessing, M., Resistance of keratinocytes to TGF beta-mediated growth restriction and apoptosis induction accelerates re-epithelialization in skin wounds. *Journal of Cell Science* 2002, 115, (10), 2189-2198.
56. Ashcroft, G. S.; Yang, X.; Glick, A. B.; Weinstein, M.; Letterio, J. J.; Mizel, D. E.; Anzano, M.; Greenwell-Wild, T.; Wahl, S. M.; Deng, C. X.; Roberts, A. B., Mice lacking Smad3 show accelerated wound healing and an impaired local inflammatory response. *Nature Cell Biology* 1999, 1, (5), 260-266.
57. Munger, J. S.; Sheppard, D., Cross talk among TGF-beta signaling pathways, integrins, and the extracellular matrix. *Cold Spring Harbor Perspectives in Biology* 2011, 3, (11) a005017.
58. Armstrong, D. G.; Jude, E. B., The role of matrix metalloproteinases in wound healing. *Journal of the American Podiatric Medical Association* 2002, 92, (1), 12-18.
59. Ravanti, L.; Kahari, V. M., Matrix metalloproteinases in wound repair (Review). *International Journal of Molecular Medicine* 2000, 6, (4), 391-407.
60. Saarialhokere, U. K.; Chang, E. S.; Welgus, H. G.; Parks, W. C., Distinct localization of collagenase and tissue inhibitor of metalloproteinases expression in wound-healing associated with ulcerative pyogenic granuloma. *Journal of Clinical Investigation* 1992, 90, (5), 1952-1957.
61. Salo, T.; Makela, M.; Kylmaniemi, M.; Autioharmainen, H.; Larjava, H., Expression of matrix metalloproteinase-2 and metalloproteinase-9 during early human wound healing. *Laboratory Investigation* 1994, 70, (2), 176-182.
62. Saarialhokere, U. K.; Pentland, A. P.; Birkedalhansen, H.; Parks, W. C.; Welgus, H. G., Distinct populations of basal keratinocytes express stromelysin-1 and stromelysin-2 in chronic wounds. *Journal of Clinical Investigation* 1994, 94, (1), 79-88.
63. Clark, R. A. F.; Lanigan, J. M.; Dellapelle, P.; Manseau, E.; Dvorak, H. F.; Colvin, R. B., Fibronectin and fibrin provide a provisional matrix for epidermal-cell migration during wound reepithelialization. *Journal of Investigative Dermatology* 1982, 79, (5), 264-269.
64. Li, J.; Zhang, Y. P.; Kirsner, R. S., Angiogenesis in wound repair: Angiogenic growth factors and the extracellular matrix. *Microscopy Research and Technique* 2003, 60, (1), 107-114.

65. Hickey, M. M.; Simon, M. C., Regulation of angiogenesis by hypoxia and hypoxia-inducible factors. *Current Topics in Developmental Biology* 2006, 76, 217-257.
66. Chen, L.; Endler, A.; Shibasaki, F., Hypoxia and angiogenesis: regulation of hypoxia-inducible factors via novel binding factors. *Experimental and Molecular Medicine* 2009, 41, (12), 849-857.
67. Breen, E. C., VEGF in biological control. *Journal of Cellular Biochemistry* 2007, 102, (6), 1358-1367.
68. Bao, P.; Kodra, A.; Tomic-Canic, M.; Golinko, M. S.; Ehrlich, H. P.; Brem, H., The role of vascular endothelial growth factor in wound healing. *Journal of Surgical Research* 2009, 153, (2), 347-358.
69. Ma, J.; Wang, Q.; Fei, T.; Han, J.-D. J.; Chen, Y.-G., MCP-1 mediates TGF-beta-induced angiogenesis by stimulating vascular smooth muscle cell migration. *Blood* 2007, 109, (3), 987-994.
70. Knighton, D. R.; Phillips, G. D.; Fiegel, V. D., Wound-healing angiogenesis - Indirect stimulation by basic fibroblast growth-factor. *Journal of Trauma-Injury Infection and Critical Care* 1990, 30, (12), S134-S144.
71. Chen, C. C.; Mo, F. E.; Lau, L. F., The angiogenic factor Cyr61 activates a genetic program for wound healing in human skin fibroblasts. *Journal of Biological Chemistry* 2001, 276, (50), 47329-47337.
72. Pola, R.; Ling, L. E.; Silver, M.; Corbley, M. J.; Kearney, M.; Pepinsky, R. B.; Shapiro, R.; Taylor, F. R.; Baker, D. P.; Asahara, T.; Isner, J. M., The morphogen Sonic hedgehog is an indirect angiogenic agent upregulating two families of angiogenic growth factors. *Nature Medicine* 2001, 7, (6), 706-711.
73. Pintucci, G.; Bikfalvi, A.; Klein, S.; Rifkin, D. B., Angiogenesis and the fibrinolytic system. *Seminars in Thrombosis and Hemostasis* 1996, 22, (6), 517-524.
74. Folkman, J., Angiogenesis and angiogenesis inhibition: an overview. *Exs* 1997, 79, 1-8.
75. Beer, H. D.; Longaker, M. T.; Werner, S., Reduced expression of PDGF and PDGF receptors during impaired wound healing. *Journal of Investigative Dermatology* 1997, 109, (2), 132-138.
76. Schiller, M.; Javelaud, D.; Mauviel, A., TGF-beta-induced SMAD signaling and gene regulation: consequences for extracellular matrix remodeling and wound healing. *Journal of Dermatological Science* 2004, 35, (2), 83-92.
77. Robson, M. C.; Phillips, L. G.; Lawrence, W. T.; Bishop, J. B.; Youngerman, J. S.; Hayward, P. G.; Broemeling, L. D.; Heggors, J. P., The safety and effect of topically applied recombinant basic fibroblast growth-factor on the healing of chronic pressure sores. *Annals of Surgery* 1992, 216, (4), 401-408.

78. Clark, R. A. F.; Nielsen, L. D.; Welch, M. P.; McPherson, J. M., Collagen matrices attenuate the collagen-synthetic response of cultured fibroblasts to TGF-BETA. *Journal of Cell Science* 1995, 108, 1251-1261.
79. Vaalamo, M.; Mattila, L.; Johansson, N.; Kariniemi, A. L.; KarjalainenLindsberg, M. L.; Kahari, V. M.; SaarialhoKere, U., Distinct populations of stromal cells express collagenase-3 (MMP-13) and collagenase-1 (MMP-1) in chronic ulcers but not in normally healing wounds. *Journal of Investigative Dermatology* 1997, 109, (1), 96-101.
80. Desmouliere, A.; Redard, M.; Darby, I.; Gabbiani, G., Apoptosis mediates the decrease in cellularity during the transition between granulation-tissue and scar. *American Journal of Pathology* 1995, 146, (1), 56-66.
81. Kerstein, M. D., The scientific basis of healing. *Advances in Wound Care : the Journal for Prevention and Healing* 1997, 10, (3), 30-6.
82. Montesano, R.; Orci, L., Transforming growth factor-BETA stimulates collagen-matrix contraction by fibroblasts - implications for wound healing. *Proceedings of the National Academy of Sciences of the United States of America* 1988, 85, (13), 4894-4897.
83. Clark, R. A. F.; Folkvord, J. M.; Hart, C. E.; Murray, M. J.; McPherson, J. M., Platelet isoforms of platelet - derived growth-factors stimulate fibroblasts to contract collagen matrices. *Journal of Clinical Investigation* 1989, 84, (3), 1036-1040.
84. Schiro, J. A.; Chan, B. M. C.; Roswit, W. T.; Kassner, P. D.; Pentland, A. P.; Hemler, M. E.; Eisen, A. Z.; Kupper, T. S., Integrin-ALPHA-2-BETA-1 (VLA-2) mediates reorganization and contraction of collagen matrices by human cells. *Cell* 1991, 67, (2), 403-410.
85. Woodley, D. T.; Yamauchi, M.; Wynn, K. C.; Mechanic, G.; Briggaman, R. A., Collagen telopeptides (cross-linking sites) plays role in collagen gel lattice contraction. *Journal of Investigative Dermatology* 1991, 97, (3), 580-585.
86. Schultz, G. S.; Barillo, D. J.; Mazingo, D. W.; Chin, G. A.; Wound Bed Advisory Board, M., Wound bed preparation and a brief history of TIME. *International Wound Journal* 2004, 1, (1), 19-32.
87. Streuli, C., Extracellular matrix remodelling and cellular differentiation. *Current Opinion in Cell Biology* 1999, 11, (5), 634-640.
88. Lamar, J. M.; Iyer, V.; DiPersio, M., Integrin alpha 3 beta 1 potentiates TGF beta-mediated induction of MMP-9 in immortalized keratinocytes. *Journal of Investigative Dermatology* 2008, 128, (3), 575-586.
89. Yuan, W. H.; Varga, J., Transforming growth factor-beta repression of matrix metalloproteinase-1 in dermal fibroblasts involves Smad3. *Journal of Biological Chemistry* 2001, 276, (42), 38502-38510.
90. Stuelten, C. H.; Byfield, S. D.; Arany, P. R.; Karpova, T. S.; Stetler-Stevenson, W. G.; Roberts, A. B., Breast cancer cells induce stromal fibroblasts to express MMP-9 via secretion of TNF-alpha and TGF-beta. *Journal of Cell Science* 2005, 118, (10), 2143-2153.

91. Philipp, K.; Riedel, F.; Germann, G.; Hormann, K.; Sauerbier, M., TGF-beta antisense oligonucleotides reduce mRNA expression of matrix metalloproteinases in cultured wound-healing-related cells. *International Journal of Molecular Medicine* 2005, 15, (2), 299-303.
92. Boniface, K.; Bernard, F. X.; Garcia, M.; Gurney, A. L.; Lecron, J. C.; Morel, F., IL-22 inhibits epidermal differentiation and induces proinflammatory gene expression and migration of human keratinocytes. *Journal of Immunology* 2005, 174, (6), 3695-3702.
93. Mast, B. A.; Schultz, G. S., Interactions of cytokines, growth factors, and proteases in acute and chronic wounds. *Wound Repair and Regeneration* 1996, 4, (4), 411-420.
94. Satish, L.; Yager, D.; Wells, A., Glu-Leu-Arg-negative CXC chemokine interferon gamma inducible protein-9 as a mediator of epidermal-dermal communication during wound repair. *Journal of Investigative Dermatology* 2003, 120, (6), 1110-1117.
95. Yates, C. C.; Whaley, D.; Kulasekeran, P.; Hancock, W. W.; Lu, B.; Bodnar, R.; Newsome, J.; Hebda, P. A.; Wells, A., Delayed and deficient dermal maturation in mice lacking the CXCR3 ELR-negative CXC chemokine receptor. *American Journal of Pathology* 2007, 171, (2), 484-495.
96. Fonder, M. A.; Lazarus, G. S.; Cowan, D. A.; Aronson-Cook, B.; Kohli, A. R.; Mamelak, A. J., Treating the chronic wound: A practical approach to the care of nonhealing wounds and wound care dressings. *Journal of the American Academy of Dermatology* 2008, 58, (2), 185-206.
97. Epstein, E. H., Molecular-genetics of epidermolysis-bullosa. *Science* 1992, 256, (5058), 799-804.
98. Niessen, F. B.; Spauwen, P. H. M.; Schalkwijk, J.; Kon, M., On the nature of hypertrophic scars and keloids: A review. *Plastic and Reconstructive Surgery* 1999, 104, (5), 1435-1458.
99. Barrick, B.; Campbell, E. J.; Owen, C. A., Leukocyte proteinases in wound healing: roles in physiologic and pathologic processes. *Wound Repair and Regeneration* 1999, 7, (6), 410-422.
100. Agren, M. S.; Steenfoss, H. H.; Dabelsteen, S.; Hansen, J. B.; Dabelsteen, E., Proliferation and mitogenic response to PDGF-BB of fibroblasts isolated from chronic venous leg ulcers is ulcer-age dependent. *Journal of Investigative Dermatology* 1999, 112, (4), 463-469.
101. Hasan, A.; Murata, H.; Falabella, A.; Ochoa, S.; Zhou, L.; Badiavas, E.; Falanga, V., Dermal fibroblasts from venous ulcers are unresponsive to the action of transforming growth factor-beta 1. *Journal of Dermatological Science* 1997, 16, (1), 59-66.
102. Stanley, A. C.; Park, H. Y.; Phillips, T. J.; Russakovsky, V.; Menzoian, J. O., Reduced growth of dermal fibroblasts from chronic venous ulcers can be stimulated with growth factors. *Journal of Vascular Surgery* 1997, 26, (6), 994-999.

103. Gottrup, F.; Apelqvist, J.; Price, P.; Outcome, E. W. M. A. P., Outcomes in controlled and comparative studies on non-healing wounds: recommendations to improve the quality of evidence in wound management. *Journal of Wound Care* 2010, 19, (6), 237-268.
104. Posnett, J.; Franks, P. J., The burden of chronic wounds in the UK. *Nursing Times* 2008, 104, (3), 44-45.
105. Kim, J. H.; Lee, S. B.; Kim, S. J.; Lee, Y. M., Rapid temperature/pH response of porous alginate-g-poly(N-isopropylacrylamide) hydrogels. *Polymer* 2002, 43, (26), 7549-7558.
106. Ferreira, M. C.; Tuma, P., Jr.; Carvalho, V. F.; Kamamoto, F., Complex wounds. *Clinics (Sao Paulo, Brazil)* 2006, 61, (6), 571-578.
107. Gentzkow, G. D.; Iwasaki, S. D.; Hershon, K. S.; Mengel, M.; Prendergast, J. J.; Ricotta, J. J.; Steed, D. P.; Lipkin, S., Use of dermagraft, a cultured human dermis, to treat diabetic foot ulcers. *Diabetes Care* 1996, 19, (4), 350-354.
108. Ruckley, C. V., Socioeconomic impact of chronic venous insufficiency and leg ulcers. *Angiology* 1997, 48, (1), 67-69.
109. Waterlow, J., Tissue viability. Prevention is cheaper than cure. *Nursing Times* 1988, 84, (25), 69-70.
110. Abbade, L. P. F.; Lastoria, S., Venous ulcer: epidemiology, physiopathology, diagnosis and treatment. *International Journal of Dermatology* 2005, 44, (6), 449-456.
111. Robson, M. C.; Cooper, D. M.; Aslam, R.; Gould, L. J.; Harding, K. G.; Margolis, D. J.; Ochs, D. E.; Serena, T. E.; Snyder, R. J.; Steed, D. L.; Thomas, D. R.; Wiersma-Bryant, L., Guidelines for the treatment of venous ulcers. *Wound Repair and Regeneration* 2006, 14, (6), 649-662.
112. Whittington, K. T.; Briones, R., National Prevalence and Incidence Study: 6-year sequential acute care data. *Advances in Skin & Wound care* 2004, 17, (9), 490-494.
113. Vanderwee, K.; Clark, M.; Dealey, C.; Gunningberg, L.; Defloor, T., Pressure ulcer prevalence in Europe: a pilot study. *Journal of Evaluation in Clinical Practice* 2007, 13, (2), 227-235.
114. Reddy, M.; Gill, S. S.; Rochon, P. A., Preventing pressure ulcers: A systematic review. *Jama-Journal of the American Medical Association* 2006, 296, (8), 974-984.
115. Freiman, A.; Bird, G.; Metelitsa, A. I.; Barankin, B.; Lauzon, G. J., Cutaneous effects of smoking. *Journal of Cutaneous Medicine and Surgery* 2004, 8, (6), 415-423.
116. Bansal, C.; Scott, R.; Stewart, D.; Cockerell, C. J., Decubitus ulcers: A review of the literature. *International Journal of Dermatology* 2005, 44, (10), 805-810.
117. Reiber, G. E., The epidemiology of diabetic foot problems. *Diabetic Medicine* 1996, 13, S6-S11.

118. Jeffcoate, W. J.; Harding, K. G., Diabetic foot ulcers. *Lancet* 2003, 361, (9368), 1545-1551.
119. National diabetes fact sheet:national estimates and general information on diabetes and prediabetes in the United States, 2011. In Prevention, C. f. D. C. a., Ed. Department of Health and Human Services, Centers for Disease Control and Prevention Atlanta, GA, U.S., 2011.
120. Gordois, A.; Scuffham, P.; Shearer, A.; Oqlesby, A.; Tobian, JA. The health care costs of diabetic peripheral neuropathy in the UK (Cost-of-illness study). *The Diabetic Foot* 2003, 6, (2), 62-73.
121. Boulton, A. J. M.; Vileikyte, L.; Ragnarson-Tennvall, G.; Apelqvist, J., The global burden of diabetic foot disease. *Lancet* 2005, 366, (9498), 1719-1724.
122. Wild, S.; Roglic, G.; Green, A.; Sicree, R.; King, H., Global prevalence of diabetes - Estimates for the year 2000 and projections for 2030. *Diabetes Care* 2004, 27, (5), 1047-1053.
123. Shaw, J. E.; Sicree, R. A.; Zimmet, P. Z., Global estimates of the prevalence of diabetes for 2010 and 2030. *Diabetes Research and Clinical Practice* 2010, 87, (1), 4-14.
124. Zhang, P.; Zhang, X.; Brown, J.; Vistisen, D.; Sicree, R.; Shaw, J.; Nichols, G., Global healthcare expenditure on diabetes for 2010 and 2030. *Diabetes Research and Clinical Practice* 2010, 87, (3), 293-301.
125. Rovee, D. T., Evolution of wound dressing and their effects on the healing process. *Clinical Materials* 1991, 8, (3-4), 183-188.
126. Mathus-Vliegen, E. M. H., Old age, malnutrition, and pressure sores: An ill-fated alliance. *Journals of Gerontology Series A-Biological Sciences and Medical Sciences* 2004, 59, (4), 355-360.
127. Thomas, D. R., Improving outcome of pressure ulcers with nutritional interventions: A review of the evidence. *Nutrition* 2001, 17, (2), 121-125.
128. Seah, C. C.; Phillips, T. J.; Howard, C. E.; Panova, I. P.; Hayes, C. M.; Asandra, A. S.; Park, H. Y., Chronic wound fluid suppresses proliferation of dermal fibroblasts through a ras-mediated signaling pathway. *Journal of Investigative Dermatology* 2005, 124, (2), 466-474.
129. Phillips, T. J.; al-Amoudi, H. O.; Leverkus, M.; Park, H. Y., Effect of chronic wound fluid on fibroblasts. *Journal of Wound Care* 1998, 7, (10), 527-532.
130. Medina, A.; Scott, P. G.; Ghahary, A.; Tredget, E. E., Pathophysiology of chronic nonhealing wounds. *Journal of Burn Care & Rehabilitation* 2005, 26, (4), 306-319.
131. Laato, M.; Niinikoski, J.; Lundberg, C.; Gerdin, B., Inflammatory reaction and blood-flow in experimental wounds inoculated with staphylococcus-aureus. *European Surgical Research* 1988, 20, (1), 33-38.

132. Bowler, P. G.; Davies, B. J., The microbiology of infected and noninfected leg ulcers. *International Journal of Dermatology* 1999, 38, (8), 573-578.
133. Bowler, P. G.; Duerden, B. I.; Armstrong, D. G., Wound microbiology and associated approaches to wound management. *Clinical Microbiology Reviews* 2001, 14, (2), 244.
134. Krasner, D., Minimizing factors that impair wound healing: a nursing approach. *Ostomy/Wound Management* 1995, 41, (1), 22-6, 28, 31-32.
135. Balin, A. K.; Pratt, L., Dilute povidone-iodine solutions inhibit human skin fibroblast growth. *Dermatologic Surgery* 2002, 28, (3), 210-214.
136. Branemar.Pi; Ekholm, R., Tissue injury caused by wound disinfectants. *Journal of Bone and Joint Surgery-American Volume* 1967, A 49, (1), 48.
137. Damour, O.; Hua, S. Z.; Lasne, F.; Villain, M.; Rousselle, P.; Collombel, C., Cytotoxicity evaluation of antiseptics and antibiotics on cultured human fibroblasts and keratinocytes. *Burns* 1992, 18, (6), 479-485.
138. Oberg, M. S.; Lindsey, D., Do not put hydrogen-peroxide or povidone iodine into wounds. *American Journal of Diseases of Children* 1987, 141, (1), 27-28.
139. Bradley, M.; Cullum, N.; Sheldon, T., The debridement of chronic wounds: a systematic review. *Health Technology Assessment* 1999, 3, (17 Pt 1), iii-iv, 1-78.
140. Wolcott, R. D.; Kennedy, J. P.; Dowd, S. E., Regular debridement is the main tool for maintaining a healthy wound bed in most chronic wounds. *Journal of Wound Care* 2009, 18, (2), 54-6.
141. Grey, J. E.; Enoch, S.; Harding, K. G., ABC of wound healing - Venous and arterial leg ulcers. *British Medical Journal* 2006, 332, (7537), 347-350.
142. Williams, D.; Enoch, S.; Miller, D.; Harris, K.; Price, P.; Harding, K. G., Effect of sharp debridement using curette on recalcitrant nonhealing venous leg ulcers: A concurrently controlled, prospective cohort study. *Wound Repair and Regeneration* 2005, 13, (2), 131-137.
143. Steed, D. L., Debridement. *American Journal of Surgery* 2004, 187, (5A), 71S-74S.
144. Konig, M.; Vanscheidt, W.; Augustin, M.; Kapp, H., Enzymatic versus autolytic debridement of chronic leg ulcers: a prospective randomised trial. *Journal of Wound Care* 2005, 14, (7), 320-323.
145. Inngjerdinger, K.; Nergard, C. S.; Diallo, D.; Mounkoro, P. P.; Paulsen, B. S., An ethnopharmacological survey of plants used for wound healing in Dogonland, Mali, West Africa. *Journal of Ethnopharmacology* 2004, 92, (2-3), 233-244.
146. Mensah, A. Y.; Houghton, P. J.; Dickson, R. A.; Fleischer, T. C.; Heinrich, M.; Bremner, P., In vitro evaluation of effects of two Ghanaian

- plants relevant to wound healing. *Phytotherapy Research* 2006, 20, (11), 941-944.
147. Zahedi, P.; Rezaeian, I.; Ranaei-Siadat, S.-O.; Jafari, S.-H.; Supaphol, P., A review on wound dressings with an emphasis on electrospun nanofibrous polymeric bandages. *Polymers for Advanced Technologies* 2010, 21, (2), 77-95.
148. Purna, S. K.; Babu, M., Collagen based dressings--a review. *Burns : Journal of the International Society for Burn Injuries* 2000, 26, (1), 54-62.
149. van Rijswijk, L., Ingredient-based wound dressing classification: a paradigm that is passe and in need of replacement. *Journal of Wound Care* 2006, 15, (1), 11-14.
150. Jones, V. J., The use of gauze: will it ever change? *International Wound Journal* 2006, 3, (2), 79-86.
151. Chang, K. W.; Alsagoff, S.; Ong, K. T.; Sim, P. H., Pressure ulcers--randomised controlled trial comparing hydrocolloid and saline gauze dressings. *The Medical Journal of Malaysia* 1998, 53, (4), 428-431.
152. SR, M., An algorithm for wound management with natural and synthetic dressing. In *Chronic wound care: a clinical source book for healthcare professionals*, D. K., Ed. King of Prussia, PA: Health Management Publications, Inc.: 1990.
153. Morgan, D., Wounds - what should a dressing formulary include? *Hospital Pharmacist* 2002, 9, 261-266.
154. Winter, G. D., Formation of scab and rate of epithelization of superficial wounds in skin of young domestic pig. *Nature* 1962, 193, (4812), 293.
155. Moshakis, V.; Fordyce, M. J.; Griffiths, J. D.; McKinna, J. A., Tegadern versus gauze dressing in breast surgery. *British Journal of Clinical Practice* 1984, 38, (4), 149-152.
156. Baker, P. D., Creating the optimal environment. An overview of dressings for chronic wounds. *Advance for Nurse Practitioners* 2005, 13, (7), 37-38.
157. Worley, C. A., So, what do I put on this wound? The wound dressing puzzle: Part III. *Dermatology Nursing / Dermatology Nurses' Association* 2005, 17, (4), 299-300.
158. Kannon, G. A.; Garrett, A. B., Moist wound-healing with occlusive dressings - A clinical review. *Dermatologic Surgery* 1995, 21, (7), 583-590.
159. Jones, V.; Milton, T., When and how to use hydrogels. *Nursing Times* 2000, 96, (23), 3-4.
160. Hampton, S., A small study in healing rates and symptom control using a new sheet hydrogel dressing. *Journal of Wound Care* 2004, 13, (7), 297-300.
161. Hollinworth, H., Pain relief. *Nurs Times* 2001, 97, (28), 63-66.

162. Eisenbud, D.; Hunter, H.; Kessler, L.; Zulkowski, K., Hydrogel wound dressings: where do we stand in 2003? *Ostomy/Wound Management* 2003, 49, (10), 52-57.
163. Lay-Flurrie, K., The properties of hydrogel dressings and their impact on wound healing. *Professional Nurse (London, England)* 2004, 19, (5), 269-273.
164. Motta, G.; Dunham, L.; Dye, T.; Mentz, J.; O'Connell-Gifford, E.; Smith, E., Clinical efficacy and cost-effectiveness of a new synthetic polymer sheet wound dressing. *Ostomy/Wound Management* 1999, 45, (10), 44-6, 48-49.
165. Thomas, D. R.; Goode, P. S.; LaMaster, K.; Tennyson, T., Acemannan hydrogel dressing versus saline dressing for pressure ulcers. A randomized, controlled trial. *Advances in Wound Care* 1998, 11, (6), 273-276.
166. Szycher, M.; Lee, S. J., Modern wound dressings: a systematic approach to wound healing. *Journal of Biomaterials Applications* 1992, 7, (2), 142-213.
167. Jones, V.; Milton, T., When and how to use hydrocolloid dressings. *Nursing Times* 2000, 96, (4 Suppl), 5-7.
168. Dealey, C., Role of hydrocolloids in wound management. *British Journal of Nursing* 1993, 2, (7), 360-362.
169. Fletcher, J., Understanding wound dressings: Hydrocolloids. *Nursing Times* 2005, 101, (46), 51.
170. Rovee, D. T., Evolution of wound dressing and their effects on the healing process. *Clinical Materials* 1991, 8, (3-4), 183-188.
171. Fletcher, J., Understanding wound dressings: Alginates. *Nursing Times* 2005, 101, (16), 53-54.
172. Taylor, B. A., Selecting wound healing products. Choices for long-term care settings. *Advance for Nurse Practitioners* 2003, 11, (5), 63-66.
173. Dumville, J. C.; O'Meara, S.; Deshpande, S.; Speak, K., Alginate dressings for healing diabetic foot ulcers. *Cochrane Database of Systematic Reviews* 2012, (2) 009110.
174. Seymour, J., Alginate dressings in wound care management. *Nursing Times* 1997, 93, (44), 49-52.
175. Segal, H. C.; Hunt, B. J.; Gilding, K., The effects of alginate and non-alginate wound dressings on blood coagulation and platelet activation. *Journal of Biomaterials Applications* 1998, 12, (3), 249-257.
176. Barnett, S. E.; Varley, S. J., The effects of calcium alginate on wound-healing. *Annals of the Royal College of Surgeons of England* 1987, 69, (4), 153-155.
177. Doyle, J. W.; Roth, T. P.; Smith, R. M.; Li, Y. Q.; Dunn, R. M., Effect of calcium alginate on cellular wound healing processes modeled in vitro. *Journal of Biomedical Materials Research* 1996, 32, (4), 561-568.

178. Thomas A., H. K., Moore K., Alginates from wound dressings activate human macrophages to secrete tumour necrosis factor- α . *Biomaterials* 2000, 21, 1797-1802.
179. Agren, M. S., Four alginate dressings in the treatment of partial thickness wounds: A comparative experimental study. *British Journal of Plastic Surgery* 1996, 49, (2), 129-134.
180. Suzuki, Y.; Tanihara, M.; Nishimura, Y.; Suzuki, K.; Yamawaki, Y.; Kudo, H.; Kakimaru, Y.; Shimizu, Y., In vivo evaluation of a novel alginate dressing. *Journal of Biomedical Materials Research* 1999, 48, (4), 522-527.
181. Berry, D. P.; Bale, S.; Harding, K. G., Dressings for treating cavity wounds. *Journal of Wound Care* 1996, 5, (1), 10-17.
182. Medicine management committee report. In *wound care guidelines* 2005; 1-33.
183. Ramos-e-Silva, M.; De Castro, M. C. R., New dressings, including tissue-engineered living skin. *Clinics in Dermatology* 2002, 20, (6), 715-723.
184. Piacquadio, D.; Nelson, D. B., Alginates - A new dressing alternative. *Journal of Dermatologic Surgery and Oncology* 1992, 18, (11), 992-995.
185. Stanton, R. A.; Billmire, D. A., Skin resurfacing for the burned patient. *Clinics in Plastic Surgery* 2002, 29, (1), 29.
186. Andreassi, A.; Bilenchi, R.; Biagioli, M.; D'Aniello, C., Classification and pathophysiology of skin grafts. *Clinics in Dermatology* 2005, 23, (4), 332-337.
187. Rose, J. K.; Herndon, D. N., Advances in the treatment of burn patients. *Burns* 1997, 23, S19-S26.
188. Fratianne RB, B. C., Improved survival of adults with extensive burns *Journal of Burn Care and Rehabilitation* 1997, 18, (4), 347-351.
189. Rheinwald, J. G.; Green, H., Serial cultivation of strains of human epidermal keratinocytes - formation of keratinizing colonies from single cells. *Cell* 1975, 6, (3), 331-344.
190. Oconnor, N. E.; Mulliken, J. B.; Banksschlegel, S.; Kehinde, O.; Green, H., Grafting of burns with cultured epithelium prepared from autologous epidermal cells. *Lancet* 1981, 1, (8211), 75-78.
191. Thivolet, J.; Faure, M.; Demidem, A.; Mauduit, G., Long-term survival and immunological tolerance of human epidermal allografts produced in culture. *Transplantation* 1986, 42, (3), 274-280.
192. Thivolet, J.; Faure, M.; Demidem, A.; Mauduit, G., Cultured human epidermal allografts are not rejected for a long period. *Archives of Dermatological Research* 1986, 278, (3), 252-254.
193. Deluca, M.; Albanese, E.; Cancedda, R.; Viacava, A.; Faggioni, A.; Zambruno, G.; Giannetti, A., Treatment of leg ulcers with cryopreserved allogenic cultured epithelium. *Archives of Dermatology* 1992, 128, (5), 633-638.

194. Limova, M., Active wound coverings: Bioengineered skin and dermal substitutes. *Surgical Clinics of North America* 2010, 90, (6), 1237.
195. Quinby, W. C.; Burke, J. F.; Bondoc, C. C., Primary excision and immediate wound closure. *Intensive Care Medicine* 1981, 7, (2), 71-76.
196. Barnett, J. R.; McCauley, R. L.; Schutzler, S.; Sheridan, K.; Hegggers, J. P., Cadaver donor discards secondary to serology. *Journal of Burn Care & Rehabilitation* 2001, 22, (2), 124-127.
197. Mathur, M.; De, A.; Gore, M., Microbiological assessment of cadaver skin grafts received in a Skin Bank. *Burns* 2009, 35, (1), 104-106.
198. Groeber, F.; Holeiter, M.; Hampel, M.; Hinderer, S.; Schenke-Layland, K., Skin tissue engineering - In vivo and in vitro applications. *Advanced Drug Delivery Reviews* 2011, 63, (4-5), 352-366.
199. Shevchenko, R. V.; James, S. L.; James, S. E., A review of tissue-engineered skin bioconstructs available for skin reconstruction. *Journal of the Royal Society Interface* 2010, 7, (43), 229-258.
200. Vercruyssen, K. P.; Prestwich, G. D., Hyaluronate derivatives in drug delivery. *Critical Reviews in Therapeutic Drug Carrier Systems* 1998, 15, (5), 513-555.
201. Luo, Y.; Kirker, K. R.; Prestwich, G. D., Cross-linked hyaluronic acid hydrogel films: new biomaterials for drug delivery. *Journal of Controlled Release* 2000, 69, (1), 169-184.
202. Voinchet, V.; Vasseur, P.; Kern, J., Efficacy and safety of hyaluronic acid in the management of acute wounds. *American Journal of Clinical Dermatology* 2006, 7, (6), 353-357.
203. Ueno, H.; Mori, T.; Fujinaga, T., Topical formulations and wound healing applications of chitosan. *Advanced Drug Delivery Reviews* 2001, 52, (2), 105-115.
204. Cullen, B.; Watt, P. W.; Lundqvist, C.; Silcock, D.; Schmidt, R. J.; Bogan, D.; Light, N. D., The role of oxidised regenerated cellulose/collagen in chronic wound repair and its potential mechanism of action. *International Journal of Biochemistry & Cell Biology* 2002, 34, (12), 1544-1556.
205. Harper, C., Permacol (TM): clinical experience with a new biomaterial. *Hospital Medicine* 2001, 62, (2), 90-95.
206. Sefton, M. V.; Woodhouse, K. A., Tissue engineering. *Journal of Cutaneous Medicine and Surgery* 1998, 3, S1 18-23.
207. Moustafa, M.; Bullock, A. J.; Creagh, T. M.; Heller, S.; Jeffcoate, W.; Game, F.; Amery, C.; Tesfaye, S.; Ince, Z.; Haddow, D. B.; MacNeil, S., Randomized, controlled, single-blind study on use of autologous keratinocytes on a transfer dressing to treat nonhealing diabetic ulcers. *Regenerative Medicine* 2007, 2, (6), 887-902.
208. Moustafa, M.; Simpson, C.; Glover, M.; Dawson, R. A.; Tesfaye, S.; Creagh, F. M.; Haddow, D.; Short, R.; Heller, S.; MacNeil, S., A new autologous keratinocyte dressing treatment for non-healing diabetic neuropathic foot ulcers. *Diabetic Medicine* 2004, 21, (7), 786-789.

209. Vanscheidt, W.; Ukat, A.; Horak, V.; Bruening, H.; Hunyadi, J.; Pavlicek, R.; Emter, M.; Hartmann, A.; Bende, J.; Zwingers, T.; Ermuth, T.; Eberhardt, R., Treatment of recalcitrant venous leg ulcers with autologous keratinocytes in fibrin sealant: A multinational randomized controlled clinical trial. *Wound Repair and Regeneration* 2007, 15, (3), 308-315.
210. Johnsen, S.; Ermuth, T.; Tanczos, E.; Bannasch, H.; Horch, R. E.; Zschocke, I.; Peschen, M.; Schopf, E.; Vanscheidt, W.; Augustin, M., Treatment of therapy-refractive ulcera cruris of various origins with autologous keratinocytes in fibrin sealant. *Vasa-Journal of Vascular Diseases* 2005, 34, (1), 25-29.
211. Supp, D. M.; Boyce, S. T., Engineered skin substitutes: practices and potentials. *Clinics in Dermatology* 2005, 23, (4), 403-412.
212. Clark, R. A. F.; Ghosh, K.; Tonnesen, M. G., Tissue engineering for cutaneous wounds. *Journal of Investigative Dermatology* 2007, 127, (5), 1018-1029.
213. Stock, U. A.; Vacanti, J. P., Tissue engineering: Current state and prospects. *Annual Review of Medicine* 2001, 52, 443-451.
214. Chong, A. K. S.; Chang, J., Tissue engineering for the hand surgeon: A clinical perspective. *Journal of Hand Surgery-American Volume* 2006, 31A, (3), 349-358.
215. Enoch, S.; Grey, J. E.; Harding, K. G., ABC of wound healing - Recent advances and emerging treatments. *British Medical Journal* 2006, 332, (7547), 962-965.
216. Schechner, J. S.; Crane, S. K.; Wang, F. Y.; Szeglin, A. M.; Tellides, G.; Lorber, M. I.; Bothwell, A. L. M.; Pober, J. S., Engraftment of a vascularized human skin equivalent. *Faseb Journal* 2003, 17, (15), 2250-2256.
217. Jones, I.; Currie, L.; Martin, R., A guide to biological skin substitutes. *British Journal of Plastic Surgery* 2002, 55, (3), 185-193.
218. Fong, J.; Wood, F., Nanocrystalline silver dressings in wound management: a review. *International Journal of Nanomedicine* 2006, 1, (4), 441-449.
219. Leaper, D. J., Silver dressings: their role in wound management. *International Wound Journal* 2006, 3, (4), 282-94.
220. Elsner, J. J.; Zilberman, M., Novel antibiotic-eluting wound dressings: An in vitro study and engineering aspects in the dressing's design. *Journal of Tissue Viability* 2010, 19, (2), 54-66.
221. Maubec, E.; Wolkenstein, P.; Lorient, M.-A.; Wechsler, J.; Mulot, C.; Beaune, P.; Revuz, J.; Roujeau, J.-C., Minocycline-induced DRESS: Evidence for accumulation of the culprit drug. *Dermatology* 2008, 216, (3), 200-204.
222. Sung, J. H.; Hwang, M.-R.; Kim, J. O.; Lee, J. H.; Il Kim, Y.; Kim, J. H.; Chang, S. W.; Jin, S. G.; Kim, J. A.; Lyoo, W. S.; Han, S. S.; Ku, S. K.; Yong, C. S.; Choi, H.-G., Gel characterisation and in vivo evaluation of

minocycline-loaded wound dressing with enhanced wound healing using polyvinyl alcohol and chitosan. *International Journal of Pharmaceutics* 2010, 392, (1-2), 232-240.

223. Lynch, S. E.; Nixon, J. C.; Colvin, R. B.; Antoniades, H. N., Role of platelet-driven growth-factor in wound-healing - Syneristic effects with other growth-factors. *Proceedings of the National Academy of Sciences of the United States of America* 1987, 84, (21), 7696-7700.

224. Sprugel, K. H.; McPherson, J. M.; Clowes, A. W.; Ross, R., Effects of growth-factors *in vivo*. 1. Cell ingrowth into porous subcutaneous chambers. *American Journal of Pathology* 1987, 129, (3), 601-613.

225. Jeschke, M. G.; Klein, D., Liposomal gene transfer of multiple genes is more effective than gene transfer of a single gene. *Gene Therapy* 2004, 11, (10), 847-855.

226. Branski, L. K.; Gauglitz, G. G.; Herndon, D. N.; Jeschke, M. G., A review of gene and stem cell therapy in cutaneous wound healing. *Burns* 2009, 35, (2), 171-180.

227. Macedo, L.; Pinhal-Enfield, G.; Alshits, V.; Elson, G.; Cronstein, B. N.; Leibovich, S. J., Wound healing is impaired in MyD88-Deficient mice - A role for MyD88 in the regulation of wound healing by adenosine A(2A) receptors. *American Journal of Pathology* 2007, 171, (6), 1774-1788.

228. Zhang, Z.; Schluesener, H. J., Mammalian toll-like receptors: from endogenous ligands to tissue regeneration. *Cellular and Molecular Life Sciences* 2006, 63, (24), 2901-2907.

229. Morbidelli, L.; Chang, C. H.; Douglas, J. G.; Granger, H. J.; Ledda, F.; Ziche, M., Nitric oxide mediates mitogenic effect of VEGF on coronary venular endothelium. *American Journal of Physiology-Heart and Circulatory Physiology* 1996, 270, (1), H411-H415.

230. Yebra, M.; Parry, G. C. N.; Stromblad, S.; Mackman, N.; Rosenberg, S.; Mueller, B. M.; Cheresch, D. A., Requirement of receptor-bound urokinase-type plasminogen activator for integrin alpha v beta 5-directed cell migration. *Journal of Biological Chemistry* 1996, 271, (46), 29393-29399.

231. Pastar, I.; Stojadinovic, O.; Krzyzanowska, A.; Barrientos, S.; Stuelten, C.; Zimmerman, K.; Blumenberg, M.; Brem, H.; Tomic-Canic, M., Attenuation of the transforming growth factor beta-signaling pathway in chronic venous ulcers. *Molecular Medicine* 2010, 16, (3-4), 92-101.

232. Chesnoy, S.; Lee, P. Y.; Huang, L., Intradermal injection of transforming growth factor-beta 1 gene enhances wound healing in genetically diabetic mice. *Pharmaceutical Research* 2003, 20, (3), 345-350.

233. Klass, B. R.; Grobbelaar, A. O.; Rolfe, K. J., Transforming growth factor beta 1 signalling, wound healing and repair: a multifunctional cytokine with clinical implications for wound repair, a delicate balance. *Postgraduate Medical Journal* 2009, 85, (999), 9-14.

234. Kopecki, Z.; Luchetti, M. M.; Adams, D. H.; Strudwick, X.; Mantamadiotis, T.; Stoppacciaro, A.; Gabrielli, A.; Ramsay, R. G.; Cowin,

- A. J., Collagen loss and impaired wound healing is associated with c-Myb deficiency. *Journal of Pathology* 2007, 211, (3), 351-361.
235. Finnerty, C. C.; Herndon, D. N.; Przkora, R.; Pereira, C. T.; Oliveira, H. M.; Queiroz, D. M. M.; Rocha, A. M. C.; Jeschke, M. G., Cytokine expression profile over time in severely burned pediatric patients. *Shock* 2006, 26, (1), 13-19.
236. Hu, Y.; Liang, D.; Li, X.; Liu, H.-H.; Zhang, X.; Zheng, M.; Dill, D.; Shi, X.; Qiao, Y.; Yeomans, D.; Carvalho, B.; Angst, M. S.; Clark, J. D.; Peltz, G., The role of interleukin-1 in wound biology. part II: in vivo and human translational studies. *Anesthesia and Analgesia* 2010, 111, (6), 1534-1542.
237. Wiegand, C.; Schoenfelder, U.; Abel, M.; Ruth, P.; Kaatz, M.; Hipler, U.-C., Protease and pro-inflammatory cytokine concentrations are elevated in chronic compared to acute wounds and can be modulated by collagen type I in vitro. *Archives of Dermatological Research* 2010, 302, (6), 419-428.
238. Mosser, D. M.; Edwards, J. P., Exploring the full spectrum of macrophage activation. *Nature Reviews Immunology* 2008, 8, (12), 958-969.
239. Rueckerl, D.; Hessmann, M.; Yoshimoto, T.; Ehlers, S.; Hoelscher, C., Alternatively activated macrophages express the IL-27 receptor alpha chain WSX-1. *Immunobiology* 2006, 211, (6-8), 427-436.
240. Heldin, C. H.; Westermark, B., Mechanism of action and in vivo role of platelet-derived growth factor. *Physiological Reviews* 1999, 79, (4), 1283-1316.
241. Lederle, W.; Stark, H.-J.; Skobe, M.; Fusenig, N. E.; Mueller, M. M., Platelet-derived growth factor-BB controls epithelial tumor phenotype by differential growth factor regulation in stromal cells. *American Journal of Pathology* 2006, 169, (5), 1767-1783.
242. Timper, K.; Seboek, D.; Eberhardt, M.; Linscheid, P.; Christ-Crain, M.; Keller, U.; Muller, B.; Zulewski, H., Human adipose tissue-derived mesenchymal stem cells differentiate into insulin, somatostatin, and glucagon expressing cells. *Biochemical and Biophysical Research Communications* 2006, 341, (4), 1135-1140.
243. Uutela, M.; Wirzenius, M.; Paavonen, K.; Rajantie, I.; He, Y. L.; Karpanen, T.; Lohela, M.; Wiig, H.; Salven, P.; Pajusola, K.; Eriksson, U.; Alitalo, K., PDGF-D induces macrophage recruitment, increased interstitial pressure, and blood vessel maturation during angiogenesis. *Blood* 2004, 104, (10), 3198-3204.
244. Buchstein, N.; Hoffmann, D.; Smola, H.; Lang, S.; Paulsson, M.; Niemann, C.; Krieg, T.; Eming, S. A., Alternative proteolytic processing of hepatocyte growth factor during wound repair. *American Journal of Pathology* 2009, 174, (6), 2116-2128.
245. Bennett, S. P.; Griffiths, G. D.; Schor, A. M.; Leese, G. P.; Schor, S. L., Growth factors in the treatment of diabetic foot ulcers. *British Journal of Surgery* 2003, 90, (2), 133-146.

246. Brem, H.; Stojadinovic, O.; Diegelmann, R. F.; Entero, H.; Lee, B.; Pastar, I.; Golinko, M.; Rosenberg, H.; Tomic-Canic, M., Molecular markers in patients with chronic wounds to guide surgical debridement. *Molecular Medicine* 2007, 13, (1-2), 30-39.
247. Li, G. C.; Gustafson-Brown, C.; Hanks, S. K.; Nason, K.; Arbeit, J. M.; Pogliano, K.; Wisdom, R. M.; Johnson, R. S., c-Jun is essential for organization of the epidermal leading edge. *Developmental Cell* 2003, 4, (6), 865-877.
248. Sano, S.; Itami, S.; Takeda, K.; Tarutani, M.; Yamaguchi, Y.; Miura, H.; Yoshikawa, K.; Akira, S.; Takeda, J., Keratinocyte-specific ablation of Stat3 exhibits impaired skin remodeling, but does not affect skin morphogenesis. *Embo Journal* 1999, 18, (17), 4657-4668.
249. Schultz, G.; Rotatori, D. S.; Clark, W., EGF and TGF-ALPHA in wound-healing and repair. *Journal of Cellular Biochemistry* 1991, 45, (4), 346-352.
250. Wu, Y.; Chen, L.; Scott, P. G.; Tredget, E. E., Mesenchymal stem cells enhance wound healing through differentiation and angiogenesis. *Stem Cells* 2007, 25, (10), 2648-2659.
251. Burd, A.; Ahmed, K.; Lam, S.; Ayyappan, T.; Huang, L., Stem cell strategies in burns care. *Burns* 2007, 33, (3), 282-291.
252. Till, J.E.; McCulloch, E.A., A direct measurement of radiation sensitivity of normal mouse bone marrow cells. *Radiat Research* 1961, 14, 1419-1430.
253. Charruyer, A.; Ghadially, R., Stem cells and tissue-engineered skin. *Skin Pharmacology and Physiology* 2009, 22, (2), 55-62.
254. Porada, C. D.; Zanjani, E. D.; Almeida-Porad, G., Adult mesenchymal stem cells: a pluripotent population with multiple applications. *Current Stem Cell Research & Therapy* 2006, 1, (3), 365-369.
255. Schabort, E. J.; Myburgh, K. H.; Wiehe, J. M.; Torzewski, J.; Niesler, C. U., Potential myogenic stem cell populations: Sources, plasticity, and application for cardiac repair. *Stem Cells and Development* 2009, 18, (6), 813-829.
256. Goestaneh N; Kokkinaki M; Pant D; Jiang J; DeStefano D; Fernandez-Bueno C; Rone JD; Haddad BR; Gallicano GI, D. M., Pluripotent stem cell derived from adult human testes. *Stem Cells Dev.* 2009, 18, (8), 1115-1126.
257. Murasawa, S.; Asahara, T., Cardiogenic potential of endothelial progenitor cells. *Therapeutic Advances in Cardiovascular Disease* 2008, 2, (5), 341-348.
258. Green, H., The birth of therapy with cultured cells. *Bioessays* 2008, 30, (9), 897-903.
259. Martinez-Santamaria, L.; Guerrero-Aspizua, S.; Del Rio, M., Skin bioengineering: preclinical and clinical applications. *Actas Dermo-Sifiliograficas* 2012, 103, (1), 5-11.

260. Nauta, A.; Gurtner, G. C.; Longaker, M. T., Wound healing and regenerative strategies. *Oral Diseases* 2011, 17, (6), 541-549.
261. Friedens.Aj; Petrakov.Kv; Kuroleso.Ai; Frolova, G. P., Heterotopic transplants of bone marrow - Analysis of precursor cells for osteogenic and hematopoietic tissue. *Transplantation* 1968, 6, (2), 230.
262. Caplan, A. I., Mesenchymal stem-cells. *Journal of Orthopaedic Research* 1991, 9, (5), 641-650.
263. Dominici, M.; Le Blanc, K.; Mueller, I.; Slaper-Cortenbach, I.; Marini, F. C.; Krause, D. S.; Deans, R. J.; Keating, A.; Prockop, D. J.; Horwitz, E. M., Minimal criteria for defining multipotent mesenchymal stromal cells. The International Society for Cellular Therapy position statement. *Cytotherapy* 2006, 8, (4), 315-317.
264. Horwitz, E. M.; Le Blanc, K.; Dominici, M.; Mueller, I.; Slaper-Cortenbach, I.; Marini, F. C.; Deans, R. J.; Krause, D. S.; Keating, A., Clarification of the nomenclature for MSC: The international society for cellular therapy position statement. *Cytotherapy* 2005, 7, (5), 393-395.
265. Pittenger, M. F.; Mackay, A. M.; Beck, S. C.; Jaiswal, R. K.; Douglas, R.; Mosca, J. D.; Moorman, M. A.; Simonetti, D. W.; Craig, S.; Marshak, D. R., Multilineage potential of adult human mesenchymal stem cells. *Science* 1999, 284, (5411), 143-147.
266. Brinchmann, J. E., Expanding autologous multipotent mesenchymal bone marrow stromal cells. *Journal of the Neurological Sciences* 2008, 265, (1-2), 127-130.
267. Caplan, A. I.; Bruder, S. P., Mesenchymal stem cells: building blocks for molecular medicine in the 21st century. *Trends in Molecular Medicine* 2001, 7, (6), 259-264.
268. Lindroos, B.; Maenpaae, K.; Ylikomi, T.; Oja, H.; Suuronen, R.; Miettinen, S., Characterisation of human dental stem cells and buccal mucosa fibroblasts. *Biochemical and Biophysical Research Communications* 2008, 368, (2), 329-335.
269. Wei G, S. G., Harder F, Müller AM., Stem cell plasticity in mammals and transdetermination in Drosophila: common themes? *Stem Cells* 2000, 18, (6), 409-414.
270. Fu, X.; Li, H., Mesenchymal stem cells and skin wound repair and regeneration: possibilities and questions. *Cell and Tissue Research* 2009, 335, (2), 317-321.
271. Kolf, C. M.; Cho, E.; Tuan, R. S., Mesenchymal stromal cells - Biology of adult mesenchymal stem cells: regulation of niche, self-renewal and differentiation. *Arthritis Research & Therapy* 2007, 9, (1) 204.
272. Wu, Y.; Wang, J.; Scott, P. G.; Tredget, E. E., Bone marrow-derived stem cells in wound healing: a review. *Wound Repair and Regeneration* 2007, 15, S18-S26.

273. Ishii, G. H.; Sangai, T.; Sugiyama, K.; Ito, T.; Hasebe, T.; Endoh, Y.; Magae, U.; Ochiai, A., In vivo characterization of bone marrow-derived fibroblasts recruited into fibrotic lesions. *Stem Cells* 2005, 23, (5), 699-706.
274. Deng, W. M.; Han, Q.; Liao, L. M.; Li, C. H.; Ge, W.; Zhao, Z. G.; You, S. G.; Deng, H. Y.; Murad, F.; Zhao, R. C. H., Engrafted bone marrow-derived Flk-1(+) mesenchymal stem cells regenerate skin tissue. *Tissue Engineering* 2005, 11, (1-2), 110-119.
275. Mori, L.; Bellini, A.; Stacey, M. A.; Schmidt, M.; Mattoli, S., Fibrocytes contribute to the myofibroblast population in wounded skin and originate from the bone marrow. *Experimental Cell Research* 2005, 304, (1), 81-90.
276. Jiang, Y. H.; Jahagirdar, B. N.; Reinhardt, R. L.; Schwartz, R. E.; Keene, C. D.; Ortiz-Gonzalez, X. R.; Reyes, M.; Lenvik, T.; Lund, T.; Blackstad, M.; Du, J. B.; Aldrich, S.; Lisberg, A.; Low, W. C.; Largaespada, D. A.; Verfaillie, C. M., Pluripotency of mesenchymal stem cells derived from adult marrow. *Nature* 2002, 418, (6893), 41-49.
277. Fathke, C.; Wilson, L.; Hutter, J.; Kapoor, V.; Smith, A.; Hocking, A.; Isik, F., Contribution of bone marrow-derived cells to skin: Collagen deposition and wound repair. *Stem Cells* 2004, 22, (5), 812-822.
278. Hao, L.; Wang, J.; Zou, Z.; Yan, G.; Dong, S.; Deng, J.; Ran, X.; Feng, Y.; Luo, C.; Wang, Y.; Cheng, T., Transplantation of BMSCs expressing hPDGF-A/hBD2 promotes wound healing in rats with combined radiation-wound injury. *Gene Therapy* 2009, 16, (1), 34-42.
279. Wilgus, T. A.; Ferreira, A. M.; Oberyszyn, T. M.; Bergdall, V. K.; DiPietro, L. A., Regulation of scar formation by vascular endothelial growth factor. *Laboratory Investigation* 2008, 88, (6), 579-590.
280. Di Rocco, G.; Gentile, A.; Antonini, A.; Ceradini, F.; Wu, J. C.; Capogrossi, M. C.; Toietta, G., Enhanced healing of diabetic wounds by topical administration of adipose tissue-derived stromal cells overexpressing stromal-derived factor-1: biodistribution and engraftment analysis by bioluminescent imaging. *Stem Cells International* 2010, 2011, 304562-304562.
281. Tian, H.; Lu, Y.; Shah, S. P.; Hong, S., 14S,21R-Dihydroxydocosahexaenoic acid remedies impaired healing and mesenchymal stem cell functions in diabetic wounds. *Journal of Biological Chemistry* 2011, 286, (6), 4443-4453.
282. Simman, R.; Craft, C.; McKinney, B., Improved survival of ischemic random skin flaps through the use of bone marrow nonhematopoietic stem cells and angiogenic growth factors. *Annals of Plastic Surgery* 2005, 54, (5), 546-552.
283. Chen, L.; Tredget, E. E.; Wu, P. Y. G.; Wu, Y., Paracrine factors of mesenchymal stem cells recruit macrophages and endothelial lineage cells and enhance wound healing. *Plos One* 2008, 3, (4) e1886.

284. Rao, M. S.; Mattson, M. P., Stem cells and aging: expanding the possibilities. *Mechanisms of Ageing and Development* 2001, 122, (7), 713-734.
285. Zuk, P. A., Tissue engineering craniofacial defects with adult stem cells? Are we ready yet? *Pediatric Research* 2008, 63, (5), 478-486.
286. Kern, S.; Eichler, H.; Stoeve, J.; Kluter, H.; Bieback, K., Comparative analysis of mesenchymal stem cells from bone marrow, umbilical cord blood, or adipose tissue. *Stem Cells* 2006, 24, (5), 1294-1301.
287. Gonda, K.; Shigeura, T.; Sato, T.; Matsumoto, D.; Suga, H.; Inoue, K.; Aoi, N.; Kato, H.; Sato, K.; Murase, S.; Koshima, I.; Yoshimura, K., Preserved proliferative capacity and multipotency of human adipose-derived stem cells after long-term cryopreservation. *Plastic and Reconstructive Surgery* 2008, 121, (2), 401-410.
288. Gimble, J. M.; Guilak, F., Adipose-derived adult stem cells: isolation, characterization, and differentiation potential. *Cytotherapy* 2003, 5, (5), 362-369.
289. Zuk, P. A.; Zhu, M.; Ashjian, P.; De Ugarte, D. A.; Huang, J. I.; Mizuno, H.; Alfonso, Z. C.; Fraser, J. K.; Benhaim, P.; Hedrick, M. H., Human adipose tissue is a source of multipotent stem cells. *Molecular Biology of the Cell* 2002, 13, (12), 4279-4295.
290. Zuk, P. A.; Zhu, M.; Mizuno, H.; Huang, J.; Futrell, J. W.; Katz, A. J.; Benhaim, P.; Lorenz, H. P.; Hedrick, M. H., Multilineage cells from human adipose tissue: Implications for cell-based therapies. *Tissue Engineering* 2001, 7, (2), 211-228.
291. Gimble, J. M.; Katz, A. J.; Bunnell, B. A., Adipose-derived stem cells for regenerative medicine. *Circulation Research* 2007, 100, (9), 1249-1260.
292. Planat-Benard, V.; Silvestre, J. S.; Cousin, B.; Andre, M.; Nibelink, M.; Tamarat, R.; Clergue, M.; Manneville, C.; Saillan-Barreau, C.; Duriez, M.; Tedgui, A.; Levy, B.; Penicaud, L.; Casteilla, L., Plasticity of human adipose lineage cells toward endothelial cells - Physiological and therapeutic perspectives. *Circulation* 2004, 109, (5), 656-663.
293. Safford, K. M.; Hicok, K. C.; Safford, S. D.; Halvorsen, Y. D. C.; Wilkison, W. O.; Gimble, J. M.; Rice, H. E., Neurogenic differentiation of murine and human adipose-derived stromal cells. *Biochemical and Biophysical Research Communications* 2002, 294, (2), 371-379.
294. Seo, M. J.; Suh, S. Y.; Bae, Y. C.; Jung, J. S., Differentiation of human adipose stromal cells into hepatic lineage in vitro and in vivo. *Biochemical and Biophysical Research Communications* 2005, 328, (1), 258-264.
295. Huang, J. I.; Zuk, P. A.; Jones, N. F.; Zhu, M.; Lorenz, H. P.; Hedrick, M. H.; Benhaim, P., Chondrogenic potential of multipotential cells from human adipose tissue. *Plastic and Reconstructive Surgery* 2004, 113, (2), 585-594.

296. Cao, Y.; Sun, Z.; Liao, L. M.; Meng, Y.; Han, Q.; Zhao, R. C. H., Human adipose tissue-derived stem cells differentiate into endothelial cells in vitro and improve postnatal neovascularization in vivo. *Biochemical and Biophysical Research Communications* 2005, 332, (2), 370-379.
297. Casteilla, L.; Planat-Benard, V.; Cousin, B.; Silvestre, J. S.; Laharrague, P.; Charriere, G.; Carriere, A.; Penicaud, L., Plasticity of adipose tissue: a promising therapeutic avenue in the treatment of cardiovascular and blood diseases? *Archives Des Maladies Du Coeur Et Des Vaisseaux* 2005, 98, (9), 922-926.
298. Planat-Benard, V.; Menard, C.; Andre, M.; Puceat, M.; Perez, A.; Garcia-Verdugo, J. M.; Penicaud, L.; Casteilla, L., Spontaneous cardiomyocyte differentiation from adipose tissue stroma cells. *Circulation Research* 2004, 94, (2), 223-229.
299. Rehman, J.; Traktuev, D.; Li, J. L.; Merfeld-Clauss, S.; Temm-Grove, C. J.; Bovenkerk, J. E.; Pell, C. L.; Johnstone, B. H.; Considine, R. V.; March, K. L., Secretion of angiogenic and antiapoptotic factors by human adipose stromal cells. *Circulation* 2004, 109, (10), 1292-1298.
300. Traktuev, D. O.; Merfeld-Clauss, S.; Li, J.; Kolonin, M.; Arap, W.; Pasqualini, R.; Johnstone, B. H.; March, K. L., A population of multipotent CD34-positive adipose stromal cells share pericyte and mesenchymal surface markers, reside in a periendothelial location, and stabilize endothelial networks. *Circulation Research* 2008, 102, (1), 77-85.
301. Kim, W.-S.; Park, B.-S.; Sung, J.-H.; Yang, J.-M.; Park, S.-B.; Kwak, S.-J.; Park, J.-S., Wound healing effect of adipose-derived stem cells: A critical role of secretory factors on human dermal fibroblasts. *Journal of Dermatological Science* 2007, 48, (1), 15-24.
302. Lu, F.; Mizuno, H.; Uysal, C. A.; Cai, X.; Ogawa, R.; Hyakusoku, H., Improved viability of random pattern skin flaps through the use of adipose-derived stem cells. *Plastic and Reconstructive Surgery* 2008, 121, (1), 50-58.
303. Moon, M. H.; Kim, S. Y.; Kim, Y. J.; Kim, S. J.; Lee, J. B.; Bae, Y. C.; Sung, S. M.; Jung, J. S., Human adipose tissue-derived mesenchymal stem cells improve postnatal neovascularization in a mouse model of hindlimb ischemia. *Cellular Physiology and Biochemistry* 2006, 17, (5-6), 279-290.
304. Song, Y.-H.; Gehmert, S.; Sadat, S.; Pinkernell, K.; Bai, X.; Matthias, N.; Alt, E., VEGF is critical for spontaneous differentiation of stem cells into cardiomyocytes. *Biochemical and Biophysical Research Communications* 2007, 354, (4), 999-1003.
305. Daher, S. R.; Johnstone, B. H.; Phinney, D. G.; March, K. L., Adipose stromal/stem cells: Basic and translational advances: The IFATS collection Introduction. *Stem Cells* 2008, 26, (10), 2664-2665.
306. Fraser, J. K.; Wulur, I.; Alfonso, Z.; Hedrick, M. H., Fat tissue: an underappreciated source of stem cells for biotechnology. *Trends in Biotechnology* 2006, 24, (4), 150-154.

307. Lindroos, B.; Suuronen, R.; Miettinen, S., The potential of adipose stem cells in regenerative medicine. *Stem Cell Reviews and Reports* 2011, 7, (2), 269-291.
308. Katz, A. J.; Llull, R.; Hedrick, M. H.; Futrell, J. W., Emerging approaches to the tissue engineering of fat. *Clinics in Plastic Surgery* 1999, 26, (4), 587.
309. Tapp, H.; Hanley, E. N., Jr.; Patt, J. C.; Gruber, H. E., Adipose-derived stem cells: Characterization and current application in orthopaedic tissue repair. *Experimental Biology and Medicine* 2009, 234, (1), 1-9.
310. De Ugarte, D. A.; Alfonso, Z.; Zuk, P. A.; Elbarbary, A.; Zhu, M.; Ashjian, P.; Benhaim, P.; Hedrick, M. H.; Fraser, J. K., Differential expression of stem cell mobilization-associated molecules on multi-lineage cells from adipose tissue and bone marrow. *Immunology Letters* 2003, 89, (2-3), 267-270.
311. Garcia-Castro, J.; Trigueros, C.; Madrenas, J.; Perez-Simon, J. A.; Rodriguez, R.; Menendez, P., Mesenchymal stem cells and their use as cell replacement therapy and disease modelling tool. *Journal of Cellular and Molecular Medicine* 2008, 12, (6B), 2552-2565.
312. Cherubino, M.; Rubin, J. P.; Miljkovic, N.; Kelmendi-Doko, A.; Marra, K. G., Adipose-derived stem cells for wound healing applications. *Annals of Plastic Surgery* 2011, 66, (2), 210-215.
313. Nie, C.; Yang, D.; Morris, S. F., Local delivery of adipose-derived stem cells via acellular dermal matrix as a scaffold: A new promising strategy to accelerate wound healing. *Medical Hypotheses* 2009, 72, (6), 679-682.
314. Trottier, V.; Marceau-Fortier, G.; Germain, L.; Vincent, C.; Fradette, J., IFATS collection: Using human adipose-derived stem/stromal cells for the production of new skin substitutes. *Stem Cells* 2008, 26, (10), 2713-2723.
315. Ebrahimian, T. G.; Pouzoulet, F.; Squiban, C.; Buard, V.; Andre, M.; Cousin, B.; Gourmelon, P.; Benderitter, M.; Casteilla, L.; Tamarat, R., Cell therapy based on adipose tissue-derived stromal cells promotes physiological and pathological wound healing. *Arteriosclerosis Thrombosis and Vascular Biology* 2009, 29, (4), 503-510.
316. Lin, Y.-C.; Grahovac, T.; Oh, S. J.; Ieraci, M.; Rubin, J. P.; Marra, K. G., Evaluation of a multi-layer adipose-derived stem cell sheet in a full-thickness wound healing model. *Acta Biomaterialia* 2013, 9, (2), 5243-5250.
317. Altman, A. M.; Yan, Y.; Matthias, N.; Bai, X.; Rios, C.; Mathur, A. B.; Song, Y.-H.; Alt, E. U., IFATS Collection: human adipose-derived stem cells seeded on a silk fibroin-chitosan scaffold enhance wound repair in a murine soft tissue injury model. *Stem Cells* 2009, 27, (1), 250-258.
318. Hong, S. J.; Jia, S.-X.; Xie, P.; Xu, W.; Leung, K. P.; Mustoe, T. A.; Galiano, R. D., Topically delivered adipose derived stem cells show an activated-fibroblast phenotype and enhance granulation tissue formation in skin wounds. *Plos One* 2013, 8, (1), e55640-e55640.

319. Kim, W.-S.; Park, B.-S.; Sung, J.-H.; Yang, J.-M.; Park, S.-B.; Kwak, S.-J.; Park, J.-S., Wound healing effect of adipose-derived stem cells: A critical role of secretory factors on human dermal fibroblasts. *Journal of Dermatological Science* 2007, 48, (1), 15-24.
320. Amos, P. J.; Kapur, S. K.; Stapor, P. C.; Shang, H. L.; Bekiranov, S.; Khurgel, M.; Rodeheaver, G. T.; Peirce, S. M.; Katz, A. J., Human adipose-derived stromal cells accelerate diabetic wound healing: impact of cell formulation and delivery. *Tissue Engineering Part A* 2010, 16, (5), 1595-1606.
321. Park, B.-S.; Jang, K. A.; Sung, J.-H.; Park, J.-S.; Kwon, Y. H.; Kim, K. J.; Kim, W.-S., Adipose-derived stem cells and their secretory factors as a promising therapy for skin aging. *Dermatologic Surgery* 2008, 34, (10), 1323-1326.
322. Huang, Y.; Onyeri, S.; Siewe, M.; Moshfeghian, A.; Madihally, S. V., In vitro characterization of chitosan-gelatin scaffolds for tissue engineering. *Biomaterials* 2005, 26, (36), 7616-7627.
323. Tan, H.; Huang, D.; Lao, L.; Gao, C., RGD modified PLGA/Gelatin microspheres as microcarriers for chondrocyte delivery. *Journal of Biomedical Materials Research Part B-Applied Biomaterials* 2009, 91B, (1), 228-238.
324. Tan, H.; Wan, L.; Wu, J.; Gao, C., Microscale control over collagen gradient on poly(L-lactide) membrane surface for manipulating chondrocyte distribution. *Colloids and Surfaces B-Biointerfaces* 2008, 67, (2), 210-215.
325. Chenite, A.; Chaput, C.; Wang, D.; Combes, C.; Buschmann, M. D.; Hoemann, C. D.; Leroux, J. C.; Atkinson, B. L.; Binette, F.; Selmani, A., Novel injectable neutral solutions of chitosan form biodegradable gels in situ. *Biomaterials* 2000, 21, (21), 2155-2161.
326. Kast, C. E.; Frick, W.; Losert, U.; Bernkop-Schnurch, A., Chitosan-thioglycolic acid conjugate: a new scaffold material for tissue engineering? *International Journal of Pharmaceutics* 2003, 256, (1-2), 183-189.
327. Berger, J.; Reist, M.; Mayer, J. M.; Felt, O.; Peppas, N. A.; Gurny, R., Structure and interactions in covalently and ionically crosslinked chitosan hydrogels for biomedical applications. *European Journal of Pharmaceutics and Biopharmaceutics* 2004, 57, (1), 19-34.
328. Hsieh, W.-C.; Chang, C.-P.; Lin, S.-M., Morphology and characterization of 3D micro-porous structured chitosan scaffolds for tissue engineering. *Colloids and Surfaces B-Biointerfaces* 2007, 57, (2), 250-255.
329. Mao, J. S.; Zhao, L. G.; de Yao, K.; Shang, Q. X.; Yang, G. H.; Cao, Y. L., Study of novel chitosan-gelatin artificial skin in vitro. *Journal of Biomedical Materials Research Part A* 2003, 64A, (2), 301-308.
330. Tan, H.; Lao, L.; Wu, J.; Gong, Y.; Gao, C., Biomimetic modification of chitosan with covalently grafted lactose and blended heparin for improvement of in vitro cellular interaction. *Polymers for Advanced Technologies* 2008, 19, (1), 15-23.

331. Yuan, Y.; Chesnutt, B. M.; Utturkar, G.; Haggard, W. O.; Yang, Y.; Ong, J. L.; Bumgardner, J. D., The effect of cross-linking of chitosan microspheres with genipin on protein release. *Carbohydrate Polymers* 2007, 68, (3), 561-567.
332. Smeds, K. A.; Grinstaff, M. W., Photocrosslinkable polysaccharides for in situ hydrogel formation. *Journal of Biomedical Materials Research* 2001, 54, (1), 115-121.
333. Leach, J. B.; Bivens, K. A.; Patrick, C. W.; Schmidt, C. E., Photocrosslinked hyaluronic acid hydrogels: Natural, biodegradable tissue engineering scaffolds. *Biotechnology and Bioengineering* 2003, 82, (5), 578-589.
334. Park, Y. D.; Tirelli, N.; Hubbell, J. A., Photopolymerized hyaluronic acid-based hydrogels and interpenetrating networks. *Biomaterials* 2003, 24, (6), 893-900.
335. Cheung, W. F.; Cruz, T. F.; Turley, E. A., Receptor for hyaluronan-mediated motility (RHAMM), a hyaladherin that regulates cell responses to growth factors. *Biochemical Society Transactions* 1999, 27, (2), 135-142.
336. Fraser, J. R. E.; Laurent, T. C.; Laurent, U. B. G., Hyaluronan: Its nature, distribution, functions and turnover. *Journal of Internal Medicine* 1997, 242, (1), 27-33.
337. Liu, L. S.; Thompson, A. Y.; Heidarani, M. A.; Poser, J. W.; Spiro, R. C., An osteoconductive collagen hyaluronate matrix for bone regeneration. *Biomaterials* 1999, 20, (12), 1097-1108.
338. Tan, H.; Wu, J.; Lao, L.; Gao, C., Gelatin/chitosan/hyaluronan scaffold integrated with PLGA microspheres for cartilage tissue engineering. *Acta Biomaterialia* 2009, 5, (1), 328-337.
339. Khairoun, I.; Magne, D.; Gauthier, O.; Bouler, J. M.; Aguado, E.; Daculsi, G.; Weiss, P., In vitro characterization and in vivo properties of a carbonated apatite bone cement. *Journal of Biomedical Materials Research* 2002, 60, (4), 633-642.
340. Komath, M.; Varma, H. K.; Sivakumar, R., On the development of an apatitic calcium phosphate bone cement. *Bulletin of Materials Science* 2000, 23, (2), 135-140.
341. Schmitt, M.; Weiss, P.; Bourges, X.; del Valle, G. A.; Daculsi, G., Crystallization at the polymer/calcium-phosphate interface in a sterilized injectable bone substitute IBS. *Biomaterials* 2002, 23, (13), 2789-2794.
342. Buschmann, M. D.; Gluzband, Y. A.; Grodzinsky, A. J.; Kimura, J. H.; Hunziker, E. B., Chondrocytes in agarose culture synthesize a mechanically functional extracellular-matrix. *Journal of Orthopaedic Research* 1992, 10, (6), 745-758.
343. Dillon, G. P.; Yu, X. J.; Sridharan, A.; Ranieri, J. P.; Bellamkonda, R. V., The influence of physical structure and charge on neurite extension in a 3D hydrogel scaffold. *Journal of Biomaterials Science-Polymer Edition* 1998, 9, (10), 1049-1069.

344. Silverman, R. P.; Passaretti, D.; Huang, W.; Randolph, M. A.; Yaremchuk, M., Injectable tissue-engineered cartilage using a fibrin glue polymer. *Plastic and Reconstructive Surgery* 1999, 103, (7), 1809-1818.
345. Zisch, A. H.; Schenk, U.; Schense, J. C.; Sakiyama-Elbert, S. E.; Hubbell, J. A., Covalently conjugated VEGF-fibrin matrices for endothelialization. *Journal of Controlled Release* 2001, 72, (1-3), 101-113.
346. Alsberg, E.; Anderson, K. W.; Albeiruti, A.; Franceschi, R. T.; Mooney, D. J., Cell-interactive alginate hydrogels for bone tissue engineering. *Journal of Dental Research* 2001, 80, (11), 2025-2029.
347. Cao, Y.; Shen, X. C.; Chen, Y.; Guo, J.; Chen, Q.; Jiang, X. Q., pH-induced self-assembly and capsules of sodium alginate. *Biomacromolecules* 2005, 6, (4), 2189-2196.
348. Stevens, M. M.; Qanadilo, H. F.; Langer, R.; Shastri, V. P., A rapid-curing alginate gel system: utility in periosteum-derived cartilage tissue engineering. *Biomaterials* 2004, 25, (5), 887-894.
349. Tate, M. C.; Shear, D. A.; Hoffman, S. W.; Stein, D. G.; LaPlaca, M. C., Biocompatibility of methylcellulose-based constructs designed for intracerebral gelation following experimental traumatic brain injury. *Biomaterials* 2001, 22, (10), 1113-1123.
350. Burdick, J. A.; Anseth, K. S., Photoencapsulation of osteoblasts in injectable RGD-modified PEG hydrogels for bone tissue engineering. *Biomaterials* 2002, 23, (22), 4315-4323.
351. Elisseeff, J.; McIntosh, W.; Anseth, K.; Riley, S.; Ragan, P.; Langer, R., Photoencapsulation of chondrocytes in poly(ethylene oxide)-based semi-interpenetrating networks. *Journal of Biomedical Materials Research* 2000, 51, (2), 164-171.
352. Lutolf, M. P.; Hubbell, J. A., Synthesis and physicochemical characterization of end-linked poly(ethylene glycol)-co-peptide hydrogels formed by Michael-type addition. *Biomacromolecules* 2003, 4, (3), 713-722.
353. Lutolf, M. P.; Raeber, G. P.; Zisch, A. H.; Tirelli, N.; Hubbell, J. A., Cell-responsive synthetic hydrogels. *Advanced Materials* 2003, 15, (11), 888.
354. Sperinde, J. J.; Griffith, L. G., Synthesis and characterization of enzymatically-cross-linked poly(ethylene glycol) hydrogels. *Macromolecules* 1997, 30, (18), 5255-5264.
355. Stile, R. A.; Healy, K. E., Thermo-responsive peptide-modified hydrogels for tissue regeneration. *Biomacromolecules* 2001, 2, (1), 185-194.
356. Lee, J. W.; Jung, M. C.; Park, H. D.; Park, K. D.; Ryu, G. H., Synthesis and characterization of thermosensitive chitosan copolymer as a novel biomaterial. *Journal of Biomaterials Science-Polymer Edition* 2004, 15, (8), 1065-1079.
357. Wang, J.; Chen, L.; Zhao, Y.; Guo, G.; Zhang, R., Cell adhesion and accelerated detachment on the surface of temperature-sensitive chitosan and

poly(N-isopropylacrylamide) hydrogels. *Journal of Materials Science-Materials in Medicine* 2009, 20, (2), 583-590.

358. Fisher, J. P.; Dean, D.; Mikos, A. G., Photocrosslinking characteristics and mechanical properties of diethyl fumarate/poly(propylene fumarate) biomaterials. *Biomaterials* 2002, 23, (22), 4333-4343.

359. Payne, R. G.; McGonigle, J. S.; Yaszemski, M. J.; Yasko, A. W.; Mikos, A. G., Development of an injectable, in situ crosslinkable, degradable polymeric carrier for osteogenic cell populations. Part 2. Viability of encapsulated marrow stromal osteoblasts cultured on crosslinking poly(propylene fumarate). *Biomaterials* 2002, 23, (22), 4373-4380.

360. Shin, H.; Ruhe, P. Q.; Mikos, A. G.; Jansen, J. A., In vivo bone and soft tissue response to injectable, biodegradable oligo(poly(ethylene glycol) fumarate) hydrogels. *Biomaterials* 2003, 24, (19), 3201-3211.

361. Timmer, M. D.; Ambrose, C. G.; Mikos, A. G., In vitro degradation of polymeric networks of poly(propylene fumarate) and the crosslinking macromer poly(propylene fumarate)-diacrylate. *Biomaterials* 2003, 24, (4), 571-577.

362. Anseth, K. S.; Metters, A. T.; Bryant, S. J.; Martens, P. J.; Elisseff, J. H.; Bowman, C. N., In situ forming degradable networks and their application in tissue engineering and drug delivery. *Journal of Controlled Release* 2002, 78, (1-3), 199-209.

363. Cellesi, F.; Tirelli, N.; Hubbell, J. A., Materials for cell encapsulation via a new tandem approach combining reverse thermal gelation and covalent crosslinking. *Macromolecular Chemistry and Physics* 2002, 203, (10-11), 1466-1472.

364. Shim, W. S.; Kim, J.-H.; Park, H.; Kim, K.; Kwon, I. C.; Lee, D. S., Biodegradability and biocompatibility of a pH- and thermo-sensitive hydrogel formed from a sulfonamide-modified poly(epsilon-caprolactone-co-lactide)-poly(ethylene glycol)-poly(epsilon-caprolactone-co-lactide) block copolymer. *Biomaterials* 2006, 27, (30), 5178-5185.

365. Jeong, B.; Bae, Y. H.; Kim, S. W., In situ gelation of PEG-PLGA-PEG triblock copolymer aqueous solutions and degradation thereof. *Journal of Biomedical Materials Research* 2000, 50, (2), 171-177.

366. Schmedlen, K. H.; Masters, K. S.; West, J. L., Photocrosslinkable polyvinyl alcohol hydrogels that can be modified with cell adhesion peptides for use in tissue engineering. *Biomaterials* 2002, 23, (22), 4325-4332.

367. Lee, K. Y.; Alsberg, E.; Mooney, D. J., Degradable and injectable poly(aldehyde guluronate) hydrogels for bone tissue engineering. *Journal of Biomedical Materials Research* 2001, 56, (2), 228-233.

368. Hou, Q. P.; De Bank, P. A.; Shakesheff, K. M., Injectable scaffolds for tissue regeneration. *Journal of Materials Chemistry* 2004, 14, (13), 1915-1923.

369. Overstreet, D. J.; Dutta, D.; Stabenfeldt, S. E.; Vernon, B. L., Injectable hydrogels. *Journal of Polymer Science Part B-Polymer Physics* 2012, 50, (13), 881-903.
370. Peppas, N. A.; Bures, P.; Leobandung, W.; Ichikawa, H., Hydrogels in pharmaceutical formulations. *European Journal of Pharmaceutics and Biopharmaceutics* 2000, 50, (1), 27-46.
371. Lu, L. C.; Zhu, X.; Valenzuela, R. G.; Currier, B. L.; Yaszemski, M. J., Biodegradable polymer scaffolds for cartilage tissue engineering. *Clinical Orthopaedics and Related Research* 2001, (391), S251-S270.
372. Klouda, L.; Mikos, A. G., Thermoresponsive hydrogels in biomedical applications. *European Journal of Pharmaceutics and Biopharmaceutics* 2008, 68, (1), 34-45.
373. Southall, N. T.; Dill, K. A.; Haymet, A. D. J., A view of the hydrophobic effect. *Journal of Physical Chemistry B* 2002, 106, (3), 521-533.
374. Li, L.; Shan, H.; Yue, C. Y.; Lam, Y. C.; Tam, K. C.; Hu, X., Thermally induced association and dissociation of methylcellulose in aqueous solutions. *Langmuir* 2002, 18, (20), 7291-7298.
375. Takahashi, M.; Shimazaki, M.; Yamamoto, J., Thermoreversible gelation and phase separation in aqueous methyl cellulose solutions. *Journal of Polymer Science Part B-Polymer Physics* 2001, 39, (1), 91-100.
376. Liu, W. G.; Zhang, B. Q.; Lu, W. W.; Li, X. W.; Zhu, D. W.; De Yao, K.; Wang, Q.; Zhao, C. R.; Wang, C. D., A rapid temperature-responsive sol-gel reversible poly(N-isopropylacrylamide)-g-methylcellulose copolymer hydrogel. *Biomaterials* 2004, 25, (15), 3005-3012.
377. Cullen, D. K.; Stabenfeldt, S. E.; Simon, C. M.; Tate, C. C.; LaPlaca, M. C., In vitro neural injury model for optimization of tissue-engineered constructs. *Journal of Neuroscience Research* 2007, 85, (16), 3642-3651.
378. Stabenfeldt, S. E.; Munglani, G.; Garcia, A. J.; LaPlaca, M. C., Biomimetic microenvironment modulates neural stem cell survival, migration, and differentiation. *Tissue Engineering Part A* 2010, 16, (12), 3747-3758.
379. Ruel-Gariepy, E.; Leroux, J. C., In situ-forming hydrogels - review of temperature-sensitive systems. *European Journal of Pharmaceutics and Biopharmaceutics* 2004, 58, (2), 409-426.
380. Bhattarai, N.; Matsen, F. A.; Zhang, M., PEG-grafted chitosan as an injectable thermoreversible hydrogel. *Macromolecular Bioscience* 2004, 5, (2), 107-111.
381. Bhattarai, N.; Ramay, H. R.; Gunn, J.; Matsen, F. A.; Zhang, M. Q., PEG-grafted chitosan as an injectable thermosensitive hydrogel for sustained protein release. *Journal of Controlled Release* 2005, 103, (3), 609-624.

382. Cho, J. H.; Kim, S. H.; Park, K. D.; Jung, M. C.; Yang, W. I.; Han, S. W.; Noh, J. Y.; Lee, J. W., Chondrogenic differentiation of human mesenchymal stem cells using a thermosensitive poly(N-isopropylacrylamide) and water-soluble chitosan copolymer. *Biomaterials* 2004, 25, (26), 5743-5751.
383. Nisbet, D. R.; Crompton, K. E.; Hamilton, S. D.; Shirakawa, S.; Prankerd, R. J.; Finkelstein, D. I.; Horne, M. K.; Forsythe, J. S., Morphology and gelation of thermosensitive xyloglucan hydrogels. *Biophysical Chemistry* 2006, 121, (1), 14-20.
384. Shirakawa, M.; Yamatoya, K.; Nishinari, K., Tailoring of xyloglucan properties using an enzyme. *Food Hydrocolloids* 1998, 12, (1), 25-28.
385. Joly-Duhamel, C.; Hellio, D.; Djabourov, M., All gelatin networks: 1. Biodiversity and physical chemistry. *Langmuir* 2002, 18, (19), 7208-7217.
386. Yang, H.; Kao, W. Y. J., Thermoresponsive gelatin/monomethoxy poly(ethylene glycol)-poly(D,L-lactide) hydrogels: Formulation, characterization, and antibacterial drug delivery. *Pharmaceutical Research* 2006, 23, (1), 205-214.
387. Ohya, S.; Matsuda, T., Poly(N-isopropylacrylamide) (PNIPAM)-grafted gelatin as thermoresponsive three-dimensional artificial extracellular matrix: molecular and formulation parameters vs. cell proliferation potential. *Journal of Biomaterials Science-Polymer Edition* 2005, 16, (7), 809-827.
388. Gil, E. S.; Frankowski, D. J.; Spontak, R. J.; Hudson, S. M., Swelling behavior and morphological evolution of mixed gelatin/silk fibroin hydrogels. *Biomacromolecules* 2005, 6, (6), 3079-3087.
389. Nakayama, M.; Okano, T.; Miyazaki, T.; Kohori, F.; Sakai, K.; Yokoyama, M. Molecular design of biodegradable polymeric micelles for temperature-responsive drug release. *Journal of Control Release* 2006, 115, (1), 46-56.
390. Pei, Y.; Chen, J.; Yang, L. M.; Shi, L. L.; Tao, Q.; Hui, B. J.; Li, R., The effect of pH on the LCST of poly(N-isopropylacrylamide) and poly(N-isopropylacrylamide-co-acrylic acid). *Journal of Biomaterials Science-Polymer Edition* 2004, 15, (5), 585-594.
391. Coughlan, D. C.; Quilty, F. P.; Corrigan, O. I., Effect of drug physicochemical properties on swelling/deswelling kinetics and pulsatile drug release from thermoresponsive poly(N-isopropylacrylamide) hydrogels. *Journal of Controlled Release* 2004, 98, (1), 97-114.
392. Liu, Y. Y.; Shao, Y. H.; Lu, J., Preparation, properties and controlled release behaviors of pH-induced thermosensitive amphiphilic gels. *Biomaterials* 2006, 27, (21), 4016-4024.
393. Yin, X.; Hoffman, A. S.; Stayton, P. S., Poly(N-isopropylacrylamide-co-propylacrylic acid) copolymers that respond sharply to temperature and pH. *Biomacromolecules* 2006, 7, (5), 1381-1385.
394. Na, K.; Park, J. H.; Kim, S. W.; Sun, B. K.; Woo, D. G.; Chung, H.-M.; Park, K.-H., Delivery of dexamethasone, ascorbate, and growth factor

(TGF beta-3) in thermo-reversible hydrogel constructs embedded with rabbit chondrocytes. *Biomaterials* 2006, 27, (35), 5951-5957.

395. Hatakeyama, H.; Kikuchi, A.; Yamato, M.; Okano, T., Bio-functionalized thermoresponsive interfaces facilitating cell adhesion and proliferation. *Biomaterials* 2006, 27, (29), 5069-5078.

396. Wei, H.; Cheng, S.-X.; Zhang, X.-Z.; Zhuo, R.-X., Thermo-sensitive polymeric micelles based on poly(N-isopropylacrylamide) as drug carriers. *Progress in Polymer Science* 2009, 34, (9), 893-910.

397. Wang, L. Q.; Tu, K. H.; Li, Y. P.; Zhang, J.; Jiang, L. M.; Zhang, Z. H., Synthesis and characterization of temperature responsive graft copolymers of dextran with poly (N-isopropylacrylamide). *Reactive & Functional Polymers* 2002, 53, (1), 19-27.

398. Ha, D. I.; Lee, S. B.; Chong, M. S.; Lee, Y. M.; Kim, S. Y.; Park, Y. H., Preparation of thermo-responsive and injectable hydrogels based on hyaluronic acid and poly(N-isopropylacrylamide) and their drug release behaviors. *Macromolecular Research* 2006, 14, (1), 87-93.

399. Tan, H.; Ramirez, C. M.; Miljkovic, N.; Li, H.; Rubin, J. P.; Marra, K. G., Thermosensitive injectable hyaluronic acid hydrogel for adipose tissue engineering. *Biomaterials* 2009, 30, (36), 6844-6853.

400. Kabanov, A. V.; Batrakova, E. V.; Alakhov, V. Y., Pluronic (R) block copolymers as novel polymer therapeutics for drug and gene delivery. *Journal of Controlled Release* 2002, 82, (2-3), 189-212.

401. Ahmed, F.; Alexandridis, P.; Shankaran, H.; Neelamegham, S., The ability of poloxamers to inhibit platelet aggregation depends on their physicochemical properties. *Thrombosis and Haemostasis* 2001, 86, (6), 1532-1539.

402. Nalbandian, R. M.; Henry, R. L.; Balko, K. W.; Adams, D. V.; Neuman, N. R., Pluronic F-127 gel preparation as an artificial skin in the treatment of 3ed-dergree burns in pigs. *Journal of Biomedical Materials Research* 1987, 21, (9), 1135-1148.

403. Cohn, D.; Sosnik, A.; Levy, A., Improved reverse thermo-responsive polymeric systems. *Biomaterials* 2003, 24, (21), 3707-3714.

404. Sosnik, A.; Cohn, D., Ethoxysilane-capped PEO-PPO-PEO triblocks: a new family of reverse thereto-responsive polymers. *Biomaterials* 2004, 25, (14), 2851-2858.

405. Cohn, D.; Sosnik, A.; Garty, S., Smart hydrogels for in situ generated implants. *Biomacromolecules* 2005, 6, (3), 1168-1175.

406. Sosnik, A.; Cohn, D., Reverse thermo-responsive poly(ethylene oxide) and poly(propylene oxide) multiblock copolymers. *Biomaterials* 2005, 26, (4), 349-357.

407. Sosnik, A.; Cohn, D.; San Roman, J. S.; Abraham, G. A., Crosslinkable PEO-PPO-PEO-based reverse thermo-responsive gels as potentially injectable materials. *Journal of Biomaterials Science-Polymer Edition* 2003, 14, (3), 227-239.

408. Liu, R.; Fraylich, M.; Saunders, B. R., Thermoresponsive copolymers: from fundamental studies to applications. *Colloid and Polymer Science* 2009, 287, (6), 627-643.
409. Ward, M. A.; Georgiou, T. K., Thermoresponsive polymers for biomedical applications. *Polymers* 2011, 3, (3), 1215-1242.
410. Lutz, J.-F.; Akdemir, O.; Hoth, A., Point by point comparison of two thermosensitive polymers exhibiting a similar LCST: Is the age of poly(NIPAM) over? *Journal of the American Chemical Society* 2006, 128, (40), 13046-13047.
411. Lutz, J.-F., Polymerization of oligo(ethylene glycol) (meth)acrylates: Toward new generations of smart biocompatible materials. *Journal of Polymer Science Part a-Polymer Chemistry* 2008, 46, (11), 3459-3470.
412. Lutz, J.-F.; Stiller, S.; Hoth, A.; Kaufner, L.; Pison, U.; Cartier, R., One-pot synthesis of PEGylated ultrasmall iron-oxide nanoparticles and their in vivo evaluation as magnetic resonance imaging contrast agents. *Biomacromolecules* 2006, 7, (11), 3132-3138.
413. Dai, S.; Ravi, P.; Tam, K. C., pH-Responsive polymers: synthesis, properties and applications. *Soft Matter* 2008, 4, (3), 435-449.
414. Schmaljohann, D., Thermo- and pH-responsive polymers in drug delivery. *Advanced Drug Delivery Reviews* 2006, 58, (15), 1655-1670.
415. Peppas, N. A.; Klier, J., Controlled release by using poly (methacrylic acid-g-ethylene glycol) hydrogels. *Journal of Controlled Release* 1991, 16, (1-2), 203-214.
416. Chen, G. H.; Hoffman, A. S., Temperature-induced phase -transition behaviors of random vs graft-copolymers of N-isopropylacrylamide and acrylic-acid. *Macromolecular Rapid Communications* 1995, 16, (3), 175-182.
417. Nagase, K.; Kobayashi, J.; Kikuchi, A.; Akiyama, Y.; Kanazawa, H.; Okano, T., Preparation of thermoresponsive cationic copolymer brush surfaces and application of the surface to separation of biomolecules. *Biomacromolecules* 2008, 9, (4), 1340-1347.
418. Determan, M. D.; Cox, J. P.; Mallapragada, S. K., Drug release from pH-responsive thermogelling pentablock copolymers. *Journal of Biomedical Materials Research Part A* 2007, 81A, (2), 326-333.
419. Varghese, S.; Hwang, N. S.; Canver, A. C.; Theprungsirikul, P.; Lin, D. W.; Elisseeff, J., Chondroitin sulfate based niches for chondrogenic differentiation of mesenchymal stem cells. *Matrix Biology* 2008, 27, (1), 12-21.
420. Bryant, S. J.; Arthur, J. A.; Anseth, K. S., Incorporation of tissue-specific molecules alters chondrocyte metabolism and gene expression in photocrosslinked hydrogels. *Acta Biomaterialia* 2005, 1, (2), 243-252.
421. DeLong, S. A.; Gobin, A. S.; West, J. L., Covalent immobilization of RGDS on hydrogel surfaces to direct cell alignment and migration. *Journal of Controlled Release* 2005, 109, (1-3), 139-148.

422. Garagorri, N.; Fermanian, S.; Thibault, R.; Ambrose, W. M.; Schein, O. D.; Chakravarti, S.; Elisseeff, J., Keratocyte behavior in three-dimensional photopolymerizable poly(ethylene glycol) hydrogels. *Acta Biomaterialia* 2008, 4, (5), 1139-1147.
423. Jongpaiboonkit, L.; King, W. J.; Lyons, G. E.; Paguirigan, A. L.; Warrick, J. W.; Beebe, D. J.; Murphy, W. L., An adaptable hydrogel array format for 3-dimensional cell culture and analysis. *Biomaterials* 2008, 29, (23), 3346-3356.
424. Hu, X.; Gao, C., Photoinitiating polymerization to prepare Biocompatible chitosan hydrogels. *Journal of Applied Polymer Science* 2008, 110, (2), 1059-1067.
425. Fedorovich, N. E.; Oudshoorn, M. H.; van Geemen, D.; Hennink, W. E.; Alblas, J.; Dhert, W. J. A., The effect of photopolymerization on stem cells embedded in hydrogels. *Biomaterials* 2009, 30, (3), 344-353.
426. Lutolf, M. P.; Tirelli, N.; Cerritelli, S.; Cavalli, L.; Hubbell, J. A., Systematic modulation of Michael-type reactivity of thiols through the use of charged amino acids. *Bioconjugate Chemistry* 2001, 12, (6), 1051-1056.
427. Pratt, A. B.; Weber, F. E.; Schmoekel, H. G.; Muller, R.; Hubbell, J. A., Synthetic extracellular matrices for in situ tissue engineering. *Biotechnology and Bioengineering* 2004, 86, (1), 27-36.
428. Vernon, B.; Tirelli, N.; Bachi, T.; Haldimann, D.; Hubbell, J. A., Water-borne, in situ crosslinked biomaterials from phase-segregated precursors. *Journal of Biomedical Materials Research Part A* 2003, 64A, (3), 447-456.
429. Shu, X. Z.; Liu, Y. C.; Palumbo, F. S.; Lu, Y.; Prestwich, G. D., In situ crosslinkable hyaluronan hydrogels for tissue engineering. *Biomaterials* 2004, 25, (7-8), 1339-1348.
430. Tan, H.; Chu, C. R.; Payne, K. A.; Marra, K. G., Injectable in situ forming biodegradable chitosan-hyaluronic acid based hydrogels for cartilage tissue engineering. *Biomaterials* 2009, 30, (13), 2499-2506.
431. Maia, J.; Ferreira, L.; Carvalho, R.; Ramos, M. A.; Gil, M. H., Synthesis and characterization of new injectable and degradable dextran-based hydrogels. *Polymer* 2005, 46, (23), 9604-9614.
432. Wang, D.-A.; Varghese, S.; Sharma, B.; Strehin, I.; Fermanian, S.; Gorham, J.; Fairbrother, D. H.; Cascio, B.; Elisseeff, J. H., Multifunctional chondroitin sulphate for cartilage tissue-biomaterial integration. *Nature Materials* 2007, 6, (5), 385-392.
433. Nishi, K. K.; Jayakrishnan, A., Preparation and in vitro evaluation of primaquine-conjugated gum arabic microspheres. *Biomacromolecules* 2004, 5, (4), 1489-1495.
434. Jia, X.; Yeo, Y.; Clifton, R. J.; Jiao, T.; Kohane, D. S.; Kobler, J. B.; Zeitel, S. M.; Langer, R., Hyaluronic acid-based microgels and microgel networks for vocal fold regeneration. *Biomacromolecules* 2006, 7, (12), 3336-3344.

435. Ruhela, D.; Riviere, K.; Szoka, F. C., Jr., Efficient synthesis of an aldehyde functionalized hyaluronic acid and its application in the preparation of hyaluronan-lipid conjugates. *Bioconjugate Chemistry* 2006, 17, (5), 1360-1363.
436. Ito, T.; Yeo, Y.; Highley, C. B.; Bellas, E.; Benitez, C. A.; Kohane, D. S., The prevention of peritoneal adhesions by in situ cross-linking hydrogels of hyaluronic acid and cellulose derivatives. *Biomaterials* 2007, 28, (6), 975-983.
437. Wang, W., Zheng, Y., Roberts, E., Duxbury, C.J., Ding, L.F., Irvine, D.J. and Howdle, S.M., Controlling chain growth: A new strategy to hyperbranched materials. *Macromolecule* 2007, 40, 7184.
438. Hoyle, C. E.; Bowman, C. N., Thiol-ene click chemistry. *Angewandte Chemie-International Edition* 2010, 49, (9), 1540-1573.

Chapter Two

Synthesis of Thermoresponsive and Photo-crosslinkable Hyperbranched Copolymer via *In-situ* Deactivation Enhanced Atom Transfer Radical Polymerization (DE-ATRP)

The majority of this chapter has previously been published in:

Dong, Y.; Gunning, P.; Cao, H.; Mathew, A.; Newland, B. E.; Saeed, A. O.; Magnusson, J. P.; Alexander, C.; Tai, H.; Pandit, A. and Wang, W. ‘Dual stimuli responsive PEG based hyperbranched polymers’ *Polymer Chemistry*, 2010, 1, 827-830

2.1 Introduction

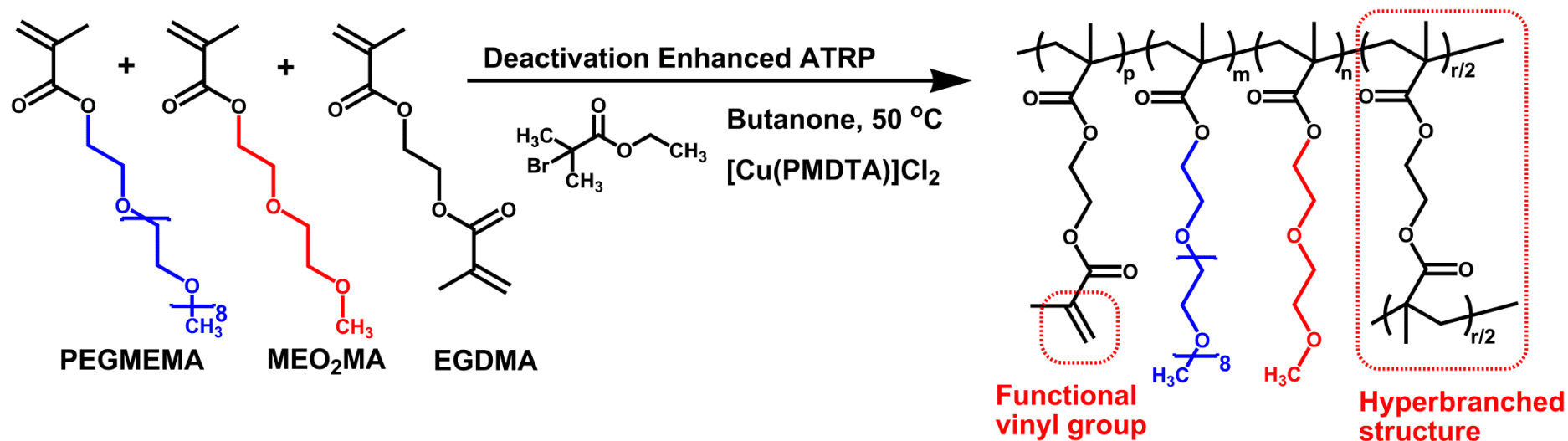
Stimuli-responsive polymers are defined as those polymers which respond with dramatic physical or chemical alterations to small external changes in their environment. Such stimuli include temperature, pH, ionic factors, electric or magnetic fields, chemical or biological agents and mechanical stress¹⁻⁴. Thermoresponsive polymers are considered as one of the most widely utilized stimuli-responsive polymers, as they are easy to apply both *in vitro* and *in vivo*⁵⁻¹⁰. Poly(N-isopropylacrylamide) (PNIPAAm) which is a classic and widely studied thermoresponsive polymer exhibits a rapid coil-to-globule conversion in aqueous solution around 32 °C¹¹. However, there are concerns over its safety for *in vivo* applications^{12, 13}. In the past few years, several thermoresponsive linear and star-shaped copolymers with PNIPAAm, poly(ethylene glycol) (PEG), oligo(ethylene glycol) methacrylate (OEGMA), poly(propylene oxide) (PPO), poly(vinyl ether)s (PVEs), poly(lactide) (PLA), poly(D,L-lactide-*co*-glycolide) (PLGA), poly(caprolactone) (PCL) and 2-(2-methoxyethoxy) ethyl methacrylate (MEO₂MA) have been developed for tissue engineering and drug delivery applications¹⁴⁻¹⁸. Among these copolymers, poly(MEO₂MA-*co*-OEGMA) was firstly reported by Lutz and colleagues¹⁶. This linear copolymer with lower critical solution temperature (LCST) around 37 °C was prepared via atom transfer radical polymerization (ATRP)^{16, 19}.

Compared to linear polymers, hyperbranched or dendritic polymers display a number of unique advantages, such as low solution and melt viscosity, and high functionality²⁰⁻²². In Lutz's study, they introduced the di-vinyl monomer of ethylene glycol dimethacrylate (EGDMA), however, only one percent of EGDMA caused the polymer gelation¹⁹. In contrast, in the present work, a higher degree of EGDMA (up to 10 % molar ratio of total feed monomers) was introduced. Instead of causing gelation, we successfully achieved a hyperbranched copolymer of poly(ethylene glycol) methyl ether methacrylate-*co*-2-(2-methoxyethoxy) ethyl methacrylate-*co*-ethylene glycol dimethacrylate (PEGMEMA-MEO₂MA-EGDMA) via a one-step *in-situ* deactivation enhanced atom transfer radical polymerization (DE-ATRP) approach (**Scheme 2.1**). As a result, the vinyl functional groups

Multifunctional Polymer Synthesis

contributed by the EGDMA component provide the copolymer with easy tailoring and photo-crosslinkable properties.

Meanwhile, by adjusting the “long” and “short” PEG chain monomers composition, we can sensitively alter the polymer hydrophobicity and control the LCST of the copolymers around body temperature. Furthermore, PEG based structure which is often considered as nontoxic, non-immunogenic and bio-compatible composition²³⁻²⁷ offers this copolymer good potential in tissue engineering and biomedical applications.



Scheme 2.1: Synthesis of hyperbranched polymers via an *in-situ* DE-ATRP copolymerization of poly(ethylene glycol) methyl ether methacrylate (PEGMEMA), 2-(2-methoxyethoxy) ethyl methacrylate (MEO₂MA) and ethylene glycol dimethacrylate (EGDMA). Ethyl 2-bromoisobutyrate and N,N,N',N'',N''-Pentamethyldiethylenetriamine (PMDTA) was used as the initiator and ligand. The dimethacrylate monomer of EGDMA provided the copolymer hyperbranched structure and the vinyl functionality.

2.2 Materials and Methods

2.2.1 Materials

The monomers of poly(ethylene glycol) methyl ether methacrylate (PEGMEMA $M_n = 475$), 2-(2-methoxyethoxy) ethyl methacrylate (MEO₂MA), and ethylene glycol dimethacrylate (EGDMA) were purchased from Sigma-Aldrich. The ethyl 2-bromoisobutyrate (98 %, Aldrich) was used as the initiator. N,N,N',N''-pentamethyldiethylenetriamine (PMDTA, 99 %, Aldrich), copper(II) chloride (CuCl₂, 97 %, Aldrich), L-ascorbic acid (AA, 99 %, Aldrich), butanone (99 %, HPLC grade, Aldrich) and hexane (95 %, Aldrich) were used as received.

2.2.2 Synthesis and Purification of PEGMEMA-MEO₂MA-EGDMA Copolymers

The copolymers were prepared in butanone using a two-necked round bottom flask (the volume ratio of total monomers to solvent was 1: 2). Copper chloride (CuCl₂, 0.25 molar equiv), ethyl 2-bromoisobutyrate (1 molar equiv) and PMDTA (0.25 molar equiv) were added into the flask and oxygen was removed by bubbling argon through the solutions for 25 min. L-ascorbic acid (AA, 0.375 molar equiv) that was diluted in deionized water was added with a microliter syringe. The solution was stirred at 800 rpm and the polymerization was conducted at 50 °C in an oil bath for a desired reaction time. The reaction was stopped by opening the flask and exposing the catalyst to air. The monomer of EGDMA was removed by dropping the solution into a large excess of hexane. The precipitated mixture was dissolved in deionized water and purified by dialysis (spectrum dialysis membrane, molecular weight cut off 6000-8000 kDa) for 4 days in dark at 4 °C. Polymer samples were obtained after freeze-drying and weighed to obtain the final yields.

2.2.3 Characterizations of PEGMEMA-MEO₂MA-EGDMA Copolymers

The copolymers were characterized by gel permeation chromatography (GPC), ¹H NMR and Fourier Transform Infrared Spectroscopy (FTIR). Weight average molecular weight (M_w), number average molecular weight

Multifunctional Polymer Synthesis

(M_n) and polydispersity index (PDI, M_w/M_n) were obtained by GPC (Polymer Laboratories) with RI detector. The columns (30 cm PLgel Mixed-C, two in series) were eluted using dimethylformamide (DMF) and calibrated with poly(methyl methacrylate) (PMMA) standards. All calibrations and analysis were performed at 40 °C and a flow rate of 1 ml/min. ^1H NMR was carried out on a 300 MHz Bruker NMR with MestReC processing software. The chemical shifts were referenced to the lock chloroform (CDCl_3). The characteristic chemical bonds were determined by FTIR (Varian 660-IR) to affirm the vinyl groups on the copolymers.

2.2.4 Thermo-responsive Behavior of PEGMEMA-MEO₂MA-EGDMA Copolymers

LCST of the copolymer solutions (0.03 % w/v) in deionized water were quantified by measuring their absorbance of 550 nm at temperatures from 20 to 55 °C (heating rate = 0.5 °C/second) with a Beckman DU-800 spectrophotometer. The data were collected every 2 seconds. The LCST value was defined as the temperature point when the A_{550} start suddenly increasing. Moreover, dynamic light scattering (DLS) was used to analyze size and distributions of copolymers in water solution on a submicron particle size analyzer (BeckmanCoulter DLS-N5). Polymer solutions (0.01 % w/v) were prepared in deionized water and filtered prior to measurements using a 0.45 μm disposable filter into a 12.5 \times 12.5 mm polystyrene disposable cuvette.

2.2.5 Preparation of Photo-crosslinked Gels and SEM Imaging

A LF215L UV lamp (365 nm, 2X15 W, UVitec, light intensity 2.0 mW/cm^2) was used for the preparation of photo-crosslinked hydrogels. The PEGMEMA-MEO₂MA-EGDMA copolymers were dissolved in 0.1 % w/v Irgacure 2959 water solution to prepare 20 % and 40 % (w/v) copolymer solutions. Photo-crosslinked gels were formed using 200 μl polymer solutions by UV exposure of 2 h. Scanning Electron Microscopy (SEM) was used to characterize the porous structure of freeze-dried gels. The samples were mounted on an aluminum stub using an adhesive carbon tab and

sputter coated with gold before images were obtained using a Hitachi Field Emission SEM machine.

2.2.6 Cytotoxicity Assessment

3T3 mouse fibroblast cell line was utilized for the polymer cytotoxicity assessment. 15,000 cells and PEGMEMA-MEO₂MA-EGDMA polymer solution (in Dulbecco's Modified Eagle's Medium, DMEM, Sigma) were seeded into each well of a 48-wells tissue culture plate (the concentration of polymers in media were 0.5 and 1 mg/ml). After one and four days of incubation at 37 °C and 5 % CO₂, alamarBlue[®] reduction method was used to assess cell activity. The absorbance at the lower wavelength filter (550 nm) was measured followed by the higher wavelength filter (595 nm) via a thermo scientific Varioskan Flash Plate Reader. The following equations were used to calculate the percentage of cell viability:

AO_{LW} = absorbance of oxidized form of alamarBlue[®] along at lower wavelength;

AO_{HW} = absorbance of oxidized form of alamarBlue[®] along at higher wavelength;

Calculated correlation factor:

$$R_o = AO_{LW} / AO_{HW}; \quad (\text{eqn. 2.1})$$

Calculated the percentage of reduced alamarBlue[®]:

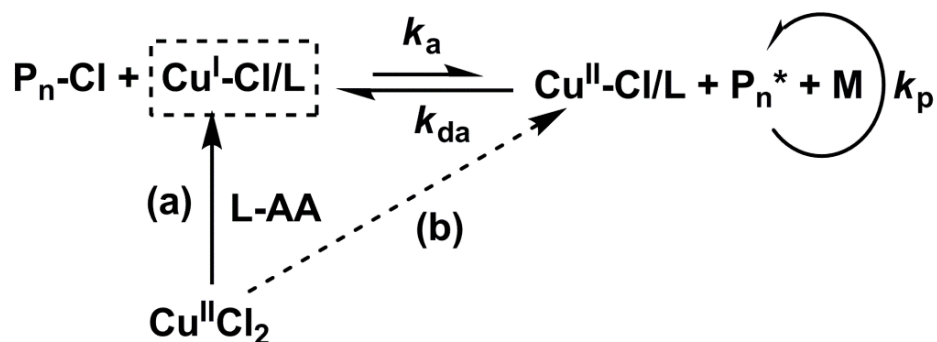
$$AR_{LW} \% = (A_{LW} - A_{HW} \times R_o) \times 100 \quad (\text{eqn. 2.2})$$

Calculated the percentage of cell metabolic activity:

$$\text{Cell activity \%} = (AR_{LW}[\text{Samples}] / AR_{LW}[\text{Cells along}]) \times 100 \quad (\text{eqn. 2.3})$$

2.2.7 Statistical Analysis

Comparisons between multiple groups were analyzed via one way-ANOVA using GraphPad Prism 5 software. Differences between two data sets were considered significant when $p < 0.05$.



Scheme 2.2: Mechanism of *in-situ* deactivation enhanced atom transfer radical polymerization (DE-ATRP). (a) *In-situ* producing Cu^{I} species from Cu^{II} species by reducing agent L-ascorbic acid (AA); (b) A small amount of AA addition ensures the excessive Cu^{II} species in the reaction system which leads to enhanced deactivation reaction, suppression of the growth rate and delayed gelation.

2.3 Results and Discussion

2.3.1 Synthesis of PEGMEMA-MEO₂MA-EGDMA Copolymers via *In-situ* DE-ATRP Approach

The DE-ATRP approach was previously reported by our group for the synthesis of dendritic copolymers^{28, 29}. In these previous studies, halogen-(Cu^I+Cu^{II})/Ligand was used as the catalyst to start the reaction instead of using the halogen-Cu^I/Ligand as in the conventional ATRP method; as a result the excessive Cu^{II} species in the DE-ATRP system enhanced the deactivation of the polymerization which slow down the reaction speed and delayed the gelation. However, using the halogen-Cu^I/Cu^{II} mixture as the catalyst resulted in some disadvantages: (i) Cu^I species are easy to be oxidized in air which may affect the repeatability of the reaction; (ii) It is more complex to study the mechanism how the deactivation agent (Cu^{II} species) control the actual reaction kinetics and influence the polymer structure.

In this study, an *in-situ* DE-ATRP approach was applied by using Cu^{II}/Ligand and a small amount of reducing agent AA to start the reaction (**Scheme 2.2**). AA reduced part of the Cu^{II} species into Cu^I, which can start the polymerization, and in the meantime the extra amounts of Cu^{II} species that remain in the reaction lead to the slow chain growth and delayed gelation. Hyperbranched copolymer of PEGMEMA-MEO₂MA-EGDMA was prepared by this approach. The reaction was monitored by GPC analysis (**Figure 2.1**). Polymer chain grew over time, for example, the total monomer conversion was 57 % after 26 h, with Mn of the copolymer as 9.9 KDa (**entry 1 in Table 2.1**). Meanwhile, the PDI value kept at a low level which demonstrated the controlled chain growth.

In addition, it was found that polymerization speed can be sensitively affected by varying the amount of the reducing agent AA (**Figure 2.2**). The same level of monomer conversion (i.e. 45 %) needed 9 h of reaction time by using 15 mol % AA, 6 h with 30 mol % AA and 1 h with 50 mol % AA. This result indicates that the slight change in the equilibrium between Cu^{II} and Cu^I could delicately adjust the activation/deactivation process of ATRP.

Interestingly, PDI value remained at the same trend by the varying AA amount (**Figure 2.3**): at the beginning stage, polymer chain grew with well controlling; while at the later stage, the broader PDI with the polymerization progressing was commonly considered as a result of the hyperbranched chain growth^{30, 31} which means the reducing agent can only influence the polymerization rate but not affect the kinetic chain growth at the molecular level.

On the other hand, a similar approach to our method is called activator generated by electron transfer (AGET) ATRP, in which the reaction is also started with Cu^{II}/Ligand and reducing agent. However, there is a significant difference between these two approaches. The AGET-ATRP usually requires an excessive reducing agent (e.g. 5 to 10 times excess of AA) to transfer Cu^{II} to Cu^I completely and rapidly in the reaction^{32, 33}. While only up to 50 mol % of reducing agent was used in the *in-situ* DE-ATRP, so that there is always an excess of Cu^{II} species in the reaction system to “deactivate” the reaction.

2.3.2 Characterization of Hyperbranched PEGMEMA-MEO₂MA-EGDMA Copolymers with Vinyl Functional Groups

The structure of the copolymers were characterized by ¹H NMR analysis (**Figure 2.4**). The characteristic peaks at chemical shifts of 6.1 and 5.6 ppm were attributed to the vinyl functional groups in the copolymer. The copolymer composition (m, n, r, p) can be calculated from the integral data C, D, E, H. assigned as indicated in **Figure 2.4**. The following equations (**eqns. 2.4 to 2.7**) demonstrate the calculating process:

$$H = p \quad (\text{eqn. 2.4})$$

$$C = 4p + 2m + 2n + 2r \quad (\text{eqn. 2.5})$$

$$D = 34m + 6n \quad (\text{eqn. 2.6})$$

$$E = 3m + 3n \quad (\text{eqn. 2.7})$$

Table 2.1: Copolymerization of poly(ethylene glycol) methyl ether methacrylate (PEGMEMA, $M_n = 475$), 2-(2-methoxyethoxy) ethyl methacrylate (MEO₂MA) and ethylene glycol dimethacrylate (EGDMA) via *in-situ* DE-ATRP.

entry	[L-AA]: [CuCl ₂]	samples	RT ^a (h)	monomer conversion ^b (%)	M_n ^c (kg/mol)	PDI ^d
1	15 mol%	S1-1	5	20	4.3	1.14
		S1-2	9	45	7.3	1.22
		S1-3	26	57	9.9	1.35
2	30 mol%	S2	6	43	10.0	1.25
3	50 mol%	S3	5	83	17.9	3.92

^a Reaction time. ^b Monomer conversion, estimated using peak areas for monomers and copolymers in GPC traces. ^c Number average molecular weight. ^d Polydispersity Index (M_w/M_n). Polymerisation conditions: 50 °C in butanone; total monomers/butanone (v/v) = 1:2; the initiator (I) / catalyst (C) / ligand (L) are ethyl 2-bromoisobutyrate / CuCl₂ / N,N,N',N'',N''-pentamethyldiethylenetriamine; the reducing agent is L-ascorbic acid (AA); the [I]/[PEGMEMA]/[MEO₂MA]/[EGDMA] (feed mole ratio) = 1:15:75:10, [I]/[C]/[L] = 1:0.25:0.25.

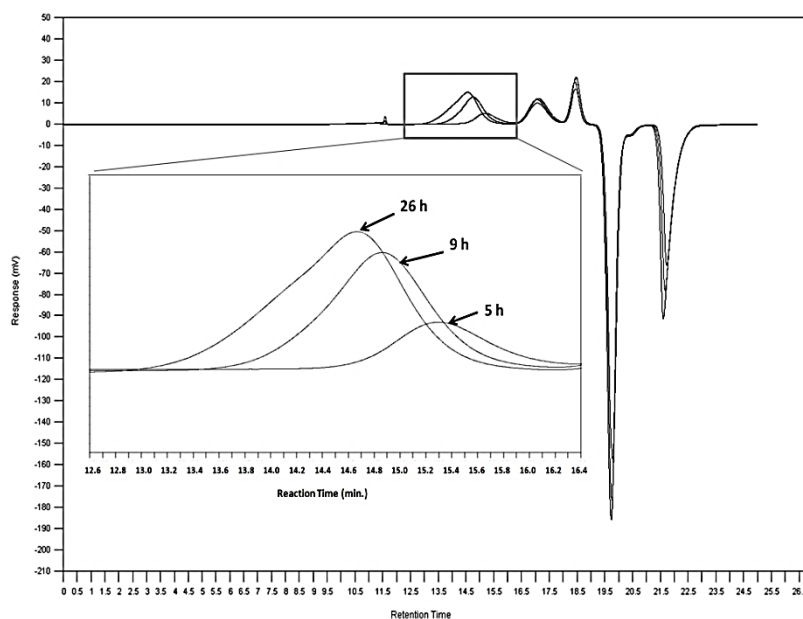


Figure 2.1: GPC traces from RI detector for the samples of entry 2 in Table 2.1. **Note:** the peak became broader and moving forward indicated that the increased molecular weights and polydispersities with monomer conversion were observed.

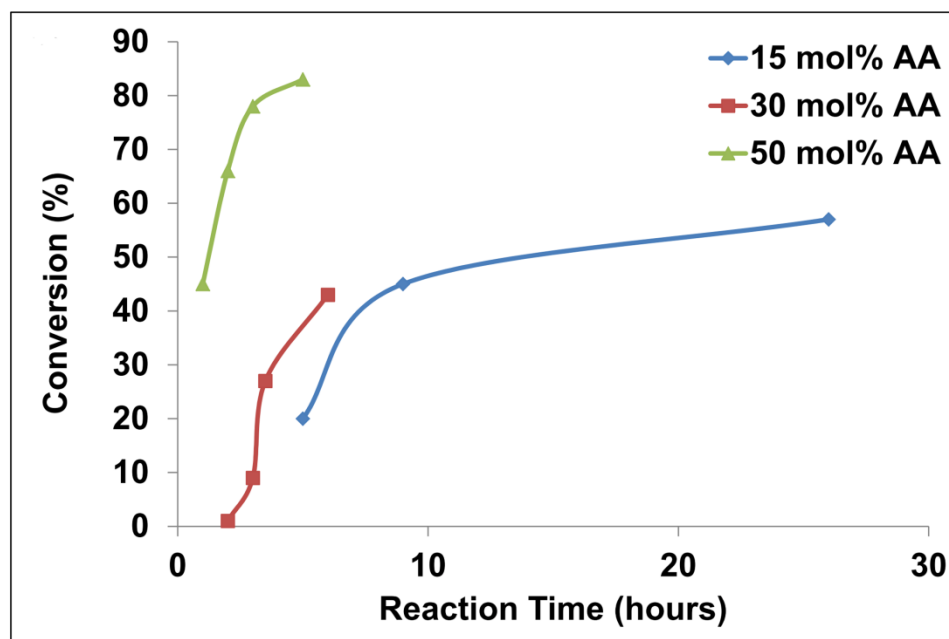


Figure 2.2: Kinetic plots of the *in-situ* DE-ATRP polymerization of PEGMEMA-MEO₂MA-EGDMA copolymers by using 15 mol %, 30 mol % and 50 mol % of reducing agent of L-ascorbic acid (AA). Increase of the monomer conversion along with the reaction progress. **Note:** the polymerization speed can be sensitively affected by varying the amount of the reducing agent AA. For example, the same level of monomer conversion (i.e. 45 %) needed 9 h of reaction time by using 15 mol % AA, 6 h with 30 mol % AA and only 1 h with 50 mol % AA.

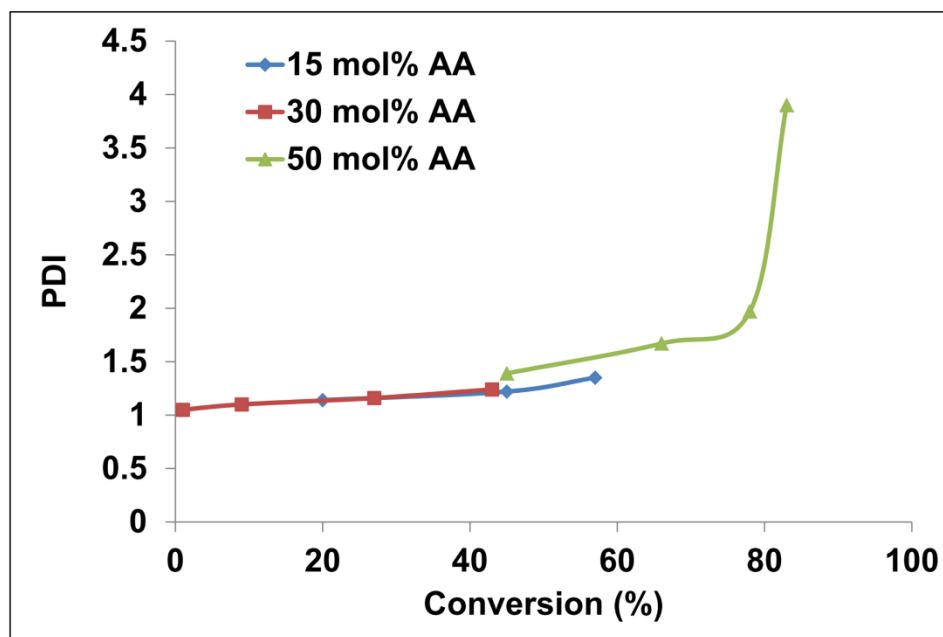


Figure 2.3: Kinetic plots of the *in-situ* DE-ATRP polymerization of PEGMEMA-MEO₂MA-EGDMA copolymers by using 15 mol %, 30 mol % and 50 mol % of reducing agent L-ascorbic acid (AA). Increase of the polydispersity Index (PDI, M_w/M_n) along with the monomer conversion.

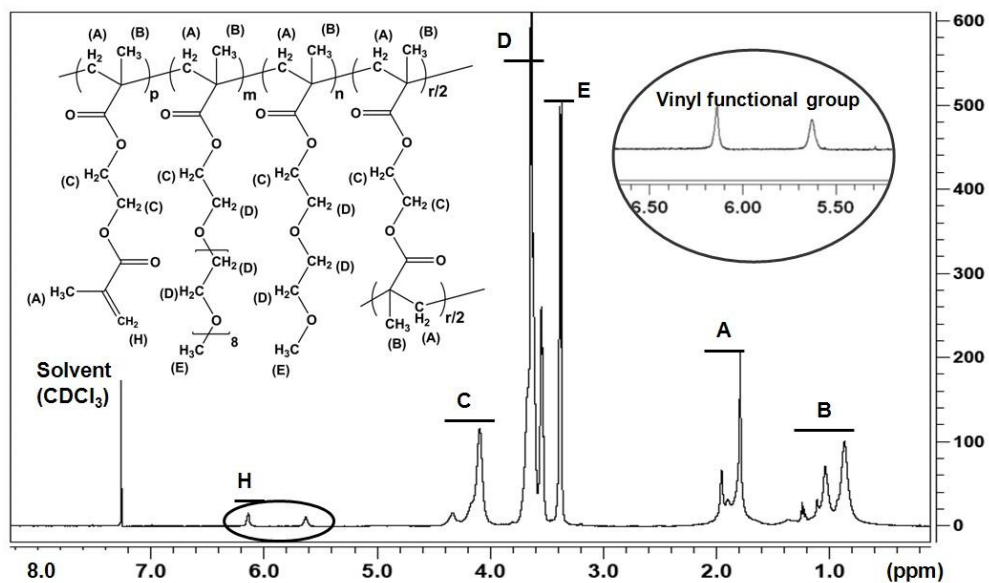


Figure 2.4: ¹H NMR for the PEGMEMA-MEO₂MA-EGDMA copolymer (entry 1 in Table 2.1) in CDCl₃. **Note:** the spectrum shows the vinyl functional group within the structure at the chemical shifts of 6.1 and 5.6 ppm (Insert).

The double bond content and the branching degree of the copolymers were calculated from **eqn. 2.8** and **eqn. 2.9**, respectively:

$$\text{Double bond content (mol\%)} = p/(m + n + r + p) \times 100 \quad (\text{eqn. 2.8})$$

$$\text{Branching degree (mol\%)} = r/(m + n + r + p) \times 100 \quad (\text{eqn. 2.9})$$

The composition, double bond content and branching degree of the copolymers are shown in **Table 2.2**. For example, the double bond and the branching structure are at 6 and 10 mol % in polymer S5. In addition, the chemical structure of the copolymer was also determined by FTIR (**Figure 2.5**).

2.3.3 Thermoresponsive Behavior of PEGMEMA-MEO₂MA-EGDMA Copolymers

LCST of the copolymers were determined by UV-vis spectrophotometer (**Figure 2.6**). The copolymers (**S4, S5 and S6 in Table 2.2**) dissolved in deionized water were quantified by measuring their absorbance of 550 nm at temperatures from 20 to 55 °C. Compared with the linear poly(OEGMA-co-MEO₂MA) copolymer as reported by Lutz *et al.*, our hyperbranched copolymer showed a lower phase transition temperature with similar polymer composition. For example they showed LCSTs of 39 and 49 °C with 10 and 20 % of PEGMEMA respectively ¹⁹, whereas our polymer exhibited 28 and 38 °C with 12 and 22 % of PEGMEMA respectively. Two reasons might be responsible: (1) The 3D hyperbranched structure and subsequently the compact space configuration of the copolymer may have resulted in stronger polymer-polymer interactions than polymer-water hydrogen bonding interaction; (2) the hydrophobic EGDMA content of the copolymer also reduces the LCST. Moreover, the high concentration of the copolymer water solution could reversible form hydrogel above the LCST (**Figure 2.6 Insert**).

In addition, DLS indicated a significant change in particle size of the copolymer in deionized water when varying the temperature. At 20 °C, the hydrodynamic radius (*R_h*) of polymer particles were ca. 7.5 nm, and at 37 °C, it was found to be 125 nm (**Figure 2.7**). This is due to the aggregation occurring at the temperatures above LCST.

Table 2.2: Properties of PEGMEMA-MEO₂MA-EGDMA copolymers

Samples	f^a ((PEGMEMA)/ [MEO ₂ MA]/ [EGDMA])	F^b ((PEGMEMA)/ [MEO ₂ MA]/ [EGDMA])	double bond content ^c	branching degree ^d	LCST °C ^e
S4	10/80/10	9/77/14	4	10	24
S5	15/75/10	12/72/16	6	10	28
S6	25/65/10	22/63/15	6	9	38

^a Monomer feed ratio. ^b Polymer composition; determined by ¹H NMR. ^{c, d} Calculated with eqs 2.4 to 2.9 (Unit: mol %). ^e Determined by UV-vis spectrophotometer.

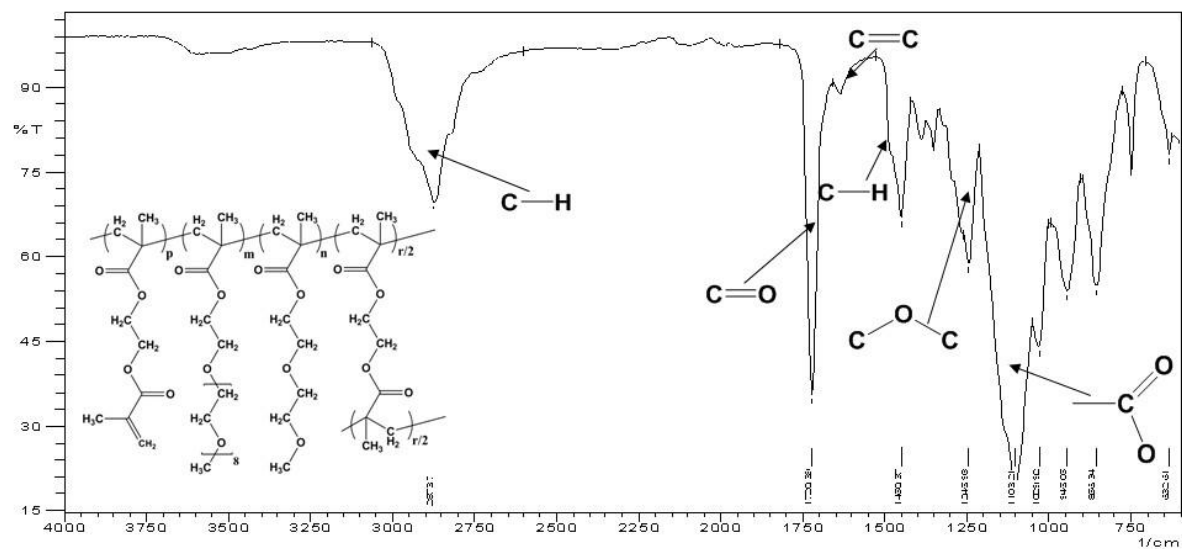


Figure 2.5: FTIR analysis of freeze-dried polymer of PEGMEMA-MEO₂MA-EGDMA (entry 1 in Table 2.1). The main chemical groups were characterized by a standard and labeled. **Note:** the spectrum shows the double bond within the polymer structure at the wavenumber around 1650 cm^{-1} .

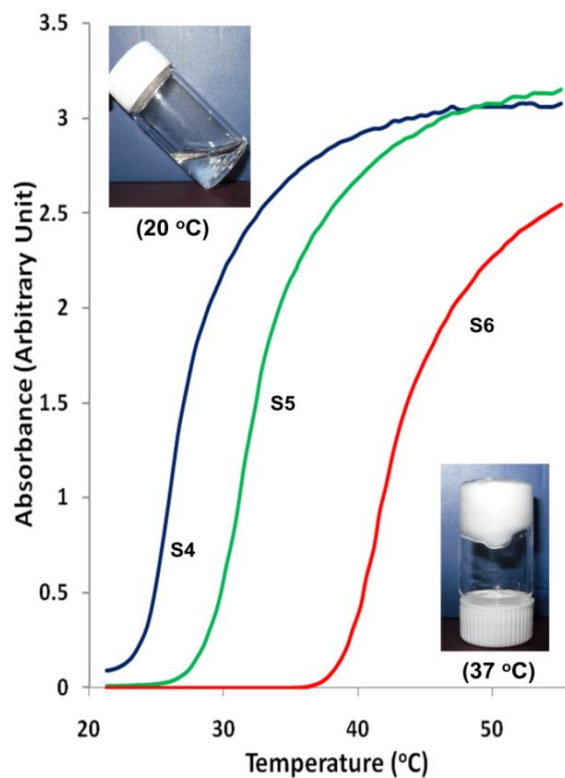


Figure 2.6: Thermoresponsive properties of PEGMEMA-MEO₂MA-EGDMA copolymers (S4, S5 and S6 in Table 2.2). LCST behavior of the copolymer in 0.03 % w/v deionized water determined by UV-vis spectrophotometer. Insert: copolymer solution (S5 in Table 2.2, 40 % w/v) became physical cross-linked gel when the temperature was raised above its LCST from 20 °C to 37 °C.

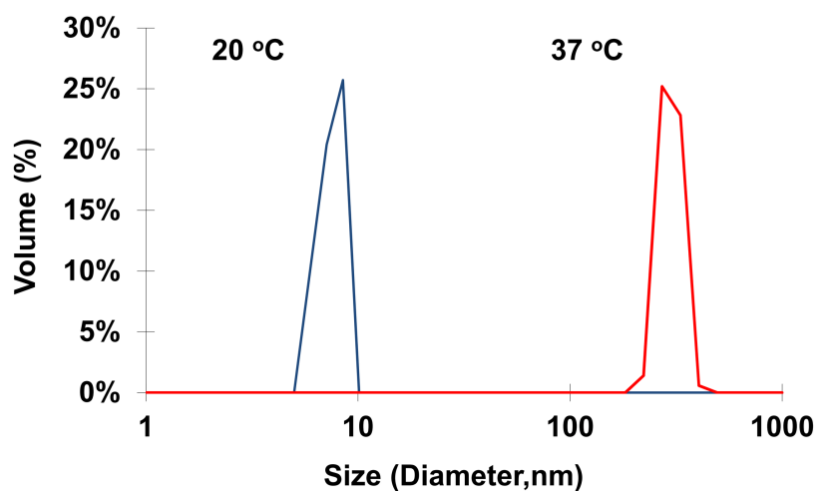


Figure 2.7: Size distribution measured by dynamic light scattering. Polymer solutions (S5 in Table 2.2, 0.01 % w/v) were prepared in deionized water and filtered prior to measurements using a 0.45 μm disposable filter. Light incident angle was 90°. **Note:** at 37 °C, polymer particles aggregated together to form the microgel structure.

2.3.4 Photo-crosslinked Hydrogels and SEM Analysis

Furthermore, after exposing the copolymer solution samples (with 0.1 % w/v of photoinitiator) to UV light (details in supporting information), the photo-crosslinking occurred to form gels. Although because the hydrogels shrank during the dehydrate process, the pore size on SEM images can not fully display the real situation in the hydrogels. It was still shown that the polymer at a higher concentration (40 % w/v) formed the photo-crosslinked gel with denser structure than at a lower concentration (20 % w/v) (**Figure 2.8**).

2.3.5 Cytotoxicity Assessment

3T3 mouse fibroblast cells were utilized for the cytotoxicity assessment of the copolymer. Cells and the polymer/DMEM solution (S5 in Table 2.2, dissolved in DMEM medium, 0.5 and 1 mg/ml) were added into each well of a 48-well tissue culture plate. It was noticed that the polymer solution formed gel particles and sank on the bottom of the culture plate at 37 °C because its thermoresponsive behavior. The alamarBlue[®] reduction method was used to assess changes in cell viability after one and four days. The results showed no significant difference of cells viability between the control (cells alone) and polymer samples after four days, indicating the copolymer is not affecting the cellular metabolism at such concentrations (**Figure 2.9**).

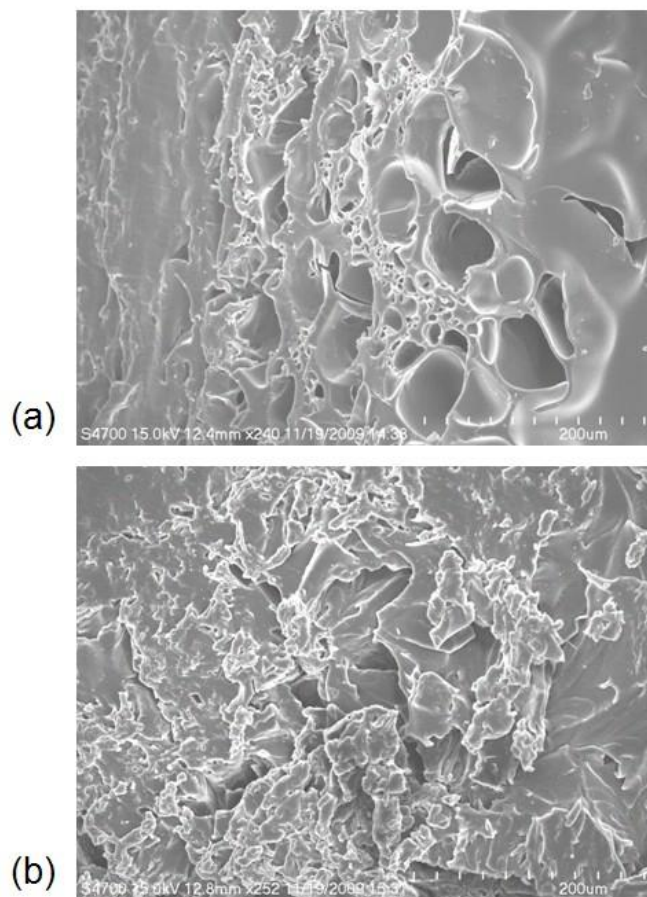


Figure 2.8: SEM images of freeze-dried photo-crosslinked gels prepared from 20 % (a) and 40 % (b) (w/v) PEGMEMA-MEO₂MA-EGDMA copolymer (S5 in Table 2.2) solution. **Note:** the photo-crosslinked gel formed using a low polymer concentration sample demonstrated more looser structure (a) than the gel formed using a high polymer concentration (b).

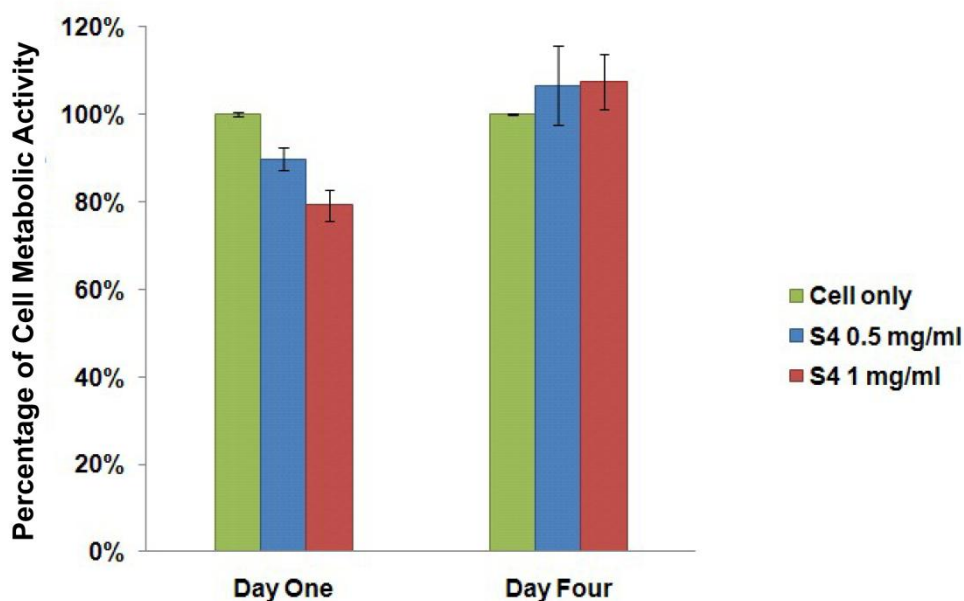


Figure 2.9: Cell metabolic activity assessment of 3T3 cells after one and four days treatment with PEGMEMA-MEO₂MA-EGDMA polymer (S5 in Table 2.2) using alamarBlue[®] assay. Cells alone as the control; the polymer concentrations were at 0.5 and 1 mg/ml. **Note:** there is no significant difference of cells viability between the control (cells alone) and polymer samples after four days (mean \pm SD, $n = 3$, $p < 0.05$).

2.4 Conclusion

A thermoresponsive and photo-crosslinkable hyperbranched copolymer PEGMEMA-MEO₂MA-EGDMA has been successfully prepared via an *in-situ* DE-ATRP approach. This copolymer exhibited the LCST around body temperature, which could be specifically adjusted by varying polymer composition. Thus at room temperature, this polymer is water soluble, while forms a physical gel at body temperature. In addition, the high degree of vinyl functional group allow this polymer photo-crosslinking by UV explosion in order to achieve a stable hydrogel structure with enhanced mechanical properties. In conclusion, this dual stimuli responsive polymer which can be easily modified further, shows great potentials for wide applications, including tissue engineering and drug delivery, polymer composites, UV cross-linkable polymer coatings, prototype mouldings, and micro patterning.

2.5 References

1. Qiu, Y.; Park, K., Environment-sensitive hydrogels for drug delivery. *Advanced Drug Delivery Reviews* 2001, 53, (3), 321-339.
2. Gil, E. S.; Hudson, S. A., Stimuli-responsive polymers and their bioconjugates. *Progress in Polymer Science* 2004, 29, (12), 1173-1222.
3. Okano, T., *Biorelated Polymers and Gels*. CA: Academic Press: San Diego, 1998.
4. Jeong, B.; Gutowska, A., Lessons from nature: stimuli-responsive polymers and their biomedical applications. *Trends in Biotechnology* 2002, 20, (7), 305-311.
5. Freiberg, S.; Zhu, X., Polymer microspheres for controlled drug release. *International Journal of Pharmaceutics* 2004, 282, (1-2), 1-18.
6. Liu, R. X.; Fraylich, M.; Saunders, B. R., Thermoresponsive copolymers: from fundamental studies to applications. *Colloid and Polymer Science* 2009, 287, (6), 627-643.
7. Kharlampieva, E.; Kozlovskaya, V.; Tyutina, J.; Sukhishvili, S. A., Hydrogen-bonded multilayers of thermoresponsive polymers. *Macromolecules* 2005, 38, (25), 10523-10531.
8. Kavanagh, C. A.; Rochev, Y. A.; Gallagher, W. A.; Dawson, K. A.; Keenan, A. K., Local drug delivery in restenosis injury: thermoresponsive co-polymers as potential drug delivery systems. *Pharmacology & Therapeutics* 2004, 102, (1), 1-15.
9. Eeckman, F.; Moes, A. J.; Amighi, K., Evaluation of a new controlled-drug delivery concept based on the use of thermoresponsive polymers. *International Journal of Pharmaceutics* 2002, 241, (1), 113-125.
10. Hruby, M.; Kucka, J.; Mackova, H.; Lebeda, O.; Ulbrich, K., Thermoresponsive polymers - from laboratory curiosity to advanced materials for medicinal applications. *Chemické Listy* 2008, 102, (1), 21-27.
11. Schild, H. G., Poly (N-Isopropylacrylamide) - experiment, theory and application. *Progress in Polymer Science* 1992, 17, (2), 163-249.
12. Chilkoti, A.; Dreher, M. R.; Meyer, D. E.; Raucher, D., Targeted drug delivery by thermally responsive polymers. *Advanced Drug Delivery Reviews* 2002, 54, (5), 613-630.
13. Vihola, H.; Laukkanen, A.; Valtola, L.; Tenhu, H.; Hirvonen, J., Cytotoxicity of thermosensitive polymers poly(N-isopropylacrylamide), poly(N-vinylcaprolactam) and amphiphilically modified poly(N-vinylcaprolactam). *Biomaterials* 2005, 26, (16), 3055-3064.
14. Kwon, I. K.; Matsuda, T., Photo-iniferter-based thermoresponsive block copolymers composed of poly(ethylene glycol) and poly(N-isopropylacrylamide) and chondrocyte immobilization. *Biomaterials* 2006, 27, (7), 986-995.

15. Li, C.; Buurma, N. J.; Haq, I.; Turner, C.; Armes, S. P.; Castelletto, V.; Hamley, I. W.; Lewis, A. L., Synthesis and characterization of biocompatible, thermoresponsive ABC and ABA triblock copolymer gelators. *Langmuir* 2005, 21, (24), 11026-11033.
16. Lutz, J.-F.; Akdemir, O.; Hoth, A., Point by point comparison of two thermosensitive polymers exhibiting a similar LCST: is the age of poly(NIPAM) over? *Journal of the American Chemical Society* 2006, 128, (40), 13046-13047.
17. Park, S. Y.; Han, D. K.; Kim, S. C., Synthesis and characterization of star-shaped PLLA-PEO block copolymers with temperature-sensitive sol-gel transition behavior. *Macromolecules* 2001, 34, (26), 8821-8824.
18. Shim, W. S.; Yoo, J. S.; Bae, Y. H.; Lee, D. S., Novel injectable pH and temperature sensitive block copolymer hydrogel. *Biomacromolecules* 2005, 6, (6), 2930-2934.
19. Lutz, J.-F.; Weichenhan, K.; Akdemir, O.; Hoth, A., About the phase transitions in aqueous solutions of thermoresponsive copolymers and hydrogels based on 2-(2-methoxyethoxy)ethyl methacrylate and oligo(ethylene glycol) methacrylate. *Macromolecules* 2007, 40, (7), 2503-2508.
20. Hult, A.; Johansson, M.; Malmstrom, E., Hyperbranched polymers. In *Branched Polymers II*, Springer-Verlag Berlin: Berlin, 1999; 143, 1-34.
21. Voit, B., New developments in hyperbranched polymers. *Journal of Polymer Science Part A-Polymer Chemistry* 2000, 38, (14), 2505-2525.
22. Seiler, M., Hyperbranched polymers: Phase behavior and new applications in the field of chemical engineering. *Fluid Phase Equilibria* 2006, 241, (1-2), 155-174.
23. Zalipsky, S., Chemistry of polyethylene glycol conjugates with biologically active molecules. *Advanced Drug Delivery Reviews* 1995, 16, (2-3), 157-182.
24. Veronese, F. M., Peptide and protein PEGylation: a review of problems and solutions. *Biomaterials* 2001, 22, (5), 405-417.
25. Nguyen, K. T.; West, J. L., Photopolymerizable hydrogels for tissue engineering applications. *Biomaterials* 2002, 23, (22), 4307-4314.
26. Kobayashi, H.; Kawamoto, S.; Saga, T.; Sato, N.; Hiraga, A.; Ishimori, T.; Konishi, J.; Togashi, K.; Brechbiel, M. W., Positive effects of polyethylene glycol conjugation to generation-4 polyamidoamine dendrimers as macromolecular MR contrast agents. *Magnetic Resonance in Medicine* 2001, 46, (4), 781-788.
27. Greenwald, R. B.; Choe, Y. H.; McGuire, J.; Conover, C. D., Effective drug delivery by PEGylated drug conjugates. *Advanced Drug Delivery Reviews* 2003, 55, (2), 217-250.
28. Tai, H.; Wang, W.; Vermonden, T.; Heath, F.; Hennink, W. E.; Alexander, C.; Shakesheff, K. M.; Howdle, S. M., Thermoresponsive and

photocrosslinkable PEGMEMA-PPGMA-EGDMA copolymers from a one-step ATRP synthesis. *Biomacromolecules* 2009, 10, (4), 822-828.

29. Tai, H.; Howard, D.; Takae, S.; Wang, W.; Vermonden, T.; Hennink, W. E.; Stayton, P. S.; Hoffman, A. S.; Endruweit, A.; Alexander, C.; Howdle, S. M.; Shakesheff, K. M., Photo-Cross-Linked hydrogels from thermoresponsive PEGMEMA-PPGMA-EGDMA copolymers containing multiple methacrylate groups: mechanical property, swelling, protein release, and cytotoxicity. *Biomacromolecules* 2009, 10, (10), 2895-2903.

30. Matyjaszewski, K.; Gaynor, S. G.; Kulfan, A.; Podwika, M., Preparation of hyperbranched polyacrylates by atom transfer radical polymerization .1. Acrylic AB* monomers in "living" radical polymerizations. *Macromolecules* 1997, 30, (17), 5192-5194.

31. Isaure, F.; Cormack, P. A. G.; Graham, S.; Sherrington, D. C.; Armes, S. P.; Butun, V., Synthesis of branched poly(methyl methacrylate)s via controlled/living polymerisations exploiting ethylene glycol dimethacrylate as branching agent. *Chemical Communications* 2004, (9), 1138-1139.

32. Li, M.; Min, K.; Matyjaszewski, K., ATRP in waterborne miniemulsion via a simultaneous reverse and normal initiation process. *Macromolecules* 2004, 37, (6), 2106-2112.

33. Min, K.; Jakubowski, W.; Matyjaszewski, K., AGET ATRP in the presence of air in miniemulsion and in bulk. *Macromolecular Rapid Communications* 2006, 27, (12), 982-982.

Chapter Three

***In-Situ* Cross-linked Semi-IPN Hydrogel Prepared from Thermoresponsive Hyperbranched Copolymer with Multi-acrylate Functionality and Hyaluronic Acid**

The majority of this chapter has previously been published in:

Dong, Y.; Hassan, W.; Zheng, Y.; Saeed, A.O.; Cao, H.; Tai, H.; Pandit, A. and Wang, W. 'Thermoresponsive hyperbranched copolymer with multi acrylate functionality for *in situ* cross-linkable hyaluronic acid composite semi-IPN hydrogel', *Journal of Materials Science: Materials in Medicine*, 2012, 23 (1), 25-35.

3.1 Introduction

In-situ cross-linkable hydrogels have attracted much attention in applications for tissue engineering and drug delivery because they can be injected directly into irregular cavities and provide a homogenous environment for cellular and bioactive molecular distribution¹⁻⁵. Thermoresponsive polymers have been widely studied for such applications to *in-situ* form physically cross-linked gels⁶⁻¹⁰. However, the physical thermal gelation is reversible and exhibits weak mechanical properties which hamper its clinical uses. Therefore, photo-polymerization or chemical cross-linking methods are used to enhance the gel mechanical properties. Drawbacks limit the applications of the photo-polymerization systems such as the extra equipment that is needed in a clinical setting, also the safety concerns of UV light in clinical uses present issues¹¹⁻¹⁴. On the other hand, the dual gelling systems by physically and chemically cross-linking via thiol-ene Michael-type addition reaction under physiological conditions have shown promising properties¹⁵⁻²⁰. Cellesi *et al.* reported the “tandem process” of thermal and chemical cross-linked gel for cell encapsulation^{21, 22}; Lee *et al.* reported the N-isopropylacrylamide (NIPAAm) based dual *in-situ* gelling system for embolization²³. However, these systems usually need the complex multi-step modification reactions to provide the polymer desired cross-linkable functionalities; in addition, some of the chemical compositions such as NIPAAm are considered to be too toxic for *in vivo* applications.

We have previously reported the synthesis of PEG-based hyperbranched thermoresponsive and photo-crosslinkable copolymers synthesized via one step deactivation enhanced atom transfer radical polymerization (DE-ATRP)²⁴ and *in-situ* DE-ATRP approach respectively²⁵. While compared to these UV photo-crosslinking systems, chemical gelation via thiol-ene Michael-type addition reaction exhibits remarkable advantages such the ease to operate, rapid gelation, the absence of chemical initiator, no specific requirement of equipment and simple gelling condition close to physiological circumstance²⁶. Therefore, to enhance the activity of vinyl groups, a new hyperbranched copolymer with high degree of multi-acrylate

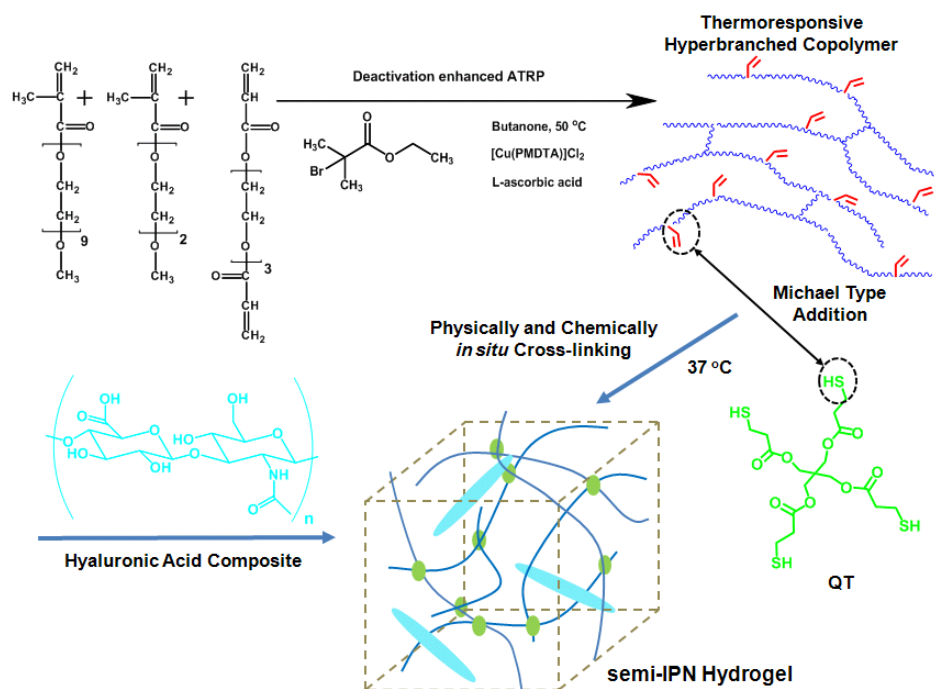
instead of methacrylate functionality has been designed and developed in this study in order to provide the polymer with the thermoresponsive and chemical *in-situ* cross-linkable properties. This hyperbranched copolymer was synthesized by co-polymerization of poly(ethylene glycol) diacrylate (PEGDA), poly(ethylene glycol) methyl ether methacrylate (PEGMEMA) and 2-(2-methoxyethoxy) ethyl methacrylate (MEO₂MA) via the *in-situ* DE-ATRP approach (**Scheme 3.1**). In addition, by varying the PEG-based hydrophilic/hydrophobic composition of the copolymers, desired phase transition temperatures were tailored close to body temperature. As a result, at room temperature, these copolymers are water-soluble, while at body temperature it forms a thermal gel. More importantly, a high concentration of PEGDA with diacrylate groups was used to achieve the hyperbranched structure while simultaneously providing the polymer with more active acrylate vinyl functionality, which significantly enhanced the activity during the thiol-ene Michael-type addition. Therefore, this copolymer led to an *in-situ* gelation system via both physical thermoresponsive gelation and chemical reaction with thiol-functional cross-linker within minutes.

To optimize the hydrogel microenvironment for cell seeding and encapsulation purposes, a semi-interpenetrated polymer network (semi-IPN) system was developed in this study by combining an extracellular matrix (ECM) biopolymer of hyaluronic acid (HA) within the hydrogel. An interpenetrating polymer network (IPN) is defined as a mixture of two or more cross-linked networks dispersed at a molecular level. If only one polymer is cross-linked in IPN and the other one is left in linear form, it is called semi-IPN structure²⁷. IPN and semi-IPN have been commonly utilized to modify the hydrogel structure and properties such as cross-linking density, swelling capacity, water content and mechanical properties for drug delivery and cell encapsulation systems²⁸⁻³⁰. HA is a linear polysaccharide with high molecular weight which has been widely used in tissue engineering for wound healing^{31, 32}, treatment of osteoarthritis^{33, 34}, cartilaginous tissue repair³⁵⁻³⁷ and drug delivery³⁸⁻⁴⁰. Here, HA macromolecule was interpenetrated within the physically and chemically cross-linking network without covalent linkage to form a semi-IPN structure

Semi-IPN Hydrogels

which increased the mesh size of gel frameworks⁴¹, enhanced the hydrogel swelling behavior and provided a large porous three dimensional microenvironment, and therefore promotes the cell adhesion and viability within the hydrogel.

Furthermore, by using the *in-situ* DE-ATRP polymerization approach, it is easy to adjust the gel properties including gelation rate, network density, pore size, mechanical properties, swelling and release kinetics by varying the acrylate content and hyperbranched structure of the copolymers, which provide this *in-situ* cross-linkable semi-IPN hydrogel system with a promising potential for controlled drug release and cell delivery applications.



Scheme 3.1: Synthesis of thermoresponsive hyperbranched PEGMEMA-MEO₂MA-PEGDA copolymer via an *in-situ* DE-ATRP approach. The copolymer can physically cross-link at body temperature and can be cross-linked with thiol cross-linker of pentaerythritol tetrakis (3-mercaptopropionate) (QT) via thiol-ene Michael-type addition. Meanwhile, by mixing with hyaluronic acid (HA) macromolecule, a semi-IPN hydrogel system was formed.

3.2 Materials and Methods

3.2.1 Materials

The monomers of poly(ethylene glycol) methyl ether methacrylate (PEGMEMA, $M_n = 475$ g/mol), 2-(2-methoxyethoxy) ethyl methacrylate (MEO₂MA), and poly(ethylene glycol) diacrylate (PEGDA, $M_n = 258$ g/mol) were purchased from Sigma-Aldrich. HA was purchased from Lifecore Biomedical inc. (research grade, 66-90 kg/mol). The ethyl 2-bromoisobutyrate (98%, Aldrich) was used as the initiator. Bis(2-dimethylaminoethyl) methylamine (99%, Aldrich), copper(II) chloride (CuCl₂, 97%, Aldrich), L-ascorbic acid (AA, 99%, Aldrich), butanone (HPLC grade, Aldrich), hexane (HPLC grade, Aldrich), diethyl ether (HPLC grade, Aldrich), sodium tetraborate (99%, Aldrich), carbazole (VetralabTM analytical standard, FLUKA) and Pentaerythritol tetrakis (3-mercaptopropionate) (QT, Aldrich) were used as received.

3.2.2 Synthesis of PEGMEMA-MEO₂MA-PEGDA Copolymers via *In-Situ* DE-ATRP

The PEGMEMA-MEO₂MA-PEGDA copolymers were synthesized by copolymerization of PEGMEMA ($M_n = 475$ g/mol), MEO₂MA and PEGDA ($M_n = 258$ g/mol) via an *in-situ* DE-ATRP approach. Briefly, the copolymers were prepared in butanone at the volume ratio of total monomers to solvent of 1:2 using a two-necked round bottom flask. Copper chloride (CuCl₂), ethyl 2-bromoisobutyrate and bis(2-dimethylaminoethyl) methylamine were added into the flask, followed by bubbling argon through the solutions for 25 min to remove the oxygen. L-ascorbic acid (molar ratio of CuCl₂ to AA was 2:1) dissolved in deionized water was added into the flask with a microliter syringe. The solution was stirred at 800 rpm and the polymerization was conducted at 50 °C in an oil bath for the required reaction time. The experiment was stopped by opening the flask and exposing the catalyst to air. The solution was diluted with acetone and dropped into a large excess of hexane/diethylether (1:1 v/v) mixture and then the precipitated mixture was dissolved in deionized water and purified by dialysis (spectrum dialysis membrane, molecular weight cut off 6000-

8000) for 4 days in dark at 4 °C to remove the monomers and catalyst. Polymer samples were obtained after freeze-drying and weighed to obtain the final yields.

3.2.3 Characterizations of PEGMEMA-MEO₂MA-PEGDA Copolymers

The resultant copolymers were characterized by gel permeation chromatography (GPC) and ¹H NMR. Weight average molecular weight (M_w), number average molecular weight (M_n) and polydispersity index (PDI, M_w/M_n) were obtained by GPC (Polymer Laboratories) with RI detector. The columns (30 cm PLgel Mixed-C, two in series) were eluted using dimethylformamide (DMF) and calibrated with poly(methyl methacrylate) standards. All calibrations and analysis were performed at 60 °C and a flow rate of 1 ml per min. ¹H NMR was carried out on a 300 MHz Bruker NMR with Delta NMR processing software. The chemical shifts were referenced to the lock chloroform (CDCl₃). Lower critical solution temperatures (LCST) of the copolymer solutions (0.03 % w/v) in deionized water were quantified by measuring their absorbance of 550 nm at temperatures from 15 to 50 °C (heating rate = 0.5 °C per sec) with a Beckman DU-800 spectrophotometer. The LCST value was defined as the temperature point when the A_{550} start suddenly increasing.

3.2.4 Preparation of Non-IPN and Semi-IPN Gels

The PEGMEMA-MEO₂MA-PEGDA copolymers were dissolved in 1 M phosphate buffered saline (PBS) at pH 7.4 to prepare copolymer solutions (10 and 20 wt %). QT (stoichiometrically molar ratio of thiol: vinyl group = 1:1) was mixed with the copolymer solution and 100 µl of the mixture was rapidly transferred to 1 ml flat bottom vials for swelling study. For preparing the semi-IPN gels, final concentration of 16 mg/ml of HA that dissolved in PBS was mixed within gelation solution followed by mixing with QT and transferred mixture to vials as described above for swelling and release studies. All samples were incubated at 37 °C for 2 h to allow for a complete gelation. Scanning Electron Microscopy (SEM) was utilized to characterize the porous structure of freeze-dried non-IPN and semi-IPN gels (polymer concentration: 20 wt %). The samples were mounted on an

aluminum stub using an adhesive carbon tab and sputter coated with gold before images were obtained using a Hitachi Field Emission SEM machine.

3.2.5 Determination of HA Retention in Semi-IPN Hydrogels

HA release study was performed to identify the retention of HA macromolecules in hydrogel after gelation and confirm the semi-IPN structure. Semi-IPN hydrogels were prepared with 10 wt % polymer solution containing 10 mg/ml and 20 mg/ml of HA separately as described in the previous section. Then 0.4 ml of PBS buffer was added to each gel sample to allow HA release at 37 °C. At each time point, 0.2 ml of the supernatant was taken after gentle shaking and the same volume of fresh PBS was added. The concentration of HA in the release samples was determined with carbazole assay as described somewhere else⁴². Briefly, standards were prepared by serial dilution of 1 mg/ml HA in PBS. 50 µl of samples and standards were placed in a 96-well plate, followed by adding 200 µl of 25 mM sodium tetraborate in sulfuric acid. The plate was heated for 10 min at 100 °C in an oven. Then the plate was cooled at room temperature for 15 min, and 50 µl of 0.125 % carbazole in ethanol were carefully added and thoroughly mixed. After heating again at 100 °C for 10 min in an oven and followed by cooling at room temperature for 15 min, the absorbance of the samples at 550 nm were determined by a microplate reader (Varioskan Flash Reader). Tests were performed in triplicate.

3.2.6 Swelling Studies

Non-IPN and semi-IPN gels were prepared as previously described. 0.5 ml of PBS buffer (pH 7.4) was added into each vial to allow gels to swell at 20 °C and 37 °C after exact weight measurement. The buffer was removed and the gels were weighed at regular time interval. Swelling ratios were calculated as below:

$$\text{swelling ratio} = \frac{w_t}{w_0} \quad (\text{eqn. 3.1})$$

where W_t represents the weight of hydrogel at a certain time point and W_0 represents the original weight of the hydrogels. 0.5 ml of fresh PBS was

added after measuring and the samples were further incubated at 20 °C and 37 °C. The swelling tests were performed in triplicate.

3.2.7 Cytotoxicity Assessment

For cellular viability studies, 3T3 mouse fibroblast cells (Passage 12) were used to study polymer cytotoxicity. 15,000 cells in Dulbecco's Modified Eagle's Medium (DMEM, Sigma, 10 % FBS, 1 % P/S,) were previously seeded into each well of a 48-wells tissue culture plate. After 24 h of incubation at 37 °C and 5 % CO₂, all the cells were attached to the bottom of culture plate and showed stable morphology under the microscope. Then PEGMEMA-MEO₂MA-PEGDA copolymer and QT solutions (0.5, 1, 5 and 10 mg/ml, dissolved in culture medium) were added into each well of the culture plate. After 48 h of incubation, the alamarBlue[®] reduction method was used to assess cellular metabolic activity. The absorbance at the lower wavelength filter (550 nm) was measured followed by the higher wavelength filter (595 nm) via a thermo scientific Varioskan[®] Flash Plate Reader. The results were calculated and normalized to the positive control (cells without treatment).

3.2.8 Cellular Viability Assessments, 2D-Cell Seeding and 3D-Cell Encapsulation Experiments

For 2D cell seeding study, PEGMEMA-MEO₂MA-PEGDA copolymers solution (10 wt % in DMEM, 10 % FBS, 1 % P/S) was filtered (0.22 µm, Corning, Germany) for sterilizing. QT (molar ratio of thiol: vinyl group = 1:1, stoichiometrically) was added into copolymer solution and mixed using a pipette for 30 s, then 80 µl of the mixture was transferred to a 4-well glass chamber slide and incubated at 37 °C for 2 h until it completely gelled. Meanwhile, HA that dissolved in culture medium was mixed with copolymer solution followed by the addition of cross-linker to prepare the semi-IPN hydrogels at the final concentration of 16 mg/ml. Rabbit adipose-derived stem cells (ADSCs, collected from NFB storage, NUIG, Passage 3) were seeded on the surface of the gels (5,000 cell/cm², with 100 µl culture medium) followed by 3 h incubation at 37 °C and 5 % CO₂ to allow the cells to adhere, and then more medium was applied. For 3D encapsulation study,

ADSCs cells (100,000 cell/ml) were mixed with gelling solutions (non-IPN or semi-IPN system) before gelation, followed by incubation at 37 °C and 5 % CO₂ for 30 min to form gel and then followed by the addition of more culture medium. The LIVE/DEAD[®] assay (Molecular Probes) was utilized to visualize the distribution of living and dead cells on the hydrogel surface after 48 h for both 2D and 3D cell culture model. Fluorescence images were taken using an Olympus 1X81 inverted microscope examining green fluorescence of living cells upon the reaction of intracellular esterase and calcein-AM, and red fluorescence utilizing ethidium homodimer-1 dye bound to the DNA of dead cells with compromised membranes.

3.3 Results and Discussion

3.3.1 Synthesis of PEGMEMA-MEO₂MA-PEGDA Copolymers via *In-Situ* DE-ATRP

DE-ATRP approach was first reported by Wang *et al.* for homopolymerization of divinyl monomers, for example divinyl benzene (DVB) or EGDMA, to successfully achieve the synthesis of dendritic homopolymers with multiple vinyl functional groups without gelation⁴³. Then this approach was further developed for the copolymerizations of monovinyl monomer and multivinyl monomers to prepare responsive dendritic polymers with well controlled chain growth and molecular structure^{24, 25}. In this study, for the first time, a high degree of diacrylate monomer of PEGDA (up to 25 molar % of monomer feed ratio) was used to provide the hyperbranched structure and significantly enhance the vinyl activity compared to methacrylate groups in the previous studies, thus leading to a rapid chemical cross-linking with thiol-functional cross-linker via thiol-ene Michael-type addition reaction. Briefly, water-soluble hyperbranched PEGMEMA-MEO₂MA-PEGDA copolymers were prepared via *in-situ* DE-ATRP approach (**Scheme 3.1**), where ethyl 2-bromoisobutyrate was utilized as the initiator and CuCl₂/PMDTA was used as the catalyst. A small amount of ascorbic acid was added into the reaction as a reducing agent that converts Cu^{II} to Cu^I; in the meantime, the extra Cu^{II}

species remained in the system which resulted in the slow chain growth and delayed gelation. By adjusting the amount of reducing agent used, the rate of molecular chain growth and the gelation point can be well controlled as previously described (see Chapter 2). The reaction was monitored by GPC analysis. Polymer chain growth over time was confirmed via GPC (**Figure 3.1**) and a final conversion of up to 78 % and 66 % of water-soluble copolymers with different degree of acrylate functionalities were obtained after 12 h and 6.5 h separately (**Table 3.1**). Moreover, the relatively low PDI value for hyperbranched structures demonstrated the controlled chain growth. At the early stage, polymerization showed linear chain growth with narrow GPC traces and the low PDI values, while at the later stage of the reaction the intermolecular cross-linking led to the hyperbranched structure and the broader PDI value.

The hyperbranched structure of the copolymer was confirmed by ^1H NMR (**Figure 3.2**). The vinyl functional groups were identified as three characteristic chemical shifts between 5.8 and 6.4 ppm. The copolymer composition (m , n , r and p) can be calculated from the integral data of C, D, E and H assigned as indicated in **Figure 3.2**. The following equations (eqns. 3.2 - 3.5) demonstrate the calculation process:

$$m = (3D - 6C - 2E)/84 \quad (\text{eqn. 3.2})$$

$$n = (10E + 2C - D)/28 \quad (\text{eqn. 3.3})$$

$$p = H \quad (\text{eqn. 3.4})$$

$$r = (3C - 2E - 12H)/12 \quad (\text{eqn. 3.5})$$

The double bond content and the branching degree of the copolymers were calculated from eqn. 3.6 and eqn. 3.7 also based on the ^1H NMR analysis:

$$\text{Double bond content (mol \%)} = p/(m + n + r + p) \times 100 \quad (\text{eqn. 3.6})$$

$$\text{Branching degree (mol \%)} = r/(m + n + r + p) \times 100 \quad (\text{eqn. 3.7})$$

Table 3.2 showed the composition, double bond content and branching degree of the copolymers. A high degree of vinyl functional groups (up to 12 mol %) was achieved in copolymers without gelation by using *in-situ* DE-ATRP approach. With this high level of vinyl groups, the copolymers

can react readily with thiol functional cross-linker via thiol-ene Michael-type addition to form chemically cross-linked network.

To study the chemical cross-linking behavior, the copolymer (entry 6 in **Table 3.1**) was dissolved in 1 M PBS at the concentrations of 10 and 20wt% at room temperature. A small amount of QT (equal molar ratio of thiol and vinyl group based on ^1H NMR analysis) was added into the copolymer solution and mixed using a pipette for 30 s followed by placement in an incubator at 37 °C. The chemical gelation occurred within 10 min, which was defined as no flow upon inversion of the vial at room temperature after a prolonged time (**Figure 3.3a**). It was also shown that the more QT (thiol/vinyl = 2:1 or 3:1) was used, the faster gelation and the denser the network identified by SEM imaging. The desired double bond content can be achieved by varying the percentage of PEGDA monomer feeding ratio via the *in-situ* DE-ATRP approach to tailor the copolymer gelation rate and network density.

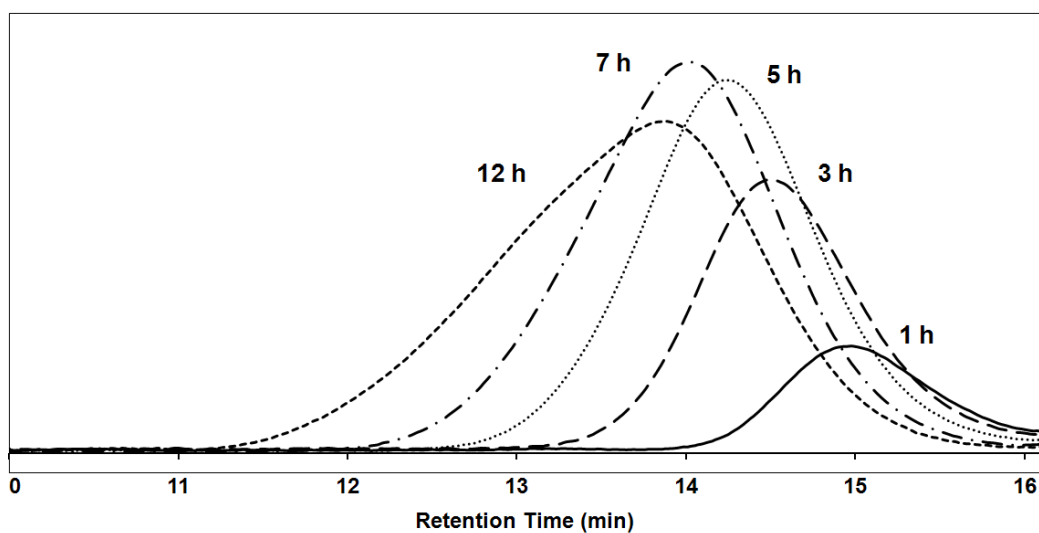


Figure 3.1: GPC traces from RI detector for the samples of entry 1-5 in Table 3.1. **Note:** the peak became broader and moving forward indicated that the increased molecular weights and polydispersities with monomer conversion were observed.

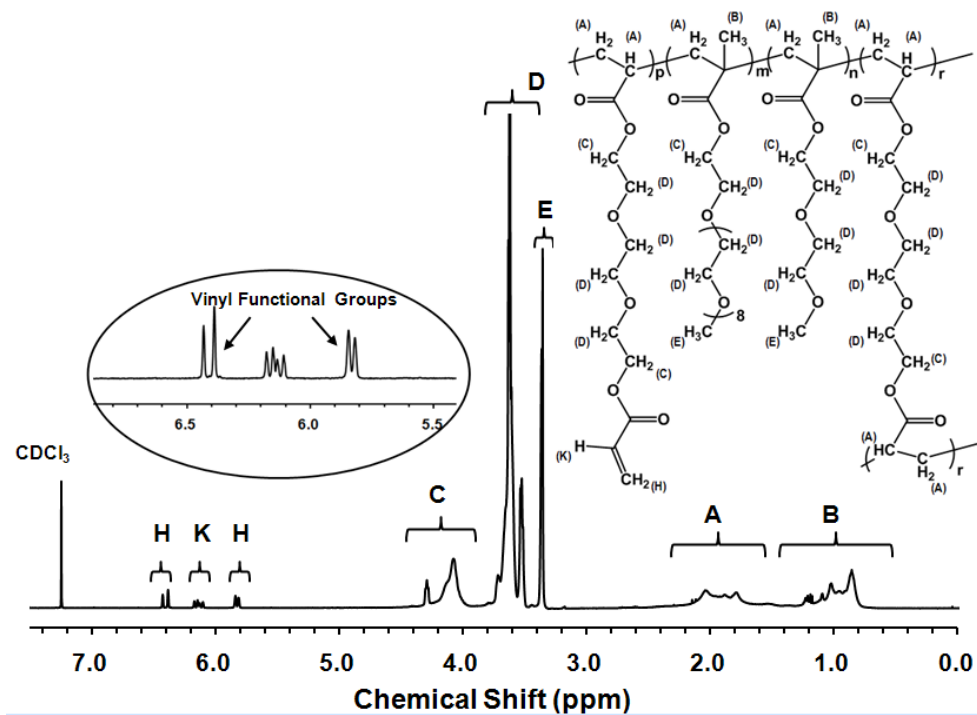


Figure 3.2: ^1H NMR for the PEGMEMA-MEO₂MA-PEGDA copolymer (entry 6 in Table 3.1) in CDCl₃. **Note:** the spectrum shows clearly the double bonds within the structure at the chemical shifts between 6.4 and 5.8 ppm (Insert).

Table 3.1: Copolymerizations of PEGMEMA-MEO₂MA-PEGDA via *in-situ* DE-ATRP

entry	monomer feed mole ratio $f_{[\text{PEGMEMA}]/[\text{MEO}_2\text{MA}]/[\text{PEGDA}]}$	RT ^a (h)	monomer conversion ^b (%)	Mn ^c (Kg mol ⁻¹)	PDI ^d
1	10/80/10	1	20	4.5	1.17
2	10/80/10	3	48	7.1	1.27
3	10/80/10	5	61	9.5	1.38
4	10/80/10	7	69	12.5	1.52
5	10/80/10	12	78	16.4	1.93
6	15/60/25	6.5	66	17.3	2.49

^a Reaction time. ^b Monomer conversion, estimated using peak areas for monomers and copolymers in GPC traces. ^c Number average molecular weight. ^d Polydispersity Index (PDI, M_w/M_n). Polymerization conditions: 50 °C in butanone; total monomers/butanone (v/v) = 1:2; the initiator (I) / catalyst (C) / ligand (L) are ethyl 2-bromoisobutyrate / CuCl₂ / bis(2-dimethylaminoethyl) methylamine; the reducing agent is L-ascorbic acid (AA); the [I]/[Monomer] = 1:100, [I]/[C]/[L]/[AA] = 1:0.25:0.25:0.125.

Table 3.2: Properties of PEGMEMA- MEO₂MA-PEGDA copolymers

entry	monomer feed mole ratio $f_{[\text{PEGMEMA}]/[\text{MEO}_2\text{MA}]/[\text{PEGDA}]}$ ^a	polymer composition $F_{[\text{PEGMEMA}]/[\text{MEO}_2\text{MA}]/[\text{PEGDA}]}$ ^b	double bond content ^c	branching degree ^d	LCST °C ^e
5	10/80/10	9/76/15	4	11	26
6	15/60/25	14/58/28	12	16	31

^a Monomer feed ratio. ^b Polymer composition; determined by ¹H NMR. ^{c, d} Calculated with eqs 1-6 (Unit: mol %). ^e Determined by UV-vis spectrophotometer.

3.3.2 Thermoresponsive Behavior of Copolymers

Different ratio of hydrophilic/hydrophobic composition can result in changes in varying the phase transition temperature of the copolymer: the more hydrophilic the copolymer was, the higher LCST would be^{25, 44}. In this study, the LCST of the copolymers are around 26 °C and 31 °C (**Table 3.2**), determined by UV-vis spectrophotometer (**Figure 3.3b**). To study the thermal gelation behavior at body temperature, the copolymers were dissolved in 1 M PBS (30 wt %) at room temperature (20 °C) and then placed at 37 °C. Gel concentration was defined as no flow upon inversion of the vial within 5 s (**Figure 3.3b insert**). It was found that the lowest thermal gelling concentrations of the copolymers at 37 °C were about 10 to 20 wt % mainly dependent on the polymer molecular weight. The higher molecular weights of the copolymers required the lower gelling concentration.

3.3.3 *In-Situ* Semi-IPN Gelation and HA Retention Assay

The HA macromolecules were mixed into the *in-situ* gelation system to create a semi-IPN system for improving the hydrogel swelling behavior and porous 3D micro-environment for cell growth, adhesion and migration. The semi-IPN hydrogels were formed within 10 min at 37 °C by chemical cross-linking with QT as similar to non-IPN (without HA) gels. The SEM images of freeze-dried gels showed that a less compact and more porous structure was achieved in semi-IPN hydrogels compared to non-IPN hydrogels (**Figure 3.4**). With the increase in the concentration of additional HA increasing, the more porous structure was achieved in the gels. It was assumed that linear HA macromolecules acted as a porogen in the semi-IPN hydrogel as the phase separation between HA and PEG based copolymers. This porous semi-IPN structure provided the hydrogel with several advantages such as increased swelling ratio and infiltration behavior, enhanced loading capacities, and providing more space for cell growth.

As hydrophilic HA macromolecules were physically mixed into system without covalent cross-linking with gelled backbone, HA release study was performed to confirm the HA retention in the hydrogel and semi-IPN structure after gelation. The HA release of semi-IPN hydrogels prepared

with low (10 mg/ml) and high (20 mg/ml) concentrations of HA were followed at 37 °C for 48 h, and then the released HA was determined with carbazole assay. It was shown that only about 15 - 20 % of HA was released from the hydrogels after two days and most elution occurred in the first 5 h which was most likely from the HA on the surface of the gels (**Figure 3.5**). After 12 h the HA release had leveled off indicating most of HA molecules (70 - 80 %) were kept in the hydrogels after gelation to form a semi-IPN structure. In addition, the semi-IPN hydrogel prepared with higher HA concentration showed slightly more release than lower group.

3.3.4 Swelling Characteristics of Non-IPN and Semi-IPN Hydrogels

Figure 3.6 shows the swelling tests of the non-IPN chemical cross-linked gels and the semi-IPN gels at room temperature (20 °C) and body temperature (37 °C). It has been demonstrated that the semi-IPN structure significantly increased the swelling ratio of the hydrogels. For example, the swelling ratio of 10 % semi-IPN gels reached about 3.1 after 4 h, while for the non-IPN gels at the same concentration it was only about 1.7 after 5 days at 20 °C. Meanwhile, the higher concentration (20 wt %) of copolymer led to lower swelling than the lower concentration (10 wt %) as it is a denser cross-linked network. Furthermore, the hydrogel showed a higher swelling ratio at 20 °C than at 37 °C as the copolymer presented more hydrophobic behavior and chain shrinking above LCST. Therefore, semi-IPN structure provided significantly enhanced swelling without varying polymer characteristics or cross-linking conditions, which is an essential property for medium absorption, cytotoxic elimination, nutrition diffusion and drug releasing in the area of controlled drug delivery and cell encapsulation.

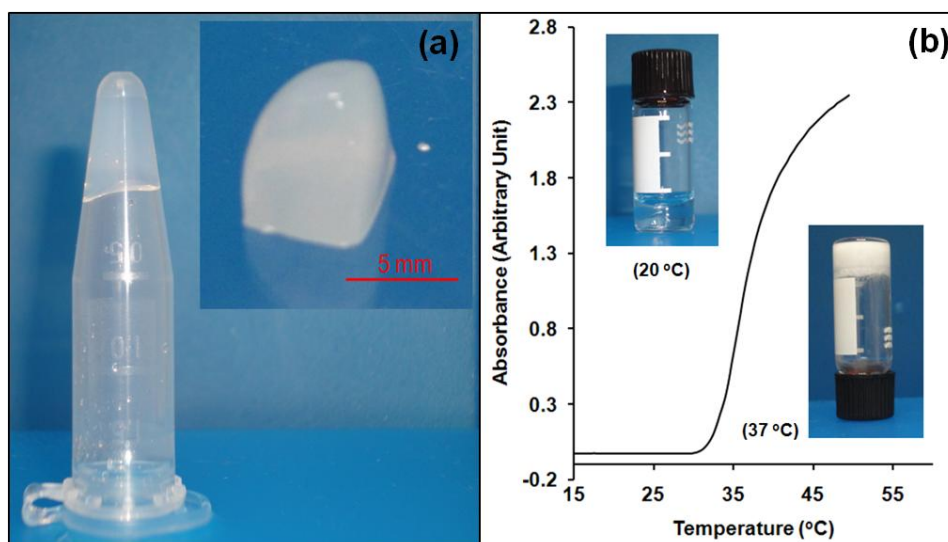


Figure 3.3: Physical and chemical cross-linking properties of PEGMEMA-MEO₂MA-PEGDA copolymer (entry 6 in Table 3.1). (a) Chemical gelation of copolymer (10 wt %) with QT (equal molar ratio of thiol and vinyl group). (b) LCST behaviour of the copolymer which was dissolved in deionized water at the concentration of 0.03 % (w/v), determined by UV-vis spectrophotometer. Insert: Polymer solution (30 wt %) became physical cross-linked gel when the temperature was raised above its LCST from 20 °C to 37 °C.

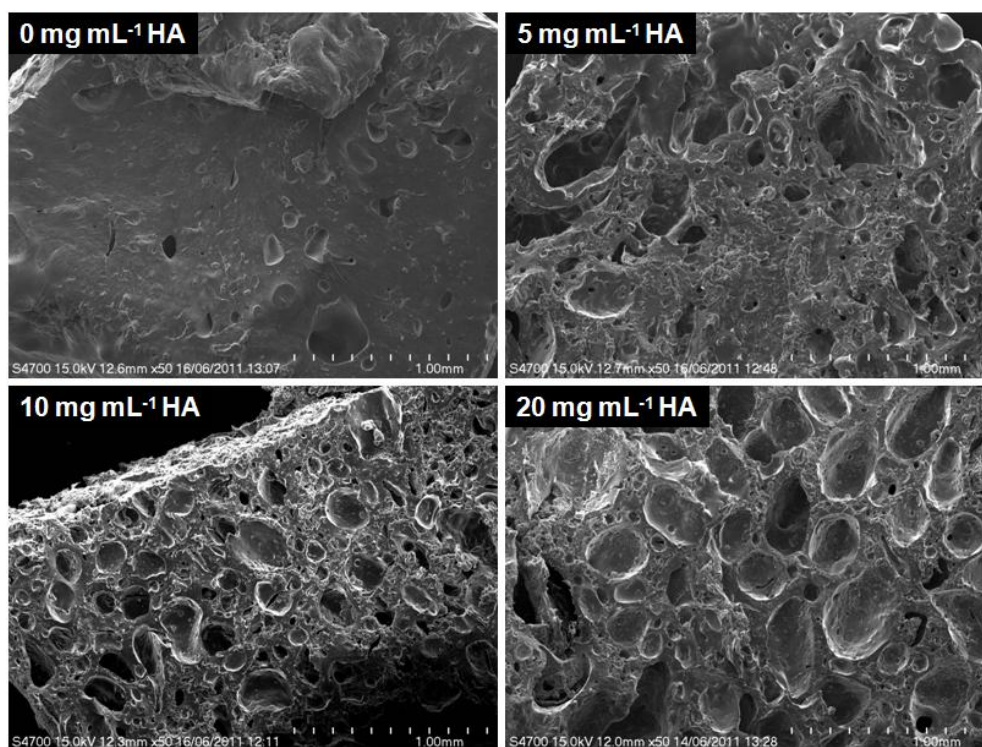


Figure 3.4: SEM images for the freeze-dried gels samples prepared from PEGMEMA-MEO₂MA-PEGDA copolymers (20 wt %) cross-linked with QT with different concentrations of HA from 0 mg/ml (non-IPN gel) to 20 mg/ml. **Note:** the higher HA concentration leads to looser hydrogel microenvironment with more space and porous structure.

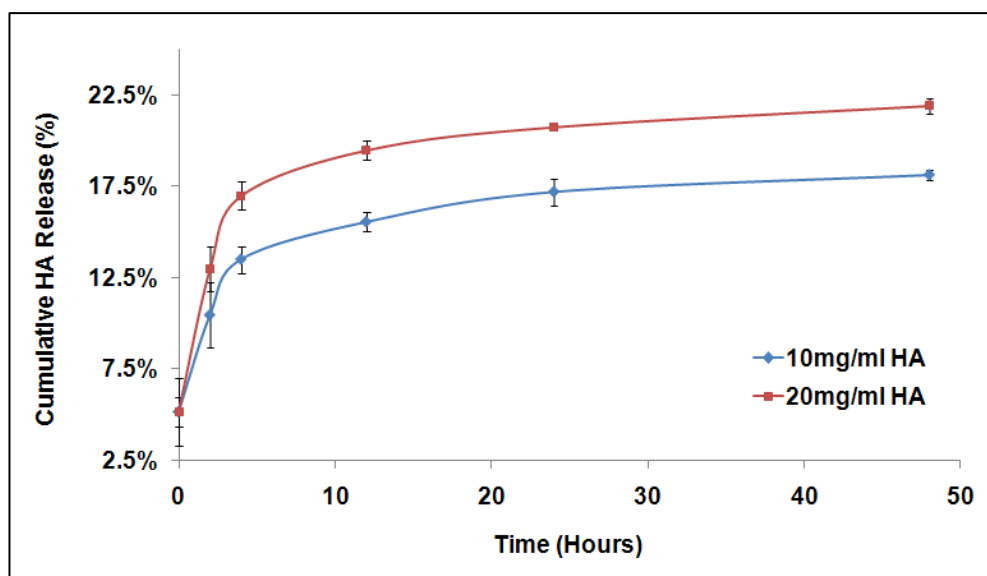


Figure 3.5: HA release study. Cumulative release of HA from semi-IPN hydrogels at 37 °C determined by carbazole assay. The absorbance of the samples at 550 nm was determined by a Varioskan Flash Reader. (Mean \pm SD, n = 3). **Note:** after 12 h the HA release had leveled off indicating most of HA molecules (70 - 80 %) were kept in the hydrogels after gelation to form a semi-IPN structure.

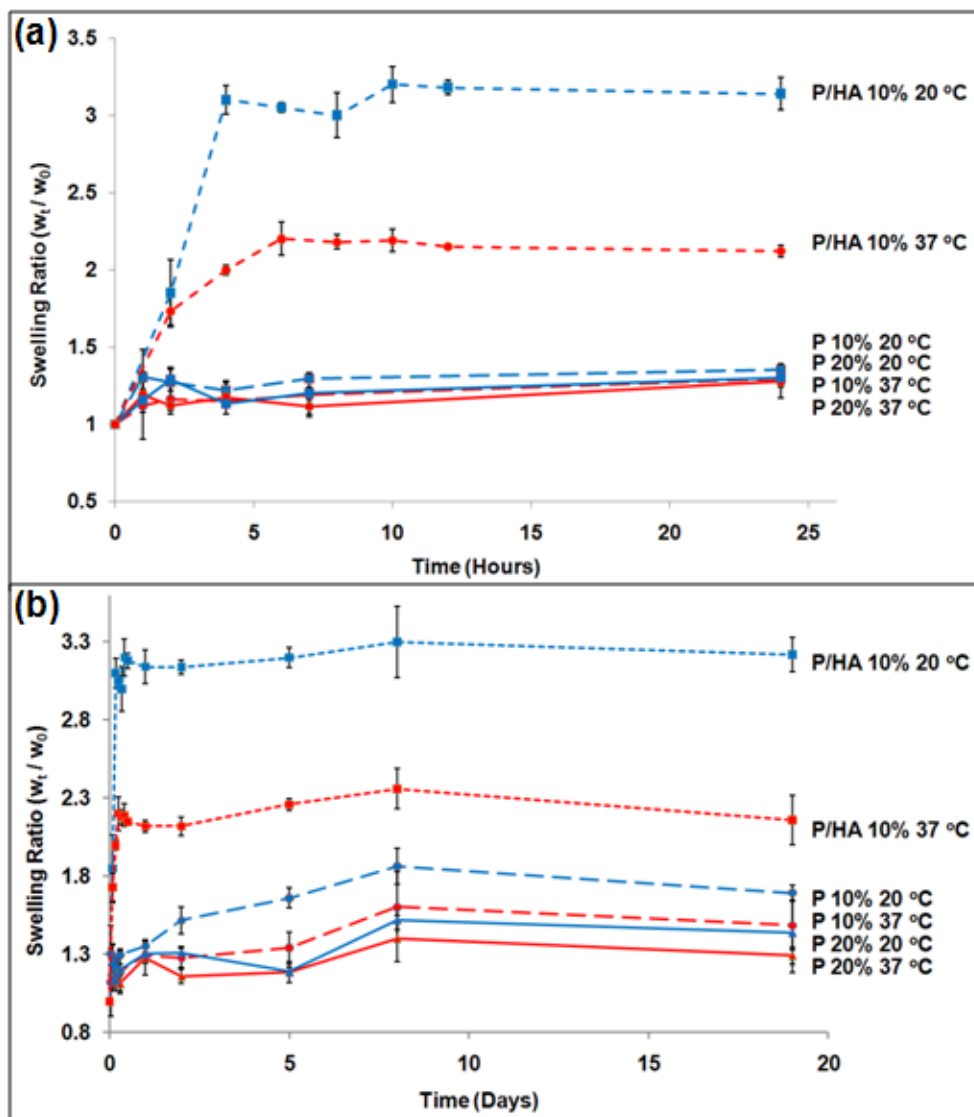


Figure 3.6: Swelling of chemically cross-linked (P) and IPN (P/HA) gels in PBS (1 M, pH 7.4) at 20 °C and 37 °C within first 24 h (a) and total 19 days (b) (Mean \pm SD, n = 3). **Note:** the lower cross-linking density (10 wt %) or at lower temperature (20 °C) demonstrated a higher swelling ratio than the higher cross-linking density (20 wt %) or at 37 °C. The IPN structure significantly enhanced the swelling capability of the gels.

3.3.5 Cytotoxicity of the Copolymer and 2D/3D Cell Culture on Non-IPN and Semi-IPN Hydrogels

The PEG based polymer is commonly considered as nontoxic and non-immunogenic materials⁴⁵⁻⁴⁸. In this study, cytotoxicity of the copolymers and QT was determined by alamarBlue[®] assay using 3T3 mouse fibroblast cells. The results showed that there was no significant difference between cell alone control and testing samples ($n = 3$, $p < 0.05$); in other words, neither copolymer nor QT influenced the metabolic activity of 3T3 cells after 48 h treatments at concentrations up to 10 mg/ml (**Figure 3.7**). Furthermore, for *in-situ* cross-linking system, the addition of small amount of HA (copolymer/HA = 6.25/1, w/w) led to a semi-IPN hydrogel which had several advantages for cell adhesion and growth. Firstly, semi-IPN system provided a more porous structure and more space for cell growth, proliferation and migration. Secondly, the enhanced swelling property makes the exchange of culture medium inside the hydrogel easier and reduces the concentration of metabolized toxic byproducts produced by cells from the microenvironment. Thirdly, the HA molecule inside the hydrogel improved the cell adhesion and viability by providing cellular “adhesive anchors”⁴⁹. Finally, combination with HA molecules results in the hydrogel system a semi-degradable behavior as HA can be degraded by specific hyaluronidase which will further improve the cell proliferation and migration for a long-term culture.

To determine the cellular compatibility of the semi-IPN hydrogel system, 2D seeding and 3D encapsulation assessments were performed with rabbit ADSCs stem cells. After 48 h culture, LIVE/DEAD[®] assay was used to visualize the distribution of living and dead cells in both 2D and 3D models. It was indicated that cells can hardly attach on the surface of non-IPN hydrogels in 2D model. Only very few living cells survived as round clusters (**Figure 3.8a**); however, many more living cells appeared on the semi-IPN gel surface and they showed spread morphology (**Figure 3.8b**). Similar results also appeared in 3D culture model. Very few cells survived inside the non-IPN hydrogel system, while in the semi-IPN system, cell survival was significantly improved (**Figure 3.8c-d**). Therefore, it was

Semi-IPN Hydrogels

demonstrated that the semi-IPN structure containing the HA biomacromolecules did improve the cell adhesion and cell viability both on the surface and inside the hydrogels. In addition, encapsulated cell viability was studied via different gelling conditions (**Figure 3.9**): (i) 7.5 % Copolymer with 1 % HA; (ii) 10 % Copolymer with 1 % HA; (iii) 10 % Copolymer with 2 % HA. Interestingly, the higher concentration of HA resulted in a significant decrease in percentage of alive cells after 6 days, which might be caused by the high viscosity of higher concentration of HA (**Figure 3.10**).

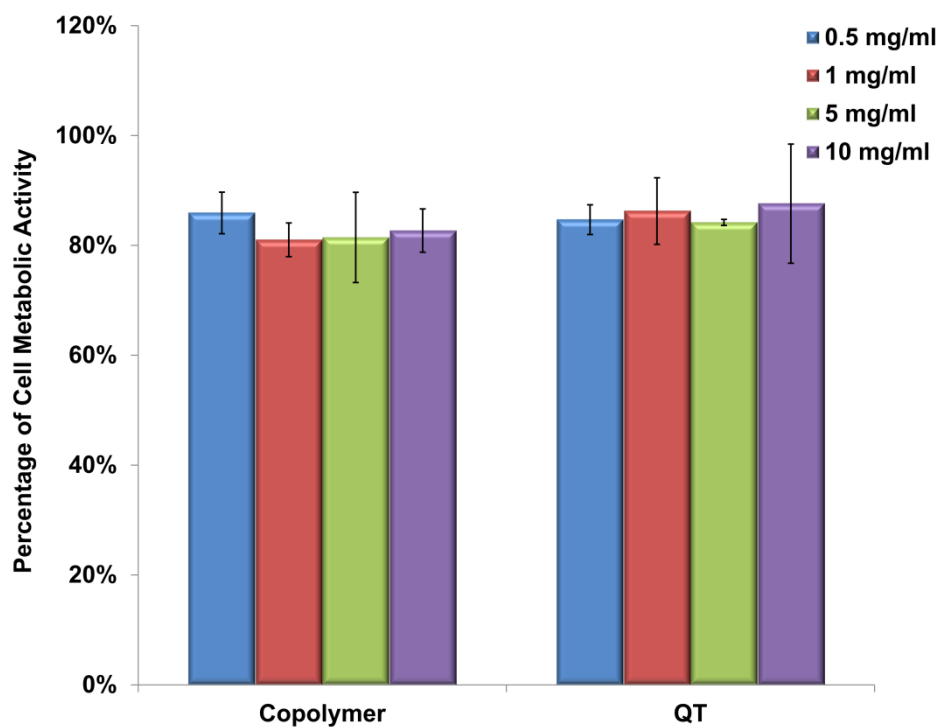


Figure 3.7: Cell metabolic activity assessment of 3T3 cells after 48 h treatment with PEGMEMA-MEO₂MA-PEGDA (entry 6 in Table 3.1) and Pentaerythritol tetrakis (3-mercaptopropionate) (QT) using alamarBlue[®] assay. **Note:** there was no significant difference between copolymer and QT treatment with control of cell alone ($n = 3, p < 0.05$).

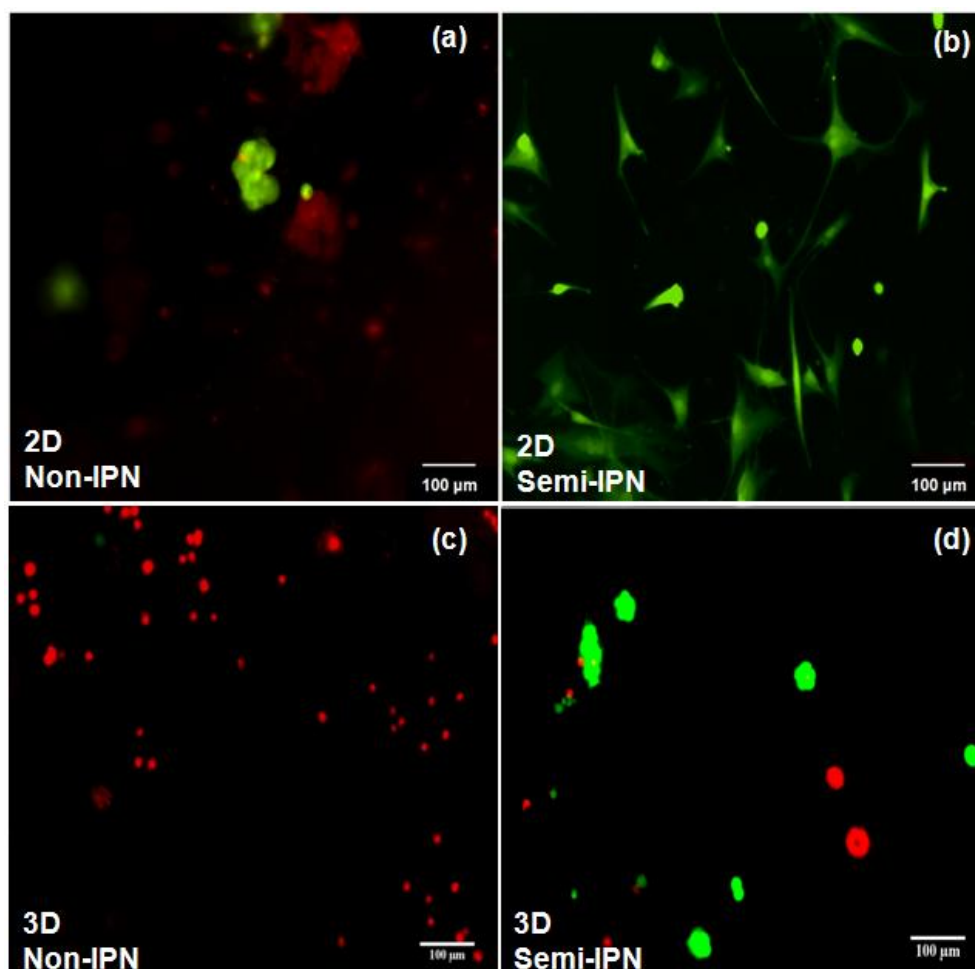


Figure 3.8: LIVE/DEAD[®] viability assay for 2D and 3D cell culture. The hydrogels were formed from 10 % w/v polymer solution in PBS and the QT was added with equal molar ratio of thiol and vinyl group. (a and b) ADSCs seeded on the surface of gels. (c and d) Cells were encapsulated into gelling system. (a, and c) Non-IPN gels without HA. (b and d) Semi-IPN gels with HA (16 mg/ml). The hydrogels fluorescently labeled with a dye that green fluoresces upon the presence of intracellular esterase activity in living cells (calcein-AM) and a dye that red fluoresces (ethidium homodimer-1) when bound to the DNA of dead cells with compromised membranes. The samples were directly visualized on an Olympus 1X81 inverted microscope. **Note:** cell adhesion and cell viability were significant improved in semi-IPN hydrogels both in 2D and 3D models.

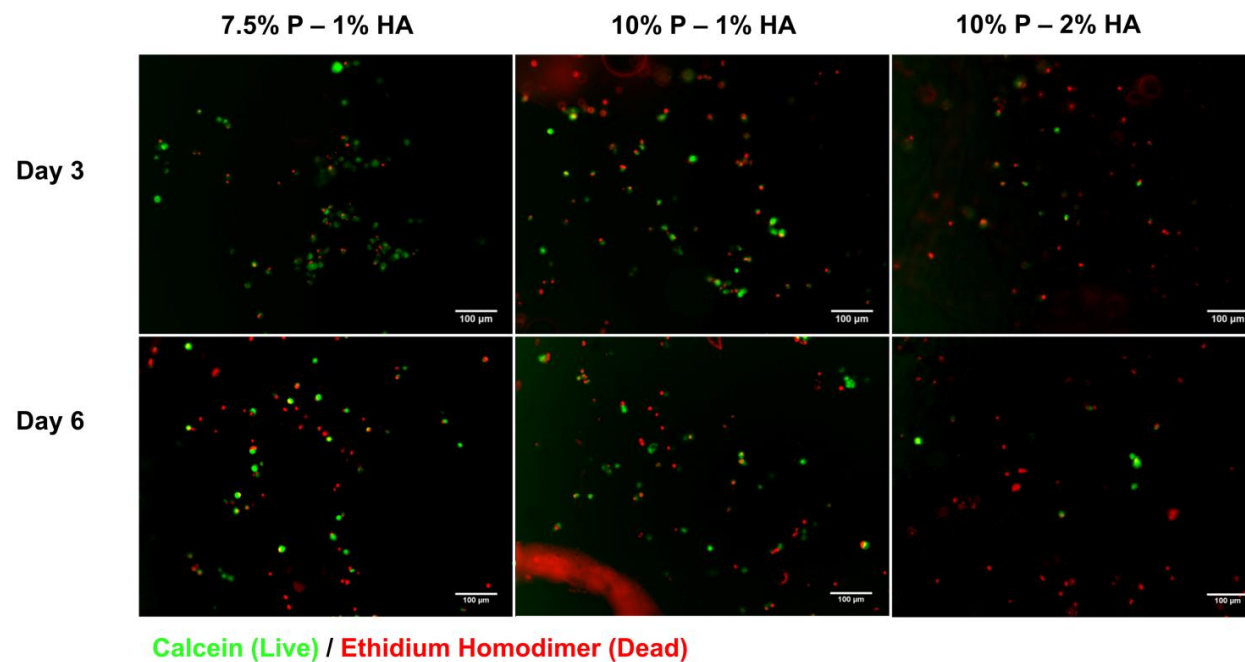


Figure 3.9: LIVE/DEAD[®] viability assay for 3D culture of ADSCs with different gelling condition after 3 and 6 days. Green fluoresces (calcein-AM) labeled living cells and red fluoresces (ethidium homodimer-1) labeled dead cells. The samples were directly visualized on an Olympus 1X81 inverted microscope. Scale bars in all cases represent 100 μm. **Note:** it seemed that the ratio of 10 % polymer with 1 % HA showed higher cell survival ratio after 6 days, which is confirmed by quantified analysis as shown.

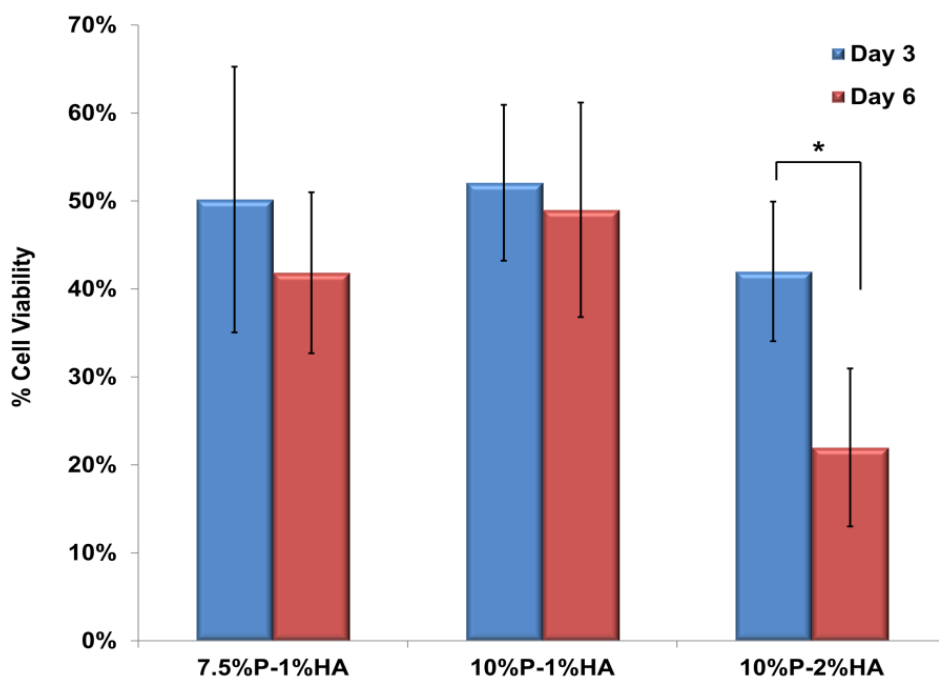


Figure 3.10: Quantification analysis of LIVE/DEAD[®] viability assay for 3D culture with different gelling condition after 3 and 6 days. Percentage of live cells to total cell number calculated from LIVE/DEAD[®] staining micrographs (Mean \pm SD, $n = 3$). **Note:** a significant drop on percentage cell viability was found in “10% P - 2% HA” group after 6 days ($n = 3$, $p < 0.05$).

3.4 Conclusion

In conclusion, a PEG-based thermoresponsive and chemical cross-linkable hyperbranched copolymers of PEGMEMA-MEO₂MA-PEGDA with multi acrylate functionality were successfully achieved via a one-step *in-situ* DE-ATRP approach. The phase transition temperature of the hyperbranched polymer close to body temperature was realized through adjusting the hydrophilic/hydrophobic polymer compositions. At room temperature, this copolymer was water-soluble while forming a gel rapidly at 37 °C. To enhance the mechanical properties of this physical cross-linked hydrogel, a thiol cross-linker of QT was utilized to chemically cross-link the hyperbranched copolymers via thiol-ene Michael-type addition reaction. In addition, with introduction of a HA biomacromolecule, a semi-IPN structure was formed which significantly improved the swelling behavior, cell adhesion in 2D culture model and cell viability in 3D culture model of the hydrogel system. With the physical and chemical cross-linkable behavior and the unique semi-IPN hydrogel structure, it can be expected that this semi-IPN hydrogel system will have good potential for the applications in controlled drug delivery and tissue engineering fields.

3.5 References

1. Anseth, K. S.; Metters, A. T.; Bryant, S. J.; Martens, P. J.; Elisseeff, J. H.; Bowman, C. N., In situ forming degradable networks and their application in tissue engineering and drug delivery. *Journal of Controlled Release* 2002, 78, (1-3), 199-209.
2. Balakrishnan, B.; Jayakrishnan, A., Self-cross-linking biopolymers as injectable in situ forming biodegradable scaffolds. *Biomaterials* 2005, 26, (18), 3941-3951.
3. Elisseeff, J., Injectable cartilage tissue engineering. *Expert Opinion on Biological Therapy* 2004, 4, (12), 1849-1859.
4. Mano, J. F., Stimuli-responsive polymeric systems for biomedical applications. *Advanced Engineering Materials* 2008, 10, (6), 515-527.
5. Yu, L.; Ding, J. D., Injectable hydrogels as unique biomedical materials. *Chemical Society Reviews* 2008, 37, (8), 1473-1481.
6. Friedrich, T.; Tieke, B.; Stadler, F. J.; Bailly, C.; Eckert, T.; Richtering, W., Thermoresponsive copolymer hydrogels on the basis of N-Isopropylacrylamide and a non-Ionic surfactant monomer: swelling behavior, transparency and rheological properties. *Macromolecules* 2010, 43, (23), 9964-9971.
7. Galperin, A.; Long, T. J.; Ratner, B. D., Degradable, thermo-sensitive poly(N-isopropyl acrylamide)-based scaffolds with controlled porosity for tissue engineering applications. *Biomacromolecules* 2010, 11, (10), 2583-2592.
8. Hatefi, A.; Amsden, B., Biodegradable injectable in situ forming drug delivery systems. *Journal of Controlled Release* 2002, 80, (1-3), 9-28.
9. Jeong, B.; Gutowska, A., Lessons from nature: stimuli-responsive polymers and their biomedical applications. *Trends in Biotechnology* 2002, 20, (7), 305-311.
10. Wang, W.; Liang, H.; Al Ghanami, R. C.; Hamilton, L.; Fraylich, M.; Shakesheff, K. M.; Saunders, B.; Alexander, C., Biodegradable thermoresponsive microparticle dispersions for injectable cell delivery Prepared using a single-step process. *Advanced Materials* 2009, 21, (18), 1809.
11. Hoare, T. R.; Kohane, D. S., Hydrogels in drug delivery: progress and challenges. *Polymer* 2008, 49, (8), 1993-2007.
12. Kwon, I. K.; Matsuda, T., Photo-iniferter-based thermoresponsive block copolymers composed of poly(ethylene glycol) and poly(N-isopropylacrylamide) and chondrocyte immobilization. *Biomaterials* 2006, 27, (7), 986-995.
13. Potta, T.; Chun, C.; Song, S. C., Dual cross-linking systems of functionally photo-cross-linkable and thermoresponsive polyphosphazene hydrogels for biomedical applications. *Biomacromolecules* 2010, 11, (7), 1741-1753.

14. Qiu, Y.; Park, K., Environment-sensitive hydrogels for drug delivery. *Advanced Drug Delivery Reviews* 2001, 53, (3), 321-339.
15. Cheng, V.; Lee, B. H.; Pauken, C.; Vernon, B. L., Poly(N-isopropylacrylamide-co-Poly(ethylene glycol))-acrylate simultaneously physically and chemically gelling polymer systems. *Journal of Applied Polymer Science* 2007, 106, (2), 1201-1207.
16. Hou, D. D.; Hao, T.; Ye, L.; Zhang, A. Y.; Wang, C. Y.; Feng, Z. G., Preparation and characterization of injectable hydrogels made via Michael-type addition reaction of dithiothreitol with 3-Arm acryloyl end-capped PEG. *Acta Polymerica Sinica* 2008, (4), 388-393.
17. Lin, C. C.; Anseth, K. S., PEG hydrogels for the controlled release of biomolecules in regenerative medicine. *Pharmaceutical Research* 2009, 26, (3), 631-643.
18. Niu, G. G.; Zhang, H. B.; Song, L.; Cui, X. P.; Cao, H.; Zheng, Y. D.; Zhu, S. Q.; Yang, Z.; Yang, H., Thiol/acrylate-modified PEO-PPO-PEO triblocks used as reactive and thermosensitive copolymers. *Biomacromolecules* 2008, 9, (10), 2621-2628.
19. Rydholm, A. E.; Bowman, C. N.; Anseth, K. S., Degradable thiol-acrylate photopolymers: polymerization and degradation behavior of an in situ forming biomaterial. *Biomaterials* 2005, 26, (22), 4495-4506.
20. Vernon, B.; Tirelli, N.; Bachi, T.; Haldimann, D.; Hubbell, J. A., Water-borne, in situ crosslinked biomaterials from phase-segregated precursors. *Journal of Biomedical Materials Research Part A* 2003, 64A, (3), 447-456.
21. Cellesi, F.; Tirelli, N.; Hubbell, J. A., Materials for cell encapsulation via a new tandem approach combining reverse thermal gelation and covalent crosslinking. *Macromolecular Chemistry and Physics* 2002, 203, (10-11), 1466-1472.
22. Cellesi, F.; Tirelli, N.; Hubbell, J. A., Towards a fully-synthetic substitute of alginate: development of a new process using thermal gelation and chemical cross-linking. *Biomaterials* 2004, 25, (21), 5115-5124.
23. Lee, B. H.; West, B.; McLemore, R.; Pauken, C.; Vernon, B. L., In-situ injectable physically and chemically gelling NIPAAm-based copolymer system for embolization. *Biomacromolecules* 2006, 7, (6), 2059-2064.
24. Tai, H., Wang, W. Vermonden, T., Heath, F. Hennink, W.E., Alexander, C., Shakesheff, K.M. and Howdle, S.M. , Thermoresponsive and photocrosslinkable PEGMEMA-PPGMA- EGDMA copolymers from a one-step ATRP synthesis. *Biomacromolecules* 2009, 10, 822-828.
25. Dong, Y.; Gunning, P.; Cao, H.; Mathew, A.; Newland, B.; Saeed, A. O.; Magnusson, J. P.; Alexander, C.; Tai, H.; Pandit, A.; Wang, W., Dual stimuli responsive PEG based hyperbranched polymers. *Polymer Chemistry* 2010, 1, (10), 827-830.
26. Hoyle, C. E.; Bowman, C. N., Thiol-ene click chemistry. *Angewandte Chemie-International Edition* 2010, 49, (9), 1540-1573.

27. Smart, J. D., An invitro assessment of some mucosa-adhesive dosage forms. *International Journal of Pharmaceutics* 1991, 73, (1), 69-74.
28. Chen, S. C.; Wu, Y. C.; Mi, F. L.; Lin, Y. H.; Yu, L. C.; Sung, H. W., A novel pH-sensitive hydrogel composed of N,O-carboxymethyl chitosan and alginate cross-linked by genipin for protein drug delivery. *Journal of Controlled Release* 2004, 96, (2), 285-300.
29. Zhang, J.; Peppas, N. A., Synthesis and characterization of pH- and temperature-sensitive poly(methacrylic acid)/poly(N-isopropylacrylamide) interpenetrating polymeric networks. *Macromolecules* 2000, 33, (1), 102-107.
30. Zhang, X. Z.; Wu, D. Q.; Chu, C. C., Synthesis, characterization and controlled drug release of thermosensitive IPN-PNIPAAm hydrogels. *Biomaterials* 2004, 25, (17), 3793-3805.
31. Chen, W. Y. J.; Abatangelo, G., Functions of hyaluronan in wound repair. *Wound Repair and Regeneration* 1999, 7, (2), 79-89.
32. Ghosh, K.; Ren, X. D.; Shu, X. Z.; Prestwich, G. D.; Clark, R. A. F., Fibronectin functional domains coupled to hyaluronan stimulate adult human dermal fibroblast responses critical for wound healing. *Tissue Engineering* 2006, 12, (3), 601-613.
33. Lo, G. H.; LaValley, M.; McAlindon, T.; Felson, D. T., Intra-articular hyaluronic acid in treatment of knee osteoarthritis - A meta-analysis. *Jama-Journal of the American Medical Association* 2003, 290, (23), 3115-3121.
34. Wang, C. T.; Lin, J.; Chang, C. J.; Lin, Y. T.; Hou, S. M., Therapeutic effects of hyaluronic acid on osteoarthritis of the knee - A meta-analysis of randomized controlled trials. *Journal of Bone and Joint Surgery-American Volume* 2004, 86A, (3), 538-545.
35. Nesti, L. J.; Li, W. J.; Shanti, R. M.; Jiang, Y. J.; Jackson, W.; Freedman, B. A.; Kuklo, T. R.; Giuliani, J. R.; Tuan, R. S., Intervertebral disc tissue engineering using a novel hyaluronic acid-nanofibrous scaffold (HANFS) amalgam. *Tissue Engineering Part A* 2008, 14, (9), 1527-1537.
36. Nettles, D. L.; Vail, T. P.; Morgan, M. T.; Grinstaff, M. W.; Setton, L. A., Photocrosslinkable hyaluronan as a scaffold for articular cartilage repair. *Annals of Biomedical Engineering* 2004, 32, (3), 391-397.
37. Yamane, S.; Iwasaki, N.; Majima, T.; Funakoshi, T.; Masuko, T.; Harada, K.; Minami, A.; Monde, K.; Nishimura, S., Feasibility of chitosan-based hyaluronic acid hybrid biomaterial for a novel scaffold in cartilage tissue engineering. *Biomaterials* 2005, 26, (6), 611-619.
38. Fang, J. Y.; Chen, J. P.; Leu, Y. L.; Hu, H. W., Temperature-sensitive hydrogels composed of chitosan and hyaluronic acid as injectable carriers for drug delivery. *European Journal of Pharmaceutics and Biopharmaceutics* 2008, 68, (3), 626-636.
39. Kurisawa, M.; Chung, J. E.; Yang, Y. Y.; Gao, S. J.; Uyama, H., Injectable biodegradable hydrogels composed of hyaluronic acid-tyramine

conjugates for drug delivery and tissue engineering. *Chemical Communications* 2005, (34), 4312-4314.

40. Luo, Y.; Kirker, K. R.; Prestwich, G. D., Cross-linked hyaluronic acid hydrogel films: new biomaterials for drug delivery. *Journal of Controlled Release* 2000, 69, (1), 169-184.

41. Kutty, J. K.; Cho, E.; Lee, J. S.; Vyavahare, N. R.; Webb, K., The effect of hyaluronic acid incorporation on fibroblast spreading and proliferation within PEG-diacrylate based semi-interpenetrating networks. *Biomaterials* 2007, 28, (33), 4928-4938.

42. Cesaretti, M.; Luppi, E.; Maccari, F.; Volpi, N., A 96-well assay for uronic acid carbazole reaction. *Carbohydrate Polymers* 2003, 54, (1), 59-61.

43. Wang, W., Zheng, Y., Roberts, E., Duxbury, C.J., Ding, L.F., Irvine, D.J. and Howdle, S.M., Controlling chain growth: A new strategy to hyperbranched materials. *Macromolecule* 2007, 40, 7184.

44. Lutz, J.-F.; Weichenhan, K.; Akdemir, O.; Hoth, A., About the phase transitions in aqueous solutions of thermoresponsive copolymers and hydrogels based on 2-(2-methoxyethoxy)ethyl methacrylate and oligo(ethylene glycol) methacrylate. *Macromolecules* 2007, 40, (7), 2503-2508.

45. Drury, J. L.; Mooney, D. J., Hydrogels for tissue engineering: scaffold design variables and applications. *Biomaterials* 2003, 24, (24), 4337-4351.

46. Hedberg, E. L.; Tang, A.; Crowther, R. S.; Carney, D. H.; Mikos, A. G., Controlled release of an osteogenic peptide from injectable biodegradable polymeric composites. *Journal of Controlled Release* 2002, 84, (3), 137-150.

47. Lih, E.; Joung, Y. K.; Bae, J. W.; Park, K. D., An in situ gel-forming heparin-conjugated PLGA-PEG-PLGA copolymer. *Journal of Bioactive and Compatible Polymers* 2008, 23, (5), 444-457.

48. Nuttelman, C. R.; Tripodi, M. C.; Anseth, K. S., In vitro osteogenic differentiation of human mesenchymal stem cells photoencapsulated in PEG hydrogels. *Journal of Biomedical Materials Research Part A* 2004, 68A, (4), 773-782.

49. Wang, C. M.; Varshney, R. R.; Wang, D. A., Therapeutic cell delivery and fate control in hydrogels and hydrogel hybrids. *Advanced Drug Delivery Reviews* 2010, 62, (7-8), 699-710.

Chapter Four

***In-Situ* Cross-linked Hybrid Hydrogel for ADSCs Encapsulation Prepared from Thermoresponsive Hyperbranched Copolymer and Thiolated Hyaluronic Acid**

The majority of this chapter has previously been published in:

Dong, Y.; Saeed, A.O.; Hassan, W.; Keigher, C.; Zheng, Y.; Tai, H.; Pandit, A. and Wang, W.; 'One-step preparation of thiol-ene clickable PEG based thermoresponsive hyperbranched copolymer for *insitu* cross-linking hybrid hydrogel', *Macromolecular Rapid Communications*, 2012, 33, 120-136.

Hassan, W.; **Dong, Y. (equally contribute)** and Wang, W. 'Encapsulation and 3D culture of human adipose derived stem cells in an in-situ crosslinked hybrid hydrogel from PEG based hyperbranched co-polymer and hyaluronic acid'. *Stem Cell Research & Therapy*. 2013, 4:32.

4.1 Introduction

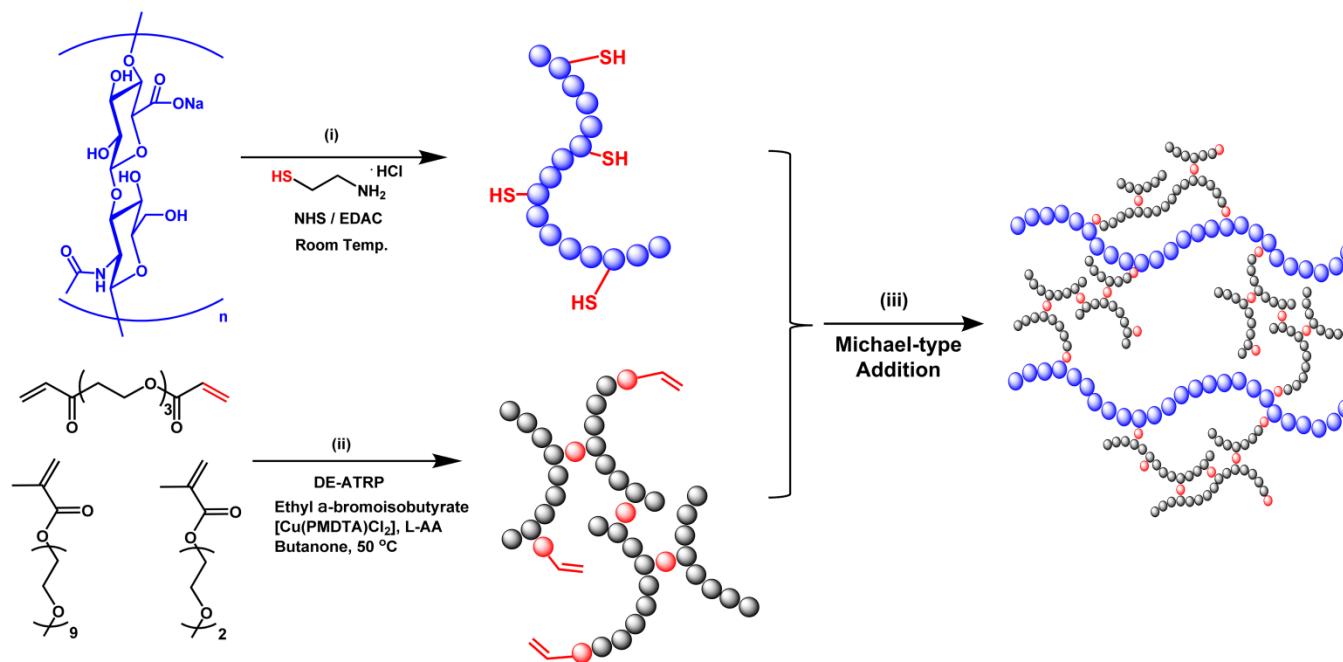
Materials that respond to external stimuli have been a focus of research for drug delivery and tissue engineering¹⁻³. Among these materials, thermoresponsive polymers, that undergo thermal phase transition phenomena, are widely explored as drug and cell delivery vehicle⁴⁻⁹. The synthetic polymers with thermoresponsive property provide a unique opportunity for the fabrication of *in-situ* cross-linking systems with injectable property, which can conform to irregular shapes, deformities at the site of delivery¹⁰⁻¹³ and minimise the invasiveness of the surgical techniques^{14, 15}.

On the other hand, naturally occurring polymers such as extracellular matrices (ECM) biopolymers have demonstrated many advantages over common synthetic materials¹⁶⁻¹⁹, due to their high water content, improved biocompatibility and tailored enzymatic biodegradation^{20, 21}. Moreover, ECM biopolymers may also provide biological cues and guide or induce tissue-specific regeneration²². Hyaluronic acid (HA), a non-sulphated glycosaminoglycan, is a major constituent of ECM which plays a vital role in cell proliferation and differentiation²³⁻²⁵. A recent example of semi-synthetic thermoresponsive hydrogel is injectable hyaluronan-dopamine/Pluronic[®] F127 hydrogel¹⁷. In this system, Pluronic F127 serves as a thermoresponsive component which was chemically modified with cysteamine to have free thiol end groups reacting with dopamine conjugated HA to form the gel via Michael-type catechol-thiol addition reaction. Other hydrogel systems have also been developed, which rely on chemical modification of PEG based thermoresponsive polymers to allow cross-linking via Michael-type addition reaction^{26, 27}. However, the chemical modification requires multi-step reactions and purification, which significantly increase the cost and complexity of preparation process. Therefore, the design of 'one-pot and one-step' synthesis of a new thermoresponsive polymer with desired end functionality to afford *in-situ* cross-linkable property is highly beneficial.

As discussed in former sections (see Chapter 2 and 3), via an advanced one-step *in-situ* deactivation enhanced atom transfer radical

polymerisation (DE-ATRP) approach, we have successfully achieved PEG-based hyperbranched copolymer with thermoresponsive behavior and photo- or chemical cross-linkable properties. In addition, in combination with ECM biopolymer of HA to form a semi-IPN hydrogel network, the hydrogel microenvironment for encapsulated cell growth has been promoted, and cell viability has been significantly increased. However, the small molecular cross-linker (QT) lead to relative dense cross-linked network, which still limited the cell survive in the hydrogel (about 50 % survival ratio after 6 days).

To overcome this limitation, in this study, we modified HA with thiol functional groups so that the multifunctional copolymer of PEGMEMA-MEO₂MA-PEGDA (see Chapter 3) can directly cross-link with the thiolated HA (HA-SH) via Michael-type addition reaction under physiological condition (**Scheme 4.1**). This copolymer exhibited the thermoresponsive behavior as described earlier (see Chapter 3) and can cross-link with HA-SH to form a stable hydrogel with strengthened mechanical property. In addition, by using this modified biopolymer as cross-linker, we hypothesised that the hydrogel microenvironment could be further optimized for encapsulated cell survive, proliferation and function.



Scheme 4.1: Synthetic route and chemical structures of PEGMEMA-MEO₂MA-PEGDA and HA-SH hydrogel. (i) modification of HA with cysteamine (EDAC-NHS) carbodiimide coupling; (ii) ‘One-pot and One-step’ *in-situ* DE-ATRP in butanone at 50 °C; (iii) hydrogel from *in-situ* cross-linking of components via thiol-ene Michael-type addition reaction at pH 7.4.

4.2 Materials and Methods**4.2.1 Materials**

The monomers of poly(ethylene glycol) methyl ether methacrylate (PEGMEMA $M_n = 475$ g/mol), 2-(2-methoxyethoxy) ethyl methacrylate (MEO₂MA), and poly(ethylene glycol) diacrylate (PEGDA $M_n = 258$ g/mol) were purchased from Sigma-Aldrich. The ethyl 2-bromoisobutyrate (EtBriB, 98 %, Aldrich) was used as the initiator. Bis(2-dimethylaminoethyl) methylamine (99 %, Aldrich), copper(II) chloride (CuCl₂, 97 %, Aldrich), N, N, N', N'', N''-Pentamethyldiethylenetriamine (PMDTA, 98 % Aldrich), N-(3-Dimethylaminopropyl)-N'-ethylcarbodiimide hydrochloride (EDAC, 98 % Fluka), N-Hydroxysuccinimide (NHS, 97 % Fluka), L-ascorbic acid (99 %, Aldrich), butanone (99 %, HPLC grade, Aldrich) and hexane (95 %, Aldrich) were used as received. Sodium hyaluronate, (HA, 1.5 MDa) was obtained from Lifecore Biomedical, Inc.

4.2.2 Synthesis of Hyperbranched PEGMEMA-MEO₂MA-PEGDA Copolymer

The Hyperbranched copolymer of PEGMEMA-MEO₂MA-PEGDA, poly(ethylene glycol) methyl ether methacrylate-*co*-2-(2-methoxyethoxy) ethyl methacrylate-*co*-poly(ethylene glycol) diacrylate was synthesized via a one-step *in-situ* DE-ATRP. The polymerization was conducted in butanone using a two-necked round bottom flask (the volume ratio of total monomers to solvent adjusted at 1:2). First, PEGMEMA (7.4 g, 0.016 mol), MEO₂MA (12.8 g, 0.068 mol), PEGDA (5.4 g, 0.021 mol), the initiator EtBriB (155 μ l, 1.05 mmol), CuCl₂ (0.032 g, 0.26 mmol), PMDTA (64 μ l, 0.26 mmol) were all added to polymerization flask in 50 ml of butanone. The mixture was stirred for complete dissolution of the components and then followed by purging with argon for 30 min to remove dissolved oxygen. L-ascorbic acid (AA, 0.011 g, 0.07 mmol) was added to the polymerisation solution under argon condition and the mixture was then heated in an oil bath at 50 °C and stirred for 6 h. The polymerization was stopped by opening the flask and exposing the

catalyst to air. The PEGDA monomer was removed by dropping the solution into a large excess of hexane/diethyl ether solution (1/1, v/v). The precipitated mixture was dissolved in deionised water and dialysis (MWCO 6-8 kDa) for 4 days in dark at 4 °C. Polymer samples were obtained after freeze-drying and weighed to obtain the final yields.

Molecular weights and molecular weight distributions of the copolymer samples were determined using GPC (Varian) with RI detector. The columns (30 cm PLgel Mixed-C, two in series) were eluted using dimethylformamide (DMF) and calibrated with poly(methyl methacrylate) (PMMA) standards. All calibrations and analysis were performed at 60 °C and a flow rate of 1 ml per min. ¹H NMR was carried out on a 300 MHz Bruker NMR with MestReC processing software. The chemical shifts were referenced to the lock chloroform (CDCl₃). The copolymer composition, the double bond content and the branching degree of the copolymer can be calculated from ¹H NMR analysis result as previously described (see Chapter 3).

4.2.3 Thermoresponsive Behavior of Copolymers

LCST of the copolymer solutions (0.03 % w/v) in deionized water were quantified by measuring their absorbance of 550 nm at temperatures from 20 to 55 °C (heating rate = 0.5 °C per sec) with a Beckman DU-800 spectrophotometer. The data were collected every 2 seconds. Moreover, oscillatory rheology tests (Advanced Rheometer AR 500) were performed to investigate the thermal gelation behaviour of the copolymer (30 wt%). Tests were performed using parallel plate geometry (40 mm in diameter), over a temperature range of 20 to 31 °C, with a frequency of 10 Hz and a strain of 0.5% and results were recorded every 30 seconds.

4.2.4 Synthesis of Thiol Derivatised Hyaluronic Acid (HA-SH)

Hyaluronic acid was modified with thiol groups by reaction of carboxylic acid with cysteamine hydrochloride, which was performed as described²⁸ with slight modification. First, 0.200 g of sodium hyaluronate was hydrated in 50 ml of demineralised water to obtain a 0.4 % (w/v) polymer solution. The pH of the reaction mixture was adjusted to 5.5 by the addition of 0.1 M

P-SH-HA Hybrid Hydrogels

HCl. Then, EDAC and NHS were added in at final concentrations of 50 mM. The pH was readjusted to 5.5 and the reaction mixture was stirred for 15 min at room temperature. Then, 0.250 g of cysteamine hydrochloride was added and the pH was readjusted to 4.75. The reaction mixture was incubated for 4 h at room temperature under stirring. The resulting conjugate was dialysed (MWCO 12 kDa) three-times against 1% NaCl and finally against demineralised water. Finally, the frozen aqueous polymer solution was freeze dried for two days. ^1H NMR was carried out for analysis of the molecular structure of thiolated HA as described earlier. The chemical shifts were referenced to the deuterium oxide (D_2O). The amount of free SH content of HA-SH (1 mg/ml in assay buffer) was determined by using Ellman's reagent quantifying free thiol groups. The quantity of free thiol groups was calculated from the standard curve obtained by solutions with increasing concentrations (0 - 2 mM) of l-cysteine hydrochloride.

4.2.5 Preparation of P-SH-HA Hybrid Hydrogel via Michael-type Addition Reaction

The hydrogel was prepared via Michael-type addition reaction between the pendant vinyl groups on the hyperbranched copolymer with free thiol contents of modified HA at physiological condition. First, HA-SH and PEGMEMA-MEO₂MA-PEGDA (10 and 15 wt%) were prepared in phosphate buffered saline (PBS, pH 7.4) in separate glass vials. The two solutions were combined (corresponding to the ratio of free thiol to vinyl groups of 1:1) and gently mixed for 15 s. The incubated solution at 37°C was observed for gel formation via solution (flow) - gel (no flow) transition and the gel state was determined by inverting the vial when no fluidity was visually observed. Moreover, the compression test were performed to the chemical cross-linked hydrogel using a dynamic mechanical analyser (DMA). Hydrogel specimens (diameter 12.5mm, thickness 2.5 mm), prepared from 15 and 30 wt% polymer solution with HA-SH, were loaded by a controlled force mode, with a force ramp from 0.001 to 1.0 N at a rate of 0.1N per min was applied to the samples at 37 °C.

4.2.6 Morphological Characterisation

Scanning Electron Microscopy (SEM) was used to determine the morphology of freeze-dried hydrogels, which was performed by a colleague of Dr Aram O. Saeed (Postdoc. researcher in our group) and the results have been published by the first-authored paper ²⁹. The hydrogels (10 and 15 wt%) were prepared as mentioned earlier and the samples were freeze-dried overnight. The freeze-dried samples were mounted on an aluminium stub using an adhesive carbon tab and sputter coated with gold before images were obtained using a Hitachi S-4700 Scanning Electron Microscope machine.

4.2.7 Swelling Behaviour

The swelling ratio of the hydrogel was determined as described ¹⁸ with slight modification, which was performed by a colleague of Dr Aram O. Saeed (Postdoc. researcher in our group) and the results have been published by the first-authored paper ²⁹. A volume of 0.6 ml of PBS 7.4 was added into the glass vials, with 0.2 ml hydrogel on the bottom prepared by combining HA-SH and varied concentration of PEGMEMA-MEO₂MA-PEGDA 10 and 15 wt% (corresponding to thiol to vinyl group ratio of 1:1). In this circumstance, the hydrogel swelling occurred uniaxially towards the upper direction of the vials. The samples were incubated at 37 °C and constant agitation at 150 rpm. The weight of the hydrogel plus the vials was recorded, after careful removing of the surface buffer, at predetermined time interval. The weight of swollen hydrogel (W_t) was determined by subtracting the vial weight from the total weight of the vial plus hydrogels. The dried weight (W_0) of the hydrogel was also determined in the same manner after freeze drying of hydrogels (dry state). The swelling ratio (Q) of the hydrogel was defined as W_t/W_0 .

4.2.8 Cell Viability, Proliferation and Metabolic Activity Analysis of ADSCs-embedded Hydrogel from PEGMEMA-MEO₂MA-PEGDA Copolymer and Commercially Available HA-SH

Free thiol groups are easily oxidized in air. Therefore to ensure the repeatability of the studies, a commercially available thiolated hyaluronic

P-SH-HA Hybrid Hydrogels

acid (HA-SH, HyStem™, Glycosan) was purchased to replace our own synthesized HA-SH from BioTime Inc., Alameda, CA.

Copolymer of PEGMEMA-MEO₂MA-PEGDA was dissolved in phosphate buffered saline (PBS, pH 7.4), mixed with ADSCs suspension (in serum-free medium) and the HA-SH (HyStem™) gently by pipette, in which the final concentration of the copolymer as 5 % (w/v), HA-SH as 0.5 % (w/v) and ADSCs as 1 million/ml. Gelation occurs within 8 min at 37 °C through Michael-type addition between vinyl groups on copolymer and thiol groups on the HA-SH.

ADSCs extracted from rat adipose tissue. The tissue was digested by type I collagenase at 0.025 % (w/v) for shaking 1 h at 37 °C, and the reaction was stopped by addition of complete medium (DMEM, 10% FBS, 1% P/S). The stromal fraction was collected by centrifugation 5 min at 1,200 rpm, re-suspended and filtered on a cell strainer (70 µm mesh size, BD Sciences, Switzerland). After 24 h of incubation at 37 °C in a humidified atmosphere of 5 % CO₂, cells were washed in order to eliminate the contaminant cells (e.g. blood cells and adipocytes). Complete culture medium was changed every 2 to 3 days and cells were maintained as sub-confluent. Adipogenic, chondrogenic and osteogenic differentiation assays were used to confirm the stemness (assessment was performed by a colleague of Robert Kennedy who is a PhD student in our group, protocol see **Appendices-I**). For the present *in vitro* and *in vivo* (see Chapter 5) studies, only rADSCs of passage 2 to 4 were used.

Cell-embedded hydrogels (40 µl each) were prepared on a hydrophobic Teflon tape surface, incubated at 37 °C for 20 min for complete gelation as described, and then transferred into each well of a 12-well culture plate and add 2 ml DMEM culture medium (10% FBS, 1% P/S). Cell- embedded hydrogels were incubated at 37 °C in a humidified atmosphere of 5 % CO₂ for 3, 7, 14 and 21 days with medium change every 2-3 days. For each time point, LIVE/DEAD® (Molecular Probes®), alamarBlue® (Invitrogen®) and PicoGreen® (Molecular Probes®) assays were used to determine the viability, metabolic activity and proliferation of the encapsulated ADSCs. LIVE/DEAD® and PicoGreen® assays were performed with recommended

procedure. For quantitatively analysis of LIVE/DEAD[®] result, 15 micrographs with the magnification of $\times 100$ were taken randomly from 3 hydrogel samples for each time point using an Olympus 1X81 inverted microscope. The cell viability was calculated by dividing the number of live cells by the total cell number in the field. All cells per area were counted using the ImagePro[®] Plus software (Meida Cybernetics, USA). For alamarBlue[®] assay, cell- embedded hydrogels were washed three times by HBSS, followed by incubation with 10 % alamarBlue[®] (v/v) in complete medium for 12 h. The absorbance at the lower wavelength filter (550 nm) was measured followed by the higher wavelength filter (595 nm) via a thermo scientific Varioskan Flash Plate Reader. The following formulae were used to calculate the percentage of cell viability:

AO_{LW} = absorbance of oxidized form of alamarBlue[®] along at lower wavelength;

AO_{HW} = absorbance of oxidized form of alamarBlue[®] along at higher wavelength;

Calculated correlation factor:

$$R_o = AO_{LW} / AO_{HW}; \quad (\text{eqn. 4.1})$$

Calculated the percentage of reduced alamarBlue[®]:

$$AR_{LW} \% = (A_{LW} - A_{HW} \times R_o) \times 100 \quad (\text{eqn. 4.2})$$

4.2.9 Determination of Growth Factor Secretion

Growth factor secretion assessment was performed by a colleague of Waqar Hassan (PhD student in our group) and the results have been published by a co-authored paper ³⁰. Briefly, Conditioned media were collected from both 2D (on tissue culture plate) and 3D culture system (P-SH-HA hydrogel system with 0.5×10^6 cells/ml of STEMPRO[®] human adipose-derived stem cells, Invitrogen[®]) after 1, 3, 5 and 7 days and stored at -80 °C. Multi-plex ELISA system was used to analyse for both the angiogenic growth factors vascular endothelial growth factor (VEGF), placental growth factor (PlGF), transforming growth factor- β (TGF- β) and pro/anti-inflammatory cytokines Interferon- γ (INF- γ),

Interleukin-2 (IL-2) and Interleukin-10 (IL-10) (mesoscale development system, MSD TH1/TH2 7-plex, MSD Human Growth factor 14-Plex).

4.2.10 Statistical Analysis

Comparisons between multiple groups were evaluated by One way ANOVA and Tukey's post analysis method. *p* value of less than 0.05 was considered as significant. The software used in the analysis was GraphPad Prism 5 software (GraphPad Software, US).

4.3 Results and Discussion

4.3.1 Polymer Synthesis

The concept in this study was to develop a facile route for the synthesis of a thermoresponsive hyperbranched copolymer with high content of acrylate vinyl functional groups via 'one-pot and one-step' DE-ATRP approach to cross-link with thiolated HA by Michael-type addition reaction. Briefly, ethyl 2-bromoisobutyrate was used to initiate the polymerization of mono-functional monomers of poly(ethylene glycol) methyl ether methacrylate (PEGMEMA, $M_n = 475$ g/mol), 2-(2-methoxyethoxy) ethyl methacrylate (MEO₂MA) and bifunctional monomer of poly(ethylene glycol) diacrylate (PEGDA, $M_n = 258$ g/mol, branching agent). The copper (Cu^{II}) and N,N,N',N'',N''-Pentamethyldiethylenetriamine (PMDTA) were utilised as catalyst system, whereas a small amount (25 mol% to Cu^{II}) of L-Ascorbic Acid (AA) was used to reduce inactive Cu^{II} into active form of Cu^{I} . By using the deficient amount of reduce agent and CuCl_2 to start the reaction, extra Cu^{II} species remained in the system during the whole reaction process, which reduced the polymer chain growth rate with better controll over the reaction. This led to a highly branched polymer structure with significantly delayed gelation point³¹. As a result, a final conversion of water soluble hyperbranched copolymer was obtained up to 45 % after 6 h of polymerisation with relatively narrow molecular weight distribution.

This indicates the controlled chain growth has been achieved via efficient DE-ATRP approach. GPC was used to determine the molecular weight

and polydispersity of the copolymers and to monitor the polymerisation process with reaction time (**Table 4.1**). Furthermore, to obtain the high content of acrylate vinyl functional groups, the high feeding ratio (20 mol %) of branching agent PEGDA was used in this study. The copolymer cross-linking reaction via thiol-ene Michael-type addition was significantly enhanced by using this acrylate bifunctional monomer instead of methacrylate monomer, compared with our previous work on UV photo-crosslinkable copolymers³². The hyperbranched structure of PEGMEMA-MEO₂MA-PEGDA was confirmed by ¹H NMR (See Chapter 3). The degree of branching and percentage of vinyl content were obtained from ¹H NMR spectra using the equations as described in supporting information. The value of 22 % and 10 % were found for the degree of branching and vinyl content respectively (**Table 4.1**). With this large number of acrylate vinyl functional groups, the copolymers efficiently performed the thiol-ene Michael-type reaction with thiolated HA, which provided *in-situ* chemical network in min. The LCST of PEGMEMA-MEO₂MA-PEGDA was determined via UV-vis Spectrophotometer, which exhibited a sharp change in temperature-time curve around 27 °C (**Figure 4.1a**), as a result the polymer solution (30 wt%) formed a reversible gel rapidly at 37 °C. In addition, the rheological result showed a dramatic increase of Loss Modulus and Storage Modulus with temperature increasing from 23 to 25 °C (**Figure 4.1b**). Furthermore, the effect on the LCST value can be easily adjusted by varying the polymer composition as described in the previous work, the higher level of hydrophilic composition resulted in higher LCST value³¹.

4.3.2 Synthesis of Thiol Derivatised Hyaluronan (HA-SH)

The hydroxyl and carboxylic acid groups on the polysaccharide repeating units of HA (D-glucuronic acid and D-N-acetylglucosamine respectively) are reported to be the main target for chemical modification. The conjugate form of HA-SH was synthesized by amide bond formation between the carboxylic acid groups and amine groups of cysteamine. As shown in **Scheme 4.1**, cysteamine was conjugated to HA (1.5×10^6

g/mol, Lifecore Biomedical) via covalent bonds formation in the presence of carbodiimide coupling agents (EDAC and NHS). Higher molar excess of cysteamine to HA was utilised in the reaction in order to maximise the degree of modification. The molecular structure of modified HA was confirmed by ^1H NMR, which showed characterized chemical shifts at 2.4 and 2.6 ppm (**Figure 4.2**). In addition, the free thiol groups on HA-SH was about 0.2 $\mu\text{mol}/\text{mg}$ which was determined by standard Ellman's assay as shown in **Figure 4.3**.

4.3.3 Fabrication of Hybrid Hydrogels

Michael-type addition between PEGMEMA-MEO₂MA-PEGDA and HA-SH to form *in-situ* cross-linkable gelling system is under physiological condition. The mechanism is described as base-catalysed reaction which involved a step growth reaction between the acrylate groups and thiolated anions under mild condition subsequently leading to formation of insoluble network between the polymer and modified HA components. The vial tilting method was used to confirm the gel formation at predetermined concentration of the PEGMEMA-MEO₂MA-PEGDA and HA-SH. As shown in **Figure 4.4**, stable hydrogels formed with the copolymer and thiolated HA at room temperature (molar ratio of thiol to vinyl groups were 1:1 and 1:2).

In addition, the mechanical property of the chemical cross-linked hydrogel was determined with a compression test using a dynamic mechanical analyser (DMA). Thermoresponsive physical gelation can only form an unstable and reversible gel which depends on the environmental temperature, while the enhancement in mechanical strength was observed for gels with the chemical cross-linking. For example, it is found that the storage modulus of 15 wt% hydrogel is about 9 kPa and about 38 kPa for 30 wt% hydrogel at 37 °C (**Figure 4.5**).

Table 4.1: Copolymerization of PEGMEMA-MEO₂MA-PEGDA via *in-situ* DE-ATRP

monomer feed molar ratio $f_{[\text{PEGMEMA}]/[\text{MEO}_2\text{MA}]/[\text{PEGDA}]}$	sample #	RT ^a (h)	monomer conversion ^b (%)	M_n^c (Kg/mol)	PDI ^d	double bond content ^e	branching degree ^e	LCST ^f (°C)
15/65/20	S1	3	18.0	6.1	1.16			
	S2	4	29.4	7.3	1.22			
	S3	6	45.0	11.6	1.33	10	22	27

^a Reaction time. ^b Monomer conversion, estimated using peak areas for monomers and copolymers in GPC traces. ^c Number average molecular weight. ^d Polydispersity Index (M_w/M_n). Polymerization conditions: 50 °C in butanone; total monomers/butanone (v/v) = 1:2; the initiator (I) / catalyst (C) / ligand (L) are ethyl 2-bromoisobutyrate / CuCl₂ / N,N,N',N'',N''- Pentamethyldiethylenetriamine (PMDTA); the reducing agent is L-ascorbic acid (AA); the [I]/[Monomer] = 1:100, [I]/[C]/[L]/[AA] = 1:0.25:0.25:0.0625. ^e Polymer composition; determined by ¹H NMR (Unit: mol %). ^f Determined by UV-vis spectrophotometer.

4.3.4 Morphological Characterisation and Swelling Behaviour of the Hydrogels

Morphological characteristic of hydrogel is an important factor in terms of tissue engineering applications. The presence of porous structure is necessary to allow for tissue growth, diffusion of nutrients and waste products. Moreover, the percentage of porosity, pore size and interconnectivity are vital parameters in determining the performance of the hydrogel. Therefore, to assess the network structure of the formed hydrogel, the freeze-dried samples were analysed by Scanning Electron Microscopy (SEM). As shown in **Figure 4.6**, the prepared hydrogel clearly demonstrated the presence of porous structure and the pores bifurcated into adjacent visible pores, which may offer advantage to optimise the hydrogel system for different tissue engineering applications that require different pore sizes and porosity.

The swelling profile of the hydrogels were obtained by soaking in PBS 7.4 at 37 °C until they reached the equilibrium state. Different time intervals were selected to monitor the change in weight of hydrated hydrogel. As shown in **Figure 4.7**, the hydrogel made with 15 wt% polymer resulted in slightly lower swelling ratio compared to 10 wt% polymer. This observation is due to the higher density of cross-linking between polymer with HA-SH at 15 wt% polymer, which is in agreement with the morphological analysis. However, the hydrogel formed with both weight percentage of the polymers were found to reach a steady state and maintained its weight. Each data point was obtained by averaging values from three samples under the same conditions, with error bars shown.

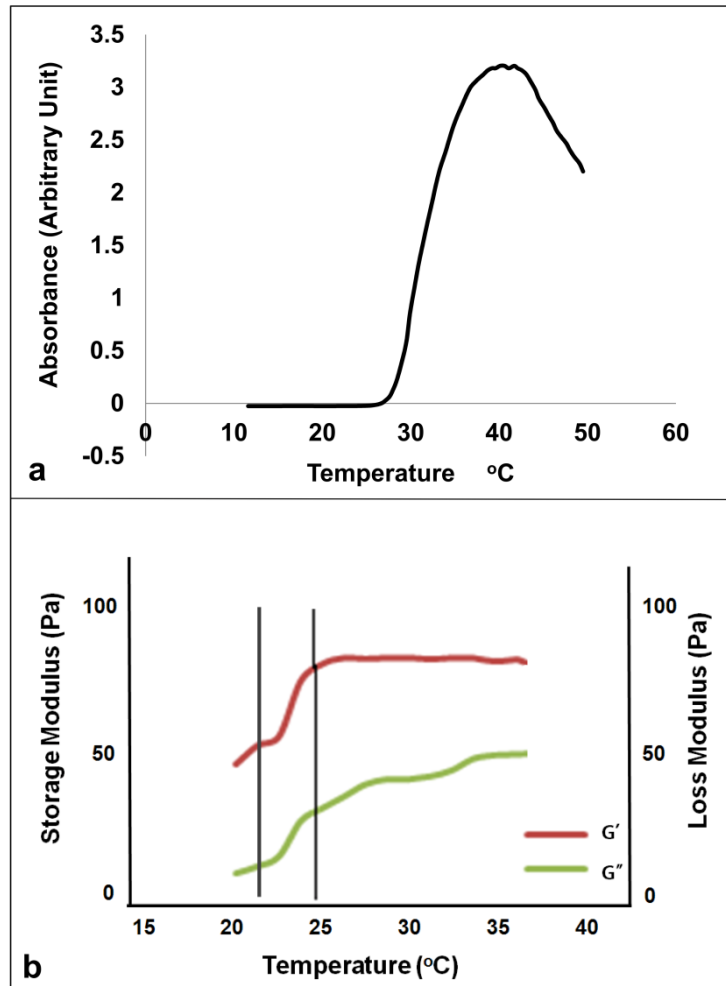


Figure 4.1: (a) LCST of the PEGMEMA-MEO₂MA-PEGDA copolymer determined by UV-vis spectrophotometer. (b) A temperature ramp rheological measurement for the copolymer (30 wt%). **Note:** the LCST of the copolymer was around 27 °C; and the rheological modulus were dramatic increased due to the aggregation of polymer particles above LCST.

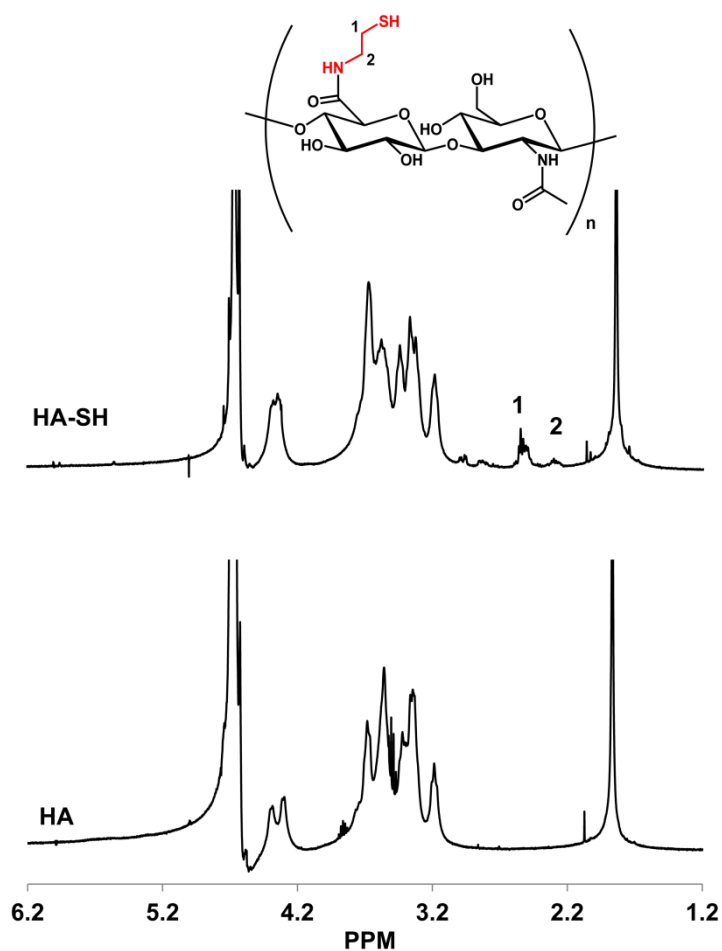


Figure 4.2: ^1H NMR (300Hz) spectrum of HA and thiolated HA (HA-SH) in DO_2 . **Note:** the protons from 2.6 (1) to 2.4 (2) ppm confirm the conjugation of thiol groups.

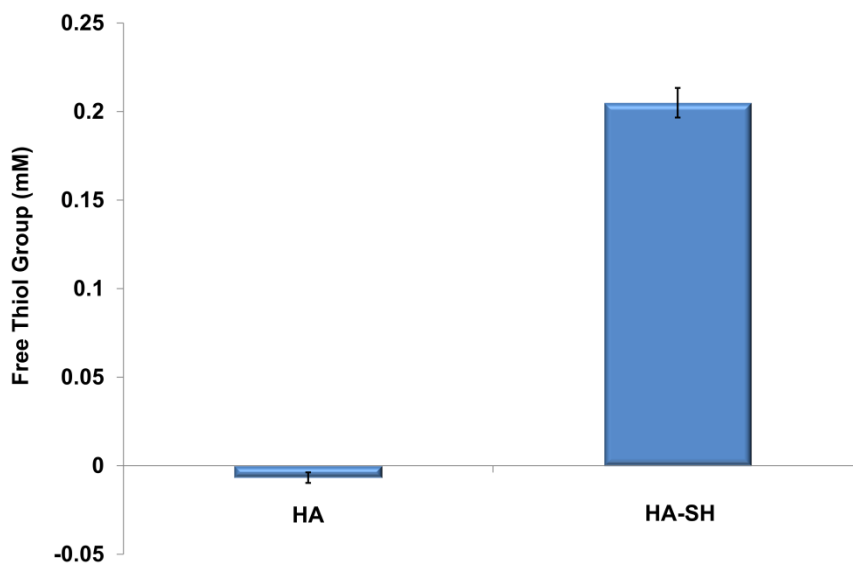


Figure 4.3: Content of free thiol groups on HA and thiolated HA (HA-SH), determined by Ellman's assay. **Note:** the content of free thiol group on the modified HA showed significant higher than control group of normal HA.

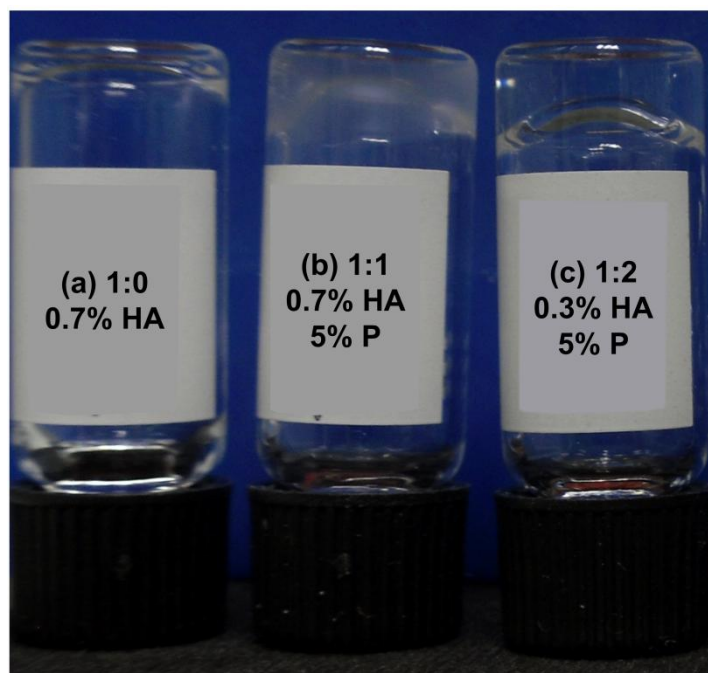


Figure 4.4: Chemical gelation via Michael-type addition between PEGMEMA-MEO₂MA-PEGDA copolymer and thiolated HA (HA-SH) at room temperature. The molar ratio between thiol groups on the HA-SH and the vinyl groups on the copolymer were (a) 1:0 (without polymer), (b) 1:1, and (c) 1:2, which were calculated based on ¹H NMR and Ellman's analysis. **Note:** HA-SH solution without polymer stay as liquid form, while in the other two groups, stable hydrogels were formed.

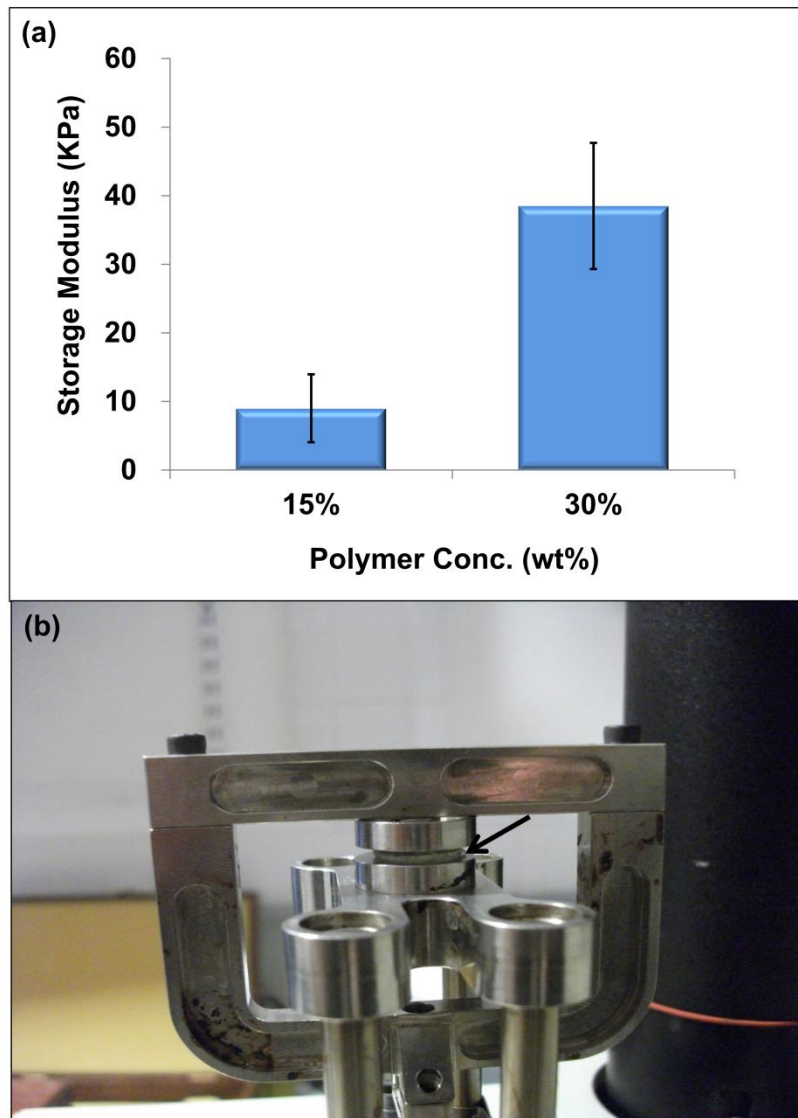


Figure 4.5: Compression tests on chemical cross-linked hydrogels fabricated from PEGMEMA-MEO₂MA-PEGDA with thiolated HA. (a) Storage Modulus of hydrogels prepared at different polymer concentration (n = 3, Mean ± SD). (b) A hydrogel sample (diameter 12.5 mm, thickness 2.5 mm) was under a compression test using DMA. **Note:** the hydrogel prepared from higher polymer concentration exhibited the strengthened mechanical properties.

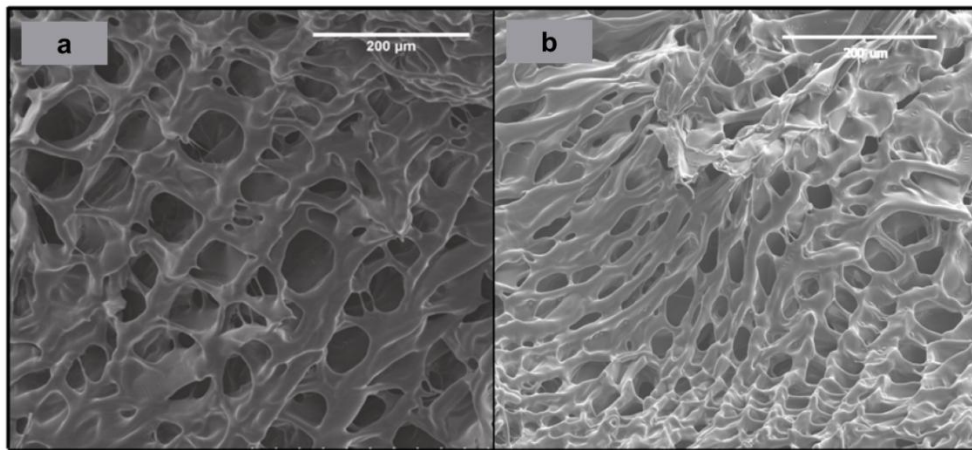


Figure 4.6: SEM images of the cross-linked hydrogel using (a) 10 wt% and (b) 15 wt% PEGMEMA-MEO₂MA-PEGDA polymer and fixed concentration of HA-SH. (The assay was performed by a colleague of Dr Aram O. Saeed (Postdoc. researcher in our group) and the results have been published by the first-authored paper ²⁹). **Note:** slight larger pore formed with lower polymer concentration.

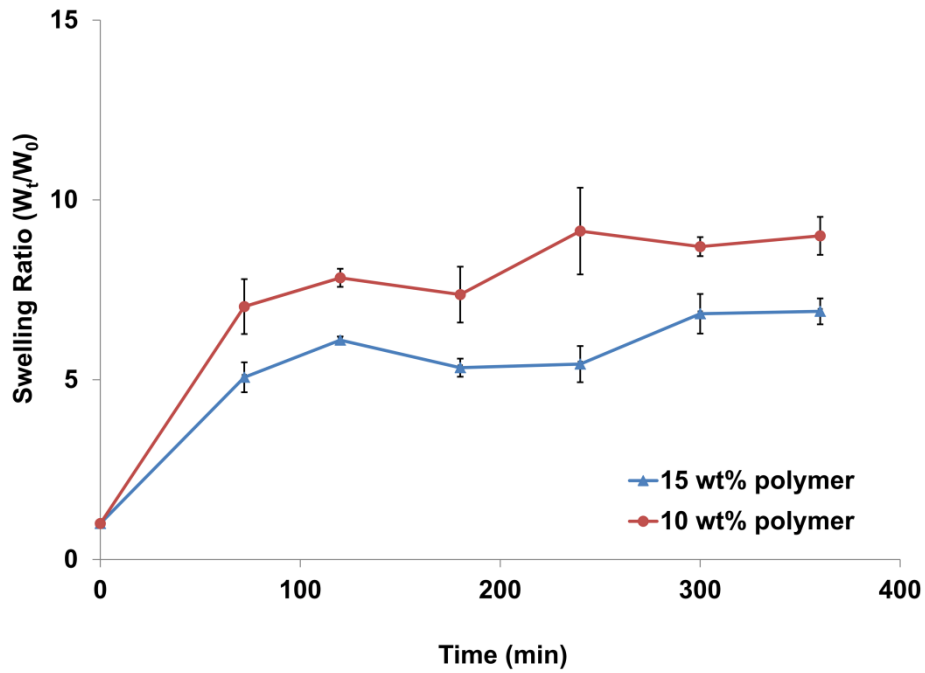


Figure 4.7: Swelling ratio of hydrogel with 10 wt% and 15 wt % PEGMEMA-MEO₂MA-PEGDA copolymer and HA-SH at 37 °C. (The assay was performed by a colleague of Dr Aram O. Saeed (Postdoc. researcher in our group) and the results have been published by the first-authored paper ²⁹).

4.3.5 Cell Metabolic Activity, Viability and Proliferation in 3D Culture

To increase the reproducibility of the studies, a commercially available thiolated hyaluronic acid (HA-SH, HyStem™, Glycosan) was used to replace our own synthesized HA-SH for *in vitro* cell viability studies. Cell viability, proliferation and metabolic activity of the encapsulated ADSCs in the P-SH-HA hydrogel were assessed *in vitro* up to three weeks in this study. LIVE/DEAD® (Molecular Probes®) staining kit was used to label the live cells (by Calcein-AM) and dead cells (by ethidium homodimer-1) in the hydrogel after 3, 7, 14 and 21 days (**Figure 4.8**). It is shown that very few dead cells (red) compare with live cells (green), and quantitative result shows no significant difference of cell viability from every time point ($n = 3$, $p < 0.05$) (**Figure 4.9**). However, although the viability of the cells in the hydrogel was 85 %, total DNA amount stopped increasing after 7 days as determined by PicoGreen® (Molecular Probes®) assay which means the proliferation of the cells were restricted (**Figure 4.10**). It is assumed that the non-degradable property of the hydrogel and the difficulty of cell attachment of ADSCs on PEG and HA based material limited the cell migration and proliferation. In addition, the results from the PicoGreen® assay were confirmed by the result from alamarBlue® (Invitrogen®) assay, in which the cell metabolic activity remained at the same level and slightly decreased at 14 days ($n = 3$, $p < 0.05$) (**Figure 4.11**).

In summary, more than eighty percent of encapsulated cells remained alive in the hydrogels up to three weeks. However, the non-degradable properties of the hydrogel limited the cell proliferation and metabolic activity at some level, but these limitations can be overcome by regularly dressing change for further clinical use. Furthermore *in vitro* modification work on the degradable and mechanical properties of the hydrogel is carried continues in our group in order to optimize the stem cell niche in this dressing system for further increase the cell proliferation and secretion.

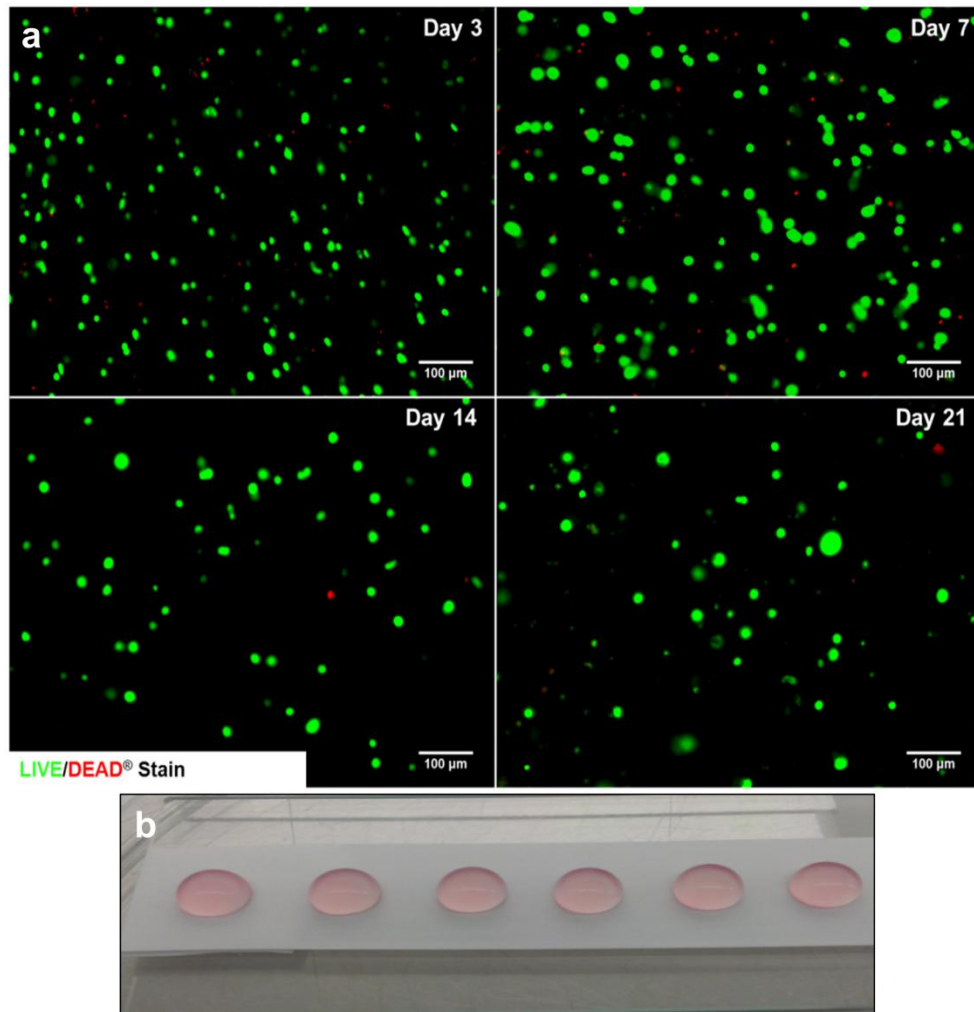


Figure 4.8: Cell viability of ADSCs encapsulated in P-SH-HA hydrogels at 3, 7, 14 and 21 days. (a) Representative fluorescent images of encapsulated ADSCs stained with calcein AM (green) for live cells and ethidium homodimer-1 (red) for dead cells by LIVE/DEAD[®] stain kit. (b) Hydrogel prepared on Teflon tape (molar ratio of thiol:vinyl as 1:1).

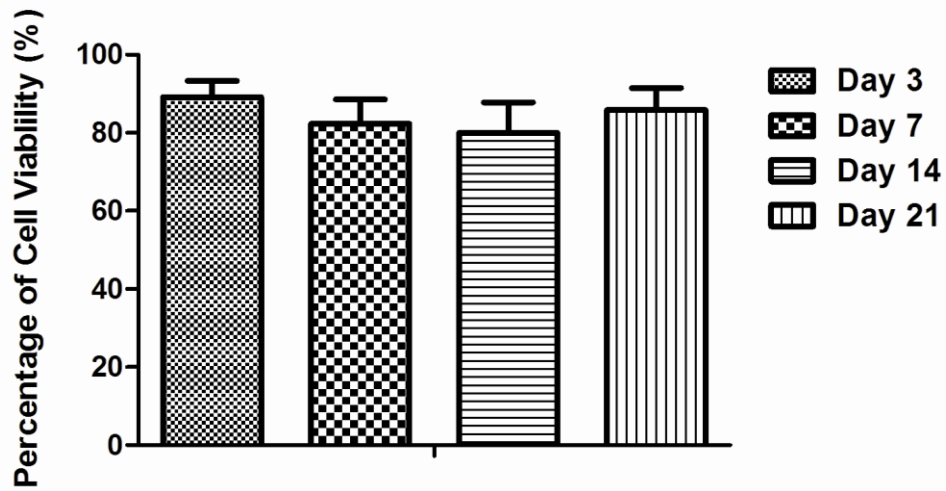


Figure 4.9: Cell viability of ADSCs encapsulated in P-SH-HA hydrogels at 3, 7, 14 and 21 days. Percentage of live cells to total cell number calculated from LIVE/DEAD[®] staining micrographs (Mean \pm SD, n = 3). **Note:** there is no significant difference of cell viability from every time point ($p < 0.05$).

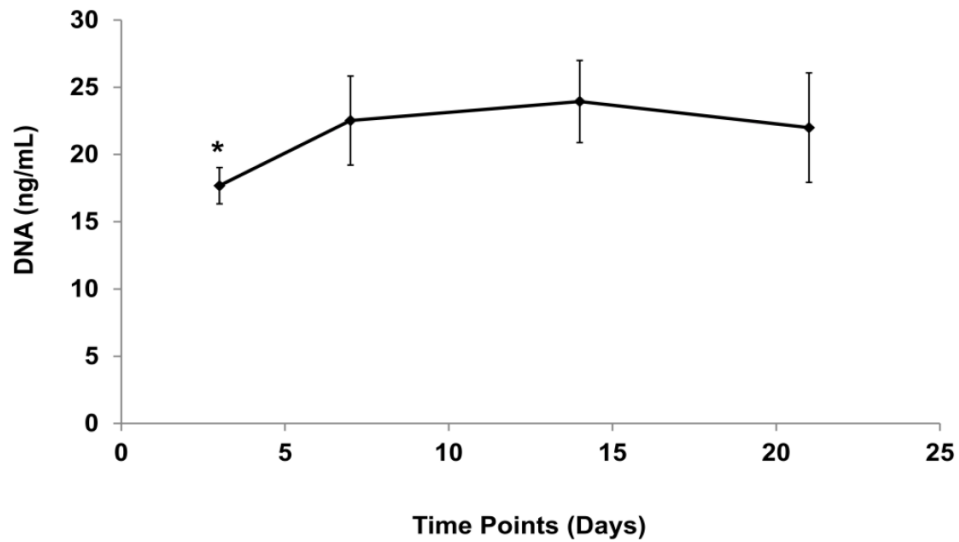


Figure 4.10: Cellular proliferation assessment by PicoGreen[®] assay. **Note:** total DNA content in the hydrogel is significant increased from 7 days (n = 3, $p < 0.05$) and maintain at the same level after that, which means the proliferation of the cells were restricted after 7 days.

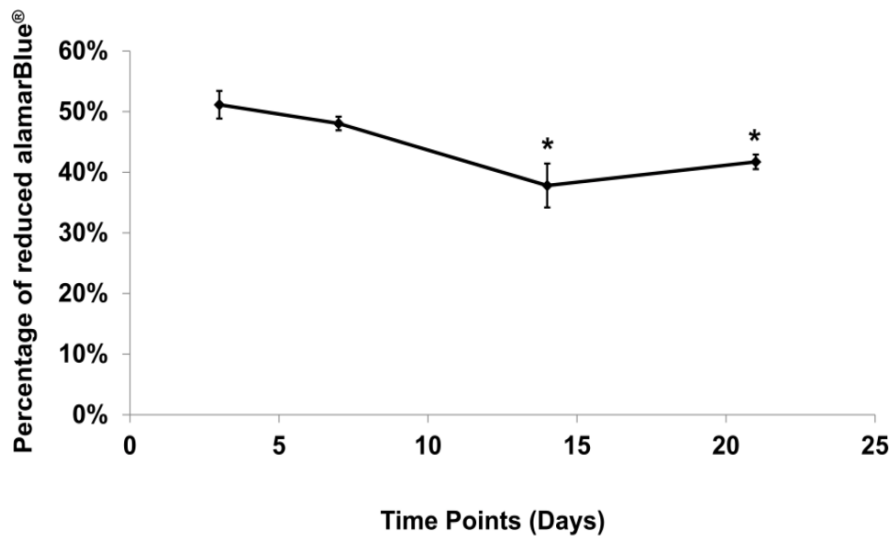


Figure 4.11: Cell metabolic activity assessment by alamarBlue[®] assay. Percentage of deduced alamarBlue[®] was calculated by the absorbance at 550 and 595 nm. **Note:** total cellular metabolic activity were significantly reduced after 14 days ($n = 3, p < 0.05$).

4.3.6 Determination of Growth Factor Secretion

As described in Chapter 1, growth factors and cytokines are essential mediators that regulate the wound healing process. In this study, we evaluated the secretion of a number of main growth factors and cytokines commonly involved in wound healing *in vitro* both in 2D (as control) and 3D culture condition, which included pro-inflammatory cytokines of IL-2 and INF- γ ; anti-inflammatory cytokines of IL-10 and angiogenic growth factors of PlGF, VEGF and TGF- β . It was found that the pro-inflammatory cytokines of IL-2 and INF- γ reduced after 7 days in 3D hydrogel microenvironment, while remained at the same level for 2D seeded cells (**Figure 4.12a-b**). At the meantime, the release level of anti-inflammatory cytokine of IL-10 in hydrogel seemed higher than 2D control (**Figure 4.12c**), which may explain the reduction of pro-inflammatory cytokines in hydrogel system as above described. In addition, release of the angiogenic growth factors of PlGF, VEGF significantly increased in hydrogel system over time (**Figure 4.13a-b**); TGF- β was also showed increased production over time in both 2D and 3D conditions, but there was no significant difference in concentration levels at any time for 3D culture (**Figure 4.12c**). In conclusion, these results suggest that hADSCs can secrete pro-angiogenic and anti-inflammatory cytokines and growth factors in our P-SH-HA hydrogel system.

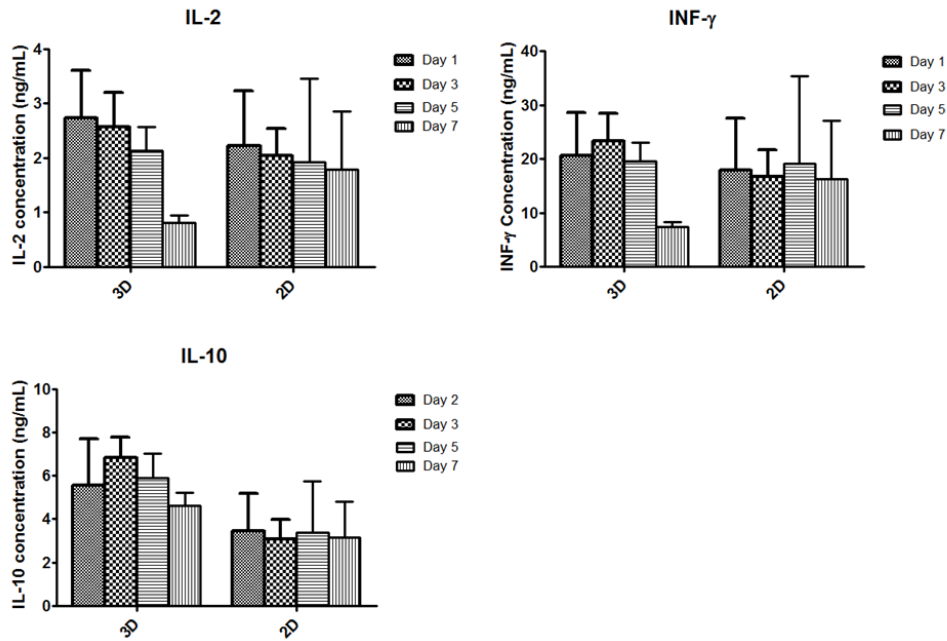


Figure 4.12: Secretion profile of cytokines of hADSCs in both P-SH-HA hydrogel (3D) and tissue culture plastic (2D) over 7 days. Cells were seeded at 0.5×10^6 cells/ml in both 3D and 2D culture conditions in 48-well plates. Supernatant from both conditions was analysed using multi-plex ELISA kit for IL-2, IL-10 and INF- γ . ($n = 3$, $p < 0.05$). The assessment was performed by a colleague of Waqar Hassan (PhD student in our group) and the results have been published by a co-authored paper ³⁰. **Note:** inflammatory cytokines of IL-2 and INF- γ reduced after 7 days in 3D hydrogel microenvironment, while remained at the same level for 2D seeded cells (a-b); anti-inflammatory cytokine of IL-10 in hydrogel seemed higher level than 2D control (c).

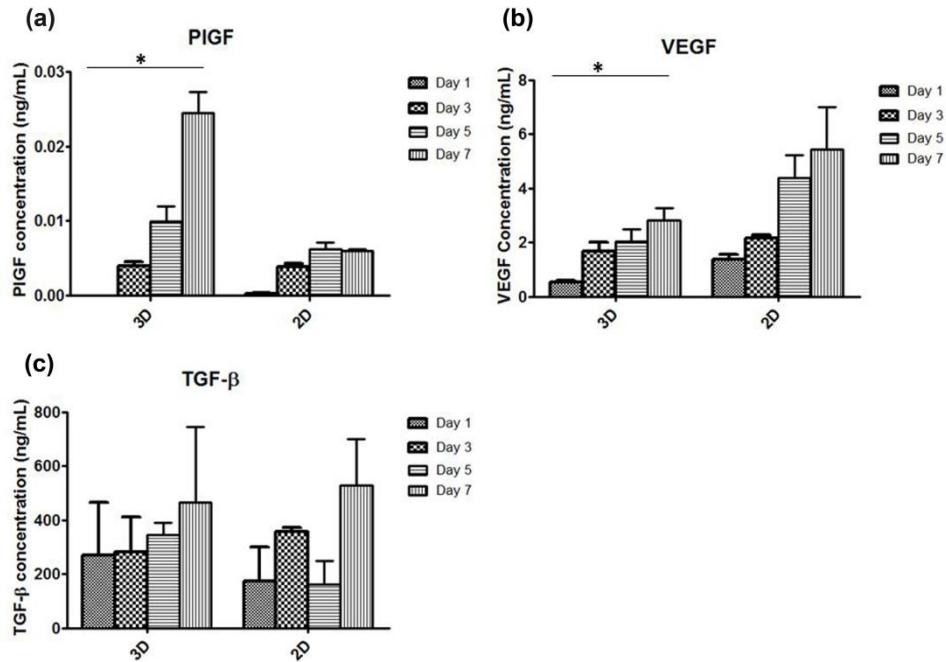


Figure 4.13: Secretion profile of growth factors of hADSCs in both P-SH-HA hydrogel (3D) and tissue culture plastic (2D) over 7 days. Cells were seeded at 0.5×10^6 cells/ml in both 3D and 2D culture conditions in 48-well plates. Supernatant from both conditions was analysed using multi-plex ELISA kit for PIGF, VEGF and TGF- β . ($n = 3$, $p < 0.05$). The assessment was performed by a colleague of Waqar Hassan (PhD student in our group) and the results have been published by a co-authored paper ³⁰. **Note:** the angiogenic growth factors of PIGF, VEGF significantly increased in hydrogel system over time (a-b); TGF- β was also showed increased production over time in both 2D and 3D conditions, but there was no significant difference in concentration levels at any time for 3D culture (c).

4.4 Conclusion

In this study, we have demonstrated the preparation of an injectable, *in-situ* cross-linking, hybrid hydrogel from the combination of thiolated hyaluronic acid and PEG-based thermoresponsive hyperbranched polymer with acrylate vinyl groups. Over 80 % of encapsulated ADSCs cells remained alive in the hydrogels up to three weeks *in vitro*, and the secretion profile of ADSCs in this P-SH-HA hydrogel system via multi-plex ELISA showed that inflammatory cytokines of IL-2 and INF- γ significantly reduced after 7 days in 3D hydrogel microenvironment, and the anti-inflammatory cytokine of IL-10 in hydrogel seemed higher level than 2D control. Furthermore, the angiogenic growth factors of PlGF, VEGF significantly increased in hydrogel system over time. In conclusion, this *in-situ* cross-linked P-SH-HA hydrogel system, in which ADSCs can be easily encapsulated and maintain their viability and secretion level, has shown promise as an injectable system for tissue engineering application.

4.5 References

1. Lee, Y.; Fukushima, S.; Bae, Y.; Hiki, S.; Ishii, T.; Kataoka, K., A protein nanocarrier from charge-conversion polymer in response to endosomal pH. *Journal of the American Chemical Society* 2007, 129, (17), 5362-5363.
2. Twaites, B. R.; Alarcon, C. D. H.; Lavigne, M.; Saulnier, A.; Pennadam, S. S.; Cunliffe, D.; Gorecki, D. C.; Alexander, C., Thermoresponsive polymers as gene delivery vectors: Cell viability, DNA transport and transfection studies. *Journal of Controlled Release* 2005, 108, (2-3), 472-483.
3. Webber, G. B.; Wanless, E. J.; Armes, S. P.; Biggs, S., Tunable diblock copolymer micelles-adapting behaviour via subtle chemical modifications. *Faraday Discussions* 2005, 128, 193-209.
4. Barichello, J. M.; Morishita, M.; Takayama, K.; Nagai, T., Absorption of insulin from Pluronic F-127 gels following subcutaneous administration in rats. *International Journal of Pharmaceutics* 1999, 184, (2), 189-198.
5. Choi, S.; Kim, S. W., Controlled release of insulin from injectable biodegradable triblock copolymer depot in ZDF rats. *Pharmaceutical Research* 2003, 20, (12), 2008-2010.
6. Fraylich, M. R.; Liu, R. X.; Richardson, S. M.; Baird, P.; Hoyland, J.; Freemont, A. J.; Alexander, C.; Shakesheff, K.; Cellesi, F.; Saunders, B. R., Thermally-triggered gelation of PLGA dispersions: Towards an injectable colloidal cell delivery system. *Journal of Colloid and Interface Science* 2010, 344, (1), 61-69.
7. Hou, Y.; Matthews, A. R.; Smitherman, A. M.; Bulick, A. S.; Hahn, M. S.; Hou, H.; Han, A.; Grunlan, M. A., Thermoresponsive nanocomposite hydrogels with cell-releasing behavior. *Biomaterials* 2008, 29, (22), 3175-3184.
8. Wang, W.; Liang, H.; Al Ghanami, R. C.; Hamilton, L.; Fraylich, M.; Shakesheff, K. M.; Saunders, B.; Alexander, C., Biodegradable thermoresponsive microparticle dispersions for injectable cell delivery prepared using a single-step process. *Advanced Materials* 2009, 21, (18), 1809.
9. Zentner, G. M.; Rathi, R.; Shih, C.; McRea, J. C.; Seo, M. H.; Oh, H.; Rhee, B. G.; Mestecky, J.; Moldoveanu, Z.; Morgan, M.; Weitman, S., Biodegradable block copolymers for delivery of proteins and water-insoluble drugs. *Journal of Controlled Release* 2001, 72, (1-3), 203-215.
10. Crompton, K. E.; Goud, J. D.; Bellamkonda, R. V.; Gengenbach, T. R.; Finkelstein, D. I.; Horne, M. K.; Forsythe, J. S., Polylysine-functionalised thermoresponsive chitosan hydrogel for neural tissue engineering. *Biomaterials* 2007, 28, (3), 441-449.
11. Jeong, B.; Kim, S. W.; Bae, Y. H., Thermosensitive sol-gel reversible hydrogels. *Advanced Drug Delivery Reviews* 2002, 54, (1), 37-51.

12. Sasaki, J. I.; Asoh, T. A.; Matsumoto, T.; Egusa, H.; Sohmura, T.; Alsberg, E.; Akashi, M.; Yatani, H., Fabrication of Three-dimensional cell constructs using temperature-responsive hydrogel. *Tissue Engineering Part A* 2010, 16, (8), 2497-2504.
13. Zimmermann, U.; Mimietz, S.; Zimmermann, H.; Hillgartner, M.; Schneider, H.; Ludwig, J.; Hasse, C.; Haase, A.; Rothmund, M.; Fuhr, G., Hydrogel-based non-autologous cell and tissue therapy. *Biotechniques* 2000, 29, (3), 564.
14. Ruel-Gariepy, E.; Leroux, J. C., In situ-forming hydrogels - review of temperature-sensitive systems. *European Journal of Pharmaceutics and Biopharmaceutics* 2004, 58, (2), 409-426.
15. Yu, L.; Ding, J. D., Injectable hydrogels as unique biomedical materials. *Chemical Society Reviews* 2008, 37, (8), 1473-1481.
16. Frisman, I.; Seliktar, D.; Bianco-Peled, H., Nanostructuring of PEG-fibrinogen polymeric scaffolds. *Acta Biomaterialia* 2010, 6, (7), 2518-2524.
17. Lee, Y.; Chung, H. J.; Yeo, S.; Ahn, C. H.; Lee, H.; Messersmith, P. B.; Park, T. G., Thermo-sensitive, injectable, and tissue adhesive sol-gel transition hyaluronic acid/pluronic composite hydrogels prepared from bio-inspired catechol-thiol reaction. *Soft Matter* 2010, 6, (5), 977-983.
18. Shu, X. Z.; Ahmad, S.; Liu, Y. C.; Prestwich, G. D., Synthesis and evaluation of injectable, in situ crosslinkable synthetic extracellular matrices for tissue engineering. *Journal of Biomedical Materials Research Part A* 2006, 79A, (4), 902-912.
19. Shu, X. Z.; Liu, Y. C.; Palumbo, F. S.; Lu, Y.; Prestwich, G. D., In situ crosslinkable hyaluronan hydrogels for tissue engineering. *Biomaterials* 2004, 25, (7-8), 1339-1348.
20. Drury, J. L.; Mooney, D. J., Hydrogels for tissue engineering: scaffold design variables and applications. *Biomaterials* 2003, 24, (24), 4337-4351.
21. Silva, E. A.; Mooney, D. J., Synthetic extracellular matrices for tissue engineering and regeneration. *Current Topics in Developmental Biology*, 2004, 64, 181-205.
22. Lutolf, M. P.; Hubbell, J. A., Synthetic biomaterials as instructive extracellular microenvironments for morphogenesis in tissue engineering. *Nature Biotechnology* 2005, 23, (1), 47-55.
23. Alini, M.; Li, W.; Markovic, P.; Aebi, M.; Spiro, R. C.; Roughley, P. J., The potential and limitations of a cell-seeded collagen/hyaluronan scaffold to engineer an intervertebral disc-like matrix. *Spine* 2003, 28, (5), 446-453.
24. Kogan, G.; Soltes, L.; Stern, R.; Gemeiner, P., Hyaluronic acid: a natural biopolymer with a broad range of biomedical and industrial applications. *Biotechnology Letters* 2007, 29, (1), 17-25.
25. Leach, J. B.; Bivens, K. A.; Patrick, C. W.; Schmidt, C. E., Photocrosslinked hyaluronic acid hydrogels: Natural, biodegradable tissue

engineering scaffolds. *Biotechnology and Bioengineering* 2003, 82, (5), 578-589.

26. Lin, C.; Zhao, P.; Li, F.; Guo, F.; Li, Z.; Wen, X., Thermosensitive in situ-forming dextran-pluronic hydrogels through Michael addition. *Materials Science and Engineering: C* 2010, 30, (8), 1236-1244.

27. Shachaf, Y.; Gonen-Wadmany, M.; Seliktar, D., The biocompatibility of Pluronic®F127 fibrinogen-based hydrogels. *Biomaterials* 2010, 31, (10), 2836-2847.

28. Kafedjiiski, K.; Jetli, R. K. R.; Foger, F.; Hoyer, H.; Werle, M.; Hoffer, M.; Bernkop-Schnurch, A., Synthesis and in vitro evaluation of thiolated hyaluronic acid for mucoadhesive drug delivery. *International Journal of Pharmaceutics* 2007, 343, (1-2), 48-58.

29. Dong, Y.; Saeed, A. O.; Hassan, W.; Keigher, C.; Zheng, Y.; Tai, H.; Pandit, A.; Wang, W., "One-step" preparation of thiol-ene clickable PEG-based thermoresponsive hyperbranched copolymer for in situ crosslinking hybrid hydrogel. *Macromolecular Rapid Communications* 2012, 33, (2), 120-126.

30. Hassan, W.; Dong, Y.; Wang, W., Encapsulation and 3D culture of human adipose-derived stem cells in an in-situ crosslinked hybrid hydrogel composed of PEG-based hyperbranched copolymer and hyaluronic acid. *Stem Cell Research & Therapy* 2013, 4.

31. Dong, Y.; Gunning, P.; Cao, H.; Mathew, A.; Newland, B.; Saeed, A. O.; Magnusson, J. P.; Alexander, C.; Tai, H.; Pandit, A.; Wang, W., Dual stimuli responsive PEG based hyperbranched polymers. *Polymer Chemistry* 2010, 1, (6), 827-830.

32. Tai, H.; Wang, W.; Vermonden, T.; Heath, F.; Hennink, W. E.; Alexander, C.; Shakesheff, K. M.; Howdle, S. M., Thermoresponsive and photocrosslinkable PEGMEMA-PPGMA-EGDMA copolymers from a one-step ATRP synthesis. *Biomacromolecules* 2009, 10, (4), 822-828.

Chapter Five

Assessment of Material Responce and Theraputic Performance of *In-situ* Formed Bioactive Stem Cell Hydrogel Dressing in Rat Dorsal Excisional Wound Model

The majority of this chapter has been submitted for publication in:

Dong, Y.; Hassan, W.; Kennedy, R.; Greiser, U.; Garcia, Y.and Wang. W.
“An *In-situ* Formed Bioactive Stem Cell Hydrogel Dressing from a PEG-
based Hyperbranched Multi-functional Copolymer”. *Biomaterials*
(BIOMAT-S-13-02170).

5.1 Introduction

Wound dressing-based treatments are the main therapeutical approaches for both acute and chronic wounds. Specific wound dressings have been developed over the years for different types and physiologic conditions of the wounds^{1, 2}. Traditional dressings were mainly used to absorb the exudates, to keep the wound bed dry and to prevent bacterial contamination, while the modern wound dressings focus more on creating an optimum moist environment to promote wound repair^{3, 4}. Appropriate amount of wound exudate not only supplies the wound bed with nutrients, but provides favorable conditions for certain cell recruitment and migration⁵⁻⁷. Among different wound dressings, hydrogel dressings made from swellable polymeric hydrophilic materials can maintain the moist wound environment, provide autolytic debridement and also cool the wound surface which lead to pain relief for patients⁸⁻¹⁰. Current commercially available hydrogel dressings include Nu-gel[®] wound dressing, Purilon[®] gel dressing, SAF-Gel[®] hydrating dermal wound dressing, Curagel[™] hydrogel wound dressing, and Carrasyn[®] gel wound dressing among others¹¹. Although significant progress has been made in the developemnt of modern wound dressings, promoting the healing process is still restricted, especially when compared to cellular skin substitutes.

Stem cells such as bone marrow derived stem cells (BMSCs)¹²⁻¹⁶ and adipose-derived stem cells (ADSCs)¹⁷⁻²⁰ have been widely studied for wound healing applications. Most of these studies focus on developing skin substitutes in which the stem cells differentiate into epidermal cell phenotypes, regulate the level of cytokines and growth factors around the wound site, and accelerate wound healing^{16, 21-23}. In the past few years, increasing evidence has emerged demonstrating the stem cell paracrine effects which play key roles in promoting the healing process. Conditioned medium of both BMSCs and ADSCs have been reported to enhance angiogenesis, epithelialization, and affect recruitment or proliferation of macrophages and endothelial progenitor cells during the healing process²⁴⁻²⁶. Furthermore, in comparison to BMSCs, ADSCs yield from adipose tissue is generally 40-fold higher²⁷. ADSCs removed in liposuction are much

easier to access because the surgical approach is considerably less painful. In addition, the isolated cells can be cryopreserved maintaining all their properties intact for up to 6 months²⁸, which provides a good potential for ADSCs to get integrated in an off-the-shelf product.

Ideally, the next step is to develop a hydrogel dressing with specific therapeutic functions, which not only act as a hydrogel dressing but also be able to deliver therapeutic agents such as growth factors or stem cells i.e. preventing unwanted inflammatory reactions and providing an ideal wound healing environment. To this end, an *in-situ* cross-linked hydrogel (i.e. P-SH-HA) cell delivery system based on a PEG based thermoresponsive hyperbranched copolymer of poly(ethylene glycol) methyl ether methacrylate-*co*-2-(2-methoxyethoxy) ethyl methacrylate-*co*-poly(ethylene glycol) diacrylate (PEGMEMA-MEO₂MA-PEGDA) was developed in our group²⁹ (see Chapter 4). At room temperature, the polymer solution can be easily mixed with cells and thiolated hyaluronic acid (HA-SH); while at body temperature physical cross-linked hydrogel forms rapidly onto the wound site. A chemical gelation between polymer and HA-SH occurs within a short time to achieve a stable hydrogel with enhanced mechanical properties. As an injectable system, this hydrogel can be easily applied to any wound size, shape or cavity, is less invasive than other approaches and minimizes patients' discomfort. Upon cross-linking an *in-situ* gelation occurs forming a three-dimensional (3D) water content polymer network via physical and chemical cross-linking which can mimic tissue microenvironment for cell growth. In addition, its relatively slow degradable and non-adherent properties provide this hydrogel dressing with the advantage to be removed chemically intact with ease at dressing changes without causing pain and/or further trauma.

In this study, as an *in-situ* cross-linked bioactive hydrogel dressing, P-SH-HA system in combination with rat extracted ADSCs was evaluated by using a rat dorsal full-thickness wound model. It was hypothesized that ADSCs could survive in the *in-situ* formed hydrogel system *in vivo*, and then promote angiogenesis and wound healing by paracrine effect.

5.2 Materials and Methods

5.2.1 Materials and Reagents

The monomers of poly(ethylene glycol) methyl ether methacrylate (PEGMEMA Mn = 475 g/mol), 2-(2-methoxyethoxy) ethyl methacrylate (MEO₂MA), and poly(ethylene glycol) diacrylate (PEGDA Mn = 258 g/mol) were purchased from Sigma-Aldrich. Ethyl 2-bromoisobutyrate (EtBriB, 98 %, Aldrich), bis(2-dimethylaminoethyl) methylamine (99 %, Aldrich), copper (II) chloride (CuCl₂, 97 %, Aldrich), L-ascorbic acid (L-AA, 99 %, Aldrich), butanone (99 %, HPLC grade, Aldrich) and hexane (95 %, Aldrich) were used as received. Thiolated hyaluronic acid (HA-SH, HyStem™, Glycosan) was purchased from BioTime Inc., Alameda, CA.

5.2.2 Polymer Synthesis and Hydrogel Fabrication

The thermoresponsive copolymer of PEGMEMA-MEO₂MA-PEGDA was synthesized by the copolymerizing of PEGMEMA (Mn = 475 g/mol), MEO₂MA and PEGDA (Mn = 258 g/mol) via *in-situ* deactivation enhanced atom transfer radical polymerization (DE-ATRP) approach as previously described²⁹. Briefly, PEGMEMA (15 molar equiv), MEO₂MA (65 molar equiv), PEGDA (20 molar equiv), EtBriB (1 molar equiv), CuCl₂ (0.25 molar equiv), bis(2-dimethylaminoethyl) methylamine (0.25 molar equiv) were all added into a two-necked round bottom flask (the volume ratio of total monomers to butanone solvent adjusted at 1:2). The mixture was completely dissolved, purged with argon for 30 min to remove oxygen, and then L-AA (0.125 molar equiv) was added to the polymerization solution under argon condition. The reaction was performed at 50 °C in an oil bath for about 6 h with monitor of gel permeation chromatography (GPC). The copolymer products were purified and characterized by GPC, ¹H NMR and UV spectrophotometer as previously described^{29, 30}. The molecular weight (Mw) of the copolymer is 72 KDa with a Polydispersity Index of 3.97. The content of vinyl functional group of the copolymer was approximate 12 mol percentage calculated by ¹H NMR analysis and the lower critical solution temperature (LCST) of this copolymer was determined around 32 °C.

Copolymer of PEGMEMA-MEO₂MA-PEGDA was dissolved in phosphate buffered saline (PBS, pH 7.4), mixed gently by pipetting to the ADSCs suspension (in serum-free medium) and commercially available thiolated HA (HA-SH). Here, the final concentration of the copolymer was 5 % (w/v), HA-SH was 0.5 % (w/v) and ADSCs was 1 million/ml. Gelation occurs within 8 min at 37 °C through Michael-type addition between vinyl groups on copolymer and thiol groups on the HA-SH.

5.2.3 *In Vivo* Model

All procedures were conducted under an animal license (no. B100/4342) authorized by the Irish Department of Health and Children and were approved by the Animal Care and Research Ethics Committee of the National University of Ireland, Galway (no. 009/10(B)). Animal care followed the Standard Operating Procedures of the Animal Facility at the National Centre for Biomedical Engineering Science, NUIG.

ADSCs were extracted from rat fat tissue and characterized as described earlier (see Chapter 4). Twenty one male Sprague Dawley rats (CD[®] IGS, CharlesRiver, UK) with body weights ranging between 275 g and 325 g were used in this study. Three time periods were designed as 3, 7 and 14 (n = 7 wounds per treatment per time point). The animals were anesthetized with isoflurane with oxygen (5 % for induction and 1-2 % for maintenance). Two full-thickness square wounds (1 cm × 1 cm) were created at each side of dorsal midline being at least 1 cm apart (see Appendices.M). Photographic images were taken for each wound. Four different treatment groups were randomized: no treatment (NA); hydrogel alone (120 µl gelling mixture solution) (H); hydrogel + rADSCs (0.12 million cells in 120 µl gelling mixture solution) (H+C); rADSCs alone (0.12 million cells in 30 µl serum-free medium) (C) (**Table 5.1**). Hydrogels with/without cells were formed *in-situ* as described above. The cells alone group was prepared by pipetting 0.12 million rADSCs in 30 µL serum-free medium to the wound surface. The wounds were covered by commercially available transparent film dressing (Tegaderm[™] Film, 3M[®]), followed by medical gauze to prevent disturbance of the wounds. Analgesia was granted by the used of Buprenorphine (0.03 mg/Kg every 8 h, Vetergesic) and inflammation due to

local contamination was prevented by the use of broad spectrum antibiotics (Enrofloxacin: 5 mg/Kg once a day) for the first three days.

5.2.4 Harvesting and Processing of Tissue

The animals were sacrificed by CO₂ asphyxiation at each time points. Gauze and film dressing were carefully removed and photographic images were taken for each wound. All samples were identified by animal number, time point and positions (AL: anterior left; AR: anterior right; PL: posterior left; PR: posterior right) to avoid analytic bias. Samples were fixed in 10 % formalin for 24 h, followed by automatic paraffin processing (Leica ASP300), blocked and sectioned perpendicularly to wound surface in 5 µm consecutive sections. The samples were stained with haematoxylin eosin (H&E), collagen type IV and CD 68 immunohistochemical staining using standard protocols developed in our lab to be subsequently analyzed stereologically.

5.2.5 Analysis for *In Vivo* Study

5.2.5.1 Wound closure

The wound areas were measured using image analysis software (ImagePro[®] Plus, Media Cybernetics, USA) on the photographic images. The percentage of reduction in the wound area at different time points was performed by comparing them with the wound area at day 0.

5.2.5.2 Wound contraction and epithelialization

Wound contraction (C) and epithelialization (E) was measured on the $\times 12.5$ images with H&E staining. The distance between dermal edges at both side of the wound was measured as wound length (W_t). The percentage of epithelialization (E %) was determined by the total epithelial layer over the wound at both side ($E_1 + E_2$) divided by the original wound length (W_0) (eqn. 5.1). The original wound size was 1 cm and roughly 10 % contraction was caused by fixing and processing processes, therefore W_0 was considered as 0.9 cm for calculation here. Percentage of wound contraction (C %) was determined by the reduction of wound length divided by the original wound length (eqn. 5.2). The identification of all the parameters can be observed in **Figure 5.1**.

$$E\% = \frac{(E_1 + E_2)}{W_0} \times 100 \quad (\text{eqn. 5.1})$$

$$C\% = \frac{(W_0 - W_t)}{W_0} \times 100 \quad (\text{eqn. 5.2})$$

5.2.5.3 Cell retention

rADSCs used for *in vivo* study were incubated with CellTrackerTM CM-Dil (Invitrogen[®]) at a concentration of 4 $\mu\text{mol/l}$ for 30 min at 37 °C. The paraffin slide samples of rADSCs alone group and Hydrogel + ADSCs were further stained by Hoechst 33258 (Invitrogen[®]), and fluorescent micrographs were taken with $\times 100$ magnification (five fields of view per slide, three slides per treatment) by Olympus 1X-81 inverted microscope. The volume fractions of rADSCs were determined by stereological analysis using a grid mask ($40 \times 40 \mu\text{m}^2$).

5.2.5.4 Determination of inflammation

The inflammatory cells including neutrophils, lymphocytes and macrophages were detected by micrographs with $\times 600$ magnification taken from H&E staining slides. In addition, ED-1 (mouse monoclonal anti-CD 68 antibody, Abcam) was used to label macrophages by standard immunohistochemical staining (AlexaFluor[®] 488 Goat anti-Mouse IgG (H+L from Invitrogen) as secondary antibody. Nucleus was stained with Hoechst 33258 (Sigma). A grid mask ($20 \mu\text{m} \times 20 \mu\text{m}$) was applied to images with $\times 200$ magnification (three fields of view per slide, three slides per treatment) and the numbers of grid intersections that touch or traverse the nucleus of CD68⁺ cells were tagged. The volume fraction (V_V) of each treatment was expressed as the fraction of tagged intersections (P_V) in relation to the total number of intersections (P_T) in the grid (eqn. 5.3).

$$V_V = \frac{P_V}{P_T} \quad (\text{eqn. 5.3})$$

Table 5.1: Treatment groups design for *in vivo* study.

No.	Treatment	No. of Treatment
I	No Treatment	7
II	P- HA-SH Hydrogel Alone (120 μ L gelling mixture solution per wound)	7
III	P- HA-SH Hydrogel + RatADSCs (0.12 million cells in 120 μ L gelling mixture solution per wound)	7
IV	RatADSCs Alone (0.12 million cells in 30 μ L serum-free medium per wound)	7

Time points: 3, 7 and 14 days

- **Wound Closure:** Digital image analysis
- **Wound Contraction & Epithelialisation:** H&E Stain
- **Cell Retention:** CellTracker™ and Hoechst fluorescent, micro-imaging
- **Inflammatory Response:** H&E stain, CD68 immunohistochemical stain
- **Angiogenesis:** Collagen type IV immunohistochemical stain

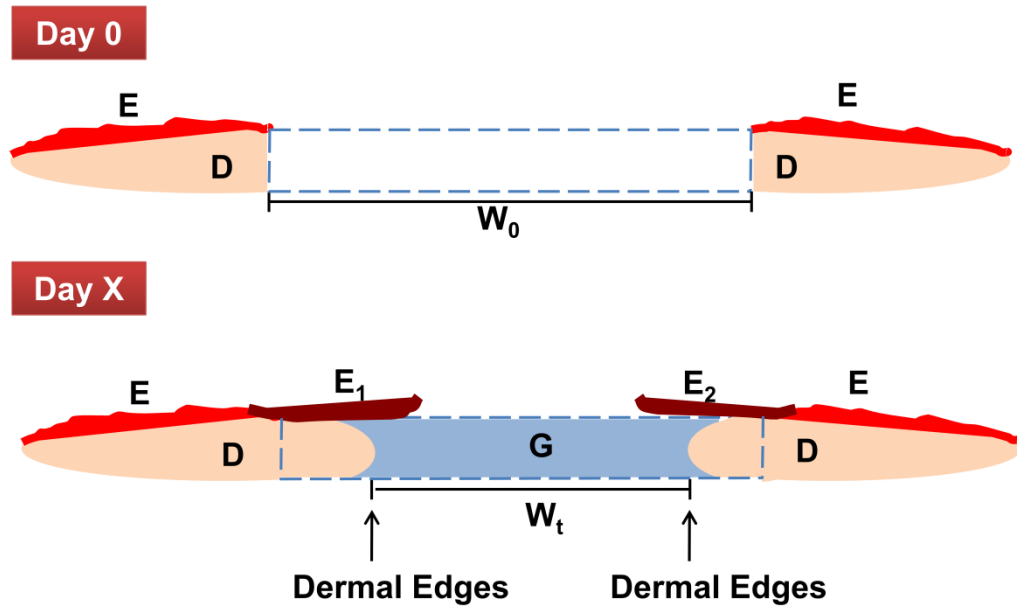


Figure 5.1: The identified parameters for measurement of wound contraction and epithelialization on H&E staining slides. E: epidermal; D: dermal; E1/E2: regenerated epidermal; G: granulation tissue. Note: wounds are contracted along with healing process.

5.2.5.5 Angiogenesis

Neoangiogenesis of the wound was determined by collagen IV immunohistochemical staining (Rabbit polyclonal antibody to collagen type IV, ab6586, Abcam plc, and AlexaFluor[®] 488 Goat anti-Rabbit IgG (H+L) as secondary antibody, Invitrogen). Stereological analysis was performed as described elsewhere³¹. Surface density (S_V), length density (L_V) were measured using a cycloid grid with known total length of cycloid lines (L) and counting the number of intersections (I) of those lines with fluorescent labeled blood vessels. Horizontal positioning grid was used for S_V and the vertical positioning grid for L_V (eqn. 5.4 and 5.5, T_S presents the thickness of sections). Wound volumes (V), surface area (S_A) and total length (L_T) were calculated by eqns. 5.6 - 5.8 (W_A presents the wound area determined by H&E staining slides).

$$S_V = 2 \times \frac{I}{L} \quad (\text{eqn. 5.4})$$

$$L_V = \frac{(2 \times (I/L))}{T_S} \quad (\text{eqn. 5.5})$$

$$V = T_S \times W_A \quad (\text{eqn. 5.6})$$

$$S_A = S_V \times V \quad (\text{eqn. 5.7})$$

$$L_T = L_V \times V \quad (\text{eqn. 5.8})$$

5.2.5.6 Statistical analysis

Comparisons between multiple groups were evaluated by One way or Two way ANOVA and Tukey's post analysis method. p value of less than 0.05 was considered as significant. The software used in the analysis was GraphPad Prism 5 software (GraphPad Software, US).

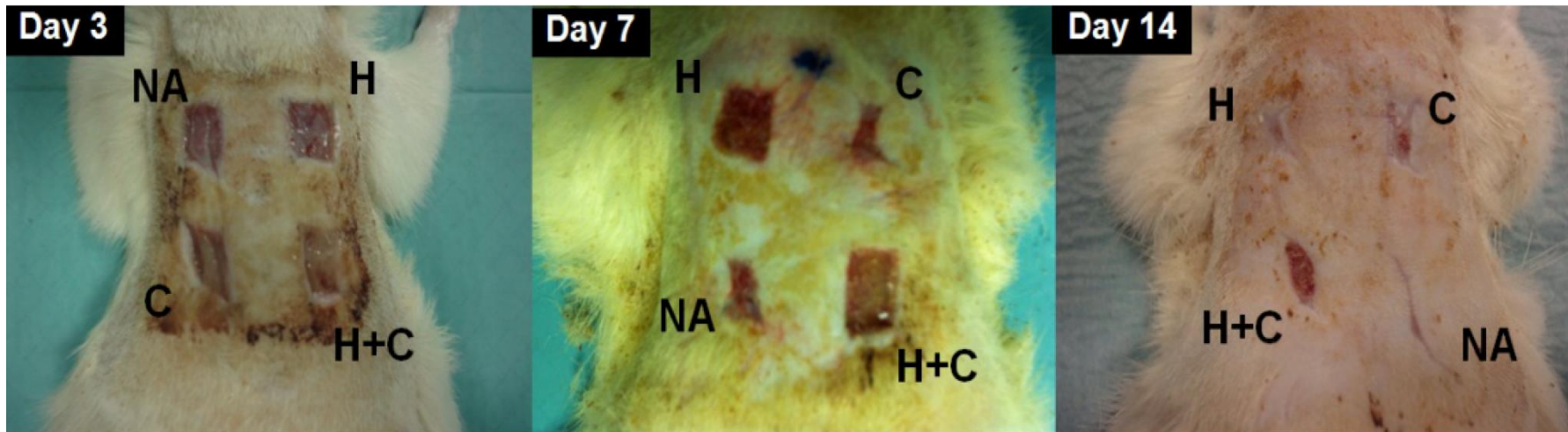


Figure 5.2: Representative photographs of wounds at 3, 7 and 14 days. NA: no treatment group; C: ADSCs cell alone group; H: hydrogel alone group; H+C: hydrogel + ADSCs group. **Note:** obvious wound contraction occurred in no treatment and cell alone control groups at 7 and 14 days.

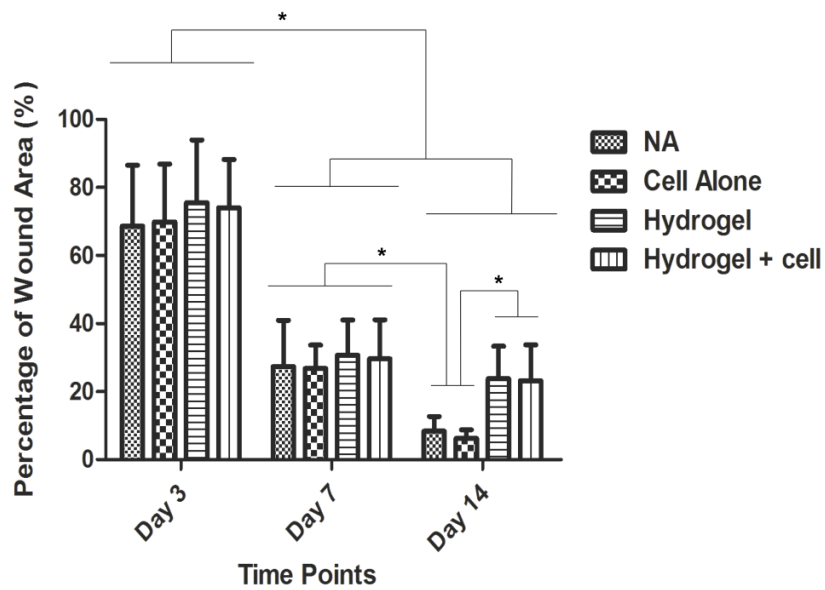


Figure 5.3: Percentage of wound area at 3, 7 and 14 days comparing to original wound area measured by ImagePro[®] Plus, (Media Cybernetics, USA). (*) labels the significant differences between each time point and groups (Two way ANOVA with Tukey’s post analysis method, Mean \pm SD, n = 7, $p < 0.05$). **Note:** wound areas of hydrogel treatment groups (with or without cells) were significantly larger than no treatment and cell alone control groups at 14 days due to the skin contraction.

5.3 Results

5.3.1 Wound Closure

Wound closure was determined by measuring the surface area from photographic images (**Figure 5.2**). As a contractive skin model, wounds with ‘no treatment’ and ‘cell alone’ treatment groups were significantly contracted during the healing process (**Figure 5.3**); the statistical result of wound area analyses showed significant reduction in wound area in the groups without hydrogels. In contrast, treatment groups of hydrogels with or without rADSCs resisted wound contraction to some extent.

5.3.2 Wound Contraction and Epithelialization

The wound contraction was calculated as percentage of wound length reduction (**Figure 5.1**) from the histological analysis. The contractive ratios of all the treatments were higher than 80 % of original wound size at 14 days, and there is no statistic significant difference between each group. However, a trend can be found that hydrogel treatment groups (with or without rADSCs) contracted less than other groups at day 7 and day 14 (**Figure 5.4**). For epithelialization measurement, it was found that the wounds were fully closed with complete re-epithelialization at 14 days in ‘no treatment’ and ‘cell alone’ treatment groups; while the re-epithelialization only occurred at the edges of the wounds in the hydrogel treatment groups (with or without cells). It appeared as if the keratinocytes ceased growing underneath the hydrogels in the center of the wound area. This observation could be explained by the inability of the keratinocytes to attach and migrate along the hydrogel surface (**Figure 5.5**). However, because of the large skin contraction, no statistical significant difference was noted for re-epithelialization between all the groups (**Figure 5.6**) at each time point.

5.3.3 Cell Retention

The cell retention ratio in the wound bed was assessed by labeling the rADSCs used in the *in-vivo* study with CellTrackerTM CM-Dil (Invitrogen[®]). The marker in this kit which conjugates with intracellular proteins reflects the cell survival rate in the hydrogels. After each time point, paraffin fixed

slides were further stained by Hoechst 33258 and determined using a fluorescent microscope. For the ‘cell alone’ group, although we applied a more concentrated cell suspension (with the same number of total cells as treatment group) and completely covered the wound with commercially available film dressing in order to prevent the cell loss from the wound bed, no labeled rADSCs could be found after 3 days. In contrast, the hydrogels provided sufficient structural support to allow their visualization after 14 days. **Figure 5.7** shows representative micrographs of implanted rADSCs (cytoplasm red and nucleus in blue) within hydrogels at three time points. The stereological quantification calculated from these microscopes showed the rADSCs volume fraction remained at the same level between each time point (**Figure 5.8**). In addition, no labeled rADSCs can be found in the host tissue; in other words, the implanted cells did not infiltrate into the host tissue from the hydrogel dressing.

5.3.4 Inflammatory

Immunohistochemistry assessment by ED-1 (anti-CD68) antibody (Abcam, UK) was used to evaluate the macrophages recruitment at each time point (**Figure 5.9**). It appeared that the hydrogel treatment groups (with or without cells) had higher inflammatory response to macrophages than the ‘no treatment group’ or ‘cell alone’ control treatment groups, but no statistically significant difference was noted between each group (**Figure 5.10**). H&E staining showed that the number of neutrophils surrounding the hydrogels was obviously increased compared with control groups at day 3, but clearly decreased at day 7, which indicated that the hydrogel triggered higher acute inflammatory response than control groups at the early stage of wound healing (**Figure 5.11 & 5.12**). In addition, the counting results for macrophages from immunohistochemistry assessment were higher than H&E analysis in all treatment groups. It might be because the CD68 was also expressed on the surface of other cell type such as monocytes, histiocytes and giant cells.

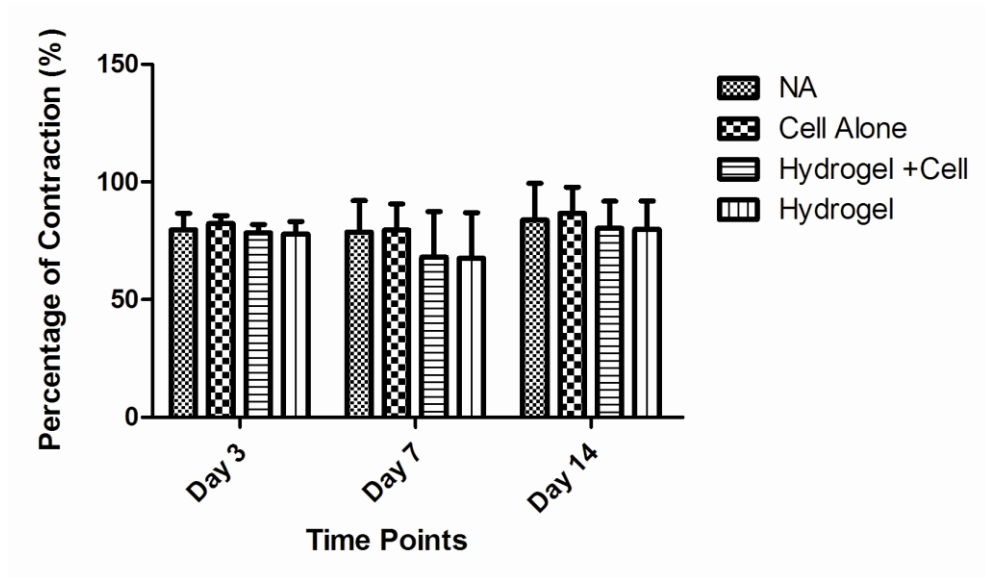


Figure 5.4: Percentage of wound contraction. **Note:** no significant difference between each treatment group at each time point (Two way ANOVA with Tukey’s post analysis method, Mean \pm SD, $n = 7$, $p < 0.05$), but a trend can be found that hydrogel treatment groups (with or without rADSCs) contracted less than other groups at 7 and 14 days.

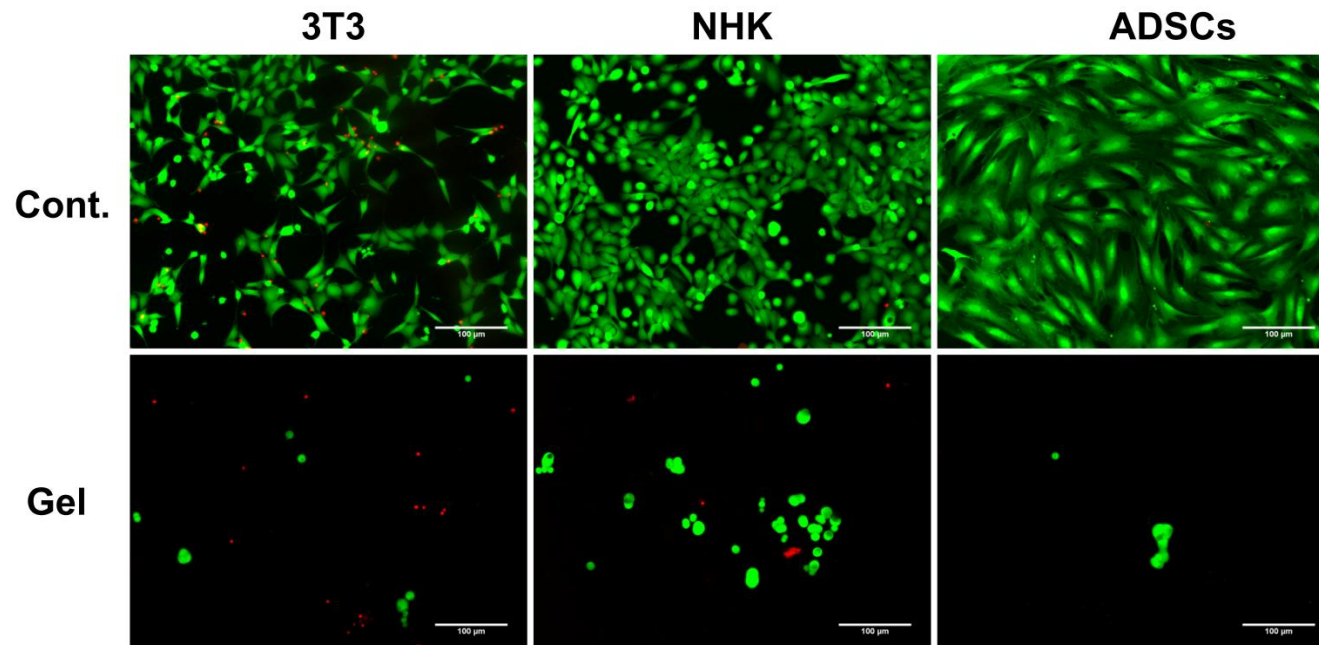


Figure 5.5: *In vitro* 2D cell attachment assessment. Fibroblast (3T3), normal human keratinocytes (NHK) and ADSCs were seeded on the cell culture plate (Cont.) and on the surface of the P-SH-HA hydrogels (Gel) and detected by LIVE/DEAD[®] stain after 48 h. Scale bars in all cases represent 100 µm. **Note:** neither of these cells can attach on the hydrogel surface compared with the cells seeded on tissue culture plates.

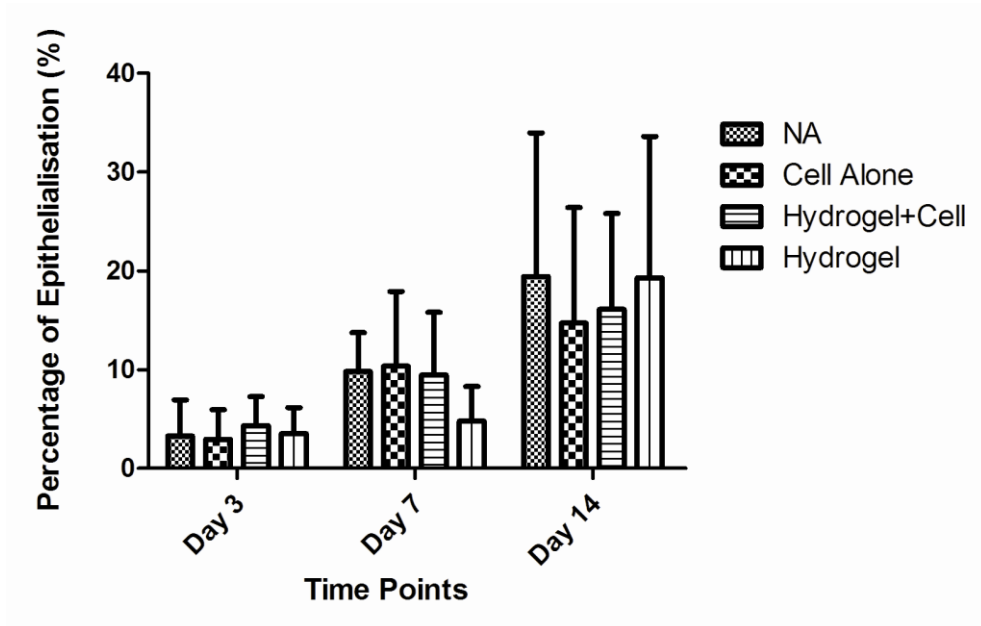


Figure 5.6: Percentage of wound epithelialization. **Note:** no significant difference between each treatment group at each time point (Two way ANOVA with Tukey’s post analysis method, Mean \pm SD, $n = 7$, $p < 0.05$).

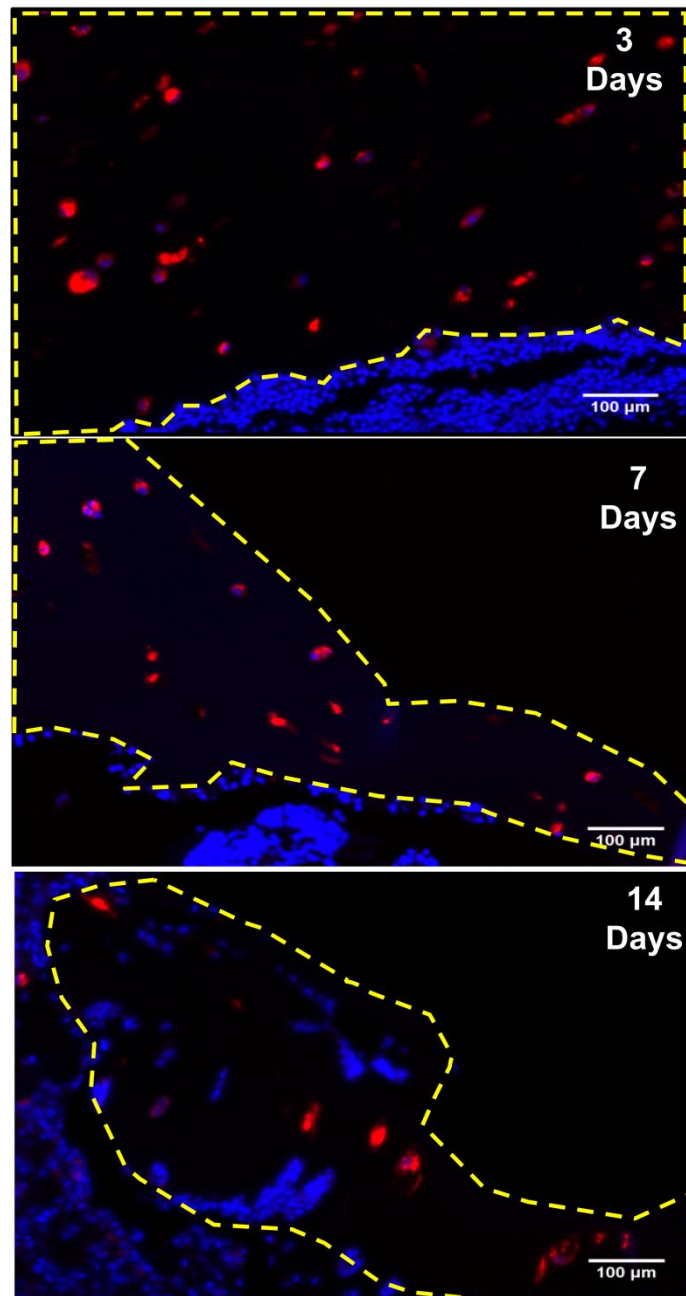


Figure 5.7: Representative fluorescent images of rADSCs embedded hydrogels at 3, 7 and 14 days. Implanted cells were marked with CellTrackerTM CM-Dil (red) counterstained with Hoechst 33258 (blue). The yellow dotted line labeled the hydrogel area above wound bed.

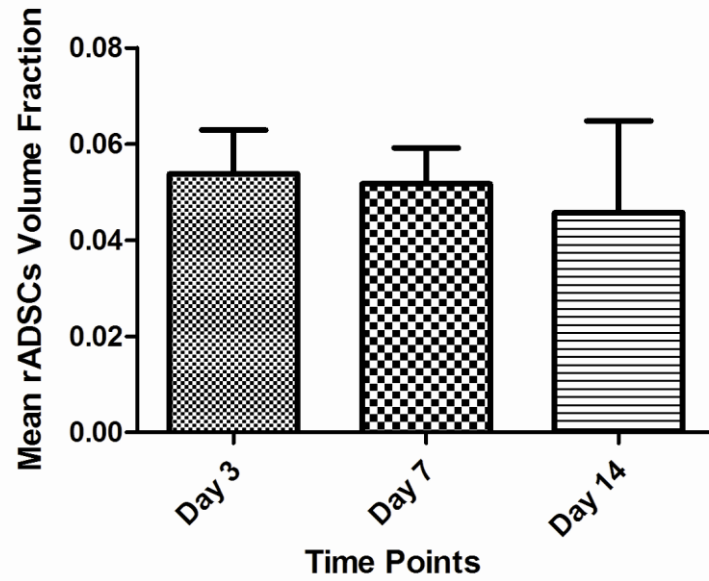


Figure 5.8: The stereological quantification of the volume fraction of implanted rADSCs based on the fluorescent images labelled by CellTrackerTM CM-Dil/Hoechst 33258. **Note:** no significant difference between each time point (Student's t-test, Mean \pm SD, $n = 7$, $p < 0.05$).

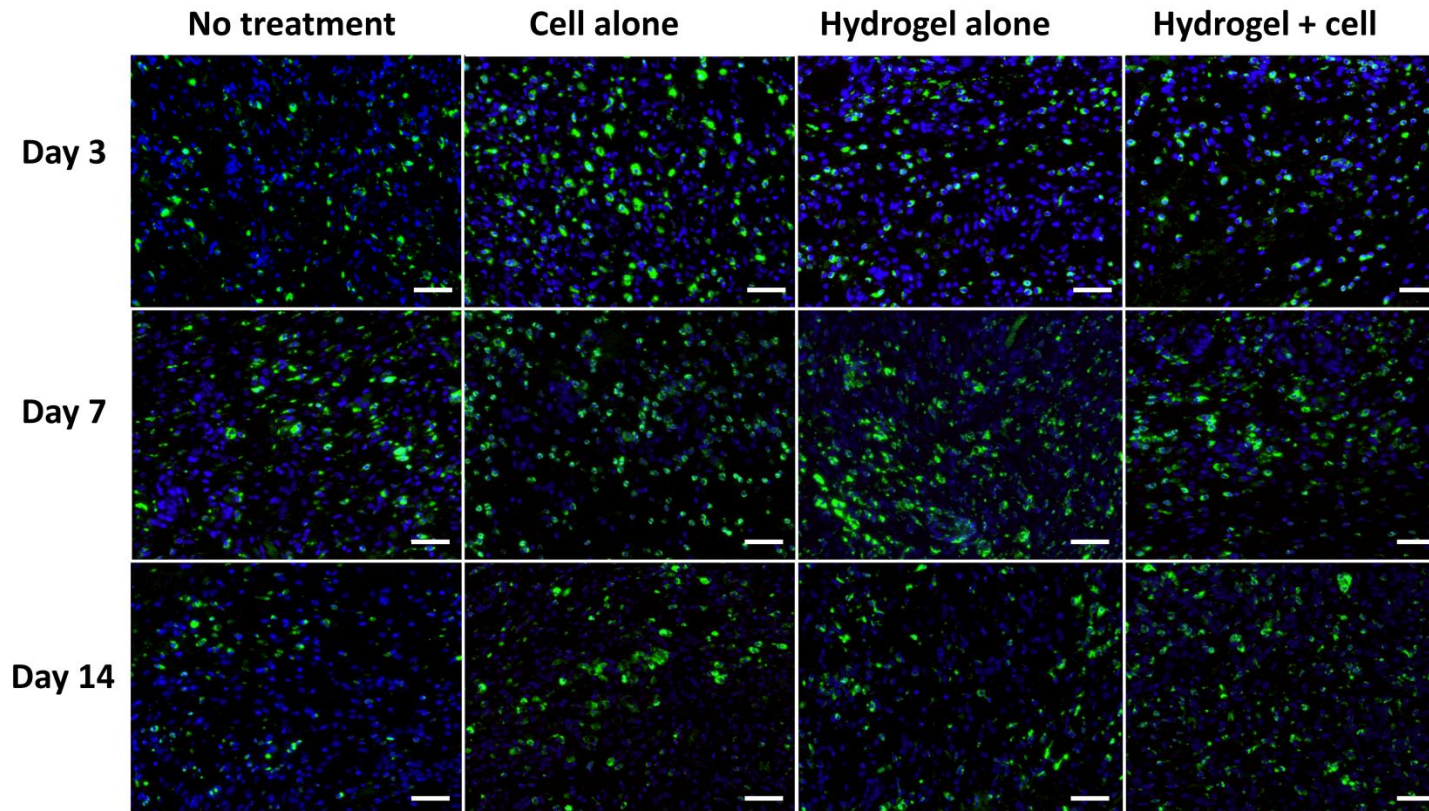


Figure 5.9: Representative fluorescent images of CD68⁺ immunohistochemistry stained macrophages (green) counterstained with Hoechst 33258 (blue) for different treatment groups at 3, 7 and 14 days. Scale bars in all cases represent 50 μ m.

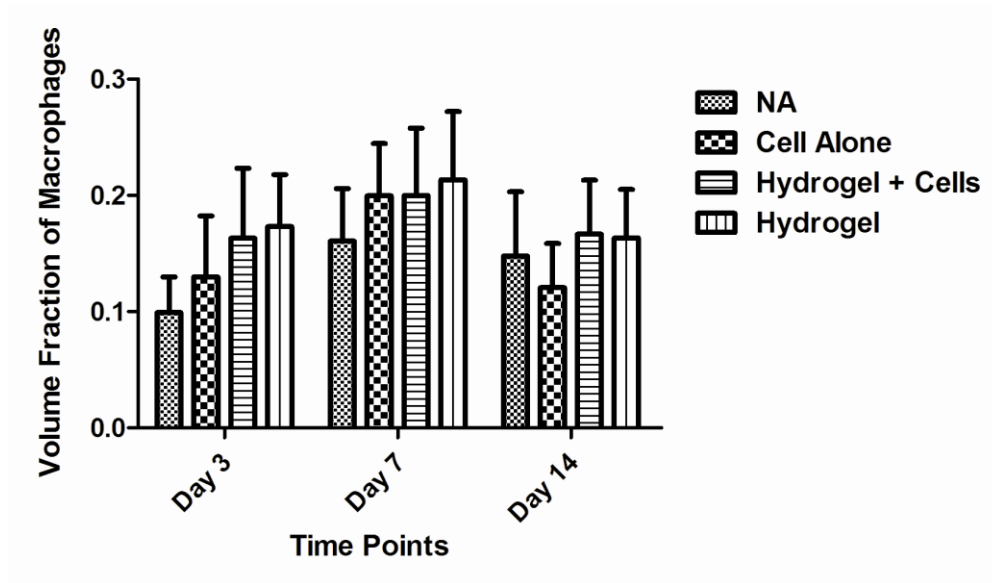


Figure 5.10: Quantification of volume fraction of macrophages at 3, 7 and 14 days based on the immunohistochemistry images (CD68⁺/Hoechst 33258). **Note:** no significant difference between each treatment group at each time point (Two way ANOVA with Tukey’s post analysis method, Mean \pm SD, n = 7, $p < 0.05$).

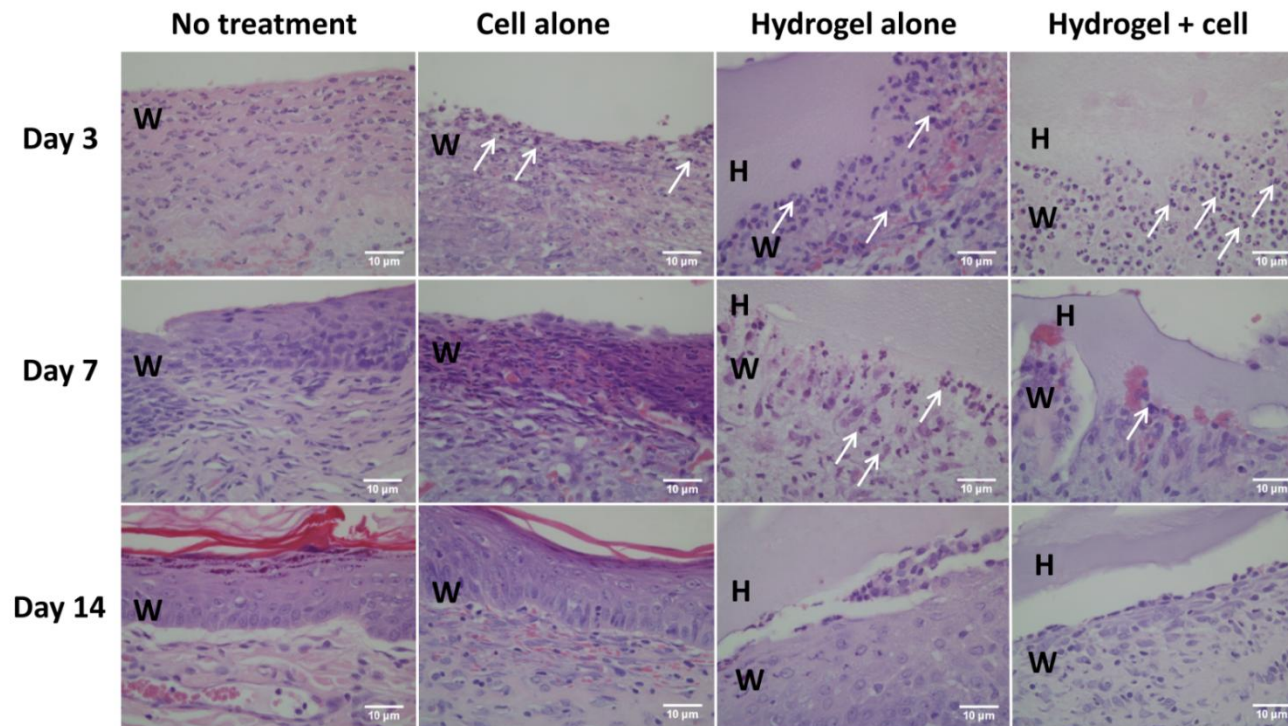


Figure 5.11: Representative images (x 600 magnification) of H&E stained tissue slides at 3, 7 and 14 days. W: skin tissue at wound area; H: hydrogel. The arrows highlight the neutrophils cells. Scale bars in all cases represent 10 μm. **Note:** the neutrophils surrounding the hydrogels was obviously more than control groups at day 3, but clearly decreased at day 7, which indicated that the hydrogel triggered higher acute inflammatory response than control groups at the early stage of wound healing.

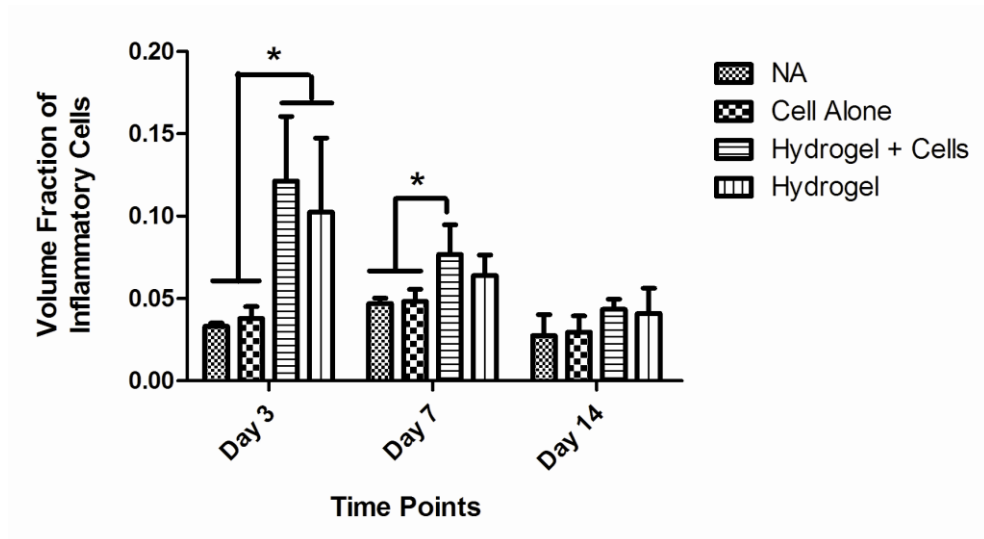


Figure 5.12: Volume fraction of total inflammatory cells at days 3, 7 and 14. Counted inflammatory cells included neutrophils, eosinophils, lymphocytes and macrophages. **Note:** because of the increased neutrophils, total inflammatory cells in Hydrogel with/without cells groups are significantly higher than control groups at day 3 and day 7 (Two way ANOVA with Tukey's post analysis method, Mean \pm SD, n = 7, $p < 0.05$).

5.3.5 Angiogenesis

Neoangiogenesis of the wound was determined by collagen IV immunohistochemical staining. No new vasculature could be found at day 3 in all the groups. The angiogenic effects of different treatments at 7 and 14 days (**Figure 5.13**) were analyzed both qualitatively and quantitatively. By visually scanning hydrogel treatment groups with or without cells showed obviously more vasculature than control groups. Furthermore, quantitative results showed that both surface density and length density of “hydrogel + cells” group was significantly higher than control groups at 14 days (**Figure 5.14 & 5.15**). This trend was also found for the parameters of total surface area (**Figure 5.16**) and total length (**Figure 5.17**) of the new vasculature; however it did not show statistically significant difference because of the high standard deviation due to the confounding roughness of wound area measurement.

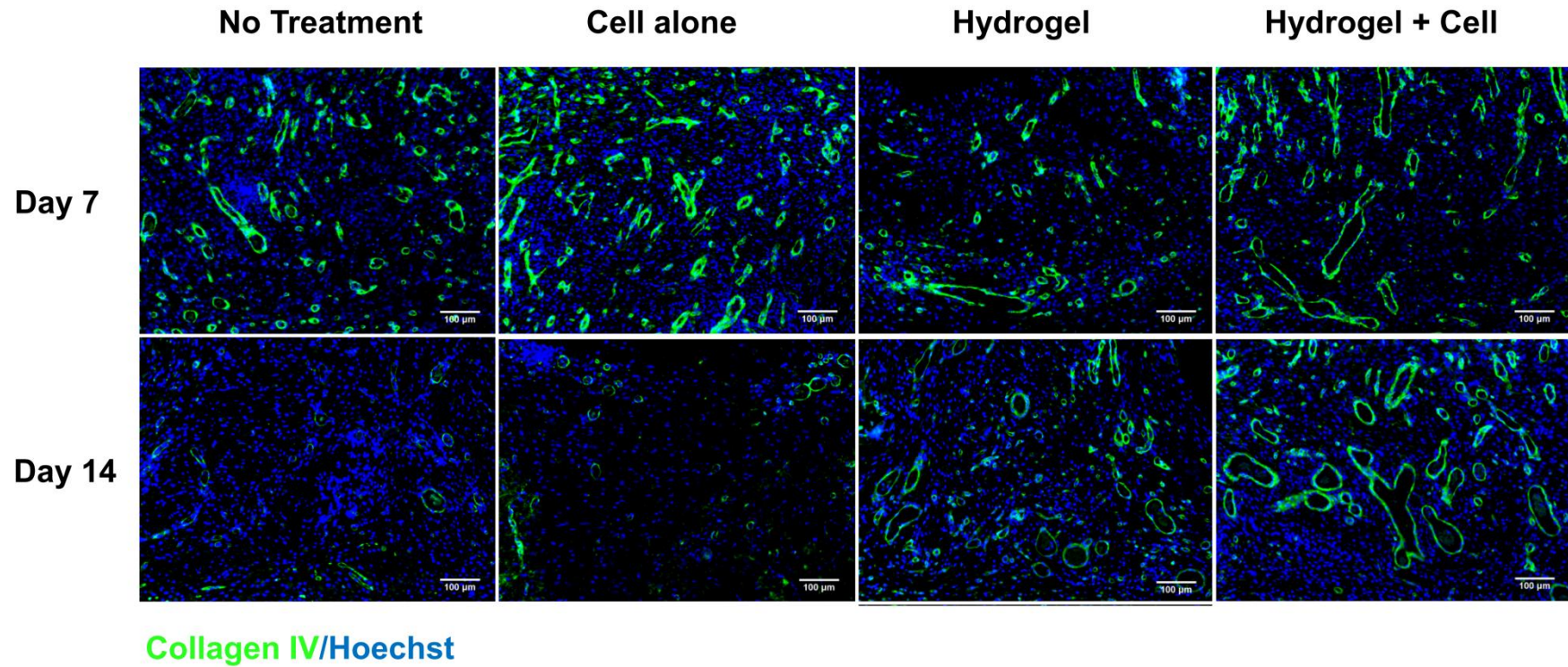


Figure 5.13: Representative fluorescent images of Collagen type IV immunohistochemical staining (green) counterstained with Hoechst 33258 (blue) for different treatment groups at each time point. Note: the angiogenesis with hydrogel treatment groups (with or without cells) were obvious increased at 14 days compared with control groups.

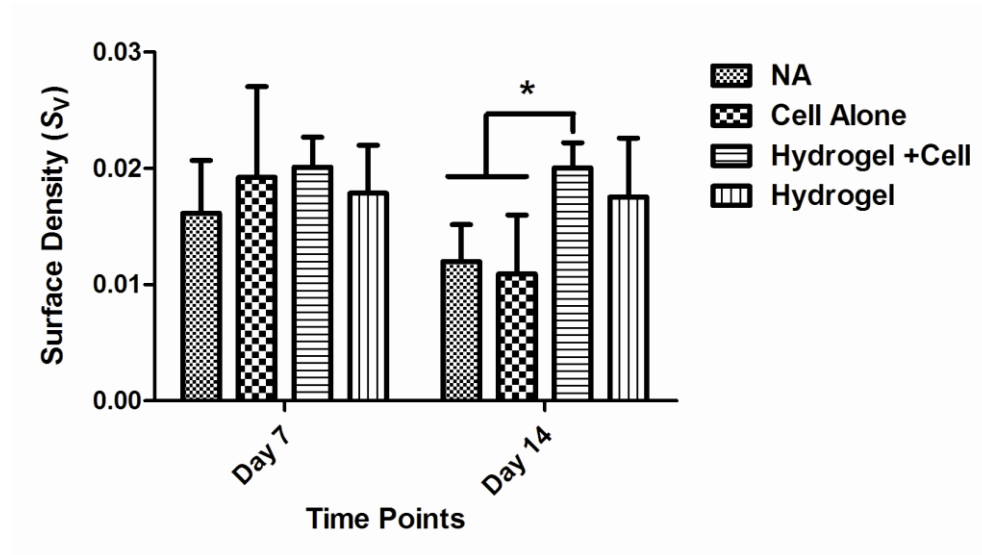


Figure 5.14: Vascular surface density at 3, 7 and 14 days. **Note:** Hydrogel + rADSCs group shows significant higher than control groups (One way ANOVA with Tukey's post analysis method, Mean \pm SD, $n = 7$, $p < 0.05$).

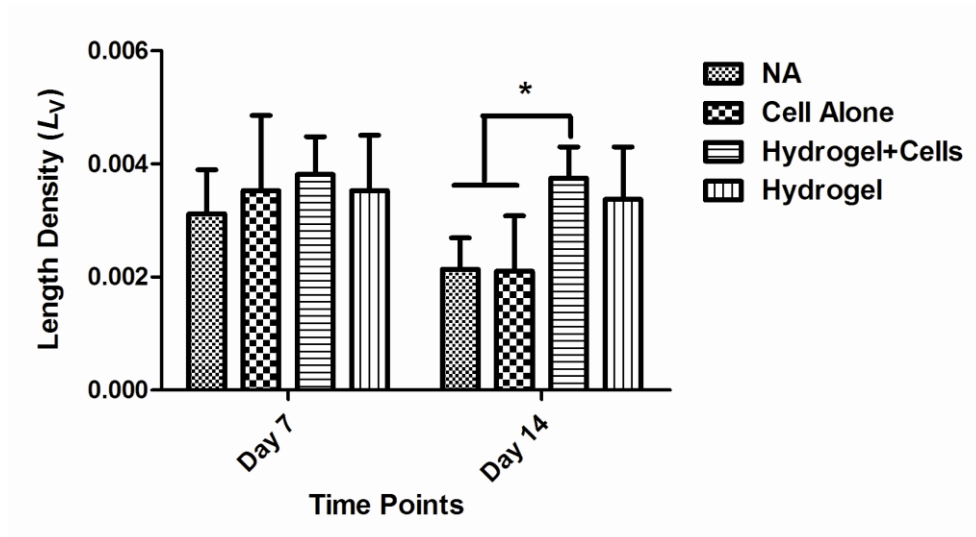


Figure 5.15: Vascular length density at 3, 7 and 14 days. **Note:** Hydrogel + rADSCs group shows significant higher than control groups (One way ANOVA with Tukey's post analysis method, Mean \pm SD, $n = 7$, $p < 0.05$).

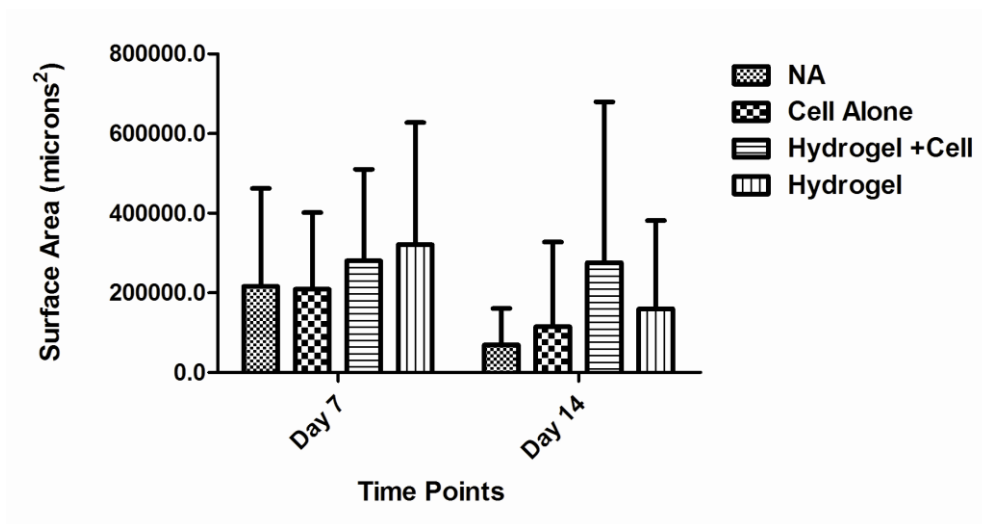


Figure 5.16: Total vascular surface area at 3, 7 and 14 days. **Note:** no significant difference between each treatment group at each time point (One way ANOVA with Tukey’s post analysis method, Mean \pm SD, n = 7, $p < 0.05$).

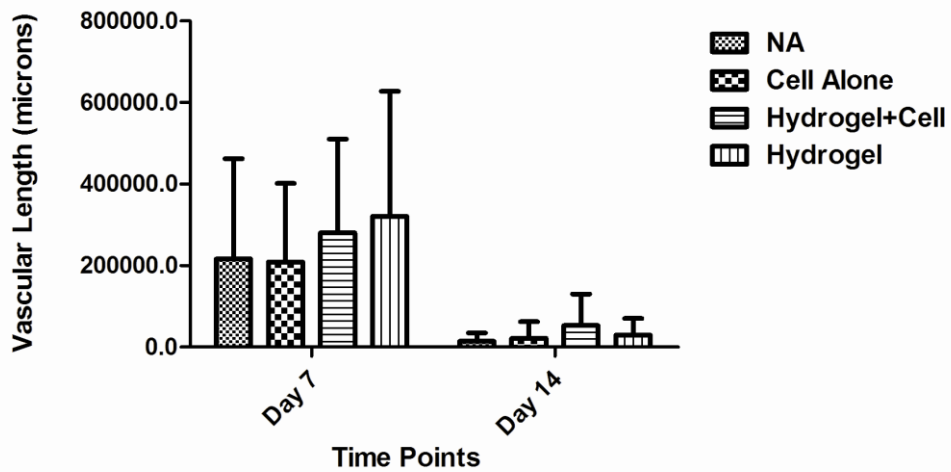


Figure 5.17: Total vascular length at at 3, 7 and 14 days. **Note:** no significant difference between each treatment group at each time point (One way ANOVA with Tukey’s post analysis method, Mean \pm SD, n = 7, $p < 0.05$).

5.4 Discussion

Current commercially available hydrogel wound dressings maintain the moist wound environment, provide autolytic debridement and provide pain reliever, however the effect on accelerating healing process by using these dressing are limited⁸⁻¹⁰. In contrast, the promising healing influence of cell therapy (especially stem cell therapy), such as enhanced angiogenesis, increased epithelialization and accelerated regenerating process has been only proved in last few years¹²⁻²⁰. In this study, we attempted to introduce the therapeutic functionality of ADSCs into an *in-situ* formed hydrogel system as a temporary bioactive dressing for wound healing.

The *in-situ* cross-linkable hydrogel system was developed previously by our group based on a thermoresponsive hyperbranched copolymer and ECM based cross-linker of thiolated HA²⁹. Here, cell behavior of encapsulated rADSCs including viability, proliferation and metabolic activity were further studied. For the purpose of designing a bioactive wound dressing which can be easily removed from the wound bed without causing further pain and trauma, host cells must not infiltrate the dressing and join implanted cells. Thus a non-degradable PEG-based polymer and a modified HA with slow degradability were used; meanwhile the hydrophilic PEG/HA-based hydrogel structure prevents the adherence of the dressing to host tissue.

One of the potential benefits of this non-degradable dressing system is preventing the wound contraction that may cause deforming scars, painful contractures and mobility dysfunction in the cases of large deep wounds such as extensive burns^{32, 33}. Although wound contraction is a complex native healing process which involves different cell phenotype (e.g. myofibroblast) and regulators such as transforming growth factor beta 1 (TGF- β 1)³⁴, the hydrogels seem to physically prevent contraction in this study. At the same time, however, the wound closure rate was also reduced by this effect in hydrogel treatment groups. As the concept of temporary dressing, we hypothesized that the keratinocytes would migrate from the wound edge to the center and form a regenerated epithelial layer underneath of the hydrogel. However, in these experimental settings re-epithelialization

only occurred at the edge of the wound, which did not form a closed epithelia layer after 14 days. We think this was mainly because the keratinocytes cannot attach and migrate along the hydrogel surface. To examine this hypothesis, a 2D *in vitro* cell attachment assessment was performed by seeding keratinocytes, fibroblasts and rADSCs on the surface of the hydrogels and detected by LIVE/DEAD[®] stain after 48 h. It was found that neither of these cells can attach on the hydrogel surface compared with seeding on tissue culture plates (**Figure 5.5**). Furthermore, the rodent skin model is not an ideal model to study the re-epithelialization ratio due to its remarkable contractive behavior. However, to overcome the attachment issue and further promote the epithelialization, an extra thin layer of acellular biomaterials such as fibrinogen or type I collagen can be used underneath the hydrogel.

The inflammatory phase is known as a complex stage during the wound healing process³⁵. Generally, inflammation occurs within 24 h after wound injury and neutrophils are firstly recruited from the circulating blood to clean the bacteria and also produce pro-inflammatory cytokines that activate the fibroblasts and macrophages^{36, 37}. Induced macrophages express a number of important cytokines and produce nitric oxide which play the important beneficial roles at the early stage of the healing process such as regulation of the migration and proliferation of epidermal cells, organization of new tissue connection, and promotion of angiogenesis³⁸⁻⁴³. In the present study, inflammatory response caused by the hydrogel system was evaluated by immunohistochemistry staining of macrophages by ED-1 (anti-CD 68) antibody. The volume fraction of macrophages in every treatment group increased at day 7 and decreased at day 14, which is consistent to normal wound healing process. A trend can be noted that the volume fraction of macrophages in the hydrogel treatment group (with or without cells) were higher than control groups at 3 days (**Figure 5.10**). Similar trend were found in H&E histological assessment, in which hydrogels triggered more neutrophils than control groups at day 3, however, this response significantly decreased after 7 days (**Figure 5.11 & 5.12**).

Angiogenesis, also known as neovascularization, plays essential role for providing nutrients and oxygen during the wound healing process⁴⁴. Lack of neovascularization is considered as one of the main reasons impairing the healing in chronic wounds^{45, 46}. Recent studies have shown that applying ADSCs to wounds enhanced the angiogenesis and promoted wound healing, not only via differentiating into various cell types, but also by paracrine secreting effects^{22, 26, 47-51}. In this study, neovascularization was enhanced by the cell embedded hydrogel treatment, which showed a statistically significant increase of the surface and length density of vasculature comparing with the control groups (no treatment and cell alone groups) at 14 days. The increased acute inflammatory response triggered by hydrogel materials may cause an enhanced angiogenesis, while the cell embedded hydrogel treatment showed higher angiogenesis than hydrogel alone group (**Figure 5.14 & 5.15**). The implanted rADSCs were not found to infiltrate into the host tissue, therefore the enhanced angiogenesis could result from paracrine effects of the rADSCs. On the other hand, small molecular HA oligosaccharides have been reported to promote angiogenesis by regulating the endothelial cells⁵². In our dressing system, thiolated HA was cross-linked with a non-degradable copolymer providing a relatively stable structure which degrade slowly in at least one month^{53, 54}. Thus, the increased neovascularization in hydrogel alone group also might be due to the un-reacted HA-SH molecules and their byproducts.

5.5 Conclusion

The injectable P-SH-HA hydrogel system based on a PEG based multi-functional hyperbranched copolymer and thiol modified HA can be easily handled and manipulated to support the rADSCs growth and maintain their viability *in vivo*. In combination with rat extracted ADSCs, this hydrogel system prevented the wound contraction and significantly enhanced the angiogenesis, which reflects the potential of this system to be used as a temporary *in-situ* formed bioactive hydrogel dressing for wound healing purpose.

5.6 References

1. Lay-Flurrie, K., The properties of hydrogel dressings and their impact on wound healing. *Professional Nurse (London, England)* 2004, 19, (5), 269-73.
2. Boateng, J. S.; Matthews, K. H.; Stevens, H. N. E.; Eccleston, G. M., Wound healing dressings and drug delivery systems: A review. *Journal of Pharmaceutical Sciences* 2008, 97, (8), 2892-2923.
3. Sibbald, R. G.; Orsted, H.; Schultz, G. S.; Coutts, P.; Keast, D.; International wound bed preparation advisory; Canadian chronic wound advisory, preparing the wound bed 2003: focus on infection and inflammation. *Ostomy/Wound Management* 2003, 49, (11), 23-51.
4. Martin, P., Wound healing - Aiming for perfect skin regeneration. *Science* 1997, 276, (5309), 75-81.
5. Mathus-Vliegen, E. M. H., Old age, malnutrition, and pressure sores: An ill-fated alliance. *Journals of Gerontology Series A-Biological Sciences and Medical Sciences* 2004, 59, (4), 355-360.
6. Freiman, A.; Bird, G.; Metelitsa, A. I.; Barankin, B.; Lauzon, G. J., Cutaneous effects of smoking. *Journal of Cutaneous Medicine and Surgery* 2004, 8, (6), 415-423.
7. Thomas, D. R., Improving outcome of pressure ulcers with nutritional interventions: A review of the evidence. *Nutrition* 2001, 17, (2), 121-125.
8. Hampton, S., A small study in healing rates and symptom control using a new sheet hydrogel dressing. *Journal of Wound Care* 2004, 13, (7), 297-300.
9. H., H., Pain relief. *Nurse Times* 2001, 97, (28), 63-66.
10. Eisenbud, D.; Hunter, H.; Kessler, L.; Zulkowski, K., Hydrogel wound dressings: where do we stand in 2003? *Ostomy/Wound Management* 2003, 49, (10), 52-57.
11. Fonder, M. A.; Lazarus, G. S.; Cowan, D. A.; Aronson-Cook, B.; Kohli, A. R.; Mamelak, A. J., Treating the chronic wound: A practical approach to the care of nonhealing wounds and wound care dressings. *Journal of the American Academy of Dermatology* 2008, 58, (2), 185-206.
12. Fathke, C.; Wilson, L.; Hutter, J.; Kapoor, V.; Smith, A.; Hocking, A.; Isik, F., Contribution of bone marrow-derived cells to skin: Collagen deposition and wound repair. *Stem Cells* 2004, 22, (5), 812-822.
13. Fu, X.; Li, H., Mesenchymal stem cells and skin wound repair and regeneration: possibilities and questions. *Cell and Tissue Research* 2009, 335, (2), 317-321.
14. Gillitzer, R.; Goebeler, M., Chemokines in cutaneous wound healing. *Journal of Leukocyte Biology* 2001, 69, (4), 513-521.

15. Kolf, C. M.; Cho, E.; Tuan, R. S., Mesenchymal stromal cells - Biology of adult mesenchymal stem cells: regulation of niche, self-renewal and differentiation. *Arthritis Research & Therapy* 2007, 9, (1) 204.
16. Wu, Y.; Wang, J.; Scott, P. G.; Tredget, E. E., Bone marrow-derived stem cells in wound healing: a review. *Wound Repair and Regeneration* 2007, 15, S18-S26.
17. Lu, F.; Mizuno, H.; Uysal, C. A.; Cai, X.; Ogawa, R.; Hyakusoku, H., Improved viability of random pattern skin flaps through the use of adipose-derived stem cells. *Plastic and Reconstructive Surgery* 2008, 121, (1), 50-58.
18. Moon, M. H.; Kim, S. Y.; Kim, Y. J.; Kim, S. J.; Lee, J. B.; Bae, Y. C.; Sung, S. M.; Jung, J. S., Human adipose tissue-derived mesenchymal stem cells improve postnatal neovascularization in a mouse model of hindlimb ischemia. *Cellular Physiology and Biochemistry* 2006, 17, (5-6), 279-290.
19. Rehman, J.; Traktuev, D.; Li, J. L.; Merfeld-Clauss, S.; Temm-Grove, C. J.; Bovenkerk, J. E.; Pell, C. L.; Johnstone, B. H.; Considine, R. V.; March, K. L., Secretion of angiogenic and antiapoptotic factors by human adipose stromal cells. *Circulation* 2004, 109, (10), 1292-1298.
20. Song, Y.-H.; Gehmert, S.; Sadat, S.; Pinkernell, K.; Bai, X.; Matthias, N.; Alt, E., VEGF is critical for spontaneous differentiation of stem cells into cardiomyocytes. *Biochemical and Biophysical Research Communications* 2007, 354, (4), 999-1003.
21. Branski, L. K.; Gauglitz, G. G.; Herndon, D. N.; Jeschke, M. G., A review of gene and stem cell therapy in cutaneous wound healing. *Burns* 2009, 35, (2), 171-180.
22. Cherubino, M.; Rubin, J. P.; Miljkovic, N.; Kelmendi-Doko, A.; Marra, K. G., Adipose-derived stem cells for wound healing applications. *Annals of Plastic Surgery* 2011, 66, (2), 210-215.
23. Cha, J.; Falanga, V., Stem cells in cutaneous wound healing. *Clinics in Dermatology* 2007, 25, (1), 73-78.
24. Wu, Y.; Chen, L.; Scott, P. G.; Tredget, E. E., Mesenchymal stem cells enhance wound healing through differentiation and angiogenesis. *Stem Cells* 2007, 25, (10), 2648-2659.
25. Chen, L.; Tredget, E.E.; Wu, P.Y.; Wu, Y., Paracrine factors of mesenchymal stem cells recruit macrophages and endothelial lineage cells and enhance wound healing. *Plos One* 2008, 3, (4) e1886.
26. Kim, W.S.; Park, B.S.; Sung, J.H.; Yang, J.M.; Park, S.B.; Kwak, S.J.; Park, J.S., Wound healing effect of adipose-derived stem cells: A critical role of secretory factors on human dermal fibroblasts. *Journal of Dermatological Science* 2007, 48, (1), 15-24.
27. Kern, S.; Eichler, H.; Stoeve, J.; Kluter, H.; Bieback, K., Comparative analysis of mesenchymal stem cells from bone marrow, umbilical cord blood, or adipose tissue. *Stem Cells* 2006, 24, (5), 1294-1301.

28. Gonda, K.; Shigeura, T.; Sato, T.; Matsumoto, D.; Suga, H.; Inoue, K.; Aoi, N.; Kato, H.; Sato, K.; Murase, S.; Koshima, I.; Yoshimura, K., Preserved proliferative capacity and multipotency of human adipose-derived stem cells after long-term cryopreservation. *Plastic and Reconstructive Surgery* 2008, 121, (2), 401-410.
29. Dong, Y.; Saeed, A. O.; Hassan, W.; Keigher, C.; Zheng, Y.; Tai, H.; Pandit, A.; Wang, W., "One-step" preparation of thiol-ene clickable PEG-based thermoresponsive hyperbranched copolymer for in situ crosslinking hybrid hydrogel. *Macromolecular Rapid Communications* 2012, 33, (2), 120-126.
30. Dong, Y.; Hassan, W.; Zheng, Y.; Saeed, A. O.; Cao, H.; Tai, H.; Pandit, A.; Wang, W., Thermoresponsive hyperbranched copolymer with multi acrylate functionality for in situ cross-linkable hyaluronic acid composite semi-IPN hydrogel. *Journal of Material Science: Material Medicine* 2012, 23, (1), 25-35.
31. Garcia, Y.; Wilkins, B.; Collighan, R. J.; Griffin, M.; Pandit, A., Towards development of a dermal rudiment for enhanced wound healing response. *Biomaterials* 2008, 29, (7), 857-868.
32. Billingham, R. E.; Medawar, P. B., Contracture and intussusceptive growth in the healing of extensile wounds in mammalian skin. *Journal of Anatomy* 1955, 89, (1), 114-123.
33. Chapman, T. T., Burn scar and contracture management. *Journal of Trauma-Injury Infection and Critical Care* 2007, 62, (6), S8-S8.
34. Gabbiani, G., The myofibroblast in wound healing and fibrocontractive diseases. *Journal of Pathology* 2003, 200, (4), 500-503.
35. Martin, P.; Leibovich, S. J., Inflammatory cells during wound, repair: the good, the bad and the ugly. *Trends in Cell Biology* 2005, 15, (11), 599-607.
36. Hubner, G.; Brauchle, M.; Smola, H.; Madlener, M.; Fassler, R.; Werner, S., Differential regulation of pro-inflammatory cytokines during wound healing in normal and glucocorticoid-treated mice. *Cytokine* 1996, 8, (7), 548-556.
37. Waldrop J, D. D., Wound-Healing physiology. In *Acute and Chronic Wounds: Nursing Management*, Ed 2 ed.; RA, B., Ed. St Louis: Mosby, 1991; 17-39.
38. Amadeu, T. P.; Costa, A. M. A., Nitric oxide synthesis inhibition alters rat cutaneous wound healing. *Journal of Cutaneous Pathology* 2006, 33, (7), 465-473.
39. Dhaunsi, G. S.; Ozand, P. T., Nitric oxide promotes mitogen-induced DNA synthesis in human dermal fibroblasts through cGMP. *Clinical and Experimental Pharmacology and Physiology* 2004, 31, (1-2), 46-49.
40. Haas, A., Wound healing. *Dermatology Nursing* 1995, 7, 28-34.

41. Leibovich, S. J.; Ross, R., Role of macrophage in wound repair - Study with hydrocortisone and antimacrophage serum. *American Journal of Pathology* 1975, 78, (1), 71-99.
42. Rappolee, D. A.; Mark, D.; Banda, M. J.; Werb, Z., Wound macrophages express TGF- α and other growth-factors in vivo - Analysis by messenger-RNA phenotyping. *Science* 1988, 241, 708-712.
43. Schaffer, M. R.; Tantry, U.; Gross, S. S.; Wasserkrug, H. L.; Barbul, A., Nitric oxide regulates wound healing. *Journal of Surgical Research* 1996, 63, (1), 237-240.
44. Li, J.; Zhang, Y. P.; Kirsner, R. S., Angiogenesis in wound repair: Angiogenic growth factors and the extracellular matrix. *Microscopy Research and Technique* 2003, 60, (1), 107-114.
45. Guo, S. D., L.A., Factors Affecting Wound Healing. *Journal of Dental Research* 2010, 89, (3), 219-229.
46. Werner, S.; Grose, R., Regulation of wound healing by growth factors and cytokines. *Physiological Reviews* 2003, 83, (3), 835-870.
47. Altman, A. M.; Yan, Y.; Matthias, N.; Bai, X.; Rios, C.; Mathur, A. B.; Song, Y.-H.; Alt, E. U., IFATS collection: Human adipose-derived stem cells seeded on a silk fibroin-chitosan scaffold enhance wound repair in a murine soft tissue injury model. *Stem Cells* 2009, 27, (1), 250-258.
48. Ebrahimian, T. G.; Pouzoulet, F.; Squiban, C.; Buard, V.; Andre, M.; Cousin, B.; Gourmelon, P.; Benderitter, M.; Casteilla, L.; Tamarat, R., Cell therapy based on adipose tissue-derived stromal cells promotes physiological and pathological wound healing. *Arteriosclerosis Thrombosis and Vascular Biology* 2009, 29, (4), 503-510.
49. Nie, C.; Yang, D.; Morris, S. F., Local delivery of adipose-derived stem cells via acellular dermal matrix as a scaffold: A new promising strategy to accelerate wound healing. *Medical Hypotheses* 2009, 72, (6), 679-682.
50. Trottier, V.; Marceau-Fortier, G.; Germain, L.; Vincent, C.; Fradette, J., IFATS collection: Using human adipose-derived stem/stromal cells for the production of new skin substitutes. *Stem Cells* 2008, 26, (10), 2713-2723.
51. Amos, P. J.; Kapur, S. K.; Stapor, P. C.; Shang, H.; Bekiranov, S.; Khurgel, M.; Rodeheaver, G. T.; Peirce, S. M.; Katz, A. J., Human adipose-derived stromal cells accelerate diabetic wound healing: Impact of cell formulation and delivery. *Tissue Engineering Part A* 2010, 16, (5), 1595-1606.
52. Chen, W. Y.; Abatangelo, G., Functions of hyaluronan in wound repair. *Wound Repair and Regeneration* 1999, 7, (2), 79-89.
53. Shu, X. Z.; Liu, Y. C.; Palumbo, F. S.; Lu, Y.; Prestwich, G. D., In situ crosslinkable hyaluronan hydrogels for tissue engineering. *Biomaterials* 2004, 25, (7-8), 1339-1348.
54. Necas, J.; Bartosikova, L.; Brauner, P.; Kolar, J., Hyaluronic acid (hyaluronan): a review. *Veterinarni Medicina* 2008, 53, (8), 397-411.

Chapter Six

Summary and Future Directions

6.1 Introduction

Wound healing, especially chronic wound healing, has become a major clinical problem all over the world. Among all the treatments for wound healing, wound dressings are the main management and therapeutic approaches for both acute and chronic wounds. However, although significant progress has been made in the development of modern wound dressings in last few years, there are still restrictions to stimulating the healing process. As an alternative to existing approaches, tissue engineering tools with stem cells therapy have been widely used for wound healing applications and showed promising therapeutic effects. Therefore, ideally, the next step is to develop a dressing with specific therapeutic functions such as delivering therapeutic agents (e.g. growth factors or stem cells) to prevent unwanted inflammatory reactions, provide an ideal wound healing environment and promote the healing process. To this end, the overall goal of this research was to develop an *in-situ* cross-linkable hydrogel cell delivery system which could easily encapsulate and support ADSCs growth and proliferation, with the potential use as a bioactive temporary hydrogel dressing for wound healing applications.

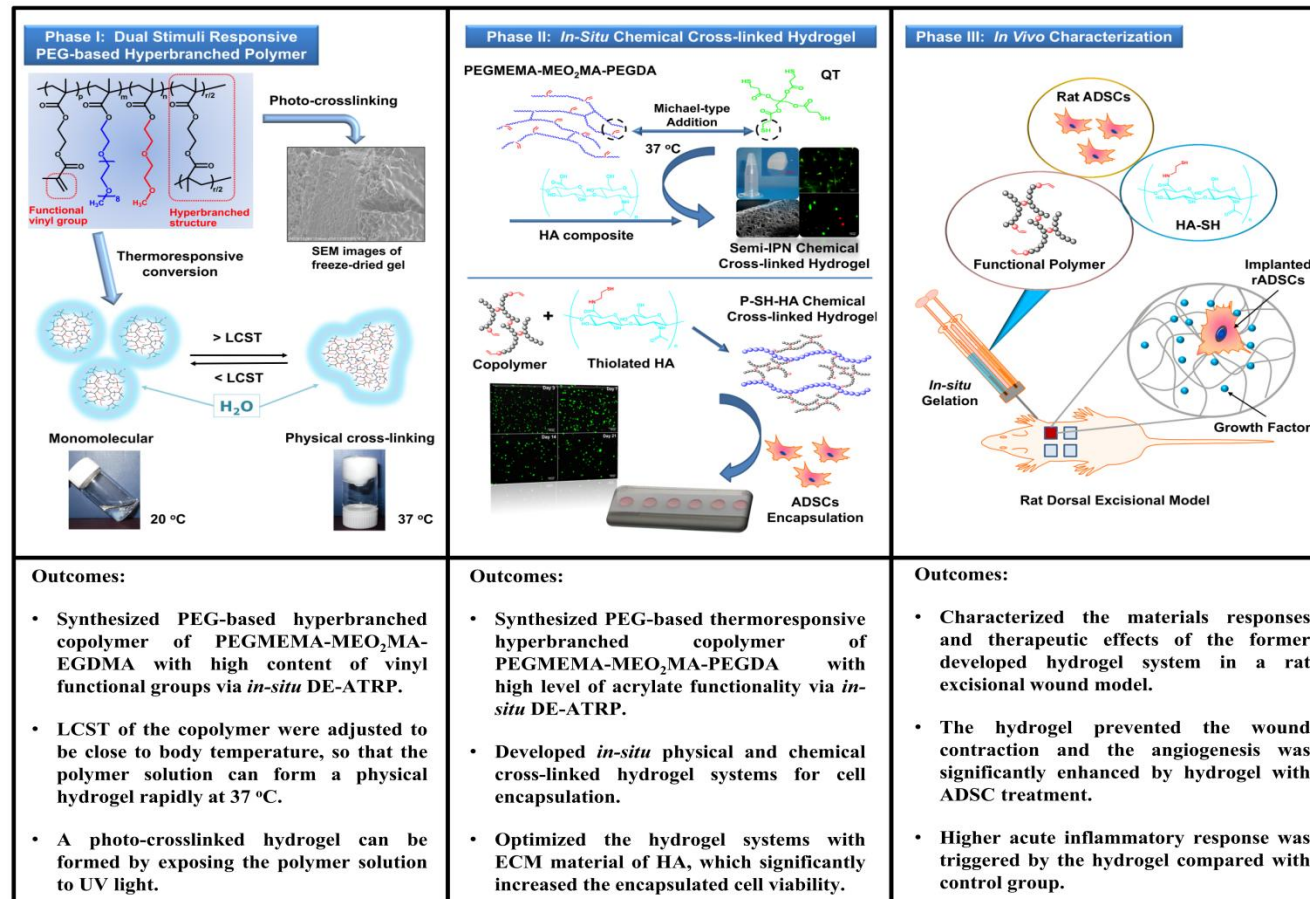


Figure 6.1: Summary of the main outcomes from each phase of this thesis.

6.2 Summary

6.2.1 Phase I: Multifunctional Polymer Synthesis

The objective of the first phase of this research was to synthesize and optimize a PEG-based multifunctional hyperbranched copolymer with thermoresponsive and *in-situ* cross-linkable properties.

PEG-based thermoresponsive copolymer with “graft” structure had been reported by Lutz and colleagues¹⁻⁴, however it is difficult to further functionalize this polymer with cross-linkable property. In this study, as described in Chapter 2, a novel polymerization method, *in-situ* DE-ATRP approach was developed, in which the extra amounts of Cu^{II} species were retained throughout the polymerization, effectively “deactivated” the reaction, leading to the slow chain growth and delayed gelation. By using this approach, we were able to introduce a high degree (up to 10 % molar ratio of total feed monomers) of divinyl monomer (EGDMA) into the copolymer without gelation, and a series of hyperbranched copolymer of PEGMEMA-MEO₂MA-EGDMA was successfully achieved via a one-step reaction. By adjusting the composition of the hydrophilic and hydrophobic PEG-based monomers, the phase change temperature (LCST) of the copolymers can be controlled around body temperature (from 24 to 38 °C). The polymer solution can rapidly form a physical hydrogel at 37 °C.

In addition, the polymerization speed could be sensitively affected by varying the amount of the reducing agent of L-ascorbic acid (AA) in DE-ATRP. The slight increase of AA could remarkably speed up the reaction without changing the molecular structure of the copolymer. The results of GPC, ¹H NMR and FTIR confirmed the hyperbranched polymer structure (around 10 mol % branching degree) with vinyl functionality (around 6 mol % double bond content). These retained vinyl functional groups provide the copolymer photo-crosslinkable behavior under UV exposure, and the porous structure of the photo-crosslinked gels was assessed by SEM imaging, which is an important parameter for cell encapsulation and growth inside the hydrogel.

Furthermore, alamarBlue[®] method was utilized to assess the cytotoxicity of the copolymer of PEGMEMA-MEO₂MA-EGDMA to 3T3 mouse fibroblast cells. The results indicated that the copolymer did not affect the cellular metabolism at the concentration up to 1 mg/ml after four days.

However, this copolymer can only be used for photo-crosslinking hydrogels. The activity of the methacrylate functional groups on this copolymer is too low to allow for rapid chemical cross-linking at the physiological condition. Some drawbacks limit the applications of the photo-crosslinked systems in clinical such as the extra equipment that is needed in a clinical setting, the dosage and safety concerns of applying UV radiation⁵⁻⁸. Being aware of these limitations, the project in later phases focused on developing the chemical cross-linked hydrogel systems.

6.2.2 Phase II: *In-situ* Chemical Cross-linked Hydrogel Fabrication

The objective of this phase was to optimize the former thermoresponsive hyperbranched copolymer and to fabricate an *in-situ* chemical cross-linked hydrogel system with enhanced mechanical properties, in which ADSCs are easily encapsulated, grow and proliferate. Two different chemical cross-linked hydrogel systems have been developed at this stage as described in Chapter 3 and Chapter 4, which are summarized separately as follows:

6.2.2.1 *Semi-IPN Hydrogel Systems*

A new PEG-based hyperbranched copolymer of PEGMEMA-MEO₂MA-PEGDA was synthesized by *in-situ* DE-ATRP as described in Chapter 3. A high degree (up to 25 % molar ratio of total feed monomers) of di-acrylate monomer of PEGDA, instead of di-methacrylate monomer of EGDMA, was applied in the polymerization to enhance the activity of vinyl functional groups, which provided this copolymer chemical *in-situ* cross-linking property. The NMR analysis suggested that the double bond content of the copolymers was around 12 mol % and branched degree around 16 mol %. Moreover, the thermoresponsive behavior of this copolymer was kept as the PEGMEMA-MEO₂MA-EGDMA which was described in the former phase. The LCST of the copolymers was controlled to remain at around 30 °C by

adjusting the monomer compositions, so that the polymer solution can form a physical hydrogel at 37 °C rapidly.

With this high level of active acrylate-vinyl groups, the copolymers can react readily with a thiol functional cross-linker of QT (equal molar ratio of thiol and vinyl group) via thiol-ene Michael-type addition to form a chemically cross-linked network. The gelation occurred within 10 min at 37 °C and the cross-linked density can be easily adjusted by varying polymer concentration, cross-linker ratio and copolymer vinyl content. The cytotoxicity of the copolymer and QT was tested by alamarBlue[®] assay and neither of them influenced the metabolic activity of 3T3 cells after two-days treatments at concentrations up to 10 mg/ml.

Furthermore, a semi-IPN system was developed by combining ECM biopolymer of HA within the hydrogel to optimize the hydrogel microenvironment for cell seeding and encapsulation purposes. The semi-IPN hydrogel with HA significantly enhanced the hydrogel swelling behavior, provided a large porous three dimensional microenvironment, improved the cell adhesion and viability both in 2D and 3D culture.

Although the viability of embedded cells in the hydrogel was significantly increased by the optimized semi-IPN microenvironment, the survival ratio of the cells was still lower than expected (about 50 % after 6 days), which was due to the high cross-linked density caused by the small molecular cross-linker. Therefore, a modified hybrid hydrogel system was designed that directly using thiolated HA as cross-linker in the following stage.

6.2.2.2 P-SH-HA Hybrid Hydrogel Systems

As described in Chapter 4, HA was modified with thiol groups by reaction of carboxylic acid with cysteamine hydrochloride. The free thiol groups on the thiolated HA (HA-SH) were determined by NMR and Ellman's assay as about 0.2 $\mu\text{mol/mg}$. Chemical cross-linked P-SH-HA hydrogels from the copolymer of PEGMEMA-MEO₂MA-PEGDA and HA-SH formed within 10 min at 37 °C. In addition, physical and mechanical properties of the hydrogels can be adjusted by varying the polymer concentration. For example, a higher concentration of the copolymer solution led to a denser

network, smaller pore size, decreased swelling ratio and enhanced mechanical properties of the hydrogels.

It was found that the free thiol groups on the copolymer were easily oxidized in air. To increase the reproducibility of the studies, a commercially available thiolated HA (HyStem™, Glycosan) was used to replace our own synthesized HA-SH for *in vitro* cell viability studies and *in vivo* study in the next phase. Over 80 % of encapsulated ADSCs cells remained alive in the hydrogels up to three weeks *in vitro*. The non-degradable properties of the hydrogel limited the cell proliferation and metabolic activity after 7 days. However, because the overall aim of this project was to develop a temporary bioactive dressing for wound healing, this limitation can be overcome by regularly dressing changes in further clinical use.

In addition, the secretion profile of ADSCs in this P-SH-HA hydrogel system compared with 2D culture condition was studied via multi-plex ELISA. It was found that inflammatory cytokines of IL-2 and INF- γ reduced after 7 days in 3D hydrogel microenvironment, while remained at the same level for 2D seeded cells; and meantime the anti-inflammatory cytokine of IL-10 in hydrogel seemed higher level than 2D control. Furthermore, the angiogenic growth factors of PlGF, VEGF significantly increased in hydrogel system over time. These results suggest that hADSCs can secrete pro-angiogenic and anti-inflammatory cytokines and growth factors in our P-SH-HA hydrogel system. Therefore, this *in-situ* cross-linked P-SH-HA hydrogel system, in which ADSCs can be easily encapsulated and maintain their viability and secretion level, has been ready for the animal studies in the next phase.

6.2.3 Phase III: *In Vivo* Assessment

The overall aim of this research project is to develop a bioactive wound dressing which can be easily removed from the wound bed without causing further pain and trauma, thus the host cells must not infiltrate the dressing and join implanted cells. It was hypothesized that the non-degradable P-SH-HA hydrogel system (as described in Chapter 4) prepared from the

Summary and Future Directions

hydrophilic PEG/HA-based hydrogel structure can prevent the adherence and infiltration of the host tissue; and meanwhile, in combination with ADSCs, this bioactive hydrogel wound dressing can promote angiogenesis and healing by paracrine effects. The objective of the final phase of this research was to evaluate the cell retention, the inflammatory response to the material, and the wound healing effect of this *in-situ* formed P-SH-HA hydrogel dressing with ADSCs *in vivo*.

As described in Chapter 5, animal study was performed by using a rat dorsal excisional full-thickness wound model with four treatment groups (i.e. no treatment, hydrogel alone, hydrogel + rADSCs and rADSCs alone) and three time points of 3, 7 and 14 days (n = 7 wounds per treatment per time point). Wound closure, wound contraction, re-epithelialization, cell retention, inflammatory response and angiogenesis were studied by imaging, histological and immunohistochemical tools after each time point.

It was found that the contractive ratio of all the treatments were higher than 80 % of original wound size after 14 days. The hydrogels seem to physically prevent the contraction, but no significant difference was observed between different treatment groups because of the high standard deviation due to the confounding roughness of wound length measurement. On the other hand, the wound closure rate was also reduced by this effect in hydrogel treatment groups. At 14 days, the wounds were fully closed with regenerated epithelial layer in 'no treatment' and 'cell alone' treatment groups; while the re-epithelialization only occurred at the edges of the wounds in the hydrogel treatment groups (with or without cells), which can be explained by the inability of the keratinocytes to attach or migrate along the hydrogel surface.

For the *in vivo* cell retention assessment, implanted cells were labeled by CellTrackerTM CM-Dil marker (Invitrogen[®]) which conjugates with the intracellular proteins and reflects the cell survival rate in the hydrogels. Although it was difficult to calculate the accurate survival ratio of implanted cells, we found no significant reduction in the volume fraction of rADSCs retention by stereological analysis after 14 days. In addition, there was no obvious infiltration of the host and implanted cells going in/out of the hydrogels as we expected.

Summary and Future Directions

The inflammatory response caused by the hydrogel system was evaluated by immunohistochemistry staining of macrophages by ED-1 (anti-CD 68) antibody and H&E staining for all of the main inflammatory cells. The volume fraction of macrophages in every treatment group increased at day 7 and decreased at day 14, which is consistent with the normal wound healing process. A trend can be noted that the volume fraction of macrophages in the hydrogel treatment group (with or without cells) was higher than control groups at 3 days. A similar trend was found in H&E histological assessment, in which hydrogels triggered obviously more neutrophils than control groups at day 3, but significantly decreased after 7 days. The angiogenesis was significantly enhanced by hydrogel+ADSCs treatment at 14 days. Although the increased acute inflammatory response triggered by hydrogel materials as described above may also cause the increased angiogenesis, the fact that the cell encapsulated hydrogel treatment showed higher angiogenesis than hydrogel alone group proved the paracrine effect of implanted rADSCs.

6.3 Limitations

One of the major limitations of this study was that the rodent skin model is not an ideal model to study the wound closure and re-epithelialization rate due to its remarkable contractive behavior, and for the purpose of evaluating the effect of this novel hydrogel dressing system to wound healing with the maximum reality, some approaches such as silicone stents which can prevent the skin contraction were not used in this study. Consequently, it was difficult to conclude from the results whether the bioactive dressing system promotes or prevents the epithelialization. However, the non-degradable behavior and the limited cell-adherent properties of this hydrogel dressing seemed to restrict the wound closure and the re-epithelialization processes. To overcome these limitations, several modified approaches could be performed with the polymer and hydrogel system, some of which are discussed in the following section as “future directions”.

Another limitation of the study design is the assessment of cell survival *in vivo*. Although the exact number and concentration of implanted cells was known at day 0, it was hard to compare the results of cell density at each time point with day 0 because the hydrogel on the tissue samples were shrinking during the fixing and tissue processing processes. Therefore, even there was no significant drop on the volume fraction of implanted rADSCs between 3 and 14 days after surgery, it was difficult to tell what the cell survival ratio was against the total implanted cells at each time point. Other advanced living image techniques (e.g. *in vivo* bioluminescence imaging⁹) would be useful for overcoming this limitation in the future. In addition, the implanted stem cell phenotype, secretion of growth factors and cytokines could be further studied by real-time quantitative PCR and multi-channel ELISA assessments.

Furthermore, the hydrogel indeed showed higher acute inflammatory response than control groups at 3 days. PEG based polymer material and HA have been widely used for wound healing applications^{10,11}. Therefore it would be interesting to find out the reason why this novel copolymer structure or hydrogel system resulted in high foreign body response, and to find out the modified approach to overcome this drawback in future studies.

6.4 Conclusions

The conclusions derived from the present research can be summarized as follows:

6.4.1 Phase I

- A PEG based hyperbranched copolymer of PEGMEMA-MEO₂MA-EGDMA with high content of vinyl functional groups has been achieved via *in-situ* DE-ATRP polymerization method.
- The polymerization speed can be sensitively controlled by varying the amount of reducing agent in *in-situ* DE-ATRP approach, thus specific polymer structure can be achieved via controlling the reaction conditions.

- LCST of the copolymer were adjusted to be close to body temperature by varying the polymer composition, and the polymer solution can form a physical hydrogel rapidly at 37 °C.
- The cytotoxicity of the copolymer was determined by alamarBlue[®] assay *in vitro*. The results suggested that the copolymer did not affect the cellular metabolism at certain concentrations.
- A photo-crosslinked hydrogel can be formed by exposing the polymer solution to UV light.

6.4.2 Phase II

6.4.2.1 Semi-IPN Hydrogel Systems

- A thermoresponsive hyperbranched copolymer of PEGMEMA-MEO₂MA-PEGDA with LCST close to body temperature and multi-acrylate functionality has been achieved via *in-situ* DE-ATRP polymerization method.
- A chemical cross-linked hydrogel can be formed by cross-linking with QT via Michael-type addition reaction within 10 min at 37 °C.
- ECM biomacromolecules of HA was introduced into the hydrogel forming a semi-IPN network to optimize the microenvironment for the encapsulation of cells.
- The semi-IPN hydrogel significantly enhanced the hydrogel swelling ratio and provided a large porous three dimensional microenvironment, which improved the cell adhesion and viability *in vitro*.

6.4.2.2 P-SH-HA Hybrid Hydrogel Systems

- HA was modified with thiol groups by reaction of carboxylic acid with cysteamine hydrochloride.
- Thiolated HA can cross-link with PEGMEMA-MEO₂MA-PEGDA copolymer via Michael-type addition reaction within 10 min at 37 °C.
- Over 80 % of embedded ADSCs cells remained alive in the hydrogels up to three weeks *in vitro*. The non-degradable properties of the hydrogel limited the cell proliferation and metabolic activity after 7 days.

- A number of anti-inflammatory cytokines (e.g IL-10) and angiogenic growth factors (e.g VEGF and PIGF) were secreted by encapsulated ADSCs in the hydrogel system.

6.4.3 Phase III

- Implanted rADSCs remained at the same level from 3 to 14 days after surgery in the *in-situ* formed P-SH-HA hydrogel system, while the cells cannot survive without hydrogel support *in vivo*.
- The hydrogel prevented the wound contraction, but also seem to limit the wound closure and re-epithelialization.
- Angiogenesis was significantly enhanced by this hydrogel dressing system in combination with rADSCs.
- Higher acute inflammatory response was triggered by the hydrogel compared with control group *in vivo*.

6.5 Future Directions

Based on the promising outcomes and limitations encountered within this research study, this section discusses the possible future directions that may follow after this project.

6.5.1 Bioactive Modification of PEG-based Hydrogels

Hydrogels have been widely used for tissue engineering applications because they provide a highly swollen 3D tissue-like environment which allows the diffusion of nutrients and cellular waste through the porous construction^{12, 13}. Compared with the natural hydrogels which are made from natural bio-polymers (e.g. collagen, fibrin, gelatin, alginate chitosan, hyaluronic acid), the synthetic hydrogels have remarkable advantages such as convenient control on material composition and hydrogel architecture, adjustable physical and mechanical properties, and can be tailored or modified with specific biofunctions¹⁴.

Among all the synthetic materials, PEG is one of the most important polymers for biomedical and tissue engineering applications because of its outstanding advantages including non-immunogenicity and resistance to

protein adsorption^{15, 16}. However, PEG-based hydrogels usually display minimal or no biological functionality due to their non-adhesive and non-degradable nature¹⁶. Therefore, much effort has been devoted to develop the bioactive modified PEG-based hydrogels that mimic the nature ECM environment¹⁷⁻²⁰. The common approaches to modified PEG-based hydrogels with bioactive molecules include post-grafting²¹⁻²⁴, photopolymerization²⁵⁻²⁷, click chemistry²⁸, Michael-type addition^{29, 30}, photo-regulation³¹⁻³³ and enzymatic reaction³⁴⁻³⁶.

To actualize these modifications, multi-step modified reactions and purification are usually required for the polymer functioning. In this project, as described in Chapter 3 and 4, a PEG-based hyperbranched polymer with high degree of acrylate functionality has been developed via *in-situ* DE-ATRP approach. By using this novel polymerization approach, we not only successfully introduced vinyl functional groups on the copolymer in “one-pot and one-step” reaction without gelation, but we also can conveniently adjust the molecular weight, branched degree and content of vinyl groups of the copolymer. Thus, the high level of active vinyl groups provides these copolymers capability of rapid cross-linking with thiol-functional molecules either via Michael-type addition reaction at physiological condition or via photo-initiated polymerization. Compared with the commercial available PEG-based acrylate functional monomers (e.g. PEGDA) or polymers (e.g. 4-arm-PEG-Acr), our copolymer exhibit advantages such as higher vinyl content, flexible and well-controlled polymer structure, and ease production via one-step reaction. Therefore, a number of bioactive modifications can be performed based on this acrylate functional polymer for specific purposes (**Figure 6.2**). Three examples are listed here:

- **Cell adhesive PEG-based hydrogels.**

One of the major limitations of PEG-based materials is lack of cell adhesion due to the hydrophilic polymer chain structure. A number of cell adhesive peptides derived from ECM proteins (e.g. fibronectin, laminin, collagen and elastin) have been widely studied. Linking PEG-based hydrogels with these adhesive peptides can significantly improve cell adhesion, increase cell viability,

proliferation and secretion, and guide cell migration and tissue reconstruction^{37, 38}. Some of these peptides have been modified by the thiol functional groups such as RGD³⁹⁻⁴¹, PHSRN⁴², IKVAV⁴³, YIGSR⁴², which can be directly cross-linked with our copolymer to form a cell specific adhesive hydrogel.

- **Enzyme-sensitive degradable PEG-based hydrogels.**

Another disadvantage of PEG-based materials is its limited degradability. One approach to overcome this limitation is incorporation of enzyme-sensitive peptide sequences in order to achieve highly desirable hydrogel degradation rate depending on different application target. For example, GPQG↓IAGQ⁴⁴, GPQG↓IWGQ⁴⁵⁻⁴⁷, YK↓NRD^{48, 49} and PEN↓FF⁴¹ are enzyme-sensitive peptides all containing the dithiol/monothiol groups, which can be used for preparing the proteolytically degradable hydrogels based on our copolymers.

- **Growth factor binding PEG-based hydrogel.**

It is always a challenge for hydrogel delivery systems used in regeneration medicine to control the release of growth factors over a long time⁵⁰⁻⁵². In order to modulate the release of growth factors, our hydrogels can be combined with modified ECM components such as proteins and glycans which provide the binding domains for growth factors. Such examples from literatures include heparin⁵³, chondroitin sulfate⁵⁴, HA⁵⁴, Biotin⁵⁵.

Based on above approaches, the bioactive wound hydrogel dressing developed in this project can be further optimized or modified, and three potential future projects for wound healing applications are proposed as follows.

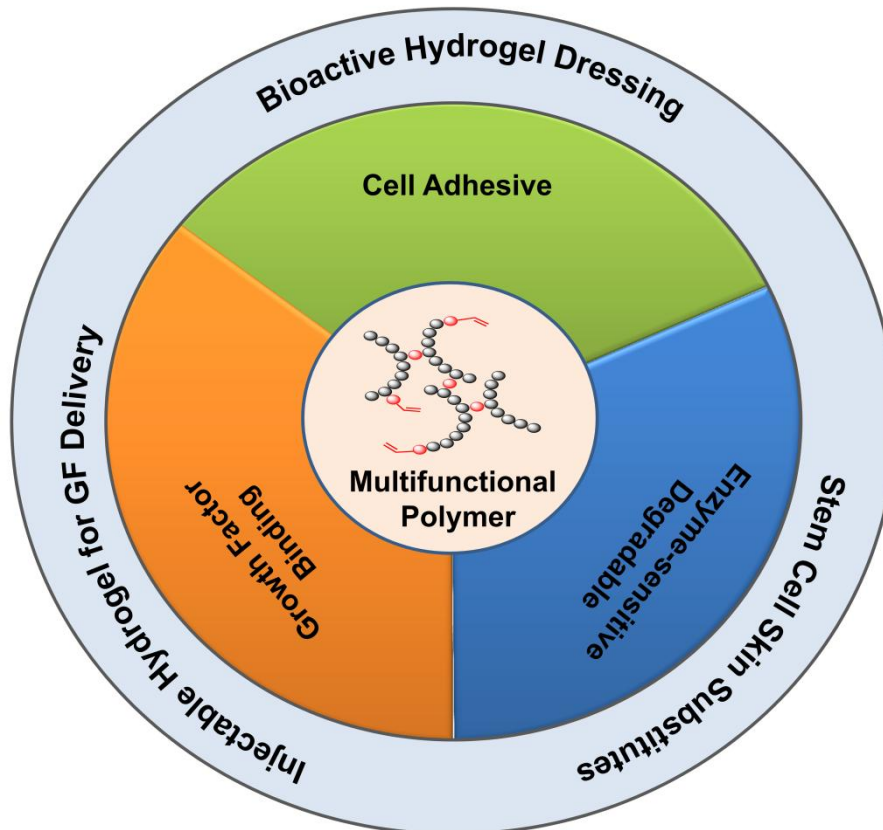


Figure 6.2: Future direction of bioactive modifications on the PEG-based hyperbranched multifunctional polymer which can be performed for specific wound healing applications.

6.5.2 Semi-degradable *In-situ* Formed Hydrogel Dressing with ADSCs

As described in Chapter 4 and 5, two major limitations were found for the P-SH-HA *in-situ* formed hydrogel dressing system: (i) low proliferation rate and metabolic activity of encapsulated cells *in vitro*; (ii) limited re-epithelialization underneath of the hydrogel dressing *in vivo*, which were due to the limited degradability and limited ability of the hydrogel to allow cells to attach. To overcome these limitations, cell adhesive peptides (e.g. RGD^{39, 41-43, 56}) and enzyme-sensitive peptide sequences (e.g. GPQG↓IAGQ⁴⁴) could be introduced to prepare a semi-degradable hydrogel with improved cell adhesion. RGD-conjugated PEG-based hydrogels have been reported to significantly improve cell adhesion of fibroblasts⁵⁷ and endothelial cells⁵⁸. In addition, appropriate degradation behavior of the hydrogel could promote the cell spreading, migration and proliferation⁵⁹. Therefore, it is hypothesized that the proliferation and secretion of the delivered ADSCs would significantly enhanced in this semi-degradable hydrogel, which would further promote the wound healing by increased paracrine effect; and also the RGD cell adhesive peptide present under surface of the hydrogel dressing would guide the keratinocytes migration and promote the epithelial layer formation underneath of the dressing. The viability, proliferation, morphology, phenotype and paracrine effect of the encapsulated ADSCs could be fully studied and an optimized hydrogel microenvironment could be found out *in vitro* first, which provides a stem cell niche to remain the ADSCs phenotype and maximally increase the cell secretion level of growth factors (e.g. VEGF, TGF- β , and IGF). Then cell paracrine effect on wound healing (e.g. growth factor secretion, wound closure, re-epithelialization, angiogenesis, inflammatory response) of using this stem cell bioactive dressing could be assessed by a specific wound model (e.g. diabetic mouse model or porcine burn wound model).

6.5.3 Degradable *In-situ* Formed Hydrogel Skin Substitutes with ADSCs

As discussed in Chapter 1, ADSCs have been proved to enhance angiogenesis, promote the recruitment of macrophage and endothelia cells, and accelerate wound closure and granulation tissue formation, either when

used as cell sheet or combined with other scaffold as skin substitutes⁶⁰⁻⁶⁶. Therefore, instead of developing a temporary bioactive wound dressing, permanent cellular wound substitutes can be also developed based on the technical outcomes of the present thesis.

In this proposed project, a degradable in situ formed hydrogel system would be developed for deliver autologous ADSCs, prepared from a multi-functional degradable PEG-based copolymer (synthesis via *in-situ* DE-ATRP), MMP-sensitive peptide cross-linker and RGD cell adhesive sequences. Mechanical property of the hydrogel would be tailored via adjusting the cross-linking density and RGD distribution, in order to mimic nature skin tissue and achieved desired the degradation rate depending on the healing profile of specific wound target. It is hypothesized that delivered ADSCs would differentiate into epidermal cell phenotype, modulating the level of growth factors and cytokines surrounding wound area, enhancing angiogenesis and accelerating the wound closure. In addition, the desired degradation rate would guide the hydrogel matrix to be gradually replaced by regenerated new tissue, and promote the remodeling process. Cell survival ratio, phenotype, secretion profile with this system would be studies both *in vitro* and *in vivo*. The therapeutic effect on wound healing such as wound closure, inflammatory response, angiogenesis, cell infiltration and collagen fiber orientation would be also assessed by using a specific wound model (e.g. diabetic mouse model or porcine burn wound model).

6.5.4 Degradable Injectable Hydrogel for Growth Factor Delivery for Wound Healing

As described in Chapter 1, wound healing is a complex process precisely regulated by local and system mediators such as cytokines, chemokines and growth factors⁶⁷⁻⁶⁹. A number of growth factors have been used to improve wound healing and skin regeneration such as EGF^{70, 71}, bFGF⁷²⁻⁷⁵, KGF^{76, 77}, VEGF⁷⁸⁻⁸⁰ and PDGF^{81, 82}. A major challenge for delivering growth factors in clinical applications is to maintain their stabilization and activity with a constant release over a long time. ECM materials (e.g. proteins and

Summary and Future Directions

glycans) may bind to growth factors via specific functional domains, which will protect them from proteolytic degradation³⁷.

In this proposed project, a degradable injectable hydrogel system would be developed for deliver single or multi growth factors for wound healing treatment, prepared from a multifunctional degradable PEG-based copolymer (synthesis via *in-situ* DE-ATRP), MMP-sensitive peptide cross-linker and thiolated ECM bio-polymers (e.g. heparin, HA and chondroitin sulfate^{53, 54}). It is hypothesized that the half-life of the implanted growth factors would be extended by binding the ECM component in the hydrogel; and with the enzyme-sensitive degradation of the hydrogels, growth factors would be released sustainably over a long time. Optimized hydrogel composition with desired degradation rate and release profile would be achieved via varying the polymer acrylate-functionality, cross-linking density and ECM material component. Growth factor release and its therapeutic effect on wound healing would be studied *in vivo* using a specific wound model (e.g. diabetic mouse model or porcine burn wound model).

6.6 References

1. Lutz, J.-F.; Akdemir, O.; Hoth, A., Point by point comparison of two thermosensitive polymers exhibiting a similar LCST: Is the age of poly(NIPAM) over? *Journal of the American Chemical Society* 2006, 128, (40), 13046-13047.
2. Lutz, J.-F., Polymerization of oligo(ethylene glycol) (meth)acrylates: Toward new generations of smart biocompatible materials. *Journal of Polymer Science Part a-Polymer Chemistry* 2008, 46, (11), 3459-3470.
3. Lutz, J.-F.; Andrieu, J.; Uezguen, S.; Rudolph, C.; Agarwal, S., Biocompatible, thermoresponsive, and biodegradable: Simple preparation of "all-in-one" biorelevant polymers. *Macromolecules* 2007, 40, (24), 8540-8543.
4. Lutz, J.-F.; Stiller, S.; Hoth, A.; Kaufner, L.; Pison, U.; Cartier, R., One-pot synthesis of PEGylated ultrasmall iron-oxide nanoparticles and their in vivo evaluation as magnetic resonance imaging contrast agents. *Biomacromolecules* 2006, 7, (11), 3132-3138.
5. Hoare, T. R.; Kohane, D. S., Hydrogels in drug delivery: Progress and challenges. *Polymer* 2008, 49, (8), 1993-2007.
6. Kwon, I. K.; Matsuda, T., Photo-iniferter-based thermoresponsive block copolymers composed of poly(ethylene glycol) and poly(N-isopropylacrylamide) and chondrocyte immobilization. *Biomaterials* 2006, 27, (7), 986-995.
7. Potta, T.; Chun, C.; Song, S. C., Dual cross-linking systems of functionally photo-cross-linkable and thermoresponsive polyphosphazene hydrogels for biomedical applications. *Biomacromolecules* 2010, 11, (7), 1741-1753.
8. Qiu, Y.; Park, K., Environment-sensitive hydrogels for drug delivery. *Advanced Drug Delivery Reviews* 2001, 53, (3), 321-339.
9. Rustad, K. C.; Wong, V. W.; Sorkin, M.; Glotzbach, J. P.; Major, M. R.; Rajadas, J.; Longaker, M. T.; Gurtner, G. C., Enhancement of mesenchymal stem cell angiogenic capacity and stemness by a biomimetic hydrogel scaffold. *Biomaterials* 2012, 33, (1), 80-90.
10. Boateng, J. S.; Matthews, K. H.; Stevens, H. N. E.; Eccleston, G. M., Wound healing dressings and drug delivery systems: A review. *Journal of Pharmaceutical Sciences* 2008, 97, (8), 2892-2923.
11. Zahedi, P.; Rezaeian, I.; Ranaei-Siadat, S.-O.; Jafari, S.-H.; Supaphol, P., A review on wound dressings with an emphasis on electrospun nanofibrous polymeric bandages. *Polymers for Advanced Technologies* 2010, 21, (2), 77-95.
12. Hoffman, A. S., Hydrogels for biomedical applications. *Advanced Drug Delivery Reviews* 2002, 54, (1), 3-12.
13. Lee, K. Y.; Mooney, D. J., Hydrogels for tissue engineering. *Chemical Reviews* 2001, 101, (7), 1869-1879.

14. Drury, J. L.; Mooney, D. J., Hydrogels for tissue engineering: scaffold design variables and applications. *Biomaterials* 2003, 24, (24), 4337-4351.
15. Alcantar, N. A.; Aydil, E. S.; Israelachvili, J. N., Polyethylene glycol-coated biocompatible surfaces. *Journal of Biomedical Materials Research* 2000, 51, (3), 343-351.
16. Lee, J. H.; Lee, H. B.; Andrade, J. D., Blood compatibility of polyethylene oxide surfaces. *Progress in Polymer Science* 1995, 20, (6), 1043-1079.
17. Cushing, M. C.; Anseth, K. S., Hydrogel cell cultures. *Science* 2007, 316, (5828), 1133-1134.
18. Lutolf, M. P., Spotlight on hydrogels. *Nature Materials* 2009, 8, (6), 451-453.
19. Lutolf, M. P.; Hubbell, J. A., Synthetic biomaterials as instructive extracellular microenvironments for morphogenesis in tissue engineering. *Nature Biotechnology* 2005, 23, (1), 47-55.
20. Tibbitt, M. W.; Anseth, K. S., Hydrogels as extracellular matrix mimics for 3D cell culture. *Biotechnology and Bioengineering* 2009, 103, (4), 655-663.
21. Albrecht, D. R.; Tsang, V. L.; Sah, R. L.; Bhatia, S. N., Photo- and electropatterning of hydrogel-encapsulated living cell arrays. *Lab on a Chip* 2005, 5, (1), 111-118.
22. Hahn, M. S.; Taite, L. J.; Moon, J. J.; Rowland, M. C.; Ruffino, K. A.; West, J. L., Photolithographic patterning of polyethylene glycol hydrogels. *Biomaterials* 2006, 27, (12), 2519-2524.
23. Perl, A.; Reinhoudt, D. N.; Huskens, J., Microcontact printing: Limitations and achievements. *Advanced Materials* 2009, 21, (22), 2257-2268.
24. Simms, H. A.; Bowman, C. A.; Anseth, K. S., Using living radical polymerization to enable facile incorporation of materials in microfluidic cell culture devices. *Biomaterials* 2008, 29, (14), 2228-2236.
25. Reddy, S. K.; Cramer, N. B.; Bowman, C. N., Thiol-vinyl mechanisms. 1. Termination and propagation kinetics in thiol-ene photopolymerizations. *Macromolecules* 2006, 39, (10), 3673-3680.
26. Salinas, C. N.; Anseth, K. S., Mixed mode thiol-acrylate photopolymerizations for the synthesis of PEG-peptide hydrogels. *Macromolecules* 2008, 41, (16), 6019-6026.
27. Zhu, J.; Tang, C.; Kottke-Marchant, K.; Marchant, R. E., Design and synthesis of biomimetic hydrogel scaffolds with controlled organization of cyclic RGD peptides. *Bioconjugate Chemistry* 2009, 20, (2), 333-339.
28. Mann, B. K.; Tsai, A. T.; Scott-Burden, T.; West, J. L., Modification of surfaces with cell adhesion peptides alters extracellular matrix deposition. *Biomaterials* 1999, 20, (23-24), 2281-2286.

29. Hiemstra, C.; van der Aa, L. J.; Zhong, Z.; Dijkstra, P. J.; Feijen, J., Rapidly in situ-forming degradable hydrogels from dextran thiols through michael addition. *Biomacromolecules* 2007, 8, (5), 1548-1556.
30. Lutolf, M. P.; Hubbell, J. A., Synthesis and physicochemical characterization of end-linked poly(ethylene glycol)-co-peptide hydrogels formed by Michael-type addition. *Biomacromolecules* 2003, 4, (3), 713-722.
31. Li, H.; Hah, J.-M.; Lawrence, D. S., Light-mediated liberation of enzymatic activity: "Small Molecule" caged protein equivalents. *Journal of the American Chemical Society* 2008, 130, (32), 10474.
32. Peters, F. B.; Brock, A.; Wang, J.; Schultz, P. G., Photocleavage of the polypeptide backbone by 2-Nitrophenylalanine. *Chemistry & Biology* 2009, 16, (2), 148-152.
33. Takahashi, I.; Kuroiwa, S.; Lindfors, H. E.; Ndamba, L. A.; Hiruma, Y.; Yajima, T.; Okishio, N.; Ubbink, M.; Hirota, S., Modulation of protein-ligand interactions by photocleavage of a cyclic peptide using phosphatidylinositol 3-kinase SH3 domain as model system. *Journal of Peptide Science* 2009, 15, (6), 411-416.
34. Ehrbar, M.; Rizzi, S. C.; Hlushchuk, R.; Djonov, V.; Zisch, A. H.; Hubbell, J. A.; Weber, F. E.; Lutolf, M. P., Enzymatic formation of modular cell-instructive fibrin analogs for tissue engineering. *Biomaterials* 2007, 28, (26), 3856-3866.
35. Ehrbar, M.; Rizzi, S. C.; Schoenmakers, R. G.; San Miguel, B.; Hubbell, J. A.; Weber, F. E.; Lutolf, M. P., Biomolecular hydrogels formed and degraded via site-specific enzymatic reactions. *Biomacromolecules* 2007, 8, (10), 3000-3007.
36. Sanborn, T. J.; Messersmith, P. B.; Barron, A. E., In situ crosslinking of a biomimetic peptide-PEG hydrogel via thermally triggered activation of factor XIII. *Biomaterials* 2002, 23, (13), 2703-2710.
37. Zhu, J. M., Bioactive modification of poly(ethylene glycol) hydrogels for tissue engineering. *Biomaterials* 2010, 31, (17), 4639-4656.
38. Jabbari, E., Bioconjugation of hydrogels for tissue engineering. *Current Opinion in Biotechnology* 2011, 22, (5), 655-660.
39. DeForest, C. A.; Polizzotti, B. D.; Anseth, K. S., Sequential click reactions for synthesizing and patterning three-dimensional cell microenvironments. *Nature Materials* 2009, 8, (8), 659-664.
40. Lutolf, M. R.; Weber, F. E.; Schmoekel, H. G.; Schense, J. C.; Kohler, T.; Muller, R.; Hubbell, J. A., Repair of bone defects using synthetic mimetics of collagenous extracellular matrices. *Nature Biotechnology* 2003, 21, (5), 513-518.
41. Salinas, C. N.; Anseth, K. S., The enhancement of chondrogenic differentiation of human mesenchymal stem cells by enzymatically regulated RGD functionalities. *Biomaterials* 2008, 29, (15), 2370-2377.
42. Fittkau, M. H.; Zilla, P.; Bezuidenhout, D.; Lutolf, M.; Human, P.; Hubbell, J. A.; Davies, N., The selective modulation of endothelial cell

mobility on RGD peptide containing surfaces by YIGSR peptides. *Biomaterials* 2005, 26, (2), 167-174.

43. Saha, K.; Irwin, E. F.; Kozhukh, J.; Schaffer, D. V.; Healy, K. E., Biomimetic interfacial interpenetrating polymer networks control neural stem cell behavior. *Journal of Biomedical Materials Research Part A* 2007, 81A, (1), 240-249.

44. Lutolf, M. P.; Lauer-Fields, J. L.; Schmoekel, H. G.; Metters, A. T.; Weber, F. E.; Fields, G. B.; Hubbell, J. A., Synthetic matrix metalloproteinase-sensitive hydrogels for the conduction of tissue regeneration: Engineering cell-invasion characteristics. *Proceedings of the National Academy of Sciences of the United States of America* 2003, 100, (9), 5413-5418.

45. Kraehenbuehl, T. P.; Zammaretti, P.; Van der Vlies, A. J.; Schoenmakers, R. G.; Lutolf, M. P.; Jaconi, M. E.; Hubbell, J. A., Three-dimensional extracellular matrix-directed cardioprogenitor differentiation: Systematic modulation of a synthetic cell-responsive PEG-hydrogel. *Biomaterials* 2008, 29, (18), 2757-2766.

46. Lutolf, M. P.; Raeber, G. P.; Zisch, A. H.; Tirelli, N.; Hubbell, J. A., Cell-responsive synthetic hydrogels. *Advanced Materials* 2003, 15, (11), 888.

47. Raeber, G. P.; Lutolf, M. P.; Hubbell, J. A., Mechanisms of 3-D migration and matrix remodeling of fibroblasts within artificial ECMs. *Acta Biomaterialia* 2007, 3, (5), 615-629.

48. Pratt, A. B.; Weber, F. E.; Schmoekel, H. G.; Muller, R.; Hubbell, J. A., Synthetic extracellular matrices for in situ tissue engineering. *Biotechnology and Bioengineering* 2004, 86, (1), 27-36.

49. Raeber, G. P.; Lutolf, M. P.; Hubbell, J. A., Molecularly engineered PEG hydrogels: A novel model system for proteolytically mediated cell migration. *Biophysical Journal* 2005, 89, (2), 1374-1388.

50. Elbert, D. L.; Pratt, A. B.; Lutolf, M. P.; Halstenberg, S.; Hubbell, J. A., Protein delivery from materials formed by self-selective conjugate addition reactions. *Journal of Controlled Release* 2001, 76, (1-2), 11-25.

51. Hiemstra, C.; Zhong, Z.; van Steenberg, M. J.; Hennink, W. E.; Feijen, J., Release of model proteins and basic fibroblast growth factor from in situ forming degradable dextran hydrogels. *Journal of Controlled Release* 2007, 122, (1), 71-78.

52. Lin, C.-C.; Anseth, K. S., PEG hydrogels for the controlled release of biomolecules in regenerative medicine. *Pharmaceutical Research* 2009, 26, (3), 631-643.

53. Tae, G.; Kim, Y.-J.; Choi, W.-I.; Kim, M.; Stayton, P. S.; Hoffman, A. S., Formation of a novel heparin-based hydrogel in the presence of heparin-binding biomolecules. *Biomacromolecules* 2007, 8, (6), 1979-1986.

54. Cai, S. S.; Liu, Y. C.; Shu, X. Z.; Prestwich, G. D., Injectable glycosaminoglycan hydrogels for controlled release of human basic fibroblast growth factor. *Biomaterials* 2005, 26, (30), 6054-6067.

55. Lin, C.-C.; Anseth, K. S., Controlling affinity binding with peptide-functionalized poly(ethylene glycol) hydrogels. *Advanced Functional Materials* 2009, 19, (14), 2325-2331.
56. Herten, M.; Jung, R. E.; Ferrari, D.; Rothamel, D.; Golubovic, V.; Molenberg, A.; Haemmerle, C. H. F.; Becker, J.; Schwarz, F., Biodegradation of different synthetic hydrogels made of polyethylene glycol hydrogel/RGD-peptide modifications: an immunohistochemical study in rats. *Clinical Oral Implants Research* 2009, 20, (2), 116-125.
57. Hern, D. L.; Hubbell, J. A., Incorporation of adhesion peptides into nonadhesive hydrogels useful for tissue resurfacing. *Journal of Biomedical Materials Research* 1998, 39, (2), 266-276.
58. Elbert, D. L.; Hubbell, J. A., Conjugate addition reactions combined with free-radical cross-linking for the design of materials for tissue engineering. *Biomacromolecules* 2001, 2, (2), 430-441.
59. Lei, Y.; Gojgini, S.; Lam, J.; Segura, T., The spreading, migration and proliferation of mouse mesenchymal stem cells cultured inside hyaluronic acid hydrogels. *Biomaterials* 2011, 32, (1), 39-47.
60. Cherubino, M.; Rubin, J. P.; Miljkovic, N.; Kelmendi-Doko, A.; Marra, K. G., Adipose-derived stem cells for wound healing applications. *Annals of Plastic Surgery* 2011, 66, (2), 210-215.
61. Nie, C.; Yang, D.; Morris, S. F., Local delivery of adipose-derived stem cells via acellular dermal matrix as a scaffold: A new promising strategy to accelerate wound healing. *Medical Hypotheses* 2009, 72, (6), 679-682.
62. Trottier, V.; Marceau-Fortier, G.; Germain, L.; Vincent, C.; Fradette, J., IFATS collection: Using human adipose-derived stem/stromal cells for the production of new skin substitutes. *Stem Cells* 2008, 26, (10), 2713-2723.
63. Ebrahimian, T. G.; Pouzoulet, F.; Squiban, C.; Buard, V.; Andre, M.; Cousin, B.; Gourmelon, P.; Benderitter, M.; Casteilla, L.; Tamarat, R., Cell therapy based on adipose tissue-derived stromal cells promotes physiological and pathological wound healing. *Arteriosclerosis Thrombosis and Vascular Biology* 2009, 29, (4), 503-510.
64. Lin, Y.-C.; Grahovac, T.; Oh, S. J.; Ieraci, M.; Rubin, J. P.; Marra, K. G., Evaluation of a multi-layer adipose-derived stem cell sheet in a full-thickness wound healing model. *Acta Biomaterialia* 2013, 9, (2), 5243-5250.
65. Altman, A. M.; Yan, Y.; Matthias, N.; Bai, X.; Rios, C.; Mathur, A. B.; Song, Y.-H.; Alt, E. U., IFATS collection: human adipose-derived stem cells seeded on a silk fibroin-chitosan scaffold enhance wound repair in a murine soft tissue injury model. *Stem Cells* 2009, 27, (1), 250-258.
66. Hong, S. J.; Jia, S.-X.; Xie, P.; Xu, W.; Leung, K. P.; Mustoe, T. A.; Galiano, R. D., Topically delivered adipose derived stem cells show an activated-fibroblast phenotype and enhance granulation tissue formation in skin wounds. *Plos One* 2013, 8, (1), e55640-e55640.
67. Werner, S.; Grose, R., Regulation of wound healing by growth factors and cytokines. *Physiological Reviews* 2003, 83, (3), 835-870.

68. Barrientos, S.; Stojadinovic, O.; Golinko, M. S.; Brem, H.; Tomic-Canic, M., Growth factors and cytokines in wound healing. *Wound Repair and Regeneration* 2008, 16, (5), 585-601.
69. Behm, B.; Babilas, P.; Landthaler, M.; Schreml, S., Cytokines, chemokines and growth factors in wound healing. *Journal of the European Academy of Dermatology and Venereology* 2012, 26, (7), 812-820.
70. Tanaka, A.; Nagate, T.; Matsuda, H., Acceleration of wound healing by gelatin film dressings with epidermal growth factor. *Journal of Veterinary Medical Science* 2005, 67, (9), 909-913.
71. Ulubayram, K.; Cakar, A. N.; Korkusuz, P.; Ertan, C.; Hasirci, N., EGF containing gelatin-based wound dressings. *Biomaterials* 2001, 22, (11), 1345-1356.
72. Akita, S.; Akino, K.; Imaizumi, T.; Hirano, A., Basic fibroblast growth factor accelerates and improves second-degree burn wound healing. *Wound Repair and Regeneration* 2008, 16, (5), 635-641.
73. Akita, S.; Akino, K.; Imaizumi, T.; Tanaka, K.; Anraku, K.; Yano, H.; Hirano, A., The quality of pediatric burn scars is improved by early administration of basic fibroblast growth factor. *Journal of Burn Care & Research* 2006, 27, (3), 333-338.
74. Kinoshita, N.; Tsuda, M.; Hamuy, R.; Nakashima, M.; Nakamura-Kurashige, T.; Matsuu-Matsuyama, M.; Hirano, A.; Akita, S., The usefulness of basic fibroblast growth factor for radiation-exposed tissue. *Wound Repair and Regeneration* 2012, 20, (1), 91-102.
75. Komori, M.; Tomizawa, Y.; Takada, K.; Ozaki, M., A single local application of recombinant human basic fibroblast growth factor accelerates initial angiogenesis during wound healing in rabbit ear chamber. *Anesthesia and Analgesia* 2005, 100, (3), 830-834.
76. Staianocoico, L.; Krueger, J. G.; Rubin, J. S.; Dlimi, S.; Vallat, V. P.; Valentino, L.; Fahey, T.; Hawes, A.; Kingston, G.; Madden, M. R.; Mathwich, M.; Gottlieb, A. B.; Aaronson, S. A., Human keratinocyte growth-factor effects in a porcine model of epidermal wound-healing. *Journal of Experimental Medicine* 1993, 178, (3), 865-878.
77. Peng, C.; He, Q.; Luo, C., Lack of keratinocyte growth factor retards angiogenesis in cutaneous wounds. *Journal of International Medical Research* 2011, 39, (2), 416-423.
78. Brem, H.; Kodra, A.; Golinko, M. S.; Entero, H.; Stojadinovic, O.; Wang, V. M.; Sheahan, C. M.; Weinberg, A. D.; Woo, S. L. C.; Ehrlich, H. P.; Tomic-Canic, M., Mechanism of sustained release of vascular endothelial growth factor in accelerating experimental diabetic healing. *Journal of Investigative Dermatology* 2009, 129, (9), 2275-2287.
79. Drinkwater, S. L.; Smith, A.; Sawyer, B. M.; Burnand, K. G., Effect of venous ulcer exudates on angiogenesis in vitro. *British Journal of Surgery* 2002, 89, (6), 709-713.
80. Ferrara, N.; Henzel, W. J., Pituitary follicular cells secrete a novel heparin-binding growth-factor specific for vascular endothelial-cells.

Summary and Future Directions

Biochemical and Biophysical Research Communications 1989, 161, (2), 851-858.

81. Greenhalgh, D. G.; Sprugel, K. H.; Murray, M. J.; Ross, R., PDGF and FGF stimulate wound-healing in the genetically diabetic mouse. *American Journal of Pathology* 1990, 136, (6), 1235-1246.

82. Uhl, E.; Rosken, F.; Sirsjo, A.; Messmer, K., Influence of platelet-derived growth factor on microcirculation during normal and impaired wound healing. *Wound Repair and Regeneration* 2003, 11, (5), 361-367.

Appendices

A. Materials and Reagents

Material	Supplier
Transparent film dressing (Tegaderm™ Film, 3M®)	3M UK & Ireland, Bracknell, UK
Mouse monoclonal anti-CD 68 antibody	Abcam, Cambridge, UK
Rabbit polyclonal antibody to collagen type IV	
Thiolated hyaluronic acid (HA-SH, HyStem™, Glycosan)	BioTime Inc., Alameda, USA
Acetone (98%)	Fisher Scientific, Dublin, Ireland
Dimethylformamide (DMF, 98 %)	
AlamarBlue®	Invitrogen, Dun Laoghaire, Ireland
AlexaFluor® 488 Goat anti-Mouse IgG (H+L)	
AlexaFluor® 488 Goat anti-Rabbit IgG (H+L)	
Celltracker™ CM-DiI	
Human adipose-derived stem cells (STEMPRO®)	
LIVE/DEAD® stain	
Picogreen®	
Sodium hyaluronate	Lifecore Biomedical, Chaska, USA
Poietics™ Human ADSCs – adipogenesis	Lonza, Muenchsteinerstrasse, Switzerland
Poietics™ Human ADSCs – Osteogenesis	
Poietics™ Human ADSCs – chondrogenesis	
2-(2-methoxyethoxy) ethyl methacrylate (MEO ₂ MA)	Sigma, Dublin, Ireland
Acetic Acid	
Alizarin Red S	
Butanone (99 %, HPLC grade)	
Calcium chloride	

Material	Supplier
Carbazole	Sigma, Dublin, Ireland
Chloroform (CDCl ₃)	
Copper(II) chloride (CuCl ₂ , 97 %)	
Cysteamine hydrochloride	
Deuterium oxide (D ₂ O)	
Dialysis membrane (MWCO 6000-8000)	
Diethyl ether (HPLC grade)	
Dullbecco's modified eagle medium (DMEM)	
Ellman's reagent	
Ethyl 2-bromoisobutyrate (98 %)	
Ethylene glycol dimethacrylate (EGDMA)	
Eosin	
Ethanol	
Ethylenediaminetetraacetic (EDTA)	
Fast Green	
Fetal bovine serum	
Fluoromount™ Aqueous Mounting Medium	
Formalin (10%)	
Goat serum	
Haematoxylin	
Hanks balanced salt solution (HBSS)	
Hexane (95 %)	
Hoechst 33258	
Hydrochloric acid	
L-ascorbic acid (AA, 99 %)	

Material	Supplier
N-(3-Dimethylaminopropyl)-N'-ethylcarbodiimide hydrochloride (EDAC, 98 %)	Sigma, Dublin, Ireland
N-hydroxysuccinimide (NHS)	
N,N,N',N'',N''-pentamethyldiethylenetriamine	
Oil Red O	
Paraformaldehyde	
Penicillin/streptomycin	
Pentaerythritol tetrakis (3-mercaptopropionate) (QT)	
Phosphate buffered saline tablets	
Poly(ethylene glycol) diacrylate (PEGDA, Mn = 258 g/mol)	
Poly(ethylene glycol) methyl ether methacrylate (PEGMEMA Mn = 475)	
Sodium chloride	
Sodium hydroxide	
Sodium tetraborate	
Safranin-O	
Sucrose	
Sulfuric acid	
Tris-hydrochloride	
Triton X-100	
TWEEN [®] 20	
Xylenes	
Buprenorphine	Vetergesic
OCT media	VWR Labshop, Batavia, USA

B. Polymer Synthesis and Purification

B.1 Polymer Synthesis

1. Design and calculate the synthesis recipe
2. Add monomers, catalyst (CuCl_2), Initiator and ligand to a two-necked round bottom flask
3. Add solvent (butanone) into flask, (the volume ratio of total monomers to solvent adjusted at 1:2)
4. Stir for 10-15 min. to dissolve CuCl_2
5. Preheat the oil bath at 50 °C
6. Purge with argon for 30 min. to remove dissolved oxygen
7. Make 5x L-ascorbic acid store solution in dH_2O (Fresh made during the purging)
8. Add L-ascorbic acid solution quickly under argon purging (avoid oxygen entre the flask), purging another 1-2 min.
9. Start reaction by heating in oil bath at 50 °C with stirring at 800 rpm
10. Take sample with argon purging and run GPC to monitor reaction (based on increased molecular weight and Polydispersity Index)
11. Stop the reaction at certain time (according to the GPC results) by opening the flask and expose the reaction solution to air

B.2 Polymer Purification

1. Add acetone to dilute the polymer solution (until not viscous)
2. Add polymer solution into 5-10 volume times of hexane/diethylether (1/1) drop by drop with stirring (quick, avoid volatilization of solvent) (remove PEGDA monomer)
3. Precipitate the solution for 1 hour (sealed the container)
4. Precipitated mixture was dissolved in deionized water and dialysis (MWCO 6-8 kDa) for 4 days in dark at 4 °C (change the water every few hours)
5. Filter the polymer solution (0.45 μl pore size)
6. Freeze dry and store at -20 °C

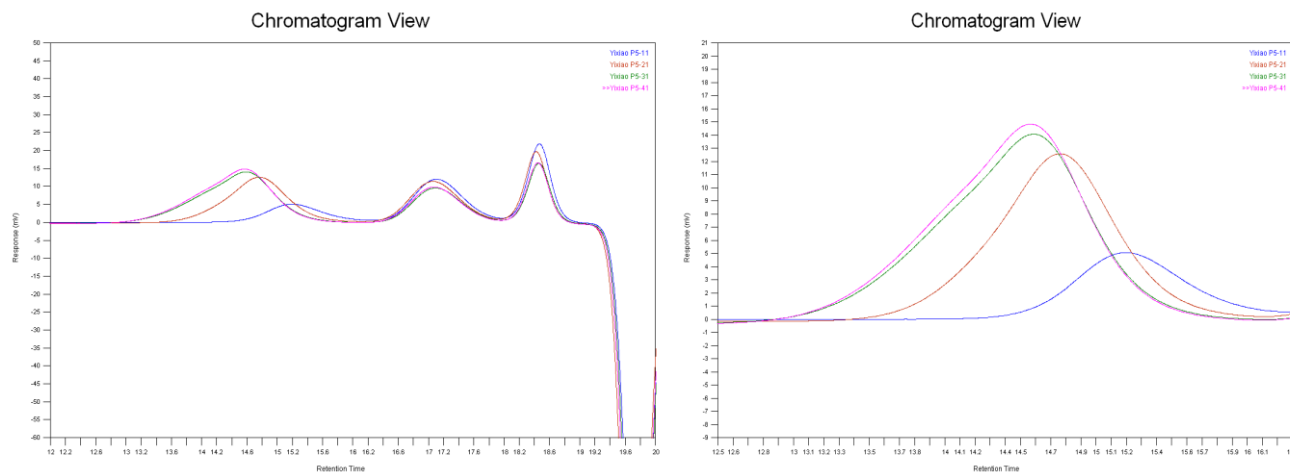
B.3 Example of Polymer Synthesis Report**PEGMEMA-MEO₂MA-EGDMA (P5) 24/07/2009****[Monomers]:[I] = 100:1; [I]:[CuCl₂] = 1:0.25; [CuCl₂]:[Ligand] = 0.25:0.25; [Agent]=15% [CuCl₂]; V_[Butanone] : V_[Monomers] = 2:1**

	Rate	Mass	Mole	MW (g/mol)	D (g/ml)	V
PEGMEMA	15	8 g	0.0168	475	1.08	7.4 ml
MEO ₂ MA	75	15.81 g	0.084	188.22	1.02	15.5 ml
EGDMA	10	2.22 g	0.0112	198.22	1.051	2.11 ml
Ethyl α -bromoisobutyrate [Initiator]	1	0.218 g	0.00112	195.06	1.315	166.1 μ l
CuCl ₂ [Catalyst]	0.25	37.65 mg	0.00028	134.45	-	-
Bis(2-dimethylaminoethyl) methylamine [L]	0.25	0.048 g	0.00028	173.3	0.83	58.46 μ l
L-Ascorbic Acid [Agent]	0.0375	7.397 mg	0.000042	176.12	($\times 5$) 36.99 mg, 80/400 μ l dH ₂ O	
Butanone			-			50 ml

<u>Start Time:</u>	10:10	24/07	
Sample 1(S1):	15:10	24/07	(5h)
Sample 1(S2):	19:10	24/07	(9h)
Sample 1(S3):	09:10	25/07	(23h)
Sample 1(S4):	12:10	25/07	(26h)

Stop the reaction

Example of Polymer Synthesis Report (GPC Monitor):



(GPC traces from RI detector for polymer samples)

Sample Name	RT	Mn	Mw	PDI
P5-S1	5 h	4293	4892	1.1395
P5-S2	9 h	7302	8908	1.2199
P5-S3	23 h	9635	12863	1.3350
P5-S4	26 h	9871	13271	1.3444

C. Swelling Assessment for Non-IPN & Semi-IPN Hydrogels

1. Prepare polymer solution of PEGMEMA-MEO₂MA-EGDMA in PBS (pH 7.4) at concentrations of 20 wt % (20% P) and 40 wt % (40 % P) (vortex until fully dissolved).
2. Prepare HA (LifeCore[®] Biomedical, 66-90 kg/mol) solution in PBS (pH 7.4) at 32 mg/ml (HA).
3. Add cross-linker of QT into polymer solution and mix properly with vortex (molar ratio of vinyl group on the polymer to thiol group on QT = 1:1.1).

	Gel	20 % P (µl)	40% P (µl)	HA (µl)	PBS (µl)	QT (µl)	Total (µl)
Semi-IPN	10 %	500	-	500	-	5.2	1005
Non-IPN	10 %	500	-	-	500	5.2	1005
	20 %	-	500	-	495	10.4	1005

4. Pipette 200 µl of the mixed solution into a 1 mL flat bottom vials (n=3) (weight the empty vial as W_v).
5. Leave the sample at 37 °C 2 h to form gel completely (gelation usually occurs at about 10 minutes) (weight the vial + gel, and calculate the weight of gel by minus W_v as W_0).
6. Add 500 µl of PBS (pH 7.4) into each vial. Leave samples at RT and 37 °C to study the effect of temperature on swelling.
7. At set time points, remove the PBS for analysis, weight and calculate the weight of the gel as W_t .
8. Add fresh PBS (500 µl) in each well and leave samples at RT and 37 °C.
9. Repeat step 7 and 8 until all the time points are tested.

Time points:	1 h	2 h	4 h	7 h	24 h	2 d	5 d	8 d	19 d
--------------	-----	-----	-----	-----	------	-----	-----	-----	------

10. Calculate swelling ratio = W_t / W_0 .

D. HA Release Assessment from Semi-IPN Hydrogel

1. Prepare polymer solution of PEGMEMA-MEO₂MA-EGDMA in PBS (pH 7.4) at concentrations of 10 wt % (P) (vortex until fully dissolved).
2. Prepare HA (LifeCore[®] Biomedical, 66-90 kg/mol) solution in PBS (pH 7.4) at 20 mg/ml (HA-20) and 40 mg/ml (HA-40).
3. Add cross-linker of QT into polymer solution and mix properly with vortex (molar ratio of vinyl group on the polymer to thiol group on QT = 1:1.1).

No.	10 % P (μl)	HA-20 (μl)	HA-40 (μl)	QT (μl)	Total (μl)
1	1000	1000	-	10.4	2020
2	1000	-	1000	10.4	2020

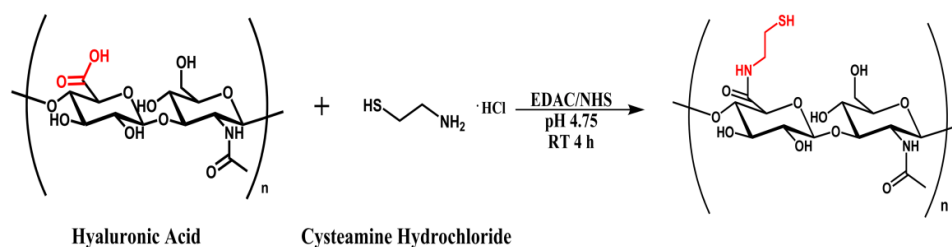
4. Pipette 400 μl of the mixed solution into a well of 48-well plate (n=3).
5. Leave the plate at 37 °C 2 h to form gel completely (gelation usually occurs at about 10 minutes).
6. Add 400 μl of PBS (pH 7.4) into each well. Leave samples at 37 °C to allow gel release.
7. At each time point, 0.2 mL of the supernatant was taken after gentle shaking and the same volume of fresh PBS was added.

The concentration of HA in the release samples was determined with carbazole assay:

8. Standards were prepared by serial dilution of 1 mg/mL HA in PBS
9. 50 μL of samples and standards were placed in a 96-well plate.
10. Add 200 μL of 25 mM sodium tetraborate in sulfuric acid to each well.
11. Heat the plate in an oven at 100 °C for 10 min.
12. Leave the plate at RT for 15 min to cool.
13. Add 50 μL of 0.125 % carbazole in ethanol and thoroughly mixed.
14. Heat the plate again in an oven at 100 °C for 10 min.
15. Leave the plate at RT for 15 min to cool.
16. Determine the absorbance of the samples at 550 nm by a microplate reader (Varioskan Flash Reader).
17. Calculate the HA concentration of each sample based on the standard curve.

E. Thiolated HA Preparation

Reaction Equation:



Materials:

- Sodium Hyaluronate: Lifecore Biomedical (1.5 MDa)
- Cysteamine hydrochloride (Mw 113.61 g/mol, Sigma)
- EDAC: 1-Ethyl-3-(3-dimethylaminopropyl) carbodiimide hydrochloride (Sigma)
- NHS: N-Hydroxysuccinimide (Sigma)

Reaction Protocol

1. 0.1 g HA dissolved in 25 mL dH₂O (0.26 mmol, 0.4%, w/v)
2. Adjust pH to 5.5 (by 0.1 M HCl)
3. Add EDAC (240 mg, 50 mM) and NHS (144 mg, 50 mM)
4. Readjust pH to 5.5
5. Stirring 15 min at RT
6. Add 0.15 g of Cysteamine hydrochloride (Mw 113.61 g/mol, 1.32 mmol, 5x)
7. Adjust pH to 4.75
8. Stirring at RT for 4 hours
9. Dialysis (6-8 kDa cut) to 0.3 mM HCl (pH3.5) and NaCl (100 mM) 2x
10. Dialysis (6-8 kDa cut) to 0.3 mM HCl (pH3.5) 2x
11. Freeze dry for 2 days
12. Protect by argon and store at -20 °C

F. Ellman’s Test

Material Preparation:

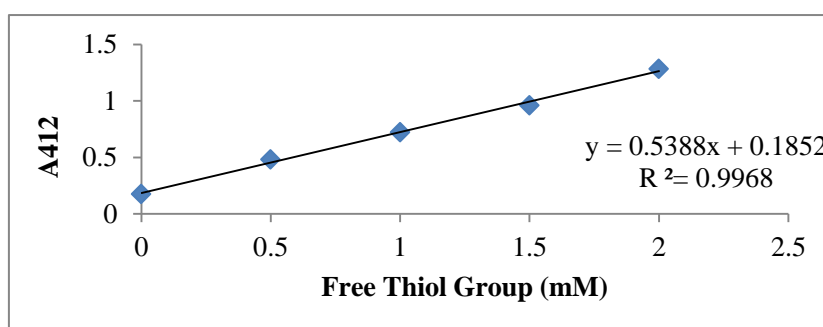
- Reaction Buffer: 0.1 M Sodium phosphate (Na_3PO_4 , Mw=163.94), pH 8.0, containing 1mM EDTA.
- Standard: Cysteine Hydrochloride Monohydrate (Mw=175.6)
 Store solution (30 mM): 10.54 mg/2mL in reaction buffer.
- Ellman’s Reagent Solution: Dissolve 4 mg Ellman’s Reagent in 1 mL of Reaction Buffer.
- Sample: HA-SH; Control: HA. 1 mg/mL x 1 mL.

Assay:

1. 50 μL Ellman’s Reagent Solution + 1 mL Reaction Buffer
2. Add 240 Standard / Sample
3. Mix and leave at RT for 15 minutes
4. Measure Absorbance 412 nm by plate reader.

Standard Curve:

	2 mM	1.5 mM	1 mM	0.5 mM	0 mM
Cysteine Store	16 μL	12 μL	8 μL	4 μL	0 μL
Top up (Buffer)	224 μL	228 μL	232 μL	236 μL	240 μL
Total	240 μL				



G. P-SH-HA Hydrogel Fabrication and Swelling Assessment

1. Prepare polymer solution of PEGMEMA-MEO₂MA-PEGDA in PBS (pH 7.4) at concentrations of 10 wt % (10% P) and 15 wt % (15 % P) (vortex until fully dissolved).
2. Prepare thiolated HA solution in PBS (pH 7.4) at 1.4 % (1.4 % HA-SH) and 2.1 % w/v (2.1 % HA-SH).
3. Add HA-SH solution into polymer solution and mix with vortex as shown in following table.

Gel	10 % P (µl)	15 % P (µl)	1.4 % HA-SH (µl)	2.1 % HA-SH (µl)	Total (µl)
10 %	500	-	500	-	1000
15 %	-	500	-	500	1000

4. Pipette 200 µl of the mixed solution into a 1 mL flat bottom vials (n=3) (weight the empty vial as W_v).
5. Leave the plate at 37 °C 2 h to form gel completely (gelation usually occurs at about 10 minutes)
6. The dried weight (W_0) of the hydrogel was also determined in the same manner after freeze drying of hydrogels
7. Add 600 µl of PBS (pH 7.4) into each vial. Leave samples at 37 °C with constant agitation at 150 rpm.
8. At set time points, remove the PBS for analysis, weight and calculate the weight of the gel as W_t (weight the vial + gel, and calculate the weight of gel by minus W_v).
9. Add fresh PBS (600 µl) in each well and leave samples at RT and 37 °C.
10. Repeat step 8 and 9 until all the time points are tested.

Time points:	1 h	2 h	3 h	4 h	5 h	6 h
--------------	-----	-----	-----	-----	-----	-----

11. Calculate swelling ratio = W_t / W_0 .

H. Rat ADSCs Cell Extraction

Isolate the fat tissue from 2 Sprague Dawley rats (CD[®] IGS, CharlesRiver, UK) 5-6 months (600-750 g).

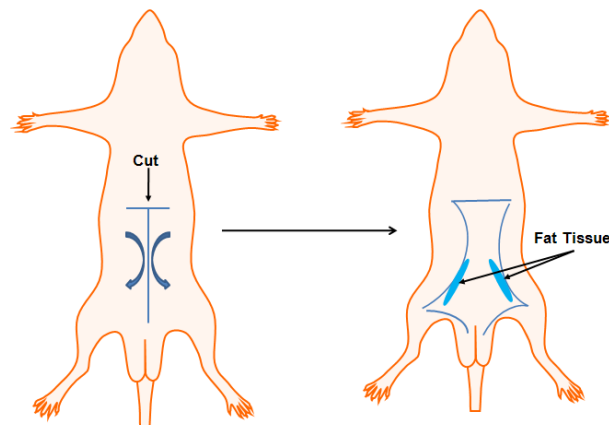
Media Prepare:

Transport medium: HBSS/DMEM 1:1 (V:V), with 10% FBS and 1% P/S

Complete media: DMEM with 10% FBS and 1% P/S (L-Glut in DMEM, if not add 1% of L-Glut)

Tissue isolation:

1. Sacrifice the rats (CO₂)
2. Sterilize working area on a table
3. Wash the rat belly with 70 % alcohol to disinfect the skin surface
4. Cut the first skin with scissors (The adipose tissue is just below this skin)



5. Add the tissue in the transport media
6. Eliminate the maximum of blood vessels.

Cells isolation (in cell culture hood):

7. Wash the tissue by HBSS to eliminate the blood potentially present (3-4x)
8. Digest by collagenase type I (collagenase crude type I A C-2674, Sigma, 0.025 % w/v)

For 15ml of tissue: 5mg of collagenase + 20 ml of HBSS

9. Cut tissue to collagenase solution (with scissors)
10. Incubate 1h at 37 °C with slowly shaking in incubator at about 60 rpm/min.(obtain a kind of cream after this step)
11. Add 1 volume of complete medium (same volume of Collagenase solution) to stop the reaction
 - Max and leave for few minutes, got two layer phases
 - Remove first layer of fat tissue (by pipetting)
12. Resuspend the last phase and filter on cell trainer 70 µm
13. Centrifuge 8 minutes at 300 g (1200 rpm)
14. Transfer cells to 15 mL tube, wash the cells with complete medium 3 times (Centrifuge and change medium each time)
15. Count cells → dilution 1/32 to count them (Cells are tiny!!)

After 24h, change the media to eliminate blood cells and adipocytes without adhesion (the other cells adhere (stick) after 72 hours).

16. Change the media every two days and conserve them sub-confluent to not have a spontaneous differentiation.

Seed at the beginning ~ 45 000 000 cells (a lot of cells will be eliminate after 24 hours) ~ 10 000 000 cells/ml

After adhesion: about 5 000 cells/cm²(big cells, so not many cells at confluence)

I. Differentiation Test for rADSCs

I.1 Adipogenic Differentiation

(Poietics™ Human ADSCs – adipogenesis, LONZA)

Prepare preadipocyte growth medium (PGM™-2):

1. Add fetal bovine serum to Preadipocyte basal medium-2 (PBM™-2) (PT 8202 – 500ml)
2. Add L-glutamine and GA- 1000 to PBM-2 bottle (PT-9502, rinse out well)

Prepare preadipocyte differentiation medium (PDM-2)

1. Pipette 100ml of PGM™-2 to sterile medium bottle
2. Add the following cryovials (PT-9502) to 100ml of PGM™-2 to sterile medium bottle:
 - Rhinsulin
 - Dexamethasone
 - IBMX
 - Indomethacin
3. This makes a 2X store solution (diluted by PGM™-2 when use)

Plating cells:

- 31,500 – 62,500 cells per cm² in 0.625 ml PGM-2 per cm²
 - 24 well plate - (1.9 cm²)
1. 70,000 cells in 1.25ml PGM™-2 per well (n=4, 3 differentiated and 1 undifferentiated)
 2. Allow cells to reach >90% confluence (24- 48 hrs)

Induction of adipogenic differentiation:

1. Remove PGM™-2
2. Add fresh PGM™-2 to undifferentiated control (1.25 ml per cm²)
3. Add 0.65 ml of PGM™-2 and 0.65 ml PDM-2 medium to differentiated cells (Don't let cells dry out)
4. Incubate at 37 °C 5% CO₂ and 90 % humidity
5. Media changes not required during 10-12 day period (analysis carried out then)

Analysis (Oil Red O staining):

1. Prepare stock solution of oil red O: 0.05g Oil Red O (Sigma-C0625) + 10ml Iso Propyl Alcohol (IPA) (Fresh made)
2. Prepare working solution: 6 ml stock solution + 4 ml ddH₂O
3. Filter working solution before use
4. Wash wells with 1X PBS (pH 7.4), x2
5. Add 70 % ethanol for 10-20 secs
6. Add Oil Red O working solution, leave at RT for 15mins
7. Remove and wash with 70 % ethanol for a few secs
8. Wash with ddH₂O
9. Counterstain with Hematoxylin (Sigma Aldrich-51275) 30 secs
10. Wash with ddH₂O
11. View under microscope via "Brightfield"
12. Lipid droplets stain bright red.

1.2 Osteogenic differentiation

(Poietics™ Human ADSCs – Osteogenesis, LONZA)

Prepare osteogenic induction medium:

(Pre-coat tissue culture surfaces with rat tail collagen I to prevent delamination)

1. Add SingleQuots™ (PT4120, contents as following) to 170ml hMSC differentiation medium - Osteogenic (PT3924)
 - L-glutamine
 - Dexamethasone
 - Ascorbate
 - pen/strep
 - MCGS
2. Rinse the SingleQuots™ vials with the medium
3. Store at 2 °C to 8 °C in the dark until needed
4. Use this medium to induce differentiation

Plating cells:

1. Add 10,000 cells per well in 1 ml ADSC growth media (ADSC-GMTM, PT 4505 bullet kit - PT-3273, PT4503) in 24 well plate (n=4, 3 differentiated and 1 undifferentiated)
2. Allow cells to attach (18- 24 hrs) then induce differentiation

Induction of osteogenic differentiation:

1. Remove ADSC- GMTM
2. Add fresh ADSC- GMTM to undifferentiated control (1ml per well)
3. Add Osteogenic induction medium to differentiated cells (1 ml per well) (Don't let cells dry out)
4. Incubate at 37 °C 5 % CO₂ and 90 % humidity
5. Change media every 3-4 days for 3-4 weeks

Analysis (Alizarin red):

(Used to demonstrate calcium in sections, confirmation of osteogenesis)

1. Add 2 g Alizarin Red (Riedel-de Haën – 33010) into 100 ml ddH₂O (C₁₄H₇O₇Na, 342.3 g/mole)
2. Adjust pH to 4.1 using 0.5 % (v/v) ammonium hydroxide (Critical required!)
3. Solution can be kept in the dark for up to 6 months, filter by filter paper before use. Avoid contact and inhalation.
4. Wash cells with HBSS
5. Fix in 10 % formalin for 30 minutes
6. Wash with HBSS 3x 10 minutes
7. Add 1mL of 40 mM ARS (pH 4.1) per well, leave at RT for 5 min.
8. Wash with ddH₂O 3x 5 minutes with gentle shaking
9. Incubate in HBSS for 15 minutes to eliminate nonspecific staining
10. View under microscope via “Brightfield”
11. Calcium deposits are stained orange-red

1.3 Chondrogenic differentiation

(PoieticsTM Human ADSCs – chondrogenesis, LONZA)

Prepare incomplete chondrogenic induction medium:

1. Add SingleQuots™ (PT3003, contents as following) to 185ml hMSC differentiation medium - chondrogenic (PT3925)
 - L-glutamine
 - Dexamethasone
 - Ascorbate
 - ITS + supplement
 - Proline
 - GA-1000
 - Sodium pyruvate
2. Rinse the SingleQuots™ vials with the medium
3. Store at 2 °C to 8 °C in the dark until needed
4. Use this medium to induce differentiation

Prepare TGF-β3

1. Resuspend the lyophilized TGF-β3 (PT- 4124) with sterile 4 mM HCl supplemented with 1 mg/ml BSA or HSA to a concentration of 20 µg/ml.
(2µg of TGF-β3 in 100 µl). **Note:** *Each µl of TGF-β3 will convert 2 ml of incomplete chondrogenic medium into complete medium.*
2. Aliquot small volumes of TGF-β3 into freezer safe tubes and store at less than -70°C for no more than 6 months. (5 µl aliquots of TGF-β3 will be sufficient to supplement 10 ml of incomplete chondrogenic induction medium.)

Prepare complete chondrogenic induction medium

1. Thaw TGFβ-3 and centrifuge briefly at a low speed to pull the small volume to the bottom of the tube (5 µl in 10 ml)
2. Pipette a volume (10 ml) of incomplete induction medium in a 15ml tube
3. Transfer a 100 µL of incomplete induction medium into TGFβ-3 tube
4. Remove and transfer to 15 ml tube with incomplete induction medium. (Final concentration of TGFβ-3 is 10 ng/ml)

5. Fresh prepared and use in 12 hrs

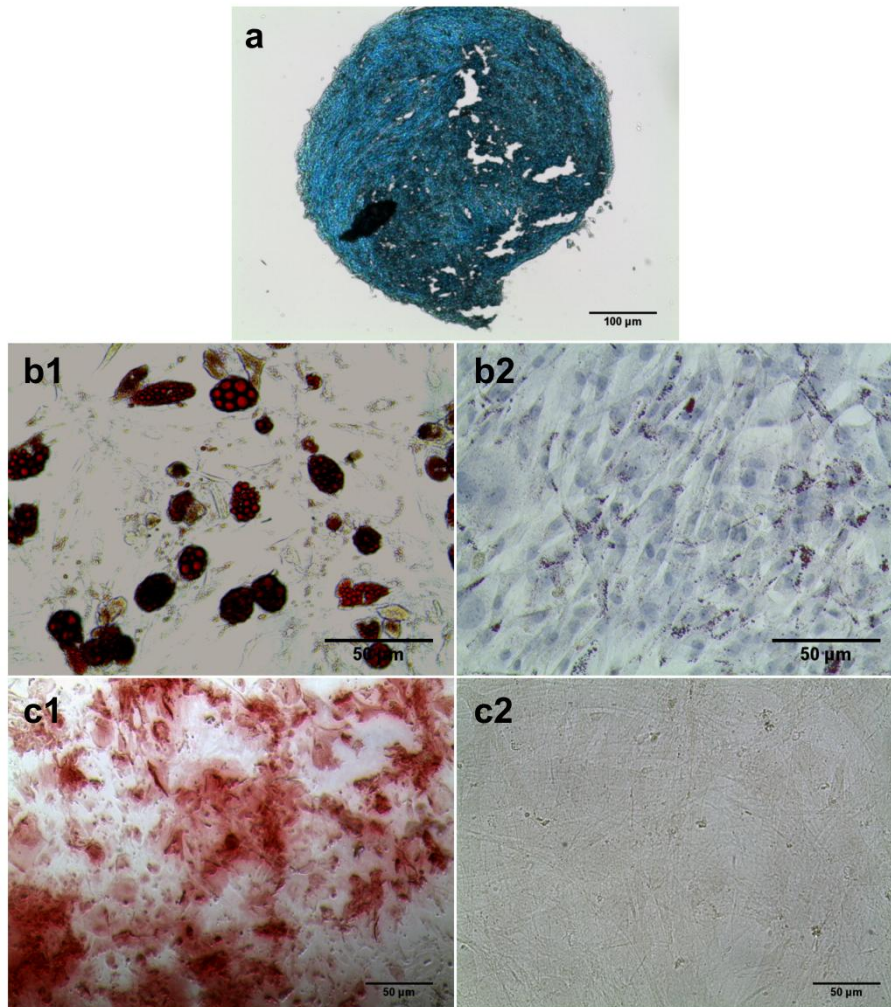
Plating cells and induction of chondrogenic differentiation:

500,000 cells required to form chondrogenic pellet, 5 pellets required

1. Wash cells with **incomplete** chondrogenic medium and transfer the amount of cells according to culture tubes and centrifuge at 150 g for 5 minutes
2. Resuspend the cells in **incomplete** chondrogenic medium (1.0×10^6 cells per ml).
3. Resuspend the cells in **complete** chondrogenic medium to a concentration of 5.0×10^5 cell per ml (2 control pellets in ADSC-GM™)
4. Aliquot 1.0 ml (5.0×10^5 cells) of the cell suspension into a 15ml polypropylene culture tubes
5. Loosen the cap of the tubes one half turn to allow gas exchange
6. Feed cell pellets every 2-3 days.
7. Replacing the medium gently flick the pellet to make sure that the pellet is not attached to the bottom of the tube.
8. 21 days in culture

Analysis (Safranin-O stain)

1. Fix cell pellet in 10 % formalin at RT for 1 hour
2. Prepare histological section
3. Wash slides in ddH₂O for 2 min
4. Stain with Iron Hematoxylin (Sigma Aldrich 51275) for 3 min (black)
5. Wash slides in ddH₂O for 3min
6. Stain with Fast Green (Sigma Aldrich F7252) for 3 min (counter stain)
7. Acetic Acid (Glacial - Fisher Scientific A/0400/PB17) for 5 seconds
8. Stain with Safranin-O (Sigma Adlrich 84120 for 3 mins (red)
9. Wash by ddH₂O for 5 mins
10. View under microscope via “Brightfield”



(Differentiation capability of rat ADSCs. (a) Safranin-O staining of histological sections of pellet after three weeks in chondrogenic differentiation conditions culture. (b) Oil red O staining after two weeks in culture in presence (b1) or absence (b2) of adipogenic differentiation medium. (c) Alizarin red staining after four weeks in culture in presence (c1) and absence (c2) of osteogenic differentiation medium.) (Assessments were performed by a colleague of Mr. Robert Kennedy who is a PhD student in our group).

J. Cell Culture

J.1 Aseptic Techniques

1. Spray the hood area with Virkon followed by 70% Ethanol
2. Spray everything entering the hood with 70% Ethanol, assume every exposed surface outside the hood is contaminated
3. Sterilize all containers, plates, flasks, tubes and media etc. if it is not sterile, and keep sterile containers sealed (usually filter culture media before using)
4. Avoid touching lids or necks of flasks or bottles with the tip of your pipette
5. If something is contaminated, do not open it in the hood (even not in the cell culture room)

J.2 Cell Recovering from Liquid Nitrogen

1. Check the cell storage record and take target vial from liquid nitrogen
2. Thaw in the 37 °C water bath for about 1 minute, the water should not touch the lids area of the vial (do not submerge the whole vial in the bath!)
3. Spray vial with 70% ethanol before putting into the hood. (Must work quickly after the cells have thawed as the DMSO is toxic!)
4. Transfer cell suspension into a sterile centrifuge tube with pipette
5. Add about 5 ml culture media drop by drop to the cells in the tube. **(Add the media slowly to reduce the osmotic shock!)**
6. Centrifuge at 1200 rpm for 5 minutes.
7. Remove the media carefully off the cell pellet
8. Resuspend the cell pellet in 2 -5 ml culture media depending on the cell concentration
9. Count cell number with haemocytometer
10. Plate out cells at 5000 cells/cm², (for a T175 flask, plate out about 875,000 – 1 million cells per flask; for ADSCs, a little bit higher concentration would promote cell proliferation)
11. Feed with media (25-30 ml for T175 flask) every 2-3 days.

J.3 Cell Feeding

1. Clean hood, spray all equipment with 70 % ethanol
2. Filter fresh culture media
3. Take flask from incubator, check cells under microscope, spray with ethanol and wipe clean with tissue paper
4. Remove media from flask (never let the liquid get up to the cotton at the top of the pipette when pipetting), or use aspirator to remove
5. Pipette in new media (T25: 3-5mL media, T75: 8-10mL media, T175: 25-30mL media)
6. Check cells under microscope and return flask to incubator

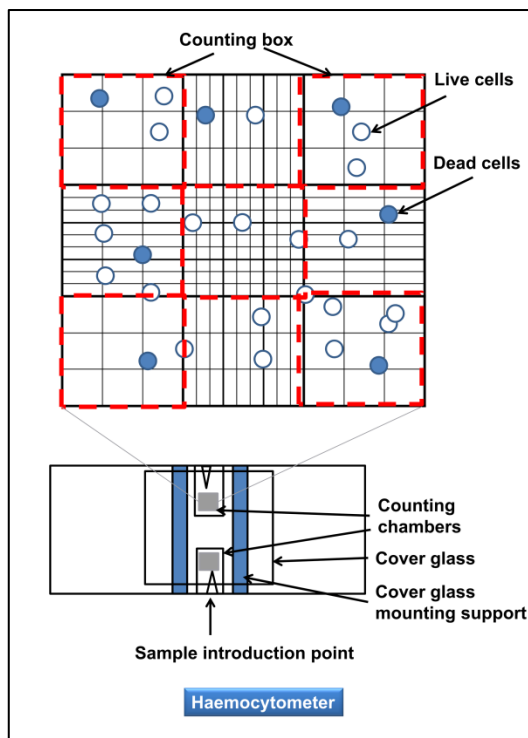
J.4 Cell Splitting

1. Remove media from flask
2. Wash flask with Hanks balanced salt solution (HBSS) by pipetting in 10 ml 1-2times (tilting the flask to get the liquid covering the full surface, then removing it)
3. Add enough 0.25% trypsin-EDTA (T/E) to cover the bottom of the flask when it's lying in the proper configuration (T25: 1 ml, T75: 3 ml, T175: 7-10 ml)
4. Put in incubator for 3-5 minutes (enzyme is active at 37 °C)
5. Take flask out and exam under microscope. (Cells should be rounded and moving around if you tap the flask. If they are still stuck to the bottom, try tapping the side of the flask gently. If they don't come off, leave it another minute or two)
6. Once all (or almost all) cells are free, spray the flask and return it to the hood
7. Add an equal volume of 10 % serum media to the flask (deactivates the trypsin)
8. Remove all of the liquid and put in a sterile 15 or 50 ml centrifuge tube
9. Centrifuge at 1200 rpm for 5 minutes.
10. Remove the media carefully off the cell pellet

11. Resuspend the cell pellet in 2 -5 ml culture media depending on the cell concentration
12. Count cell number with haemocytometer
13. Seed desired number of into new flasks as needed

J.5 Cell Counting

1. Add 90 μ l trypan blue into a well of 96-well plate (dilute 1/10), 2x
2. Take 10 μ l of the cell suspension, add into each well with trypan blue and mix with pipette gently
3. Add 10 μ l of mixture of cell/trypan blue suspension to each side of a haemocytometer (trypan blue is excluded by live cells – blue cells are dead, clear cells are alive)
4. Count cells on both sides of haemocytometer and get the average (five box per side as shown in the image)
5. To calculate the cell concentration and total number:
6. Cell concentration = average cell no./box $\times 10^4 \times$ dilution factor (in this case $\times 10$)
7. Total cell number = Cell concentration \times original total volume of cell suspension



J.6 2D Cell Seeding on Hydrogel Surface

All performance in hood

1. Prepare polymer solution of PEGMEMA-MEO₂MA-PEGDA in serum free DMEM media at certain concentration
2. Prepare the cross-linker (e.g. QT or HA-SH in PBS)
3. Mix polymer solution and cross-linker as certain ratio
4. Transfer mixture into 48-well plate (100-200 µl per well) or glass well slides (80 µl per well in 4 well-slides).
5. Leave in incubator for 1 h to completely form gel
6. Wash gel by HBSS, 10 min in incubator 3 times
7. Wash gel by culture media, 20 min in incubator 2 times
1. Split, count cells and concentrate/dilute cell suspension to 100,000 cell/ml in culture media (DMEM+1%PS+10%FBS)
8. Add 100 µl (about 10,000 cell per well for 48 well-plate or 4 well-slides) cell suspension on the gel surface
9. Leave plate in incubator for 2-4 h to let cell attach on the gel
10. Add more culture media drop by drop carefully (1 ml per well for 48 well-plate, 200 µl per well for 4 well-slides)
11. Culture in incubator, change media every 1-2 days
12. Staining cells (e.g. LIVE/DEAD[®] Stain) and exam using fluorescence microscope at certain time point

J.7 3D Cell Culturing in Hydrogel (P-SH-HA hydrogel as example)

All performance in hood

1. Prepare polymer solution of PEGMEMA-MEO₂MA-PEGDA in serum free DMEM media at 20% (200 mg/mL)
2. Dissolve HA-SH in water (all from HyStem[™] kit, 1%)
3. Prepare sterile glass slides covered by Teflon tape (hydrophobic surface)
4. Split, count cells and concentrate/dilute cell suspension to 4 million cell/ml in culture media (DMEM+1%PS+10%FBS)
5. Mix 40 uL polymer (20%) with 80 uL HA-SH (1%) and 40 uL cells (4 M/mL)

6. Take 40 μ L on prepared slide and put in incubator for 15 min to form gel

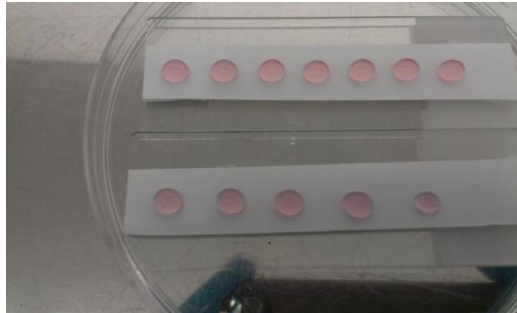


(Photo of hydrogel on glass slides covered by Teflon tape)

7. Transfer gels to 48 well plats and add 1-2 mL culture media
8. Staining cells (e.g. LIVE/DEAD[®] Stain) and exam using fluoresce microscope at certain time point

J.8 LIVE/DEAD[®] Staining

1. Take out kit (in Freezer), defrost tubes, spun down (quick spin)
2. Transfer seeded scaffolds into HBSS/PBS to wash and remove serum, wash 2x
3. (if you wish to have a dead control, immerse scaffold in 70% Methanol or other killing solution)
4. Prepare Staining Solution(s)
 - Calcein (live) is at 5-10 μ M
 - Ethidium Homodimer-1 (dead) is at 1.5-2 μ M
 - If staining with both, add both to the same staining solution.

PROTECT FROM LIGHT

5. Add enough stain to cover the scaffolds (ie. 500 μ l)
6. Incubate 30 minutes in the incubator or 45 minutes in the hood. (if your scaffold is very dense, it might need longer to penetrate, but note the dye is cytotoxic so you can't leave it too long.)
7. Exam under X81 fluorescence microscope):

Live: FITC filter / Dead: Texas Red filter

K. Cell Metabolic Assessment (alamarBlue[®] Assay)

1. Add 1000 µl of Hank's balanced salt solution (HBSS) into the required number of wells in the sterile 24 well plate i.e. same number as samples to be tested.
2. Make up the solution of alamarBlue[®] in HBSS (Culture medium for 3D, ratio 1:9 respectively). 500 µl is required per well.
3. Transfer the seeded scaffolds/tissue culture inserts from their original well plate to the HBSS well plate using the sterile tweezers.
4. Remove the HBSS from each well.
5. Cover the scaffolds and positive control (empty wells washed with HBSS) with 500 µl of the alamarBlue[®] in HBSS (ratio 1:9).
6. Incubate for 2 hours (15 h for 3D) at 37 °C
7. After incubating, transfer 150-200 µl of the dye into the clear 96 well plate
8. Measure the absorbance at 550 nm and 595 nm (0.5 seconds per well).
9. Calculate a viability value according to 'simplified method of calculating percent reduction' available in the alamarBlue[®] handbook.
10. Subtract the absorbance values of HBSS only from the absorbance values of the alamarBlue[®] in HBSS (ratio 1:9). Call this AO_{LW} = absorbance of oxidized form at lower wavelength, and AO_{HW} = absorbance of oxidized form at higher wavelength.
11. Calculate correlation factor: R_O .

$$R_O = AO_{LW}/AO_{HW}$$

12. To calculate the percent of reduced alamarBlue[®]:

$$AR_{LW} = [A_{LW} - (A_{HW} \times R_O)] \times 100$$

13. Percent of cell viability:

$$\text{Cell viability \%} = AR_{LW}(\text{test})/AR_{LW}(\text{cell alone}) \times 100$$

L. Cell Proliferation Assessment (Picogreen[®] Assay)

(Invitrogen[™]: Quant-iT[™] PicoGreen[®] dsDNA Reagent and kits)

- **The manipulation must be realized with gloves (DNA intercalant)**
- **Protect the picogreen with cook foil: Picogreen light sensitive**

Before Beginning

- Make up 1X TE buffer in DNase-free H₂O (initial solution in kit is 20X)
- Make up 2 µg/ml DNA stock solution (100 µg/ml DNA standard in working TE buffer)

1. Remove the media and wash the structure by HBSS
2. If a classic culture on TCP in 24 well plate:
 - Remove media and gently rinse cells with HBSS.
 - Add 250 µl of DNase free water
 - Repeatedly freeze-thaw cells 3 times (freeze at -80 °C during 15 minutes minimum and defreeze at room temperature until completely de-freezing.)

If culture on/in a Collagen scaffold/hydrogel:

- Wash the constructs with HBSS
- After transfer of the construct in an eppendorf, digest it by 1 ml of proteinase K (1 mg/mL, ≈ 30 U/mL, Sigma P2308, dissolve in working TE buffer) overnight at 37 °C, 100 rpm.
- Use the product of digestion directly or freeze it at -20 °C.

If culture on/in a PEGDA-SH-HA hydrogel:

- Wash the constructs with HBSS
- After transfer of the construct in an eppendorf, digest it by 460 µL of proteinase K (for 40 µl gel. 1 mg/mL, ≈30 U/mL, Sigma P2308, dissolve in working TE buffer) & hyaluronidase (2 mg/mL, ≈ 1500 U/mL, Sigma H3506, dissolve in working TE buffer) overnight at 37 °C, 100 rpm.
- Use the product of digestion directly or freeze it at -20 °C.

3. Prepare a standard curve (n=3):

Final DNA concentration (ng/ml)	Volume (µl) of DNase Free H ₂ O	Volume (µl) of 2 µg/ml DNA stock	Volume (µl) of 50ng/ml DNA stock	Total Volume
1000	200	200	--	400
500	300	100	--	400
100	380	20	--	400
50	780	20	--	800
25	200	--	200	400
10	320	--	80	400
5	360	--	40	400
0	400	--	--	400

4. Transfer 100 µl of each sample in the 96 Corning flat bottom well-plate (Black/White).
5. Make up diluted PicoGreen solution (1/200): 7.96 mL 1X TE + 40 µl concentrated PicoGreen (*enough for the standard curve in triplicate and 50 samples, Prevent from light*)
6. Add 100 µl of diluted PicoGreen to each well.
7. Incubate at room temperature 2-5 minutes in the **DARK**.
8. Read the plate with the protocol:
 - Shake (5 ss, speed 600)
 - Fluorometrial (480/520 nm; 12; AutoRange; 100)
8. Plot on a graph the concentration vs. the reading. Determine the concentration of DNA in function of this standard curve.

M. Procedures for Animal Studies

All procedures were conducted under an animal license (no. B100/4342) authorized by the Irish Department of Health and Children and were approved by the Animal Care and Research Ethics Committee of the National University of Ireland, Galway (no. 009/10(B)). Animal care followed the Standard Operating Procedures of the Animal Facility at the National Centre for Biomedical Engineering Science, NUIG.

M.1 Pre-surgery

Sterilize all the surgical tools and equipment as needed (One day before surgery)

Prepare rat ADSCs:

1. Prepare cell tracker solution at 4 μM (CM-DiL Invitrogen C7000, resuspend the powder in 1mL of DMSO, then dilute in serum free medium)
2. Wash cells (T175 culture flask) with HBSS 2x
3. Add cell tracker to cover cells
4. Put in incubate for 30 min
5. Wash cells with HBSS and trypsinize cells
6. Count cells and make concentrated cell suspension (4 million/ml, aliquot into sterile 500 μl eppendorf vial, each vial for one animal)
7. Keep cells on ice (cell viability can be remained for at least 9-10 hours)

Prepare polymers and HA-SH:

1. Prepare polymer solution of PEGMEMA-MEO₂MA-PEGDA in serum free DMEM media at 20 % (200 mg/ml)
2. Aliquot into sterile 1 ml eppendorf vial, each vial for one animal
3. Dissolve HA-SH in water (all from HyStem™ kit, 1%)
4. Keep everything on ice

M.2 Surgical Procedure

1. Prepare surgical area (sterilize and prepare tools).
2. Analgesia animals by injecting with Buprenorphine (0.03 mg/Kg, Vetergesic), 30 min before surgery
3. Weight, anaesthetize rats using isoflurane (5 to 2%) and oxygen (2 l/min) and label the rat No. (on the Tail).
4. Clipped/shaved dorsal area
5. Mark the surgical area (4 points per wound) and swab the surgical area with 4% chlorhexidine or povidone iodine to control bacterial (2 times)
6. Four full thickness wound (1cm x1cm) will be created on the dorsum of the rat (4 cut for each wound)
7. Image with ruler by digital camera
8. At meantime, another person prepares cells and samples (mix at certain ratio)
9. Put the mixture (120 µl) on to each wound to in situ form a hydrogel.
10. A standard bio-occlusive transparent dressing will cover the wounds (TegadermTM Film, 3M[®])
11. Antibiotics injection (Enrofloxacin: 5 mg/Kg).
12. Cover the rat by a medial bandage.
13. Put animal into a new cage and put in recover room once it wake

M.3 Post-surgery Animal Caring

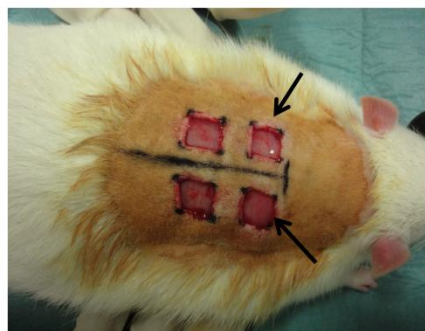
- Inject with Buprenorphine (0.03 mg/Kg every 8 hours, Vetergesic) and antibiotics (Enrofloxacin: 5 mg/Kg once a day) for first 3 days after surgery
- Weight animals once a day to record animal weight lose
- Monitor appearance, food and water intake and dressings everyday



a. anesthesia



b. wound creation



c. wound with hydrogel



d. covered by Tegaderm™ Film



e. covered by medical bandage

(Photos of surgical procedure in animal study)

M.4 Example of Records for Animal Study

RAT SURGICAL RECORD

Title: Rat Dorsal Excisional Wound Model **Date:** 9/5/12
Rat ID: A2 N5 D14 **Time:** 11:40
Strain: Sprague Dawley (male)
Born Date: 12-01-12 **Arrival Date:** 15-03-12 **Age (Month):** 4
Initial Weight (g): 527

Purpose:	Tissue Response Healing Response
Method:	1cm x 1cm full thickness wound (4 wounds per animal) In situ hydrogel formation Wound Dressing
Duration:	Day 3 Day 7 <u>Day 14</u> Day 21
Anaesthesia	Isoflurane/O ₂ ✓ Time: 11:37
Analgesia	Buprenorphine (Vetergesic) 0.01-0.05mg/kg SC. Half hour before surgery Time: 10:20 Dose: 55.

Procedure 11:45

Wound Traced: **Wounds photographed:**

Position	Group	Treatment
AL		NA.
AR		C
PL		H
PR		H+C

AL	AR
PL	PR

Time end of procedure: 12:30.

Recovery time: 12:35.

Comments on recovery from anaesthesia:

(Surgery Record)

Medication Logbook

Study Title: Excisional Rat wound model
 Animal No: A2 N 5 D14 Species: Rat
 Breed: Sprague Dawley Sex: Male Age: 4 m
 Initial Date: 9/5 Initial Weight: 527
 P.I./Researcher: Wenxin Wang/ Yixiao Dong

Date:	Time	Weight (g):	Drug Used:	Quantity	Route	Comments
9/5	10:20	527	BP	SC	55	
	12:30		BT	SC	55	
	17:10		BP	SC	55	
	23:00		BP	SC	55	
10/5	10:20	524	BP	SC	55	
			BT	SC	55	
	16:32		BP	SC	55	
	24:18		BP	SC	55	
11/5	08:35	512	BP	SC	50	
			BT	SC	50	
	16:05		BP	SC	50	
	23:25		BP	SC	50	
12/5	9:10	506	BP	SC	50	
			BT	SC	50	
	16:35		BP	SC	50	
13/5	9:10	501				
14/5	9:45	471				
15/5	11:00	460				
16/5	12:40	455				
17/5	15:50	450				
18/5	13:20	450				
19/5	11:35	456				
21/5	11:00	460				
22/5	12:00	460				

BP: Buprenorphine BT: Baytril

(Medication logbook)

N. Tissue Harvest and Slides Preparation

1. The animals were sacrificed by CO₂ asphyxiation at each time points.
2. Remove gauze and film dressing carefully.
3. Take photographic images of each wound with a ruler next to the wound. (Keep the distance and angle of the camera from the wound the same).
4. Cut off the whole area of the skin with four wounds and split to each wound.
5. Cut each wound in two from the middle.
6. Fix one half with 10 % formalin at RT for 24 h followed by automatic paraffin processing (Leica ASP300, “routine overnight, 16 h” program).
7. Embed samples in wax (section surface down in the plastic mould, Lennox). Keep at 4 °C at least overnight before sectioning
8. Sectioning perpendicularly to wound surface in 5 µm consecutive sections.
9. Collect sections from hot water bath (about 45-50 °C) with labeled slides
10. Dry the slides in air.
11. (Fix the other half sample by 4 % paraformaldehyde overnight at 4 °C, followed by sinking in 30 % sucrose at 4 °C, embedding in O.C.T and freezing in liquid nitrogen, so samples are ready for cryo-sectioning).

Harvesting Record – Hypertrophic Scar Model

Animal ID: A2 N5 D14 **Date:** 23/5.
Species: Rat **Breed:** Sprague Dawley
Sex: Male **Initial Wight:** 527
Time Point: 14 days **Wight:** 457.
P.I./Researcher: Wenxin Wang/ Yixiao Dong

Agents Used for Euthanasia:

Method	Admin. Time	Date	Comments
CO ₂	13:00	23/5	

Harvesting Notes:

Wound Traced: **Wounds photographed:**

Comments on wound sites:

Sample in 10% of Formalin:
Sample to 4% PFA:

(Example of Tissue Harvest Records for Animal Study)

O. Hematoxylin and Eosin (H&E) Staining

1. Preheat slides in 50 °C oven for 2 minutes
2. Xylene 8 min 2x
3. 100% Ethanol Dip
4. 95% Ethanol Dip
5. 80% Ethanol Dip
6. 70% Ethanol Dip
7. 50% Ethanol Dip

(For cryosections, start with running water 2 min here)

8. Distilled H₂O Dip
9. Haematoxylin 10 min
10. Running Water 15 min
11. Distilled H₂O Dip
12. 50% Ethanol Dip
13. 70% Ethanol Dip
14. 80% Ethanol Dip
15. 95% Ethanol Dip
16. Eosin 2 min
17. 95% Ethanol 2 min
18. 95% Ethanol Dip 2x
19. 100% Ethanol Dip 3x
20. 50% Ethanol/50% Xylene 4 min
21. Xylene 4 min 2x
22. Clean cover slip with xylene
23. Mountain by DPX
24. Dry overnight in hood

P. Immunohistochemistry**Equipment and Reagents:**

- Samples on charged slides
- Oven
- Xylene
- Ethanol
- Deionised water
- Troughs/Slide racks and rack baths
- Humidifier chamber (Keep reagents do not drain off)
- Absorbent tissue paper
- Scientific microwave (T/T MEGA, Multifunctional Microwave Histoprocessor, Medical Supply Co Ltd.)
- **Antigen Retrieval Buffer:**
10 mM Sodium citrate, 0.05% Tween[®] 20, pH 6.0
 - Trisodium Citrate Dihydrate: 2.94 g (Sigma-S1804, 294.1 g/mol)
 - Distilled water: 1000 ml
 - Adjust to pH 6.0 with 1 N HCl
 - Add 0.5 mL of Tween[®] 20 (Fisher BP337) and mix well.
 - Store at RT for 3 months or at 4 °C for longer storage.
- **H₂O₂** (30% H₂O₂ Diluted in 1/20) **make fresh every time.**
- **10X TBS** (Tris Buffered Saline pH:7.6-7.8):
 - TrisHCl: 24.23 g (Sigma-T3253, 157.6 g/mol)
 - Sodium chloride: 80.06 g (Fluka 71381, 58.44 g/mol)
 - Distilled water: 800 ml
 - Adjust to pH 7.6
 - Top up to 1000 ml
- **TBS 0.025% Triton X-100**
 - 10X TBS: 100 ml
 - Distilled water: 899.75 ml
 - Triton X-100: 250 µl (Fisher-BP151-100)

- **5% Normal Goat's Serum (NGS)**
50 µl Goat's Serum (Sigma-G9023) in 950 µl 1X TBS
Prepare fresh (no more than 2-3 days in the fridge); 50-100 µl per sample, **Doubled** as the primary antibody are diluted in this blocking solution.
- **Primary Antibody**
 - Rabbit polyclonal antibody to collagen type IV for angiogenesis analysis (Abcam plc, Cambridge, UK)
 - Mouse monoclonal anti-CD 68 antibody for macrophages, (Abcam Abcam plc, Cambridge, UK)
 - Dilution: 1/200 in 5% NGS
- **Secondary Antibody**
 - AlexaFluor[®] 488 Goat anti-rabbit IgG (H+L) for angiogenesis analysis (Invitrogen).
 - AlexaFluor[®] 488 Goat anti-Mouse IgG (H+L) for macrophages (Invitrogen)
 - Dilution: 1/1000 in TBS
- **Aqueous Mounting Medium:** Fluoromount[™] Aqueous Mounting Medium (Sigma-F4680-25 ml)

Procedure:

1. Deparaffinizing and rehydrating sections:

- Warm the slides 1-2 minutes in an oven at 40-50°C to facilitate the removal of paraffin.
- 100% xylene ----- 8 minutes (x2)
- 50% xylene+50% ethanol ----- 4 minutes
- 100% ethanol ----- 5 minutes (x2)
- 95% ethanol ----- 5 minutes
- 70% ethanol ----- 5 minutes
- 50% ethanol ----- 5 minutes
- 1X TBS ----- 2 minutes

(Do Not allow slides dry. Non-specific binding can occur with high background in dry slides)

2. Antigen retrieval:

- Add antigen retrieval buffer to the microwave vessel allowing enough volume for evaporation (500 mL).
- Pre-heating the scientific microwave at 98 °C. (Antigen Retrieval-Citrate Heating 98 °C)
- Place sections in the vessel and avoid positioning the rack directly above the magnetic stirrer in the microwave so the turbulences will not disturb the samples and detach them
- Program the scientific microwave as “15 slides 20 min.”, maximum stirring speed
- When the time has elapsed, remove the vessel from microwave and place slides rack in cold tap water for 15 minutes for cooling down.

3. Immuno-histochemical staining:

- TBS-Triton X ----- 5 minutes (x2, change every time)
- Drain slides with Absorbent tissue paper, place in humidified chamber
- 5% NGS in TBS ----- 1 hours (Blocking)
- Drain slides with Absorbent tissue paper
- Apply primary antibody, diluted **1/200** in blocking solution (5% NGS in TBS)
- **Overnight at 4°C in humidified chamber**
- Leave chamber at RT ----- 60 minutes (to acclimatize)
- Tap and dry around
- TBS-Triton X ----- 5 minutes (x3, change every time)
- Tap and dry around
- 1.5% H₂O₂ in TBS-Triton X in humidified chamber ----- 15 minutes
- Drain slides with Absorbent tissue paper
- TBS-Triton X ----- 5 minutes (x2, change every time)
- Apply secondary antibody, diluted **1/250** in TBS
- Incubate at RT ----- 60 minutes
- TBS ----- 5 minutes (x2, on shaker)
- Hoechst ----- 15 minutes (1/4000)
- TBS ----- 5 minutes (x2, on shaker)
- dH₂O ----- 10 minutes (on shaker)

- Mounting by Fluoromount™ Aqueous Mounting Medium

4. Exam under X81 fluorescence microscope:

Green (FITC filter) - Blue (DAPI filter)

Q. Hoechst Stain (for Cell Retention Analysis)

1. Preheat slides in 50 °C oven for 2 minutes
2. Xylene 8 min 2x
3. 100% Ethanol Dip
4. 95% Ethanol Dip
5. 80% Ethanol Dip
6. 70% Ethanol Dip
7. 50% Ethanol Dip
8. Distilled H₂O Dip
9. PBS 3 min
10. Drain slides with Absorbent tissue paper
11. Stain with Hoechst 33258 (1/4000, Invitrogen®) for 15 min
12. PBS 5 min
13. Mounting by Fluoromount™ Aqueous Mounting Medium

R. Stereology

R.1 Wound Contraction and Epithelialization

1. Place H&E stained slide under bright field light.
2. Capture an image of whole wound at 1.25X objective.
3. Open image by Image Pro® software and calibrate the image at 12.5X magnification.
4. Identify one of the wounds edges, (based on the change in epithelium thickness, collagen (blue) density, cellularity, and the lack of skin appendages.

5. Measure the wound length (W_t) between two wound edges using line command, (parallel with epithelium line).
6. Measure the length of regenerated epithelia layer (E_1 & E_2) from both side (identify based on the change in epithelium thickness and the difference of cell organization).
7. The original wound size was 1 cm and roughly 10 % contraction was caused by fixing and processing processes, therefore W_0 was considered as 0.9 cm for calculation.
8. The percentage of epithelialization (E %) was determined by the total epithelial layer over the wound at both side (E_1+E_2) divided by the original wound length (W_0).

$$E \% = \frac{(E_1 + E_2)}{W_0} \times 100$$

9. Percentage of wound contraction (C %) was determined by the reduction of wound length divided by the original wound length (W_0).

$$C \% = \frac{(W_0 - W_t)}{W_0} \times 100$$

R.2 Cell Retention

1. Exam Hoechst stained slides (“cell alone” and “hydrogel + cell” groups) under X81 fluorescence microscope:
 - Transplanted cells with CellTrackerTM CM-Dil (Invitrogen[®]): Texas Red filter;
 - Nucleus stained with Hoechst 33258: DAPI filter.
 - Automate take images from both filter and merge.
2. Capture five random images of hydrogel area at 10X objective.
3. Open images by Image Pro[®] software and calibrate the image at 100X magnification.
4. The volume fractions of rADSCs were determined by stereological analysis using a line grid mask ($40 \times 40 \mu\text{m}^2$, with 20 μm margins).

- Count the intersections against implanted cells (P_V) and grid intersections hit hydrogel area (P_T). volume fraction (V_V) of implanted cells was expressed as follows:

$$V_V = \frac{P_V}{P_T}$$

R.3 Inflammation

- Exam CD68 immunohistochemical stained slides under X81 fluorescence microscope:
 - Macrophages (CD68+): FITC filter;
 - Nucleus stained with Hoechst 33258: DAPI filter.
 - Automate take images from both filter and merge.
- Capture three random images of wound area at 20X objective.
- Open images by Image Pro[®] software and calibrate the image at 200X magnification.
- The volume fractions of macrophages were determined by stereological analysis using a line grid mask ($20 \times 20 \mu\text{m}^2$, with $10 \mu\text{m}$ margins).
- Count the intersections against CD68+ cells (P_V) and grid intersections hit hydrogel area (P_T). volume fraction (V_V) of macrophages was expressed as follows:

$$V_V = \frac{P_V}{P_T}$$

R.4 Angiogenesis

- Exam Collagen-Type IV immunohistochemical stained slides under X81 fluorescence microscope:
 - Collagen-Type IV +: FITC filter;
 - Nucleus stained with Hoechst 33258: DAPI filter.
 - Automate take images from both filter and merge.
- Capture three random images of wound area at 10X objective.

3. Open images by Image Pro[®] software and calibrate the image at 100X magnification.
4. All images are analyzed under cycloid grid.
5. To measure surface density, place cycloid grid on the image with radius of 20 μm , spacing of 40 μm and margin at 20 μm .
6. Total length (L) of test line is calculated by number of arcs on the reference space multiply by 40.
7. Count the number of intersections (I) of blood vessels and the cycloid arcs, and calculate surface density according to the following equation:

$$S_V = 2 \times \frac{I}{L}$$

8. Rotate each image by 90 degrees.
9. Apply the same grid as in surface density.
10. Count the intersections of blood vessels and cycloid arcs and use the following equation to calculate length density, T_S presents the thickness of sections (i.e. 5 μm).

$$L_V = \frac{(2 \times (I/L))}{T_S}$$

11. Wound volumes (V), surface area (S_A) and total length (L_T) were calculated by following equations:

$$V = T_S \times W_A$$

$$S_A = S_V \times V$$

$$L_T = L_V \times V$$

All stereological analysis was performed as described elsewhere:

“Garcia, Y.; Wilkins, B.; Collighan, R. J.; Griffin, M.; Pandit, A., Towards development of a dermal rudiment for enhanced wound healing response. *Biomaterials* 2008, 29, (7), 857-868”

S. Publications

S.1 Accepted or Printed Article Publications

1. **Dong, Y.**; Aied, A.; Li, J.; Wang, Q.; Hu, X.; Wang, W. 'An *in vitro* approach for production of non-scar minicircle DNA vectors.' *Journal of Biotechnology*, 2013, 166: 84-87
2. Hassan, W.; **Dong, Y.** (equally contribute) and Wang, W. 'Encapsulation and 3D culture of human adipose derived stem cells in an *in-situ* crosslinked hybrid hydrogel from PEG based hyperbranched co-polymer and hyaluronic acid'. *Stem Cell Research & Therapy*. 2013, 4:32
3. **Dong, Y.**; Hassan, W.; Zheng, Y.; Saeed, A.O.; Cao, H.; Tai, H.; Pandit, A.; Wang, W.; 'Thermoresponsive hyperbranched copolymer with multi acrylate functionality for *in situ* cross-linkable hyaluronic acid composite semi-IPN hydrogel', *Journal of Materials Science: Materials in Medicine*, 2012, 23 (1), 25-35.
4. **Dong, Y.**; Saeed, A.O.; Hassan, W.; Keigher, C.; Zheng, Y.; Tai, H.; Pandit, A.; Wang, W.; 'One-step preparation of thiol-ene clickable PEG based thermoresponsive hyperbranched copolymer for *in situ* crosslinking hybrid hydrogel', *Macromolecular Rapid Communications*, 2012, 33, 120-136.
5. Zheng, Y.; Cao, H.; Newland, B.; **Dong, Y.**; Pandit, A.; Wang, W.; '3D single cyclized polymer chain structure from controlled polymerisation of multi-vinyl monomers: Beyond Flory-Stockmayer theory' *Journal of American Chemical Society*, 2011, 133, 13130-13137.
6. Cao, H.; **Dong, Y.**; O'Rorke, S.; Wang, W.; Pandit, A. 'PEG based hyperbranched polymeric hollow nanospheres' *Nanotechnology*, 2011, 22, 065604
7. **Dong, Y.**; Gunning, P.; Cao, H.; Mathew, A.; Newland, B. E.; Saeed, A. O.; Magnusson, J. P.; Alexander, C.; Tai, H.; Pandit, A.; Wang, W. 'Dual stimuli responsive PEG based hyperbranched polymers' *Polymer Chemistry*, 2010, 1, 827-830

S.2 Submitted Manuscripts

Dong, Y.; Hassan, W.; Kennedy, R.; Greiser, U.; Garcia, Y. and Wang, W. ‘An *in-situ* formed bioactive stem cell hydrogel dressing from a PEG-based hyperbranched multi-functional copolymer’ *Biomaterials*, (Ref. BIOMAT-S-13-02170.)

S.3 Conference Abstracts and Presentations

1. **Dong, Y.**; Saeed, A.O.; Hassan, W.; Tai, H.; Pandit, A.; Wang, W., ‘Thiol-ene clickable PEG-based thermoresponsive hyperbranched copolymer for in situ crosslinking hybrid hydrogel’. Podium presentation at The 3rd TERMIS World Congress, Vienna, Austria, Sep. 2012
2. **Dong, Y.;** Saeed, A.O.; Hassan, W.; Tai, H.; Pandit, A.; **Wang, W.**, ‘Thiol-ene clickable PEG-based thermoresponsive hyperbranched copolymer for in situ crosslinking hybrid hydrogel’, Podium presentation at The 9th World Biomaterials Congress, Chengdu, China, Jun. 2012
3. **Dong, Y.**; Hassan, W.; Abu-Rub, M.; Pandit, A.; Wang, W., ‘In-situ cross-linked hydrogel from thermoresponsive PEG-based hyperbranched copolymer’, Podium presentation at The 24th European Conference on Biomaterials, Dublin, Ireland, Sep. 2011
4. Cao, H.; Aied, A.; **Dong, Y.;** **Wang, W.** and Pandit, A., ‘A pH-sensitive hyperbranched polymer for nucleic acid delivery.’ Podium presentation at The 24th European Conference on Biomaterials, Dublin, Ireland, Sep. 2011
5. **Aied, A.**; Cao, H.; **Dong, Y.;** Zheng, Y.; Pandit, A.; Wang, W. ‘Biodegradable disulfide-cationic polymer for the gene therapy of recessive dystrophic epidermolysis bullosa’, Podium presentation at The 24th European Conference on Biomaterials, Dublin, Ireland, Sep. 2011
6. **Dong, Y.**; Hassan, W.; Abu-Rub, M.; Pandit, A.; Wang, W., ‘In-situ cross-linked hydrogel from thermoresponsive PEG-based hyperbranched copolymer’, Podium presentation at The Tissue

- Engineering Regenerative Medicine International Society – EU Meeting, Granada, Spain. Jun. 2011
7. Newland, B., **Dong, Y.**; Zheng, Y., Yao, J., Wang, W., Pandit, A., ‘Single cyclised polymer for gene transfection’, Podium presentation at The Tissue Engineering Regenerative Medicine International Society – EU Meeting, Granada, Spain. Jun. 2011
 8. **Dong, Y.**; Zheng, Z.; Pandit, A.; Wang, W., ‘Biodegradable disulfide-cationic polymer for the gene therapy of recessive dystrophic epidermolysis bullosa’, Aied, A.; Cao, H.; Podium presentation at The Tissue Engineering Regenerative Medicine International Society – EU Meeting, Granada, Spain. Jun. 2011
 9. Zheng, Y.; Cao, H.; Newland, B.; **Dong, Y.**; and Wang, W. ‘Celtic knot’ - a new class of polymer structure created from the deactivation enhanced controlled polymerisation of multi-vinyl monomers: Beyond Flory-Stockmayer theory’, Podium presentation at American Chemical Society 241th National Meeting & Exposition, Anaheim, California, USA. Mar. 2011
 10. Cao, H.; **Dong, Y.**; Aied. A.; Wang, W.; Pandit. A. ‘A pH-sensitive cross-linker based on a hyperbranched acetal-polymer’, Podium presentation at 2011 MRS Spring Meeting, San Francisco, California, USA, Apr. 2011
 11. **Dong, Y.**; Saeed, A.O.; Alexander, C.; Tai, H.; Pandit, A. and Wang, W. ‘Dual stimuli responsive PEG based hyperbranched polymers’, Poster presentation at The Tissue Engineering Regenerative Medicine International Society – EU Meeting, Galway, Ireland, Jun. 2010.
 12. **Dong, Y.**; Brown, S., Saeed, A.O.; Alexander, C.; Tai, H.; Pandit, A. and Wang, W. ‘Dual stimuli responsive PEG based hyperbranched polymers’, Poster presentation, The Annual conference of the European Society for Biomaterials, Finland, Jul. 2010.
 13. **Dong, Y.**, Wang, W. ‘Thermo-responsive PEGMEMA-MEO₂MA-EGDMA copolymer for wound healing dressing’, Poster presentation at The DEBRA International Conference, Vienna, Austria, Sep. 2009